Drought Tolerance and its Evolution in Conifers Including UK Commercial Species

Gabriele Rizzuto

Linacre College

Department of Plant Sciences

University of Oxford

Thesis submitted for the degree of

Doctor of Philosophy

Michaelmas Term, 2022

Supervisors: Professor John MacKay and Professor Emily Flashman

INDEX

Acknowledgements

This thesis is a personal milestone and life achievement. It wouldn't have been possible without the help given by many friends, colleagues, staff members and academics at the departments of Plant Sciences and Chemistry. I would like to thank them for their kindness.

I am deeply grateful to my supervisors, Prof. John MacKay and Prof. Emily Flashman, for their patience, trust and guidance.

I would like to thank all MacKay lab members, past and present, for providing help anytime it was needed. Thanks to Dr. Cyril Vanghelder and Dr. Dapeng Wang for guiding me in my first steps in bioinformatics and giving me access to the conifer transcriptomes used in this thesis. Thanks, in particular to Henry, Laura, Barley Rose, Hayley and Heather for spending hours in a hot greenhouse with me and for their contribution to solve statistics and bioinformatic issues. Thanks to Rebecca Latter, Dona Gunawardana and Anna Dirr for giving me access to their laboratory and for their help with protein work.

Thanks to Henry, Tatiana, Razia and Tom, for the amazing time spent together in Oxford since the beginning of this journey and their unconditional friendship.

Thanks to Deniz, who brought some reason where it was needed, and to Jacopo for his lovely criticism. Thanks to Andrew, for his good heart. Friendship has no national borders.

Thanks to Domenico, Fulvio, Gabriele (Piro), Luigi, Marco C., Marco M., Marina and Riccardo. You have seen it all.

And thanks to my family for always being there for me. This thesis is the fruit of your hard work too.

Finally, this work is dedicated to my loved ones who passed before seeing it complete. They are deeply missed.

List of figures

General introduction

Chapter 1

Supplementary figure 1. MWP progression during experimental drought.

Supplementary figure 2. Curvilinear and linear relationships between MWP and SWC. Red line: Linear regression model of MWP against % volumetric SWC. Black dashed line: second order polynomial regression. R^2, P-values and slope for the ordinary linear model are shown.

Supplementary figure 3. MAFFT multiple sequence alignment (MSA) of putative and model NCED protein sequences.

Supplementary figure 4. MAFFT MSA of putative and model ABA1 protein sequences.

Supplementary figure 5. MAFFT MSA of putative and model AAO protein sequences.

Supplementary figure 6. MAFFT MSA of putative and model CYP707A protein sequences

Supplementary figure 7. ABA peak as detected by Liquid Chromatography-Mass Spectrometry (LC-MS) and standard curve.

Chapter 2

Figure 1. Detail of the CCD/NCED catalytic centre.

Figure 2. Zea mays (Z. mays) VIVIPAROUS 14 (VP14) 3D structure.

Figure 3. MEME (Multiple Em for Motif Elicitation) results.

Figure 4. MSA showing structural features based on reference sequence of Z. mays VP14. Target region comprising residues between position 214 and 265.

Figure 5. MSA showing structural features based on reference sequence of Z. mays VP14. Target region comprising residues between position 300 and 400.

Figure 6. MSA showing structural features based on reference sequence of Z. mays VP14. Target region comprising residues between position 478 and 502.

Figure 7. Protein-membrane interaction simulations for putative conifer NCED structures.

Figure 8. Ligand docking simulation run by Swiss-dock web server and visualised on CHIMERA viewdock tool.

Figure 9. Coomassie-stained SDS-page gel (sodium dodecyl sulfate–polyacrylamide gel electrophoresis), showing expressed recombinant protein segregation between extraction pellet and

lysate and His-stained version of the same SDS page gel, confirming the presence of an His-tagged protein.

Figure 10. Coomassie-stained SDS-page gel, showing recombinant His-MBP-PsNCED1 (Histidine-Maltose Biding Protein-Picea sitchensis NCED1) and control His-MBP tag extraction and purification steps.

Supplementary figure 1. MAFFT multiple sequence alignment (MSA) of putative and model NCED and CAROTENOID CLEAVAGE DIOXYGENASES (CCD) protein sequences.

Supplementary figure 2. MSA showing structural features based on reference sequence of Z. mays VP14. Target region comprising residues between position 499 and 503.

Supplementary figure 3. Reference ZmVP14 known crystal structure and putative conifer NCED structures predicted by AlphaFold2 colab ab initio algorithm.

Supplementary figure 4. ProSa web server model local quality estimates.

Supplementary figure 5. ProSa web server model global quality estimates.

Supplementary figure 6. Ligand docking simulation based on modelling by Swiss-dock web server and visualised on CHIMERA viewdock tool.

Supplementary figure 7. Structure quality summary of PsNCED1 as returned by SwissModel web server.

Chapter 3

Figure 1. A: Time course of experimental Photosynthetic Active Radiation (PAR), Air Temperature and Air Relative Humidity, measured daily at morning by greenhouse sensors.

Figure 2. Time course of volumetric SWC, MWP, stomatal conductance to H_2O (g_s) and leaf transpiration (E), for Picea sitchensis (P. sitchensis) and Picea lutzii (P. lutzii) hybrids upon drought treatment.

Figure 3. Time course of net photosynthetic carbon assimilation (A), substomatal CO_2 (C_i), intrinsic water use efficiency (WUE_i) and instantaneous water use efficiency (WUE_{ins}), for P. sitchensis and P. lutzii hybrids upon drought treatment.

Figure 4. Correlation matrix based on Spearman's correlation test for relationships between physiological responses following drought treatment in P. lutzii hybrids.

Figure 5. Correlation matrix based on Spearman's correlation test for relationships between physiological responses following drought treatment in P. sitchensis.

Figure 6. Principal component analysis (PCA) of water status and photosynthesis parameters. All samples and families pooled together.

Figure 7. Relationship between SWC and MWP, g_s and E and net A for P. lutzii and P. sitchensis upon drought treatment.

*Figure 8. Relationship between (**A**) net A and stomatal conductance to H_2O (g_s), (**B**) net A and C_i and (C) stomatal conductance to H_2O (g_s) and substomatal CO_2 concentration (C_i) in P. sitchensis and P. lutzii subjected to drought treatment and recovery.*

Supplementary figure 1. Differences in stem diameter of P. sitchensis (Ps111-118) and P. lutzii (Pl700-703) at 2 and 30 days since the onset of drought, compared by Student's t-test.
Supplementary figure 2. Differences in stem height of P. sitchensis (Ps111-118) and P. lutzii (Pl700-703) at 2 and 30 days since the onset of drought, compared by Student's t-test.

*Supplementary figure 3. (**A**) Relationship between WUE_i and g_s and (**B**) WUE_i and C_i in P. lutzii and P. sitchensis subjected to drought treatment and recovery.*

*Supplementary figure 4. (**A**) Relationship between WUE_{ins} and g_s and (**B**) WUE_{ins} and C_i in P. lutzii and P. sitchensis subjected to drought treatment and recovery.*

List of tables

Chapter 1

Chapter 2

Supplementary table 1. TargetP – 2.0 output table.

Chapter 3

Table 1. Provenance and type of material of the full-sibling families of Sitka and P. lutzii used in this experiment.

Table 2. Summary of non-parametric analysis of variance of P. lutzii and P. sitchensis water status and photosynthesis parameters.

Table 3. Summary of non-parametric analysis of variance and post hoc multiple comparisons by Student's t-test of P. lutzii and P. sitchensis water status and photosynthesis parameters.

Table 4. Summary of analysis of variance of P. lutzii and P. sitchensis light response curve parameters.

Table 5. Summary of analysis of variance and post hoc multiple comparisons by Tukey test of P. lutzii light response curve parameters.

Table 6. Summary of analysis of variance and post hoc multiple comparisons by Tukey test of P. sitchensis light response curve parameters.

Supplementary table 1. Summary of analysis of variance of P. lutzii and P. sitchensis growth parameters.

Statement of authorship

This thesis is the product of the work carried out by the author, Gabriele Rizzuto, with contributions by:

Dapeng Wang (PhD, Senior Bioinformatician in Integrative Analysis, University of Oxford, The Wellcome Centre for Human Genetics) for the assembly of conifer transcriptomes;

Lisa Folkes (formerly Senior Bioanalysis Scientist, Oxford Institute for Radiation Oncology, Department of Oncology) for the HPLC-MS quantitative analysis of abscisic acid samples collected during experimental procedures of Chapter 1;

Rebecca Latter (D.Phil. student, University of Oxford, Department of Chemistry) for the LC-MS quantitative analysis of *Ps*NCED1 in vitro assays of Chapter 2;

Dona Gunawardana (PhD, University of Oxford, Department of Chemistry) for her guidance in protein SDS gel production and staining.

MacKay lab members, and in particular: Dr. Tin Hang "Henry" Hung (PhD), Laura Guillardin Calvo (D.Phil. student), Barley Rose Collier Harris (D.Phil. student) and Oliver Spacey (Graduate student) for sample collection and midday xylem water potential and anatomical measurements of Chapter 3.

General abstract

This work seeks to contribute to our understanding of conifer tree responses to drought. Research in this field has historically privileged the study of the changing anatomy, physiology, and metabolism of trees under adverse environmental conditions. The main reason for this lies in the size and complexity of conifer genomes, which posed limitations to genetic studies in this important plant group. Recently, fast-evolving sequencing technologies have unlocked conifer "mega-genomes" and made a considerable number of genetic resources available for researchers. Here, we investigate the genetic mechanisms governing the responses to soil water deficit of diverse conifer species, that are relevant to the UK forestry market but are faced with human-made climate change. We explored how dynamic expression of key genes involved in abscisic acid (ABA) biosynthesis and catabolism may relate to the *isohydry* paradigm. Several frameworks have been proposed, that include a range of traits and definitions to explain diverging water regulation responses falling along the isohydric spectrum. We developed new evidence for the role of selected candidate genes, in particular 9-*cis*-epoxycarotenoid dioxygenases (*NCEDs*), based on their expression in conifer species with contrasting responses. These may be the master regulators of contrasting ABA accumulation profiles in conifer foliage. We also characterised genes encoding putative NCEDs in detail, comparing three key conifer species and model angiosperms, through *in silico* analyses, and produced a recombinant protein from *P. sitchensis* (PsNCED1) to enable functional characterisation *in vitro*. We found a high degree of 1D-3D sequence conservation, indicating that conifers may have evolved a rate limiting step for ABA biosynthesis. This information forms a basis for new gene functional studies on conifers, which is important in the context of newly developing forest management programs. Finally, we studied *P. sitchensis* and its natural hybrid with *P. glauca*, *P. lutzii*. *P. sitchensis* is widely exploited in the UK timber market and represents a large portion of planted forests. We selected an array of cultivars, including hybrids, and tested their phenotypic variability in relation to drought stress. Although similarly conservative, cultivars deployed variable drought responses that differed in their use of water. Exploring drought adaptability by use of hybrids is one approach for developing resilient forests, which will be of interest to tree breeders looking for alternative planting materials. We believe that this work will contribute to bridge the gap between phenotypic and genomic studies in conifers and will help establish better breeding practices.

General introduction

This thesis will explore the molecular bases of diverging drought responses in conifer species of interest for the UK forestry sector. Conifers adapted to dry environments by the means of contrasting strategies of water status regulation, characterized as conservative and risk-taking species, respectively [1,2]. They did this by evolving a dual system of hydraulic and metabolic traits, including stomatal control of xylem water potential through abscisic acid (ABA) accumulation in the leaf [1,2]. Fine-tuning of ABA biosynthesis and catabolism is required to produce species-specific accumulation profiles that characterise conservative and risk-taking types [3]. We set out to investigate genes and proteins hypothesized to contribute to the distinct behaviours observed across conifer clades that nowadays are faced with climate change. Droughts represent one of the greatest threats to crops and forests around the world [4]. It is crucial to understand how diverse plant species and types will respond to such global change in the short to long term. Knowledge of plant physiology, anatomy, metabolism, and genetics is needed to preserve ecosystems and improve crop productivity in the face of climate change [4–6].

This work seeks to improve our understanding of the molecular mechanisms that control diverging conifer responses to drought, by integrating across disciplines and levels of diversity. Most of the research conducted on this topic falls in the field of eco-physiology, while genes and biochemical pathways in conifer species are understudied [3–5]. Here, we scan diverse taxa and investigate to what extent differential expression of key metabolic genes, such as the rate-limiting epoxycarotenoid dioxygenases (*NCEDs*), may vary in relationship to characteristic ABA accumulation profiles that have been linked to the isohydry paradigm. We then attempt to characterise a clear drought responsive NCED protein from *Picea sitchensis (P. sitchensis)* by using *in silico* and *in vitro* studies. Finally, we focussed on phenotypic variability among breeding families *P. sitchensis* and its hybrid with *Picea glauca* - *Picea lutzii*, to assess the potential for selecting forest reproductive materials with a higher level of drought tolerance. We believe that this work will contribute to bridging the gap between phenotypic and molecular studies in conifer species relevant to the forestry sector and will help establish better breeding practices for a more sustainable future.

This chapter will introduce the reader to the diverse – and sometimes imbalanced – fields of research and key findings of the last two decades concerning plant responses to water stress, with a particular focus on conifers. First, drought events will be defined and their impact on forest survival across the globe will be described. Then, the physiological and metabolic mechanisms by which plants cope

with drought will be illustrated, dissecting the cellular pathways involved and their evolution in land plants. Finally, a summary of present and future solutions for sustainable forestry in a fast-changing world is presented.

Trees in a dry world

Climate change

Future climate forecasts

Yearly reports of the IPCC (Intergovernmental Panel on Climate Change) highlight the urgency to curb human-made carbon emissions to mitigate global warming. Climate models predict that temperatures will reach 1.5 °C above pre-industrial levels between 2030 and 2052 with high confidence, with long-lasting effects on ecosystems, human health and well-being and socio-economic structures if anthropogenic pollution does not drastically decrease [7]. Global and regional climate change patterns may vary, and their effects are difficult to predict, given the possible feedbacks involving different factors other than global mean temperature [8,9]. Ultimately, temperatures seem to rise even faster than expected and could reach higher than 2 °C above pre-industrial levels due to reinforcing feedbacks and cascading effects [10–12].

Tipping elements and tipping points

In this catastrophic domino effect, tipping elements play a fundamental role. These are macro-components of the Earth system that interact and stabilise each other in what we know as recurrent climatic phenomena, biomes, and oceanic streams [13–15]. The list of tipping elements has been growing in the last two decades, but all of them have one feature in common: a tipping point [13]. Climate tipping points (CTPs) are critical thresholds that define the capacitance of tipping elements to endure applied stress. Once a tipping point is exceeded, the corresponding tipping element will face a qualitative change that becomes self-perpetuating and may affect other tipping elements and Earth functions, compromising the stability of the global climate system [11,15,16]. A clear example is the melting ice sheets of Greenland and West Antarctica. Arctic Sea-ice, the Greenland Ice Sheet (GIS) and the West Antarctic Ice Sheet (WAIS) are tipping elements that have received much attention in recent years and are the most vulnerable, with existing evidence pointing at an early breaking of their tipping

points [7,11,13]. In fact, recent modelling efforts have predicted that GIS and WAIS are most of the times initiators of tipping cascades [16] that affect downstream elements.

Extreme climate events

While the effects of global warming will likely require centuries to unfold completely, we can already observe some early signs, the most obvious being extreme climate events (ECEs). Smith defines ECEs as "an episode or occurrence in which a statistically rare or unusual climatic period alters ecosystem structure and/or function well outside the bounds of what is considered typical or normal variability" [17]. There is mounting evidence that extreme events are becoming more frequent, and they are oftentimes driven by global warming [18–26], including heatwaves, fires, storms, frost, and drought. All of these happen outside what is accepted as the common experience of seasonal weather variability and will impact ecosystems and human activities on the short term to an extent that is difficult to predict entirely [20–26]. The most common ECEs – and most recognisable signature of climate change - are heatwaves and droughts. A seminal paper by Meehl and Tebaldi predicted increasing long-lasting heatwaves across Europe and North America, because of anthropogenic pollution [27]. Indeed, compound drought and heatwave (CDHW) events have increased in 5 continents out of 6, and especially in the Northern Hemisphere [28], with some of the hottest years on record occurring in the last two decades. Hot summers such that of 2003 in Europe will become more frequent [29]. The excessive and prolonged heat (4 °C above the mean), a long-lasting drought, higher solar irradiance, and low humidity [30] resulted in 70,000 excess deaths [31] and unprecedented losses in primary productivity and crop yields [32]. The summer of 2010 was the hottest ever recorded in Russia: heat, wildfires and smoke caused 56,000 deaths, forest industry losses estimated at US$ 330M and agricultural losses for US$ 1.4bn [33]. Increased frequency of droughts and heatwaves has been observed in India [34], China [35], United States [36], Brazil [37] and Europe [38].

Drought definitions and indexes

Drought stands out as an important component of ecological stability, extreme events affecting forest ecosystem primary production [39–41] and altering the terrestrial carbon cycle [42,43] under the drive of global warming in the 21st century [44]. Research on drought has been ongoing for over a century [45] and yet there is no agreement on a univocal definition of this phenomenon [46–48]. Many different indices have been produced to describe drought events in terms of their duration, severity, and intensity [49–51]. Drought indices can be divided in two general groups: those that measure the supply of moisture from precipitation only, and those that use a combination of diverse meteorological elements,

evapotranspiration, and reservoirs [48,52]. It is also possible to classify droughts in four categories [52]. Meteorological drought happens because of a precipitation deficit that lasts for a few weeks. Hydrological drought occurs when water reservoirs, either on the surface or subsurface, are exhausted. Agricultural droughts refer to drying soil and crop die-off and depend on factors that drive meteorological and hydrological droughts in combination with biological features of the plants and physico-chemical features of the soil. Finally, socio-economic drought happens when shortage in water resources affects the supply of other economic goods [52]. A recent review by AghaKouchak and collaborators has coined a new category of drought, the anthropogenic drought [53]. This definition considers drought as a multidimensional process made of natural and human-induced changes and feedbacks, impacting land water resources. Finally, time and space must also be accounted for when approaching to study the drought phenomena. Most drought events are localised at the regional level but depending on land-atmosphere feedbacks they can travel several hundreds of kilometres across continents and possibly reach critical intensity and duration thresholds that make them extreme [54]. It is important to consider the time scale of droughts, as well. Droughts are normally measured in years, a time scale that often applies in the context of regional events, or months, which are better suited to describe agricultural droughts [52].

Trees and drought

Reports of forest mortality across the globe

Regional to sub-continental scale drought events can lead to extensive damage to forest ecosystems by tree canopy die-off, depending on their intensity, duration, and interaction with compound events such as heatwaves [55–60]. Widespread drought-related mortality events have been recorded with increasing frequency in recent years in a variety of forest ecosystems [56] from arid regions [55,61], to temperate and central Europe [58,59,62,63] and boreal forests [64,65]. While drought is the main driver of forest die-back, there are some concurring factors that can eventually result in tree death. Hotter droughts, i.e., drought occurring with heatwaves, may induce faster tree death by increased atmospheric evaporative demand and accelerated soil dry-down [66]. The association between drought and biotic outbreaks (often bark beetles or pathogenic fungi) has been widely studied [67–71]. Drought-driven wildfires represent an additional - and increasingly frequent - disturbance affecting forest health, structure, and composition, from the wet Amazonian Forest [72] to Europe [73] and Borneo [74] and even in ecosystems that are naturally subject to periodical fire such as the boreal forest ecosystems of western North America [75]. Recent research highlights the intrinsic connection between increasing

drought and tree mortality, dating back as far as 1987 [57,58]. While the entire consequences of extensive and long-lasting changes in forest cover and composition are yet to be fully understood [76], it is possible to predict increasing vulnerability of forest ecosystems to pests, pathogens and wildfires, radical shift in nutrient use and carbon resources allocation patterns and drastic reductions in global gross primary production under current greenhouse gas emission scenarios [77,78].

Mechanism of tree mortality under drought

Rising temperatures will likely bring more intense droughts, even if not causing them directly [79], compounding the effect of water deficit on the physiology of woody plants by accelerating drying rates and eventually leading to widespread mortality events [80–82]. Forests occupy ~30% of earth's land surface, storing ~45% of terrestrial carbon, contributing ~50% of land net primary production and sustaining nutrient and hydrological cycles [83]. Moreover, forests uptake ~30% of human-made carbon emissions, representing an important terrestrial carbon sink [83,84]. It is therefore compelling to understand the mechanistic basis of tree mortality in response to climate change. However, this is not an easy task. Despite intense research in this field, the mechanisms of tree death are still debated. Ultimately, tree death under drought conditions is due to catastrophic failure of water and carbon transportation and the exhaustion of their pools inside the plant tissues, with consequent impairment of the plant defences against biotic attacks [4]. Several mechanistic models have been proposed to explain the complex interactions and feedbacks between physiological and metabolic processes that result in tree death, but these are based on different experimental conditions, hypotheses and methodologies and no unambiguous definition has been produced [85–88].

Water transport in the tree

The main determinant of woody-plant mortality is a critical threshold of tissue water content [89,90], beyond which cell membrane integrity is compromised and meristematic activity ceases [90,91]. The first step in the sequence of events that leads to this lethal threshold is a breakpoint in whole-plant water conductance, from roots to leaves. Plants transport water in the form of sap thanks to a negative pressure, defined as the difference of water potential between the atmosphere and the soil that creates a capillary suction force through the xylem conduits [92]. Water moves from the soil to the atmosphere, and plant tissues act as a conductor. Stomata – the pores on the leaf surfaces - function as regulators of this pulling force by opening and closing in response to the leaf water content [93]. Stomatal control of the plant water potential – interposed between that of the atmosphere and that of the soil - has evolved as a means of avoiding high negative pressures in the xylem that may lead to the formation

of emboli [94]. When water is scarce in the soil and the evaporative demand by the atmosphere remains high, the pulling force in the plant vessels may exceed water molecule cohesion and induce a change of phase from liquid to gas, producing air bubbles that can travel across and between conduits by air seeding, blocking their lumen [95–97]. If embolism spreads through the plant organs, catastrophic failure of the hydraulic system can happen and mark a crucial step towards death [4].

Hydraulic failure under drought

Differences in resistance to embolism have been observed between plant organs in the hydraulic system. These observations form the basis of the "hydraulic vulnerability segmentation hypothesis", according to which distal organs of woody plants are more vulnerable to embolism than the proximal ones [98,99]. Hydraulic conductance and stomatal control of water potential coordinate to keep the plant in an operative safety margin zone and prevent emboli formation [100–102]. Proximal, carbon rich, organs normally present a larger safety margin, allowing the tree to sacrifice distal, expendable, and easier to repair parts such as the leaves to drastically reduce transpiration and prevent catastrophic embolism in costly stems [99,100]. Roots may also suffer from early emboli formation, as they have been observed to operate with smaller safety margins compared to shoots [103,104], particularly smaller roots [105]. Root damage starts from fine roots. Unsuberised fine roots are the main entry point of water from the soil into woody-plant hydraulic systems [106] . Cortical cells of fine roots suffer mechanical damage early during mild drought stress, limiting root hydraulic conductivity and decoupling roots from the soil to allow preservation of water pools in the canopy [107,108]. Increasing drought stress may eventually induce root shrinkage and emboli formation in the xylem of fine roots and later coarse roots [107]. Roots make up 81% of the total plant hydraulic resistance under normal conditions, but this contribution increases up to 95% under moderate drought stress with cortical cell damage and root disconnection from the soil [108]. Reduced hydraulic conductance induces stomatal closure to limit canopy conductance and slow down water loss [99–101,108]. With safety measures such as root-soil decoupling and stomatal closure in place, trees would appear to achieve a certain degree of isolation and conserve their water pools [109]. Instead, trees continue to lose water by cuticular transpiration, stomatal leakiness and even through the bark [2,110–113]. Trees can further contrast increasing xylem tension by adjusting deep root water uptake through aquaporins according to canopy evaporative demand [114], reversibly collapsing minor leaf veins to protect major conduits from embolism [115] and realising water from cellular stores [116]. As drought progresses, xylem tension will eventually induce formation of emboli that can spread through vessels and lead to systemic hydraulic failure and consequent tree death if critical thresholds are passed, hampering recovery [117,118].

Carbon economy under drought

Stomata are the entry point of CO_2 inside the leaf. Hence, drought will affect photosynthesis either transiently by diffusive limitation imposed by stomatal closure [119–122] or, if drought is long enough for compounding factors to intervene, by permanent metabolic damage to the photosynthetic apparatus inside the chloroplast [121,123–125]. It has been postulated that prolonged drought and photosynthesis impairment may eventually lead to whole-tree carbon imbalance and death by carbon starvation [86]. According to this hypothesis, trees can die because of exhaustion of carbon resources, mainly in the form of non-structural carbohydrates (NSC – sugars deriving from starch mobilisation) and the inability to maintain metabolic, defence and transport processes dependent on carbon pools in the long term [86,126]. Although this hypothesis lacks conclusive supporting evidence and the phenomena may vary between individuals [127–129], carbon starvation could be a concurring cause of tree mortality together with hydraulic dysfunction [87,88,130,131]. Ultimately, as may be expected, hydraulic failure and NSC depletion are interdependent. NSCs seem to improve drought resistance and resilience, promoting higher xylem water potential, refilling of cavitated vessels and osmoregulation [132,133]. On the other hand, failure in water transport during drought stress can affect nutrient and carbon transport to sink tissues through phloem collapse and increased phloem sap viscosity [126,134–137] and the concomitant use of this resource for growth, defences, osmoregulation and embolised xylem refilling can initiate self-reinforcing feedbacks, that will lead to tree death [87,88,126]. Finally, roots may be more sensitive to carbon starvation than shoots, as they benefit from carbon supply only after crown tissues [138] and NSC falling below a critical threshold of 5-6% could compromise root structural integrity [139]. Interestingly, roots are the first carbon sink to be restored once drought is released [140], demonstrating their importance in accessing newly available soil water. Overall, tree survival under drought depends on whether carbon offer meets demand from different organs and tissues [4].

Biotic factors of tree mortality

Drought stress and biotic stressors interact, often leading to widespread infestation and regional scale outbreaks that are either the primary, the concurring cause or the consequence of forest mortality [67,141–144]. Reduced water availability will affect tree defences against attacks by insects [71,145–149] and fungal pathogens [67,150–152]. In fact, tree defences against biotic aggressors rely on both water and carbon resources, feeding back on their respective pools once they are mobilised and hence influencing the whole-plant carbon and water balance [4]. Defence compounds are secondary metabolites (hence, not involved in growth and reproduction) such as resin and terpenes, that are

carbon rich, and their production and efficacy depend in the first place on nutrient availability, transport, and allocation [153,154]. Reduction of photosynthetic rate during drought stress, in combination with steady-state leaf respiration, can limit photosynthate availability for export and phloem loading, hampering the capacity to osmotically draw water from the xylem [155–157]. At the same time, impaired xylem hydraulic conductivity due to high tension or embolism will limit water exchange with phloem vessels [137,158,159]. Increasing phloem viscosity slows down sugar translocation across the plant and carbon resource allocation to tissues and biological functions [137,155,156,158–160]. Drought stress can also affect phloem vessel number and diameter [156,159,161] or induce turgor collapse [135], with reduced overall conductance capacity. Reduced carbohydrate availability and/or translocation will limit defence compound production, alter the phloem sap chemical profile, and decrease tree resistance against pathogens [149,162–168]. Moreover, infestations deflect carbon resource allocation from growth, development, and reproduction functions in favour of resin and secondary metabolites, leading in the long term to starch reserve exhaustion, possible organ starvation and an inability to maintain cell turgor [164–168]. Biotic aggressors directly damage tree tissues, by chewing or occluding xylem vessels and stomata, disrupting water uptake and transport and reducing transpiration [169–171]. Thus, biotic attacks compound the adverse effect of drought in self-reinforcing feedback that increases the chances of leading a tree to death [164,172,173].

Forest adaptation to drought

Means of adaptation

Climate change is likely to cause significant shifts in forest ecosystem structure, composition and extent as trees succumb to unfavourable conditions or migrate towards favourable ones [174–180]. Phenotypic traits have been widely studied in response to changing environmental conditions and have been used to model changes in forest cover and composition, but modelling efforts lack the contribution of the genetic information underlying quantitative traits [5,181]. Phenotypic responses to climate change can be the product of plasticity or evolution, or both, but their adaptive power is unclear [182]. Plant species have been documented to migrate towards higher elevations [177,179,180,183], higher latitudes [179,184] or sometimes southwards [184] as local conditions change, and a mismatch develops between adaptation and new conditions. Dispersal as a means of tracking favourable environmental conditions may not be sufficient, as strong selection pressures can interrupt gene flow, especially under fast changing climate [185–189] and plant species may have to rely on genetic diversity,

phenotypic plasticity, fast recruitment, and shorter generation times to adapt to new conditions and persist in their current range [186–195].

Genes and phenotype variation

Both genetic and phenotypic variation, and their interactions, shape the adaptation capacity of tree species to environmental conditions and will determine whether species will persist or migrate, but research is still needed to identify key signatures [5,196]. Genetic investigations on association between genes and phenotypic traits involved in local adaptation are complicated by the polygenic nature of forest tree phenotypic traits and genome size, especially in the case of conifer mega-genomes [5,197–202]. The study of the genetic mechanisms underlying phenotypic variation is complicated by the fact that natural selection at a given location operates on many genes, often with epistatic interactions, that have small individual effects on adaptive phenotypic traits, producing weak signals of polygenic local adaptation and making it difficult to identify relevant traits and related allelic markers [181,199,201–203]. Ultimately, existing standing variation within and between species populations will favour adaptation to rapidly changing local conditions and species with large continuous cover will likely have more chances of survival compared to those with fragmented distribution, as they will benefit from improved gene flow, high genetic diversity due to clinal variation and rapid fixation of allelic variants [181,190,191], but only if harbouring enough fecundity and heritability. If forests lag behind fast climate change, they will become maladapted and lose fitness with patterns dependent on species and local population genetic diversity and phenotypic plasticity at a particular site, resulting in geographical and functional shifts [188,204–207].

Conifer ecosystems

Dynamic range shifts in response to climate change are part of the evolutionary history of forest species, but conifers have experienced the most dramatic changes, facing several extinction events during the Cenozoic and Quaternary era that contributed to angiosperms becoming dominant in many modern ecosystems [208–213]. Conifer species distribution across the Northern and Southern hemisphere are the result of processes of extirpation, migration to track climatic optima or adaptive shift and persistence in climatic refugia during global glacial and interglacial periods [209,212,213]. Considering their evolutionary history, it is not surprising that conifers are nowadays among the most threatened and vulnerable species in the world, facing important range contractions and species composition shifts in the face of global warming [192,214–219]. Coniferous forests may become particularly maladapted to future climate scenarios, incurring into reductions of growth, productivity and diversity in response

to climate-related disturbances, compared to broadleaf and mixed forests [206,215,220–227]. The risk of maladaptation for conifer populations depends on genetic pools [202], which may not harbour large diversity for some conifers [228,229] but also on trait-climate associations and species responsiveness to changing conditions. Species or populations with weak trait-climate association and low intraspecific differentiation may be generalist enough to quickly adapt to new conditions and outcompete those with strong trait-climate associations, that are extremely specialised in occupying a restricted step in a cline [205,206,230,231]. Boreal conifer populations, growing at the northern edge of species distribution ranges, are at greater risk as they show higher sensitivity to climate variables such as increasing temperature and water availability, compared to southern ones [206,220,224,226,231].

Conifer research

Conifers dominate several ecosystems, especially in the Northern hemisphere, support biodiversity, represent large carbon sinks, participate in carbon, water and nutrient cycles, and provide ecosystem services. It is therefore crucial to explore and understand key functional traits associated with growth but also photosynthesis, hydraulic function, leaf traits and gas exchange, that may contribute to forest tree adaptation to future climate scenarios, and their link with genetic variation in relation to the environment, between and within species [5,196,200,202,232–235]. There is a need to integrate approaches and methodologies coming from different disciplines that can complement findings in the fields of genetics, genomics and plant physiology and anatomy. While genome-wide association studies can tell us much about the evolutionary capability of trees, gene expression and transcriptome analyses can provide insights into plasticity and rapid responses to environmental change with adaptive power, but knowledge of the traits involved in plant resistance and resilience is needed [5,6,196].

Tree functional traits under drought

Functional traits and mechanistic frameworks

Tree functional traits provide useful metrics for assessing single species and plant communities' capacity to withstand stress in their habitats, and therefore must be included in vegetation models considering climate change [132,236]. Despite much uncertainty around which set of traits to include in these models (e.g., anatomical, morphological, or physiological), traits associated with hydraulic function are particularly important in forest mortality forecasts as they are universally linked to drought-related tree death, posing critical thresholds for tree survival under limiting water conditions

[237–240]. Stomatal control of transpiration to avoid cavitation-inducing pressures in the hydraulic system has been widely investigated and recognised as a key trait for tree survival under drought [237,241–243]. Hydraulic frameworks accounting for plant water status, stomatal regulation of transpiration, water conductivity and their operative safety margins have been developed to explain the mechanisms of differential tree responses to drought [238,242,244–247]. One such framework has attempted to reduce the diversity - and complexity - of plant hydraulic responses to drought by grouping them into two opposite types, isohydric and anisohydric ones, based on sensitivity of regulation of leaf water potential [244,248].

The iso/anisohydry paradigm

First developed to describe daily fluctuations in plant water status [248], the iso/anisohydric dichotomy was later applied to the study of plant responses to soil water deficit on longer timescales [86,243–245,249]. Within this framework, plants that maintain a relatively stable leaf water potential are isohydric, whereas those that allow their leaf water potential to drop during drought are anisohydric [244,248,249]. Owing to its simplicity, this model has been widely used to investigate plant hydraulic strategies, not without criticism concerning its reduction of diversity to a dual contrast that does not fully apply to a real-world scenario, made of environmental clines and rich plant communities [249–254]. A step forward in the use of this concept was the recognition that plant species (and sometimes cultivars) move along a continuum of isohydric to anisohydric responses, and that the dichotomy previously proposed only applies to its extremes [244,245,249]. Different metrics of isohydry have been proposed, trying to quantify the stringency of regulation of plant water homeostasis. The first and widely used metric was the slope value of the regression line between plant and soil water potential [244], where values from 0 to 1 indicate transition from isohydric to anisohydric behaviour, respectively. Stomatal control over water potential was soon adopted as a proxy of sensitivity to water deficit, with plants being classified as iso or anisohydric according to the stringency of control of water potential through stomatal closure. Klein and collaborators [249] proposed a system of classification based on the sensitivity of g_s to changes in midday leaf water potential, where plants with a tighter stomatal control over water potential were isohydric, compared with less control in anisohydric plants. Eventually, it was found that leaf water potential regulation is not necessarily associated with the degree of stomatal sensitivity [250], because of the complexity of the soil-plant continuum, where the difference in water potential depends also on xylem conductivity, timing of stomatal closure and changing soil water potential. From this point of view, contrasting regulation of leaf water potential does not necessarily explain differential predisposition to death under drought. One step in this direction was taken by Skelton and collaborators [245], who proposed an integrated system incorporating stomatal regulation of water

potential and xylem vulnerability that allowed direct predictions of plant mortality under drought in biodiverse communities. Finally, the only classification system that may hold despite variation in site-specific water availability is based on the calculation of the area between the 1:1 line and the regression line of midday leaf water potential versus predawn leaf water potential, defined as hydroscape [246].

Why still use iso/anisohydry classification?

To date, no agreement has been reached on an unambiguous definition of what seems to be a system of coevolved and coordinated traits, rather than a discrete plant trait [242,249–253,255,256]. The sources of variability may be too many for a species or cultivar to be described unequivocally as iso or anisohydric, making drought-related mortality predictions inconsistent across studies [250,252]. Therefore, when approaching the study of iso/anisohydric responses, it is important to acknowledge which environmental conditions are being considered and which definition and metrics are being used [253]. Despite its caveats, the iso/anisohydric framework can still provide useful insights into plant responses to drought, especially if used to compare coexisting species [245,257–262] and complemented by evidence coming from other fields, such as genetics [263–267]. The iso/anisohydric contrast has also been employed to assess ecosystem responses and vulnerability to drought in tree mortality studies, also within the mechanistic framework of the hydraulic failure and carbon starvation hypotheses [86,88,141,259,268,269], although species predisposition to mortality may not vary linearly across the isohydric continuum, with only extreme types suffering highest death rates during extreme events [270]. The inclusion of the iso/anisohydric concept in such studies derives from the obvious implications of differential control of stomatal closure as a means of water use regulation and its systemic link to hydraulic function and xylem vulnerability to embolism, possibly acting on both hydraulic failure and carbon starvation [86]. It is not surprising to find variation in multiple plant traits associated with the discrimination between iso/anisohydric types. Anisohydric trees have been found to be less vulnerable to xylem embolism, withstanding very low water potentials, compared to isohydric ones [245,249,269]. Significant differences exist also in photosynthesis regulation, with anisohydric trees adopting faster stomatal opening, activation of photosynthesis, showing greater phososynthetic capacity and lower water use efficiency [246,269]. Anisohydric trees may also hold higher osmoregulation capacity through non-structural carbohydrates (NSC) mobilisation, needed to maintain efficient osmoregulation at low water potentials [257,258,271]. Finally, isohydric behaviour appears to be controlled by high ABA levels in the foliage, inducing tight stomatal closure, whereas anisohydric behaviour would rely on a transient increase in hormone levels followed by water potential-driven loose stomatal closure [1,2,271].

Abscisic acid

ABA and drought

The role of ABA in controlling iso/anisohydric responses to water deficit was first recognised by Tardieu and Simonneau [248]. Later work confirmed how different strategies relate to differences in stomatal sensitivity to this hormone as well as variation in ABA-related gene expression [1,263,265,267,271]. Research on ABA dates to the mid 1900s. Early work in the 1940s identified a molecule involved in bud dormancy [272,273]. The same molecule was later found to be involved in both growth inhibition [274] and the abscission of the cotton fruit [275] and leaves under two different names, dormin and abscissin II [276], and was finally called ABA [277]. ABA was found to accumulate in water-stressed leaves and to control stomatal aperture [278–280]. Phenotyping and genetic studies on mutants of several model angiosperms revealed new functions and key metabolic steps for this plant hormone [281–285]. It was apparent that ABA controlled leaf water homeostasis in dry conditions [283,286–288], but was also involved in seed germination and plant growth [286,289–291] and development [292]. To date, ABA metabolism, functions and mechanisms of action have been extensively investigated. ABA is a C15 isoprenoid molecule that is synthesised in the 2-C-methyl-D-erythritol-4-phosphate (MEP) pathway through the cleavage of C40 carotenoid precursors [293], also called the "indirect pathway". This pathway is shared by photosynthetic organisms, but ABA is also synthesised through a "direct pathway", or mevalonate pathway, in some pathogenic fungi [294–299]. ABA has also been identified in animal tissues and even some prokaryotes [297,300], suggesting an ancestral origin as a universal growth regulator [301]. Genetic studies on viviparous mutants (VP) of *Zea mays (Z. mays)* have been crucial in dissecting the biosynthetic pathway of ABA in land plants. In these mutants, the transition between the embryo and post-embryo stage is unregulated, resulting in the early germination of seeds into seedlings attached to the maternal plant. It was discovered that several *vp* mutants of maize are insensitive to ABA-mediated inhibition because of the disruption of a variety of biosynthesis and signalling mechanisms, resulting in precocious germination and associated characters such as albinism and necrosis [284,302–306]. Research on the mechanisms of ABA deficiency in angiosperms greatly advanced thanks to studies on the model plant *Arabidopsis thaliana (A. thaliana)*, so that in the last 30 years the metabolic and signalling pathways have been widely uncovered (reviewed by [307–309]).

ABA biosynthesis

ABA synthesis begins inside the plastid with the epoxidation of zeaxanthin to all-trans-violaxanthin by the zeaxanthin epoxidase (ZEP) enzyme, discovered with mutational studies in *Nicotiana plumbaginifolia* [310] and isolated in *A. thaliana* loss-of-function *aba1* mutants [285,311–313]. Subsequently, all-trans-violaxanthin needs to be isomerised to 9-cis-violaxanthin and 9-cis-neoxanthin by the combined action of AtABA4 [314] and NXD1 [315]. The next step is the key rate-limiting reaction, which is considered the bottleneck of the pathway [316,317]. Nine-*cis*-epoxycarotenoid dioxygenases (NCEDs) catalyse the cleavage of neoxanthin and violaxanthin to yield a C15 product called xanthoxin [318–320]. This activity was first observed in maize *vp14* mutants and later several other *nced* mutants have been found in maize, *A. thaliana*, tomato, avocado and other plant species [316–318,321–323], making *NCEDs* a well-studied, multi-gene family, showing functional redundancy [323–326]. The next steps in the pathway occur in the cytosol, where xanthoxin is converted to an intermediate abscisic aldehyde molecule by ABA2, a short-chain alcohol dehydrogenase [327,328]. Finally, the abscisic aldehyde is oxidised to ABA by an abscisic aldehyde oxidase (AAO), first identified through genetic screening of *flacca* and *sitiens* mutants of tomato [281] and later characterised as AAO3 in *A. thaliana* [329]. This reaction requires a molybdenum cofactor (MoCo), which is biosynthesised by the AtABA3 Molybdenum Cofactor Sulfurase in *A. thaliana* [313,330].

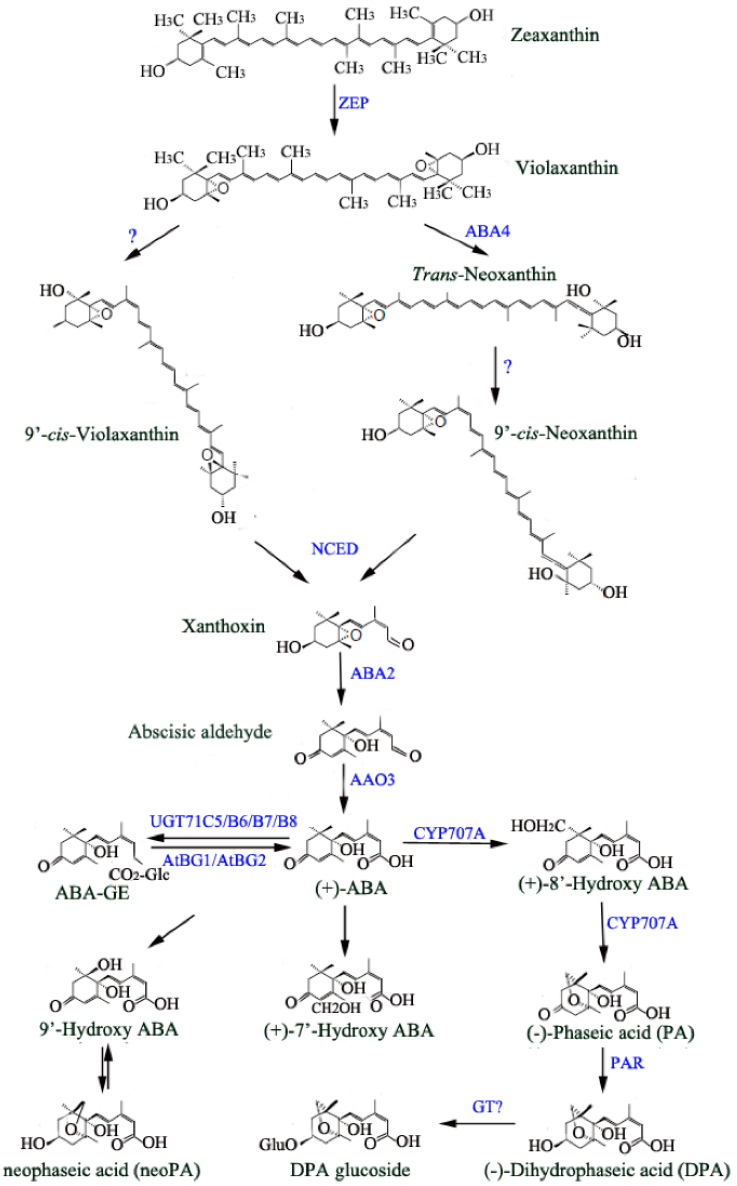

Figure 1. ABA biosynthesis pathway. Enzymes that catalyse each step are shown in blue. Image from Ma and collaborators, 2018.

ABA catabolism

Once ABA has been synthetized, its signal is attenuated by either hydroxylation or conjugation. The latter is a catabolic reaction based on the rapid sequestration of ABA in the vacuole in its glycosylated and inactive form, ABA-glucose ester (ABA-GE) [331–334], which is catalysed by a UDP-glucosyltransferase (UGT) coded by AtUGT71C5 in *A. thaliana*. The converse reaction, the fast mobilisation of ABA from vacuole ABA-GE stores into its active form, is catalysed by β-glucosidases coded by AtBG1 and AtBG2 [331–333].

The main mechanism of ABA inactivation through catabolism is hydroxylation to phaseic acid (PA) by 8′-hydroxylases which are cytochrome P450 monooxygenases (P450s), encoded by the *CYP707As* multi-gene family in *A. thaliana* [335–338]. Within this gene family, *CYP707A3* has been identified as the best candidate for controlling ABA levels in the vascular bundle of the leaf [339,340]. Phaseic acid is then catabolised to dihydrophaseic acid (DPA) by a phaseic acid reductase (PAR) and further to 4′-O-β-D-glucoside (DPAG) by a glycosyltransferase (GT) [341–345].

ABA transport

A third mechanism of ABA removal is transport between cells and organs. ABA can diffuse through plasma membranes in its protonated form (ABAH) under weak acid conditions, but drought stress increases the apoplastic pH, reducing ABAH mobility [346,347]. Thus, active transport is required to translocate active pools of ABA. Transporters act in concert to export and import ABA in and out of cells and tissues and have been extensively reviewed [307,348,349]. ATP-BINDING CASSETTE transporters belonging to the G subfamily (ABCG) are among the best studied ABA transporters in *A. thaliana* and some other model angiosperms. AtABCG25 and AtABCG31 are important for stomata and embryo sensitivity to ABA, respectively. In fact, AtABCG25 exports ABA from cells around the vascular tissue to active sites inside guard cells [350–353]. Moreover, AtABCG25 coordinates with AtABCG31 in the export of ABA outside of the endosperm, to be imported by AtABCG30 and AtABCG40 inside the embryo [354,355]. An *A. thaliana* NITRATE TRANSPORTER 1/PEPTIDE TRANSPORTER FAMILY (NPF), AtNPF4.6, previously identified as a low-affinity nitrate transporter on the plasma membrane, seems to have high affinity for ABA and functions as an importer, contributing to regulation of hormone homeostasis within the vascular parenchyma cells and hence stomatal aperture [356]. Reverse genetic studies on a protein belonging to the MULTIDRUG AND TOXIN EFFLUX (MATE) transporter family, called AtDTX50, revealed that it could coordinate with AtABCG25 and AtNPF4.6 to export ABA when expressed in the vascular parenchyma but could also control efflux from guard cells and hence stomatal aperture [357].

ABA signalling core

Once ABA is imported into the guard cells, a battery of nine soluble intracellular PYRABACTIN RESISTANCE1/PYR1-LIKE/ REGULATORY COMPONENT OF ABA RECEPTOR (PYR/PYL/RCAR) is ready to bind it [358–362]. ABA activates PYR/PYL/RCAR receptors which start signal transduction by binding and inhibiting clade-A type-2C protein phosphatases (PP2Cs) so that

they can release multiple SUCROSE NONFERMENTING 1 (SNF1)-RELATED PROTEIN KINASE 2 (SnRK2s), which are kept inactive by PP2C-mediated dephosphorylation in the absence of ABA [358,359,361,363–366]. SnRK2s are then free to autophosphorylate or be phosphorylated by other kinases [367–370] and in turn phosphorylate downstream targets, such as transcription factors and ion channels such as the S-type anion channel SLAC1, allowing membrane depolarisation and hence guard cell deflation [371–376]. The same channels can also be activated by ABA through a Ca^{2+}-dependent pathway that relies on the aperture of calcium channels in the plasma membrane [377,378] and the creation of a pulse of Ca^{2+} ions that may stimulate phosphorylation of SLAC1 by calcium-dependent protein kinase [375,379]. The brief synthesis presented here shows what is known as the core signalling complex of ABA inside guard cells, but other components are involved and extensive crosstalk between this and other nodes forms a signalling network that is actively studied and has been reviewed elsewhere [307,308].

Evolution of the ABA metabolic pathway

While ABA has been detected in all land plants, the degree of conservation of its metabolic and signalling pathways as well as the nature of ABA-related stomatal movements in early diverging taxa are still debated [3,380–383]. ABA probably evolved in early land plants adapting to periodically dry environments as a means of promoting desiccation tolerance and possibly regulating sporulation in bryophytes [384–389], as well as sexual development and leaf morphology in ferns [390–392]. Evidence suggests that the ABA metabolic pathway may be at least partially conserved in non-vascular and seedless plants. Homologous sequences of *A. thaliana ZEP* and *NCED3* in moss *Syntrichia caninervis* were responsive to dehydration treatment in gene expression studies [393]. Mutational studies targeting ZEP in *Physcomitrium patens (P. patens)* produced an ABA-deficient phenotype [394]. Microarray analysis in *P. patens* identified *NCED* sequences that were differentially expressed in response to salt osmotic stress [395]. Phylogenetic reconstructions found orthologous sequences of *A. thaliana AAO3* in *P. patens* and *Selaginella moellendorffii (S. moellendorffii)* [396]. Exogenous ABA applications down-regulated *ZEP*, *NCED3*, *ABCG25* and *ABCG40* in fern *Polystichum proliferum* [381].

Evolution of the ABA signalling pathway

While the components of the core signalling pathway have been found in all representatives of land plants, their degree of functional conservation remains unclear. Bryophytes present homologs of the main genes involved in the ABA signal transduction in their genomes, including PYR/RCAR

receptors, PP2C phosphatases, SnRK2-OST1 kinases and SLAC1 channels [389,397–402], which may be involved in dehydration tolerance [389,397,401–403]. Further molecular studies show that a *P. patens* SLAC1 channel was activated by a SnRK-OST1 kinase in a *Xenopus* oocyte system [404]. Recent evidence suggests that stomata only open once in the sporophyte of modern bryophytes to allow for desiccation and release of spores [405,406] and may not be associated with photosynthetic regulation. Moreover, most physiological studies on bryophyte stomata have been based on high levels of exogenous ABA that elicit only small responses and do not match natural conditions [381,398,407–409]. There are few molecular studies in early vascular taxa lycophytes and ferns [381], but a recent report indicated no activation of SLAC1 channels by SnRK-OST1 in the lycophyte *S. moellendorffii* and fern *Ceratopteris richardii (C. richardii)* [392]. The same authors also showed that mutation of SnRK-OST1 in *C. richardiii* did not have any effect on stomatal behaviour, but it did impact spore dormancy and sexual determination in the gametophyte.

Stomata and ABA evolution

Previous work proved that the stomata of ferns and lycophytes do not respond to high endogenous ABA levels [410], in line with passive, water potential-driven, guard cell movements [411,412]. This adds to the line of evidence in favour of a gradual evolution of stomata and their active, ABA-dependent, regulation [408,411], although conclusive findings are lacking as systems and conditions change among studies [409,413]. According to this argument, stomata evolved as a means of desiccation tolerance passively regulated by environmental water fluctuations in non-vascular and seedless plants. They form metabolically controlled valves to regulate gas exchange in coordination with the hydraulic system of seed and flowering plants [3,414]. Gymnosperms are in an intermediate position, being the first land plant taxa to show clear active stomatal regulation [3,414]. Conifers respond to short-term changes in atmospheric water availability with passive movements of guard cells but accumulate high levels of ABA during drought [3,414]. Furthermore, species with highly embolism-resistant xylem still use passive stomatal closure and only synthesise ABA in the early stages of drought stress, while species with low embolism resistance display high sensitivity of stomata to ABA and tend to exponentially increase hormone foliage levels during drought [2]. Finally, angiosperms have lost the ancestral turgor-driven stomal closure and evolved a fast system of active regulation of guard cells movements that allows them to quickly respond to slight fluctuations in environmental water, light and CO_2 conditions, based on efficient SnRK-OST1 activation of SLAC1 channels [382,415–418] and fast *NCED* gene expression [417].

Tree breeding for safer forests

Improving the resilience of conifers to drought

Despite the wide array of genetic, genomic and phenotyping tools developed to study tree adaptation to abiotic and biotic stresses, tree improvement programmes that could benefit from their application are constrained by intrinsic limitations. The long generation times represent the most obvious constraint on breeding programs, with some trees taking up to 15 years to breed [235] and some selection traits measured on young trees possibly not matching mature tree characteristics at 50 years growth [235,419]. Another constraint is posed by the large size of most forest trees, making measurements difficult. Overall, field trials need to be large-scale and long-term, they are costly and represent an investment that may not pay off in terms of economic gains and ideal wood traits, in the case of commercial plantations.

Phenomics and genomics for tree breeding

The development of high-throughput phenomics technologies can aid the management and improve the efficiency of breeding programs, by simplifying time-consuming and subjective screening on the ground, enabling the scale-up of experiments and linking of genetic information with desired traits [420]. Remote sensing of chlorophyll fluorescence and hyperspectral imaging allow the detection of the early onset of biotic and abiotic stresses on large populations of trees [421–423]. Thermal image analysis has proven effective in monitoring the performance of several genotypes in large populations under field conditions and the early prediction of suitable growth traits in progeny trials [424,425]. Fast and cost-effective high-throughput DNA sequencing and genotyping technologies have produced a large amount of valuable information and resources in the form of genomes, transcriptomes, genetic maps and single nucleotide polymorphism (SNP) arrays, pushing traditional tree breeding into a new generation of genetic selection [5,235,426,427]. Breeders can now make use of detailed information on complex genetic traits and their causative effects on phenotypic traits, highly characterised gene families, genomic maps and different scaling of gene expression profiles [5,235,426,427]. This is particularly useful for conifers, which are understudied, harbour complex large genomes and are particularly slow growing [200,428,429].

Genomic selection

While marker-assisted selection (MAS) and Quantitative Trait Loci (QTL) allowed exploration of the association between genes with large effects on simple phenotypic traits, they had limited power when applied to multigenic traits in large, diversified populations, which result in complex inheritance patterns [430–432]. Genomic selection (GS) represents the most promising avenue of next-generation breeding programs [432]. This new approach is based on the detection of thousands of genome-wide genetic markers and characterisation of quantitative traits in a breeding population, which is used as a training set to estimate the simultaneous effect of each marker (QTL) on each phenotypic trait. The predictive model is then validated on a test population and can be further used to predict the genomic estimated breeding value (GEBV), or phenotypic value, of candidate uncharacterised individuals based on genotypic data [432]. GS is more efficient than standard MAS because it does not need previous knowledge of genetic architecture and its association with phenotypic traits, and it uses high-density genomic markers with small relative effects on traits of interest. GS is highly accurate [433,434] and speeds up the process of selection, eliminating the need of long field trials and shortening the breeding cycle, as it can be applied on young seedlings [432].

Alternative avenues of forest conservation

Forest genetics and next-generation tree breeding are promising approaches to improve individual species resistance and resilience to climate change. To date, most of the advances in forest research are based on studies on commercial tree species and managed plantations, rather than natural populations, for which traits of interest may be different in the face of increasing drought risk [4]. Thus, alternative ways of conserving or improving forest adaptive potential to climate change-driven disturbances must be considered for natural tree stands. A response can come from the implementation of ecosystem-specific silvicultural planning, aimed at maintaining the ecological and economical value of regional forests in the face of changing climate [435–437]. The applicability of such planning is still debated [438], but some efforts are being made to find the best framework for each changing scenario. These include conservation or restoration of genetic and species diversity in degraded landscapes, where they can promote resilience of ecosystem functions and plant health [435,439], or restoration of key-stone species by promoting generational turnover and recruitment and by assisted migration [437,440]. The translocation of populations and species to aid their range expansion and preserve them from extinction [441] is debated, for its ethical implications and its risk associated with ecosystem manipulation [57,442–444]. Nevertheless, with a cautious cost/benefit analysis, accurate choice of endangered species/population, target climate and site, science-based collection strategies, assisted

migration may be the most direct way of filling the gap between fast-changing climate and forest adaptation [57,441].

Project rationale

Conifers are typically understudied due to their size, long generation time, slow growth, and large genomes. Nonetheless they represent some of the most important forest species, often dominant in many ecosystems. Recent advances in the field of genomics, thanks to next-generation sequencing technologies, and increasingly accurate phenotyping tools, allow new insights into this important plant group and better planning and management strategies of planted and natural populations. This work seeks to improve our knowledge of the genetic mechanisms underpinning the drought physiology and metabolism of conifer species of commercial interest for the UK forestry market.

From genes to phenotype

The project was developed in partnership with Maelor Forest Nurseries Ltd. and Forestart Ltd., the largest tree nursery and forest tree seed supplier in the UK, respectively. Maelor are actively involved in selecting the best performing progenies of *P. sitchensis*, its hybrid with *P. glauca*, *P. lutzii*, and many other species. Tree breeding looks at the future, which is now uncertain. A warmer climate will bring more frequent and hotter regional droughts, hence breeding efforts must account now for future tree growing conditions. Research in the field of plant stress responses has yielded a large amount of data on the way plants cope with drought. The bulk of information now available mainly focus on plant ecophysiology, especially in the case of conifers, for which good quality genomic data are only recently being published. In the previous paragraphs, we have seen how important is to bridge the gap between genes and phenotypes and build solid bases for the establishment of better breeding practices. To do this, this project crossed disciplines, from genomic data analysis to single protein isolation. We provide molecular evidence that explains diverging drought responses among conifer families and species, namely the iso/anisohydric strategies in conjunction with Peaking/Rising ABA accumulation types. Discerning the genetic mechanisms controlling such contrasting response patterns, could help decision making in applied silviculture. Furthermore, we explored the degree of photosynthesis-related trait variation among breeding families of *P. sitchensis* and *P. lutzii* spruce and analysed their significance under drought stress. We believe that these studies may provide tree breeders with valuable information for better selection strategies.

Hypotheses, objectives, and experimental approach

Species drought response comparison

The first part of our work was based on three hypotheses. First, NCED genes may control the iso/anisohydric (rising/peaking types) phenotypes observed in diverging conifer species. In order to do this, NCEDs need to be conserved among conifer families, representing a bottleneck in the ABA biosynthetic pathway of conifers as in model angiosperms. Moreover, contrasting ABA accumulation types should follow differential expression of NCED genes in time under drought conditions.

We set four objectives to verify these hypotheses:

1) Screen the water status of study species and compare them for their stringency in the maintenance of leaf water potential in response to soil drought;

2) Model species-specific ABA profiles over the course of the drought and characterise rising vs peaking types;

3) Identify putative NCEDs and other ABA-related gene sequences, through phylogenetic analyses and ortholog searches;

4) Test the responsiveness of candidate genes to applied water deficit and relate their expression profiles to ABA and water potential profiles.

We conducted a controlled drought experiment in a greenhouse setting, including 9 conifer species that represented the 3 main phylogenetic families – Pinaceae, Cupressaceae and Taxaceae. Using time response measurements, we investigated how species and families differed in their water homeostasis management with drying soil. We used in-house transcriptomes and others sourced from NCBI (The National Center for Biotechnology Information, **https://www.ncbi.nlm.nih.gov**), to identify candidate genes for the key steps of the ABA metabolic pathway. Gene sequences were used for phylogenetic analyses, aimed at identifying patterns of divergence among conifer families and homology relations with other land plant groups. Selected conifer orthologs of *A. thaliana* ABA-related genes, including NCEDs, were used in downstream gene expression assays for 3 species representing 3 families – *Picea sitchensis (P. sitchensis)* (Pinaceae), *Chamaecyparis lawsoniana* (C. lawsoniana) (Cupressaceae) and *Taxus baccata (T. baccata)* (Taxaceae). We finally compared differential gene expression profiles to foliage ABA accumulation profiles, in order to determine relative contribution of biosynthesis and catabolism to the production of characteristic Peaking/Rising types.

NCED protein isolation

Here, we aimed at confirming the identity and role of selected NCED enzymes in ABA biosynthesis. We hypothesised that drought-responsive gene sequences would translate into structurally and functionally conserved NCED proteins. We set three objectives:

1) Establish the degree of sequence similarity and motif conservation across six putative NCED, compared with model *Z. mays* VP14 and *A. thaliana* NCED3;

2) Verify 3D protein structure conservation, based on combined 1D-3D predictive modelling approaches;

3) Test candidate proteins *in silico* for their functional conservation (membrane and substrate binding);

4) Clone, isolate and test *in vitro* the best candidate protein for its catalytic activity.

NCED protein sequences of the same 3 species were used for *in silico* structural and functional analyses. Using multiple screening tools, we collected more evidence in support of our experimental conclusions and to further confirm the identity of the candidate ortholog sequences used in gene expression assays. Finally, we selected one of the candidates NCED sequences from *P. sitchensis*, based on its response to drought treatment and industrial interest. This sequence was cloned using an *Escherichia coli* system and isolated. We concluded our experiments by attempting to test the purified protein *in vitro* and prove its catalytic activity.

Breeding families and hybrids

In the third and final part of our work, we set out to compare several full-sibling families of *P. sitchensis* and its hybrid *Picea lutzii,* for their physiological performance under drought conditions. We hypothesised that full-sibling breeding families of closely related species of conifers may harbour enough inter- and intra-specific variation in responses to the same drought event. *P. sitchensis* and *P. lutzii* are hypothesised to vary in drought tolerance. The objectives were:

1) Monitor and distinguish changes in water relations among breeding families.

2) Study variation of photosynthesis-related traits in response to drought.

3) Calculate water use efficiency and potential growth differences among breeding families.

We investigated photosynthesis-related traits variation in breeding families provided by our industrial partner. We set up a larger greenhouse drought experiment, including 8 full-sibling families (4 *P. sitchensis* and 4 *P. lutzii*) and a rewatering phase. We monitored growth parameters, leaf water status and leaf gas exchange in relation to drying soil. Photosynthesis parameters and water use efficiency estimates were extrapolated from gas exchange readings. The experimental outcomes could inform on best performing species or hybrids, and breeding families under our experimental conditions.

Literature cited

1. Brodribb TJ, McAdam SAM. Abscisic Acid Mediates a Divergence in the Drought Response of Two Conifers. *Plant Physiology*. 2013;162(3):1370-1377. doi:10.1104/PP.113.217877
2. Brodribb TJ, McAdam SAM, Jordan GJ, Martins SCV. Conifer species adapt to low-rainfall climates by following one of two divergent pathways. *Proceedings of the National Academy of Sciences*. 2014;111(40):14489-14493. doi:10.1073/pnas.1407930111
3. McAdam SAM, Sussmilch FC. The evolving role of abscisic acid in cell function and plant development over geological time. *Seminars in Cell and Developmental Biology*. 2021;109:39-45. doi:10.1016/J.SEMCDB.2020.06.006
4. McDowell NG, Sapes G, Pivovaroff A, et al. Mechanisms of woody-plant mortality under rising drought, CO_2 and vapour pressure deficit. *Nature Reviews Earth & Environment*. 2022;3(5):294-308. doi:10.1038/s43017-022-00272-1
5. Moran E, Lauder J, Musser C, Stathos A, Shu M. The genetics of drought tolerance in conifers. *New Phytologist*. 2017;216(4):1034-1048. doi:10.1111/NPH.14774
6. Baldi P, la Porta N. Toward the genetic improvement of drought tolerance in conifers: an integrated approach. *Forests*. 2022;13(12). doi:10.3390/F13122016
7. Masson-Delmotte V, Zhai P, Pörtner HO, et al. Global Warming of 1.5°C; An IPCC Special Report on the impacts of global warming of 1.5°C above pre-industrial levels and related global greenhouse gas emission pathways, in the context of strengthening the global response to the threat of climate change, sustainable development, and efforts to eradicate poverty. Published online 2019.
8. Steffen W, Rockström J, Richardson K, et al. Trajectories of the Earth System in the Anthropocene. *Proceedings of the National Academy of Sciences*. 2018;115(33):8252-8259. doi:10.1073/PNAS.1810141115

9. Arnell NW, Lowe JA, Challinor AJ, Osborn TJ. Global and regional impacts of climate change at different levels of global temperature increase. *Climate Change*. 2019;155(3):377-391. doi:10.1007/S10584-019-02464-Z/
10. Ceppi P, Nowack P. Observational evidence that cloud feedback amplifies global warming. *Proceedings of the National Academy of Sciences*. 2021;118(30):e2026290118. doi:10.1073/PNAS.2026290118
11. Cai W, Santoso A, Collins M, et al. Changing El Niño–Southern Oscillation in a warming climate. *Nature Reviews Earth & Environment* 2021;2(9):628-644. doi:10.1038/s43017-021-00199-z
12. Climate Change 2022: Impacts, Adaptation and Vulnerability | Climate Change 2022: Impacts, Adaptation and Vulnerability. Accessed January 2, 2023. https://www.ipcc.ch/report/ar6/wg2/
13. Lenton TM, Held H, Kriegler E, et al. Tipping elements in the Earth's climate system. *Proceedings of the National Academy of Sciences*. 2008;105(6):1786-1793. doi:10.1073/PNAS.0705414105
14. Lenton TM, Rockström J, Gaffney O, et al. Climate tipping points — too risky to bet against. *Nature.* 2019;575(7784):592-595. doi:10.1038/d41586-019-03595-0
15. McKay DIA, Staal A, Abrams JF, et al. Exceeding 1.5°C global warming could trigger multiple climate tipping points. *Science. 2022;* 377(6611). doi:10.1126/SCIENCE.ABN7950
16. Wunderling N, Donges JF, Kurths J, Winkelmann R. Interacting tipping elements increase risk of climate domino effects under global warming. *Earth System Dynamics*. 2021;12(2):601-619. doi:10.5194/ESD-12-601-2021
17. Smith MD. An ecological perspective on extreme climatic events: a synthetic definition and framework to guide future research. *Journal of Ecology*. 2011;99(3):656-663. doi:10.1111/J.1365-2745.2011.01798.X
18. Diffenbaugh NS, Singh D, Mankin JS, et al. Quantifying the influence of global warming on unprecedented extreme climate events. *Proceedings of the National Academy of Sciences*. 2017;114(19):4881-4886. doi:10.1073/PNAS.1618082114
19. Herring SC, Christidis N, Hoell A, Kossin JP, Schreck CJ, Stott PA. Explaining Extreme Events of 2016 from a Climate Perspective. *Bulletin of the American Meteorological Society*. 2018;99(1):S1-S157. doi:10.1175/BAMS-EXPLAININGEXTREMEEVENTS2016.1
20. Wigley TML. The effect of changing climate on the frequency of absolute extreme events. *Climate Change*. 2009;97(1):67-76. doi:10.1007/S10584-009-9654-7

21. Walther GR. Community and ecosystem responses to recent climate change. *Philosophical Transactions of the Royal Society B: Biological Sciences*. 2010;365(1549):2019-2024. doi:10.1098/RSTB.2010.0021
22. Monier E, Gao X. Climate change impacts on extreme events in the United States: an uncertainty analysis. *Climate Change*. 2015;131(1):67-81. doi:10.1007/S10584-013-1048-1
23. Ummenhofer CC, Meehl GA. Extreme weather and climate events with ecological relevance: a review. *Philosophical Transactions of the Royal Society B: Biological Sciences*. 2017;372(1723). doi:10.1098/RSTB.2016.0135
24. Bell JE, Brown CL, Conlon K, et al. Changes in extreme events and the potential impacts on human health. Journal of the Air & Waste Management Association. 2018;68(4):265-287. doi:10.1080/10962247.2017.1401017
25. Babcock RC, Bustamante RH, Fulton EA, et al. Severe continental-scale impacts of climate change are happening now: Extreme climate events impact marine habitat forming communities along 45% of Australia's coast. *Frontiers in Marine Science*. 2019;6(7):411. doi:10.3389/FMARS.2019.00411/
26. Raymond C, Horton RM, Zscheischler J, et al. Understanding and managing connected extreme events. *Nature Climate Change.* 2020;10(7):611-621. doi:10.1038/s41558-020-0790-4
27. Meehl GA, Tebaldi C. More intense, more frequent, and longer lasting heat waves in the 21st century. *Science*. 2004;305(5686):994-997. doi:10.1126/SCIENCE.1098704
28. Mukherjee S, Mishra AK. Increase in Compound Drought and Heatwaves in a Warming World. *Geophysical Research Letters*. 2021;48(1). doi:10.1029/2020GL090617
29. Christidis N, Jones GS, Stott PA. Dramatically increasing chance of extremely hot summers since the 2003 European heatwave. *Nature Climate Change.* 2014;5(1):46-50. doi:10.1038/nclimate2468
30. Rebetez. Heat and drought 2003 in Europe: a climate synthesis. *Annals of Forest Science* 2006;63:569-577. doi:10.1051/forest:2006043
31. Robine JM, Cheung SLK, le Roy S, et al. Death toll exceeded 70,000 in Europe during the summer of 2003. *Comptes Rendus Biologies*. 2008;331(2):171-178. doi:10.1016/J.CRVI.2007.12.001
32. Ciais P, Reichstein M, Viovy N, et al. Europe-wide reduction in primary productivity caused by the heat and drought in 2003. *Nature;* 2005;437(7058):529-533. doi:10.1038/nature03972
33. Re M., TOPICS GEO, Natural catastrophes 2010.

34. Sharma S, Mujumdar P. Increasing frequency and spatial extent of concurrent meteorological droughts and heatwaves in India. *Scientific Reports;*2017;7(1):1-9. doi:10.1038/s41598-017-15896-3

35. Kong Q, Guerreiro SB, Blenkinsop S, Li XF, Fowler HJ. Increases in summertime concurrent drought and heatwave in Eastern China. *Weather and Climate Extremes*. 2020;28:100242. doi:10.1016/J.WACE.2019.100242

36. Mazdiyasni O, AghaKouchak A. Substantial increase in concurrent droughts and heatwaves in the United States. *Proceedings of the National Academy of Sciences*. 2015;112(37):11484-11489. doi:10.1073/PNAS.1422945112

37. Geirinhas JL, Russo A, Libonati R, Sousa PM, Miralles DG, Trigo RM. Recent increasing frequency of compound summer drought and heatwaves in Southeast Brazil. *Environmental Research Letters*. 2021;16(3):034036. doi:10.1088/1748-9326/ABE0EB

38. Brás TA, Seixas J, Carvalhais N, Jagermeyr J. Severity of drought and heatwave crop losses tripled over the last five decades in Europe. *Environmental Research Letters*. 2021;16(6):065012. doi:10.1088/1748-9326/ABF004

39. Doughty CE, Metcalfe DB, Girardin CAJ, et al. Drought impact on forest carbon dynamics and fluxes in Amazonia. *Nature.*2015;519(7541):78-82. doi:10.1038/nature14213

40. Du L, Mikle N, Zou Z, et al. Global patterns of extreme drought-induced loss in land primary production: Identifying ecological extremes from rain-use efficiency. *Science of The Total Environment*. 2018;628-629:611-620. doi:10.1016/J.SCITOTENV.2018.02.114

41. Schwalm CR, Anderegg WRL, Michalak AM, et al. Global patterns of drought recovery. *Nature.* 2017;548(7666):202-205. doi:10.1038/nature23021

42. Schwalm CR, Williams CA, Schaefer K, et al. Reduction in carbon uptake during turn of the century drought in western North America. *Nature Geoscience.*2012;5(8):551-556. doi:10.1038/ngeo1529

43. Reichstein M, Bahn M, Ciais P, et al. Climate extremes and the carbon cycle. *Nature;* 2013;500(7462):287-295. doi:10.1038/nature12350

44. Chiang F, Mazdiyasni O, AghaKouchak A. Evidence of anthropogenic impacts on global drought frequency, duration, and intensity. *Nature Communications.* 2021;12(1):1-10. doi:10.1038/s41467-021-22314-w

45. Gorham E, Kelly J. A History of Ecological Research Derived from Titles of Articles in the Journal "Ecology," 1925–2015. *The Bulletin of the Ecological Society of America*. 2018;99(1):61-72. doi:10.1002/BES2.1380

46. Crausbay SD, Ramirez AR, Carter SL, et al. Defining Ecological Drought for the Twenty-First Century. *Bulletin of the American Meteorological Society*. 2017;98(12):2543-2550. doi:10.1175/BAMS-D-16-0292.1
47. Slette IJ, Post AK, Awad M, et al. How ecologists define drought, and why we should do better. *Global Change Biology*. 2019;25(10):3193-3200. doi:10.1111/GCB.14747
48. Ault TR. On the essentials of drought in a changing climate. *Science*. 2020;368(6488):256-260. doi:10.1126/SCIENCE.AAZ5492
49. Zargar A, Sadiq R, Naser B, Khan FI. A review of drought indices. *Environmental Reviews*. doi:10.1139/A11-013
50. Touma D, Ashfaq M, Nayak MA, Kao SC, Diffenbaugh NS. A multi-model and multi-index evaluation of drought characteristics in the 21st century. *Journal of Hydrology*. 2015;526:196-207. doi:10.1016/J.JHYDROL.2014.12.011
51. Mukherjee S, Mishra A, Trenberth KE. Climate Change and Drought: a Perspective on Drought Indices. *Curr Climate Change Rep*. 2018;4(2):145-163. doi:10.1007/S40641-018-0098-X
52. Mishra AK, Singh VP. A review of drought concepts. *Journal of Hydrology*. 2010;391(1-2):202-216. doi:10.1016/J.JHYDROL.2010.07.012
53. AghaKouchak A, Mirchi A, Madani K, et al. Anthropogenic Drought: Definition, Challenges, and Opportunities. *Reviews of Geophysics*. 2021;59(2):e2019RG000683. doi:10.1029/2019RG000683
54. Herrera-Estrada JE, Satoh Y, Sheffield J. Spatiotemporal dynamics of global drought. *Geophysical Research Letters*. 2017;44(5):2254-2263. doi:10.1002/2016GL071768
55. Breshears DD, Cobb NS, Rich PM, et al. Regional vegetation die-off in response to global-change-type drought. *Proceedings of the National Academy of Sciences*. 2005;102(42):15144-15148. doi:10.1073/PNAS.0505734102
56. Allen CD, Macalady AK, Chenchouni H, et al. A global overview of drought and heat-induced tree mortality reveals emerging climate change risks for forests. *Forest Ecology and Management*. 2010;259(4):660-684. doi:10.1016/J.FORECO.2009.09.001
57. Williams MI, Dumroese RK. Preparing for Climate Change: Forestry and Assisted Migration. *Journal of forestry*. 2013;111(4):287-297. doi:10.5849/JOF.13-016
58. Senf C, Buras A, Zang CS, Rammig A, Seidl R. Excess forest mortality is consistently linked to drought across Europe. *Nature Communications.* 2020;11(1):1-8. doi:10.1038/s41467-020-19924-1

59. Gazol A, Camarero JJ. Compound climate events increase tree drought mortality across European forests. *Science of The Total Environment*. 2022;816:151604. doi:10.1016/J.SCITOTENV.2021.151604

60. Hammond WM, Williams AP, Abatzoglou JT, et al. Global field observations of tree die-off reveal hotter-drought fingerprint for Earth's forests. *Nature Communications*. 2022;13(1):1-11. doi:10.1038/s41467-022-29289-2

61. Madakumbura GD, Goulden ML, Hall A, et al. Recent California tree mortality portends future increase in drought-driven forest die-off. *Environmental Research Letters*. 2020;15(12):124040. doi:10.1088/1748-9326/ABC719

62. Siwecki R, Ufnalski K. Review of oak stand decline with special reference to the role of drought in Poland. *European Journal of Forest Pathology*. 1998;28(2):99-112. doi:10.1111/J.1439-0329.1998.TB01171.X

63. Cailleret M, Nourtier M, Amm A, Durand-Gillmann M, Davi H. Drought-induced decline and mortality of silver fir differ among three sites in Southern France. *Annals of Forest Science* 2014;71(6):643-657. doi:10.1007/S13595-013-0265-0/

64. Michaelian M, Hogg EH, Hall RJ, Arsenault E. Massive mortality of aspen following severe drought along the southern edge of the Canadian boreal forest. *Global Change Biology*. 2011;17(6):2084-2094. doi:10.1111/J.1365-2486.2010.02357.X

65. Peng C, Ma Z, Lei X, et al. A drought-induced pervasive increase in tree mortality across Canada's boreal forests. *Nature Climate Change.* 2011;1(9):467-471. doi:10.1038/nclimate1293

66. Allen CD, Breshears DD, McDowell NG. On underestimation of global vulnerability to tree mortality and forest die-off from hotter drought in the Anthropocene. *Ecosphere*. 2015;6(8):1-55. doi:10.1890/ES15-00203.1

67. Desprez-Loustau ML, Marçais B, Nageleisen LM, Piou D, Vannini A. Interactive effects of drought and pathogens in forest trees. *Annals of Forest Science* 2006;63(6):597-612. doi:10.1051/FOREST:2006040

68. Negrón JF, McMillin JD, Anhold JA, Coulson D. Bark beetle-caused mortality in a drought-affected ponderosa pine landscape in Arizona, USA. *Forest Ecology and Management*. 2009;257(4):1353-1362. doi:10.1016/J.FORECO.2008.12.002

69. Jactel H, Petit J, Desprez-Loustau ML, et al. Drought effects on damage by forest insects and pathogens: a meta-analysis. *Global Change Biology*. 2012;18(1):267-276. doi:10.1111/J.1365-2486.2011.02512.X

70. Netherer S, Matthews B, Katzensteiner K, et al. Do water-limiting conditions predispose Norway spruce to bark beetle attack? *New Phytologist*. 2015;205(3):1128-1141. doi:10.1111/NPH.13166

71. Netherer S, Panassiti B, Pennerstorfer J, Matthews B. Acute Drought Is an Important Driver of Bark Beetle Infestation in Austrian Norway Spruce Stands. *Frontiers in Forests and Global Change*. 2019;2:39. doi:10.3389/FFGC.2019.00039/

72. Pontes-Lopes A, Silva CVJ, Barlow J, et al. Drought-driven wildfire impacts on structure and dynamics in a wet Central Amazonian Forest. *Proceedings of the Royal Society B*. 2021;288(1951). doi:10.1098/RSPB.2021.0094

73. Gudmundsson L, Rego FC, Rocha M, et al. Predicting above normal wildfire activity in southern Europe as a function of meteorological drought. E*nvironmental Research Letters*. 2014;9(8):084008. doi:10.1088/1748-9326/9/8/084008

74. Taufik M, Torfs PJJF, Uijlenhoet R, Jones PD, Murdiyarso D, van Lanen HAJ. Amplification of wildfire area burnt by hydrological drought in the humid tropics. *Nature Climate Change* 2017;7(6):428-431. doi:10.1038/nclimate3280

75. Whitman E, Parisien MA, Thompson DK, Flannigan MD. Short-interval wildfire and drought overwhelm boreal forest resilience. *Scientific Reports.* 2019;9(1):1-12. doi:10.1038/s41598-019-55036-7

76. Anderegg WRL, Kane JM, Anderegg LDL. Consequences of widespread tree mortality triggered by drought and temperature stress. *Nature Climate Change* 2012;3(1):30-36. doi:10.1038/nclimate1635

77. Schlesinger WH, Dietze MC, Jackson RB, et al. Forest biogeochemistry in response to drought. *Global Change Biology*. 2016;22(7):2318-2328. doi:10.1111/GCB.13105

78. Xu C, McDowell NG, Fisher RA, et al. Increasing impacts of extreme droughts on vegetation productivity under climate change. *Nature Climate Change*. 2019;9(12):948-953. doi:10.1038/s41558-019-0630-6

79. Trenberth KE, Dai A, van der Schrier G, et al. Global warming and changes in drought. *Nature Climate Change 2014 4:1*. 2013;4(1):17-22. doi:10.1038/nclimate2067

80. Duan H, Amthor JS, Duursma RA, O'Grady AP, Choat B, Tissue DT. Carbon dynamics of eucalypt seedlings exposed to progressive drought in elevated [CO_2] and elevated temperature. *Tree Physiology*. 2013;33(8):779-792. doi:10.1093/TREEPHYS/TPT061

81. McDowell NG, Williams AP, Xu C, et al. Multi-scale predictions of massive conifer mortality due to chronic temperature rise. *Nature Climate Change*. 2016;6(3):295-300. doi:10.1038/nclimate2873

82. Adams HD, Barron-Gafford GA, Minor RL, et al. Temperature response surfaces for mortality risk of tree species with future drought. *Environmental Research Letters*. 2017;12(11):115014. doi:10.1088/1748-9326/AA93BE
83. Bonan GB. Forests and climate change: Forcings, feedbacks, and the climate benefits of forests. *Science*. 2008;320(5882):1444-1449. doi:10.1126/SCIENCE.1155121
84. Pan Y, Birdsey RA, Fang J, et al. A large and persistent carbon sink in the world's forests. *Science*. 2011;333(6045):988-993. doi:10.1126/SCIENCE.1201609
85. Martínez-Vilalta J, Piñol J, Beven K. A hydraulic model to predict drought-induced mortality in woody plants: an application to climate change in the Mediterranean. *Ecological Modelling*. 2002;155(2-3):127-147. doi:10.1016/S0304-3800(02)00025-X
86. Mcdowell N, Pockman WT, Allen CD, et al. Mechanisms of Plant Survival and Mortality during Drought: Why Do Some Plants Survive while Others Succumb to Drought. *New Phytologist*. 2008;178(4):719-739.
87. McDowell NG. Mechanisms Linking Drought, Hydraulics, Carbon Metabolism, and Vegetation Mortality. *Plant Physiology*. 2011;155(3):1051-1059. doi:10.1104/PP.110.170704
88. McDowell NG, Beerling DJ, Breshears DD, Fisher RA, Raffa KF, Stitt M. The interdependence of mechanisms underlying climate-driven vegetation mortality. *Trends in Ecology & Evolution*. 2011;26(10):523-532. doi:10.1016/J.TREE.2011.06.003
89. Martinez-Vilalta J, Anderegg WRL, Sapes G, Sala A. Greater focus on water pools may improve our ability to understand and anticipate drought-induced mortality in plants. *New Phytologist*. 2019;223(1):22-32. doi:10.1111/NPH.15644
90. Mantova M, Menezes-Silva PE, Badel E, Cochard H, Torres-Ruiz JM. The interplay of hydraulic failure and cell vitality explains tree capacity to recover from drought. *Physiologia Plantarum*. 2021;172(1):247-257. doi:10.1111/PPL.13331
91. Guadagno CR, Ewers BE, Speckman HN, et al. Dead or Alive? Using Membrane Failure and Chlorophyll a Fluorescence to Predict Plant Mortality from Drought. *Plant Physiology*. 2017;175(1):223-234. doi:10.1104/PP.16.00581
92. Dixon HH, Dixon HH. *Transpiration and the Ascent of Sap in Plants*. Macmillan and co., limited; 1914. doi:10.5962/bhl.title.1943
93. Buckley TN. How do stomata respond to water status? *New Phytologist*. 2019;224(1):21-36. doi:10.1111/NPH.15899
94. Brodribb TJ, McAdam SAM. Evolution of the Stomatal Regulation of Plant Water Content. *Plant Physiology*. 2017;174(2):639-649. doi:10.1104/PP.17.00078

95. Crombie D, Hipkins M, Milburn J. Gas Penetration of Pit Membranes in the Xylem of Rhododendron as the Cause of Acoustically Detectable Sap Cavitation. *Functional Plant Biology*. 1985;12(5):445-453. doi:10.1071/PP9850445
96. Sperry JS, Tyree MT. Mechanism of Water Stress-Induced Xylem Embolism. *Plant Physiology*. 1988;88(3):581-587. doi:10.1104/PP.88.3.581
97. Sperry JS, Saliendra NZ, Pockman WT, et al. New evidence for large negative xylem pressures and their measurement by the pressure chamber method. *Plant, Cell & Environment*. 1996;19(4):427-436. doi:10.1111/J.1365-3040.1996.TB00334.X
98. Zimmermann MH. Hydraulic architecture of some diffuse-porous trees. *Canadian Journal of Botany*. 2011;56(18):2286-2295. doi:10.1139/B78-274
99. Liu YY, Song J, Wang M, Li N, Niu CY, Hao GY. Coordination of xylem hydraulics and stomatal regulation in keeping the integrity of xylem water transport in shoots of two compound-leaved tree species. *Tree Physiology*. 2015;35(12):1333-1342. doi:10.1093/TREEPHYS/TPV061
100. Brodribb TJ, Holbrook NM. Stomatal protection against hydraulic failure: a comparison of coexisting ferns and angiosperms. *New Phytologist*. 2004;162(3):663-670. doi:10.1111/J.1469-8137.2004.01060.X
101. Meinzer FC, Johnson DM, Lachenbruch B, McCulloh KA, Woodruff DR. Xylem hydraulic safety margins in woody plants: coordination of stomatal control of xylem tension with hydraulic capacitance. *Functional Ecology*. 2009;23(5):922-930. doi:10.1111/J.1365-2435.2009.01577.X
102. Creek D, Lamarque LJ, Torres-Ruiz JM, et al. Xylem embolism in leaves does not occur with open stomata: evidence from direct observations using the optical visualization technique. *Journal of Experimental Botany*. 2020;71(3):1151-1159. doi:10.1093/JXB/ERZ474
103. Pratt RB, MacKinnon ED, Venturas MD, Crous CJ, Jacobsen AL. Root resistance to cavitation is accurately measured using a centrifuge technique. *Tree Physiology*. 2015;35(2):185-196. doi:10.1093/TREEPHYS/TPV003
104. Johnson DM, Wortemann R, McCulloh KA, et al. A test of the hydraulic vulnerability segmentation hypothesis in angiosperm and conifer tree species. *Tree Physiology*. 2016;36(8):983-993. doi:10.1093/TREEPHYS/TPW031
105. Sperry JS, Ikeda T. Xylem cavitation in roots and stems of Douglas-fir and white fir. *Tree Physiology*. 1997;17(4):275-280. doi:10.1093/TREEPHYS/17.4.275

106. Gambetta GA, Fei J, Rost TL, et al. Water Uptake along the Length of Grapevine Fine Roots: Developmental Anatomy, Tissue-Specific Aquaporin Expression, and Pathways of Water Transport. *Plant Physiology*. 2013;163(3):1254-1265. doi:10.1104/PP.113.221283
107. Cuneo IF, Knipfer T, Brodersen CR, McElrone AJ. Mechanical Failure of Fine Root Cortical Cells Initiates Plant Hydraulic Decline during Drought. *Plant Physiology* 2016;172(3):1669-1678. doi:10.1104/PP.16.00923
108. Rodriguez-Dominguez CM, Brodribb TJ. Declining root water transport drives stomatal closure in olive under moderate water stress. *New Phytologist*. 2020;225(1):126-134. doi:10.1111/NPH.16177
109. Plaut JA, Yepez EA, Hill J, et al. Hydraulic limits preceding mortality in a piñon-juniper woodland under experimental drought. *Plant, Cell & Environment*. 2012;35(9):1601-1617. doi:10.1111/J.1365-3040.2012.02512.X
110. Kerstiens G. Cuticular water permeability and its physiological significance. *Journal of Experimental Botany*. 1996;47(12):1813-1832. doi:10.1093/JXB/47.12.1813
111. Burghardt M, Riederer M. Ecophysiological relevance of cuticular transpiration of deciduous and evergreen plants in relation to stomatal closure and leaf water potential*. *Journal of Experimental Botany*. 2003;54(389):1941-1949. doi:10.1093/JXB/ERG195
112. Wolfe BT. Bark water vapour conductance is associated with drought performance in tropical trees. *Biology Letters*. 2020;16(8). doi:10.1098/RSBL.2020.0263
113. Machado R, Loram-Lourenço L, Farnese FS, et al. Where do leaf water leaks come from? Trade-offs underlying the variability in minimum conductance across tropical savanna species with contrasting growth strategies. *New Phytologist*. 2021;229(3):1415-1430. doi:10.1111/NPH.16941
114. McElrone AJ, Bichler J, Pockman WT, Addington RN, Linder CR, Jackson RB. Aquaporin-mediated changes in hydraulic conductivity of deep tree roots accessed via caves. *Plant, Cell & Environment*. 2007;30(11):1411-1421. doi:10.1111/J.1365-3040.2007.01714.X
115. Zhang YJ, Rockwell FE, Graham AC, Alexander T, Michele Holbrook N. Reversible Leaf Xylem Collapse: A Potential "Circuit Breaker" against Cavitation. *Plant Physiology* .2016;172(4):2261-2274. doi:10.1104/PP.16.01191
116. Borchert R, Pockman WT. Water storage capacitance and xylem tension in isolated branches of temperate and tropical trees. *Tree Physiology*. 2005;25(4):457-466. doi:10.1093/TREEPHYS/25.4.457
117. Brodribb TJ, Cochard H. Hydraulic Failure Defines the Recovery and Point of Death in Water-Stressed Conifers. *Plant Physiology* 2009;149(1):575. doi:10.1104/PP.108.129783

118. Anderegg WRL, Berry JA, Smith DD, Sperry JS, Anderegg LDL, Field CB. The roles of hydraulic and carbon stress in a widespread climate-induced forest die-off. *Proceedings of the National Academy of Sciences*. 2012;109(1):233-237. doi:10.1073/PNAS.1107891109
119. Jones HG. Stomatal control of photosynthesis and transpiration. *Journal of Experimental Botany*. 1998;49(Special_Issue):387-398. doi:10.1093/JXB/49.SPECIAL_ISSUE.387
120. Medrano H, Escalona JM, Bota J, Gulías J, Flexas J. Regulation of Photosynthesis of C3 Plants in Response to Progressive Drought: Stomatal Conductance as a Reference Parameter. *Annals of Botany*. 2002;89(7):895-905. doi:10.1093/AOB/MCF079
121. Flexas J, Medrano H. Drought-inhibition of Photosynthesis in C3 Plants: Stomatal and Non-stomatal Limitations Revisited. *Annals of Botany*. 2002;89(2):183-189. doi:10.1093/AOB/MCF027
122. Santos VAHF dos, Ferreira MJ, Rodrigues JVFC, et al. Causes of reduced leaf-level photosynthesis during strong El Niño drought in a Central Amazon Forest. *Global Change Biology*. 2018;24(9):4266-4279. doi:10.1111/GCB.14293
123. Chaves MM. Effects of Water Deficits on Carbon Assimilation. *Journal of Experimental Botany*. 1991;42(1):1-16. doi:10.1093/JXB/42.1.1
124. Flexas J, Bota J, Loreto F, Cornic G, Sharkey TD. Diffusive and Metabolic Limitations to Photosynthesis under Drought and Salinity in C3 Plants. *Plant Biology.* 2008;6(3):269-279. doi:10.1055/S-2004-820867
125. Teskey R, Wertin T, Bauweraerts I, Ameye M, McGuire MA, Steppe K. Responses of tree species to heat waves and extreme heat events. *Plant, Cell & Environment*. 2015;38(9):1699-1712. doi:10.1111/PCE.12417
126. Kono Y, Ishida A, Saiki ST, et al. Initial hydraulic failure followed by late-stage carbon starvation leads to drought-induced death in the tree Trema orientalis. *Communications Biology*. 2019;2(1):1-9. doi:10.1038/s42003-018-0256-7
127. Sala A. Lack of direct evidence for the carbon-starvation hypothesis to explain drought-induced mortality in trees. *Proceedings of the National Academy of Sciences*. 2009;106(26):E68-E68. doi:10.1073/PNAS.0904580106
128. Hartmann H. Carbon starvation during drought-induced tree mortality – are we chasing a myth? *Journal of Plant Hydraulics*. 2015;2:e005. doi:10.20870/jph.2015.e005
129. Adams HD, Zeppel MJB, Anderegg WRL, et al. A multi-species synthesis of physiological mechanisms in drought-induced tree mortality. *Nature Ecology & Evolution*. 2017;1(9):1285-1291. doi:10.1038/s41559-017-0248-x

130. Sevanto S, Mcdowell NG, Dickman LT, Pangle R, Pockman WT. How do trees die? A test of the hydraulic failure and carbon starvation hypotheses. *Plant, Cell & Environment*. 2014;37(1):153-161. doi:10.1111/PCE.12141
131. Nardini A, Casolo V, Dal Borgo A, et al. Rooting depth, water relations and non-structural carbohydrate dynamics in three woody angiosperms differentially affected by an extreme summer drought. *Plant, Cell & Environment*. 2016;39(3):618-627. doi:10.1111/PCE.12646
132. O'Brien MJ, Leuzinger S, Philipson CD, Tay J, Hector A. Drought survival of tropical tree seedlings enhanced by non-structural carbohydrate levels. *Nature Climate Change*. 2014;4(8):710-714. doi:10.1038/nclimate2281
133. Tomasella M, Petrussa E, Petruzzellis F, Nardini A, Casolo V. The Possible Role of Non-Structural Carbohydrates in the Regulation of Tree Hydraulics. *International Journal of Molecular Sciences 2020, Vol 21, Page 144*. 2019;21(1):144. doi:10.3390/IJMS21010144
134. McDowell NG, Sevanto S. The mechanisms of carbon starvation: how, when, or does it even occur at all? *New Phytologist*. 2010;186(2):264-266. doi:10.1111/J.1469-8137.2010.03232.X
135. Sevanto S. Phloem transport and drought. *Journal of Experimental Botany*. 2014;65(7):1751-1759. doi:10.1093/JXB/ERT467
136. Mencuccini M, Minunno F, Salmon Y, Mart J. Coordination of physiological traits involved in drought-induced mortality of woody plants. *New Phytologist*. 2015; 208(2):396-409. doi: 10.1111/nph.13461
137. Hesse BD, Goisser M, Hartmann H, Grams TEE. Repeated summer drought delays sugar export from the leaf and impairs phloem transport in mature beech. *Tree Physiology*. 2019;39(2):192-200. doi:10.1093/TREEPHYS/TPY122
138. Landhäusser SM, Lieffers VJ. Defoliation increases risk of carbon starvation in root systems of mature aspen. *Trees - Structure and Function*. 2012;26(2):653-661. doi:10.1007/S00468-011-0633-Z
139. Wiley E, Hoch G, Landhäusser SM. Dying piece by piece: carbohydrate dynamics in aspen (Populus tremuloides) seedlings under severe carbon stress. *Journal of Experimental Botany*. 2017;68(18):5221-5232. doi:10.1093/JXB/ERX342
140. Hagedorn F, Joseph J, Peter M, et al. Recovery of trees from drought depends on belowground sink control. *Nature Plants*. 2016;2(8):1-5. doi:10.1038/nplants.2016.111
141. McDowell NG. Mechanisms Linking Drought, Hydraulics, Carbon Metabolism, and Vegetation Mortality. *Plant Physiology* 2011;155(3):1051-1059. doi:10.1104/pp.110.170704

142. Anderegg WRL. Spatial and temporal variation in plant hydraulic traits and their relevance for climate change impacts on vegetation. *New Phytologist*. 2015;205(3):1008-1014. doi:10.1111/nph.12907
143. Ghanbary E, Fathizadeh O, Pazhouhan I, et al. Drought and Pathogen Effects on Survival, Leaf Physiology, Oxidative Damage, and Defense in Two Middle Eastern Oak Species. *Forests 2021, Vol 12, Page 247*. 2021;12(2):247. doi:10.3390/F12020247
144. Gomez-Gallego M, Galiano L, Martínez-Vilalta J, et al. Interaction of drought- and pathogen-induced mortality in Norway spruce and Scots pine. *Plant, Cell & Environment*. 2022;45(8):2292-2305. doi:10.1111/PCE.14360
145. Rouault G, Candau JN, Lieutier F, Nageleisen LM, Martin JC, Warzée N. Effects of drought and heat on forest insect populations in relation to the 2003 drought in Western Europe. *Annals of Forest Science* 2006;63(6):613-624. doi:10.1051/FOREST:2006044
146. Dobbertin M, Wermelinger B, Bigler C, et al. Linking Increasing Drought Stress to Scots Pine Mortality and Bark Beetle Infestations. *The Scientific World Journal*. 2007;7(SUPPL. 2):231-239. doi:10.1100/TSW.2007.58
147. Kaiser KE, Mcglynn BL, Emanuel RE. Ecohydrology of an outbreak: mountain pine beetle impacts trees in drier landscape positions first. *Ecohydrology*. 2013;6(3):444-454. doi:10.1002/ECO.1286
148. Kolb T, Keefover-Ring K, Burr SJ, Hofstetter R, Gaylord M, Raffa KF. Drought-Mediated Changes in Tree Physiologyogical Processes Weaken Tree Defenses to Bark Beetle Attack. *Journal of Chemical Ecology*. 2019;45(10):888-900. doi:10.1007/S10886-019-01105-0
149. Suárez-Vidal E, Sampedro L, Voltas J, Serrano L, Notivol E, Zas R. Drought stress modifies early effective resistance and induced chemical defences of Aleppo pine against a chewing insect herbivore. *Environmental and Experimental Botany*. 2019;162:550-559. doi:10.1016/J.ENVEXPBOT.2019.04.002
150. Camarero JJ, Gazol A, Sangüesa-Barreda G, Oliva J, Vicente-Serrano SM. To die or not to die: early warnings of tree dieback in response to a severe drought. *Journal of Ecology*. 2015;103(1):44-57. doi:10.1111/1365-2745.12295
151. Klutsch JG, Shamoun SF, Erbilgin N. Drought stress leads to systemic induced susceptibility to a nectrotrophic fungus associated with mountain pine beetle in Pinus banksiana seedlings. *PLoS One*. 2017;12(12):e0189203. doi:10.1371/JOURNAL.PONE.0189203
152. Devkota P, Enebak SA, Eckhardt LG. The impact of drought and vascular-inhabiting pathogen invasion in pinus taeda health. *International Journal of Forestry Research*. 2018; doi:10.1155/2018/1249140

153. Gershenzon J. Metabolic costs of terpenoid accumulation in higher plants. *Journal of Chemical Ecology 1994 20:6*. 1994;20(6):1281-1328. doi:10.1007/BF02059810
154. Franceschi VR, Krokene P, Christiansen E, Krekling T. Anatomical and chemical defenses of conifer bark against bark beetles and other pests. *New Phytologist*. 2005;167(2):353-376. doi:10.1111/J.1469-8137.2005.01436.X
155. Sevanto S. Drought impacts on phloem transport. *Current Opinion in Plant Biology.* 2018;43:76-81. doi:10.1016/J.PBI.2018.01.002
156. Salmon Y, Dietrich L, Sevanto S, Hölttä T, Dannoura M, Epron D. Drought impacts on tree phloem: from cell-level responses to ecological significance. *Tree Physiology*. 2019;39(2):173-191. doi:10.1093/TREEPHYS/TPY153
157. Hikino K, Danzberger J, Riedel VP, et al. High resilience of carbon transport in long-term drought-stressed mature Norway spruce trees within 2 weeks after drought release. *Global Change Biology*. 2022;28(6):2095-2110. doi:10.1111/GCB.16051
158. Hölttä T, Vesala T, Sevanto S, Perämäki M, Nikinmaa E. Modeling xylem and phloem water flows in trees according to cohesion theory and Münch hypothesis. *Trees - Structure and Function*. 2006;20(1):67-78. doi:10.1007/S00468-005-0014-6
159. Hölttä T, Mencuccini M, Nikinmaa E. Linking phloem function to structure: Analysis with a coupled xylem–phloem transport model. *Journal of Theoretical Biology*. 2009;259(2):325-337. doi:10.1016/J.JTBI.2009.03.039
160. Epron D, Cabral OMR, Laclau JP, et al. In situ $13CO_2$ pulse labelling of field-grown eucalypt trees revealed the effects of potassium nutrition and throughfall exclusion on phloem transport of photosynthetic carbon. *Tree Physiology*. 2016;36(1):6-21. doi:10.1093/TREEPHYS/TPV090
161. Dannoura M, Epron D, Desalme D, et al. The impact of prolonged drought on phloem anatomy and phloem transport in young beech trees. *Tree Physiology*. 2019;39(2):201-210. doi:10.1093/TREEPHYS/TPY070
162. Goodsman DW, Lusebrink I, Landhäusser SM, Erbilgin N, Lieffers VJ. Variation in carbon availability, defense chemistry and susceptibility to fungal invasion along the stems of mature trees. *New Phytologist*. 2013;197(2):586-594. doi:10.1111/NPH.12019
163. Wiley E, Rogers BJ, Hodgkinson R, Landhäusser SM. Nonstructural carbohydrate dynamics of lodgepole pine dying from mountain pine beetle attack. *New Phytologist*. 2016;209(2):550-562. doi:10.1111/NPH.13603

164. Oliva J, Stenlid J, Martínez-Vilalta J. The effect of fungal pathogens on the water and carbon economy of trees: implications for drought-induced mortality. *New Phytologist*. 2014;203(4):1028-1035. doi:10.1111/NPH.12857

165. Caretto S, Linsalata V, Colella G, Mita G, Lattanzio V. Carbon Fluxes between Primary Metabolism and Phenolic Pathway in Plant Tissues under Stress. *International Journal of Molecular Sciences* 2015;16(11):26378-26394. doi:10.3390/IJMS161125967

166. Marler TE, Cascasan ANJ. Carbohydrate depletion during lethal infestation of aulacaspis yasumatsui on cycas revoluta. *International Journal of Plant Sciences*. 2018;179(6):497-504. doi:10.1086/697929

167. Roth M, Hussain A, Cale JA, Erbilgin N. Successful Colonization of Lodgepole Pine Trees by Mountain Pine Beetle Increased Monoterpene Production and Exhausted Carbohydrate Reserves. *Journal of Chemical Ecology*. 2018;44(2):209-214. doi:10.1007/S10886-017-0922-0

168. Rissanen K, Hölttä T, Bäck J, Rigling A, Wermelinger B, Gessler A. Drought effects on carbon allocation to resin defences and on resin dynamics in old-grown Scots pine. *Environmental and Experimental Botany*. 2021;185:104410. doi:10.1016/J.ENVEXPBOT.2021.104410

169. Croisé L, Lieutier F, Cochard H, Dreyer E. Effects of drought stress and high density stem inoculations with Leptographium wingfieldii on hydraulic properties of young Scots pine trees. *Tree Physiology*. 2001;21(7):427-436. doi:10.1093/TREEPHYS/21.7.427

170. Manter DK, Kavanagh KL. Stomatal regulation in Douglas fir following a fungal-mediated chronic reduction in leaf area. *Trees - Structure and Function*. 2003;17(6):485-491. doi:10.1007/S00468-003-0262-2

171. Hubbard RM, Rhoades CC, Elder K, Negron J. Changes in transpiration and foliage growth in lodgepole pine trees following mountain pine beetle attack and mechanical girdling. *Forest Ecology and Management*. 2013;289:312-317. doi:10.1016/J.FORECO.2012.09.028

172. Gori Y, Cherubini P, Camin F, la Porta N. Fungal root pathogen (Heterobasidion parviporum) increases drought stress in Norway spruce stand at low elevation in the Alps. *European Journal of Forest Research*. 2013;132(4):607-619. doi:10.1007/S10342-013-0698-X

173. Lahr EC, Sala A. Sapwood Stored Resources Decline in Whitebark and Lodgepole Pines Attacked by Mountain Pine Beetles (Coleoptera: Curculionidae). *Environmental Entomology*. 2016;45(6):1463-1475. doi:10.1093/EE/NVW138

174. Parmesan C, Yohe G. A globally coherent fingerprint of climate change impacts across natural systems. *Nature.* 2003;421(6918):37-42. doi:10.1038/nature01286

175. Thuiller W, Lavorel S, Araújo MB, Sykes MT, Prentice IC. Climate change threats to plant diversity in Europe. *Proceedings of the National Academy of Sciences*. 2005;102(23):8245-8250. doi:10.1073/PNAS.0409902102
176. Morin X, Viner D, Chuine I. Tree species range shifts at a continental scale: new predictive insights from a process-based model. *Journal of Ecology*. 2008;96(4):784-794. doi:10.1111/J.1365-2745.2008.01369.X
177. Kelly AE, Goulden ML. Rapid shifts in plant distribution with recent climate change. *Proceedings of the National Academy of Sciences*. 2008;105(33):11823-11826. doi:10.1073/PNAS.0802891105
178. Angert AL, Crozier LG, Rissler LJ, Gilman SE, Tewksbury JJ, Chunco AJ. Do species' traits predict recent shifts at expanding range edges? *Ecology Letters*. 2011;14(7):677-689. doi:10.1111/J.1461-0248.2011.01620.X
179. Chen IC, Hill JK, Ohlemüller R, Roy DB, Thomas CD. Rapid range shifts of species associated with high levels of climate warming. *Science*. 2011;333(6045):1024-1026. doi:10.1126/SCIENCE.1206432
180. Fadrique B, Báez S, Duque Á, et al. Widespread but heterogeneous responses of Andean forests to climate change. *Nature*. 2018;564(7735):207-212. doi:10.1038/s41586-018-0715-9
181. Alberto FJ, Aitken SN, Alía R, et al. Potential for evolutionary responses to climate change – evidence from tree populations. *Global Change Biology*. 2013;19(6):1645-1661. doi:10.1111/GCB.12181
182. Franks SJ, Weber JJ, Aitken SN. Evolutionary and plastic responses to climate change in terrestrial plant populations. *Evolutionary Applications*. 2014;7(1):123-139. doi:10.1111/EVA.12112
183. Anderson JT, Wadgymar SM. Climate change disrupts local adaptation and favours upslope migration. *Ecology Letters*. 2020;23(1):181-192. doi:10.1111/ELE.13427
184. Boisvert-Marsh L, Périé C, de Blois S. Shifting with climate? Evidence for recent changes in tree species distribution at high latitudes. *Ecosphere*. 2014;5(7):1-33. doi:10.1890/ES14-00111.1
185. Savolainen O, Pyhäjärvi T, Knürr T. Gene Flow and Local Adaptation in Trees. 2007;38:595-619. doi:10.1146/ANNUREV.ECOLSYS.38.091206.095646
186. Loarie SR, Duffy PB, Hamilton H, Asner GP, Field CB, Ackerly DD. The velocity of climate change. *Nature*. 2009;462(7276):1052-1055. doi:10.1038/nature08649

187. Kuparinen A, Savolainen O, Schurr FM. Increased mortality can promote evolutionary adaptation of forest trees to climate change. *Forest Ecology and Management*. 2010;259(5):1003-1008. doi:10.1016/J.FORECO.2009.12.006

188. Kremer A, Ronce O, Robledo-Arnuncio JJ, et al. Long-distance gene flow and adaptation of forest trees to rapid climate change. *Ecology Letters*. 2012;15(4):378-392. doi:10.1111/J.1461-0248.2012.01746.X

189. Shaw RG, Etterson JR. Rapid climate change and the rate of adaptation: insight from experimental quantitative genetics. *New Phytologist*. 2012;195(4):752-765. doi:10.1111/J.1469-8137.2012.04230.X

190. Aitken SN, Yeaman S, Holliday JA, Wang T, Curtis-McLane S. Adaptation, migration or extirpation: climate change outcomes for tree populations. *Evolutionary Applications*. 2008;1(1):95-111. doi:10.1111/J.1752-4571.2007.00013.X

191. Rehfeldt GE, Leites LP, Bradley St Clair J, et al. Comparative genetic responses to climate in the varieties of *Pinus ponderosa* and *Pseudotsuga menziesii*: Clines in growth potential. *Forest Ecology and Management*. 2014;324:138-146. doi:10.1016/J.FORECO.2014.02.041

192. Kroiss SJ, Hillerislambers J, D'Amato AW. Recruitment limitation of long-lived conifers: implications for climate change responses. *Ecology*. 2015;96(5):1286-1297. doi:10.1890/14-0595.1

193. Carja O, Plotkin JB. Evolutionary Rescue Through Partly Heritable Phenotypic Variability. *Genetics*. 2019;211(3):977-988. doi:10.1534/GENETICS.118.301758

194. Kelly M. Adaptation to climate change through genetic accommodation and assimilation of plastic phenotypes. *Philosophical Transactions of the Royal Society B*. 2019;374(1768). doi:10.1098/RSTB.2018.0176

195. Razgour O, Forester B, Taggart JB, et al. Considering adaptive genetic variation in climate change vulnerability assessment reduces species range loss projections. *Proceedings of the National Academy of Sciences*. 2019;116(21):10418-10423. doi:10.1073/PNAS.1820663116

196. Aubin I, Munson AD, Cardou F, et al. Traits to stay, traits to move: a review of functional traits to assess sensitivity and adaptive capacity of temperate and boreal trees to climate change. *Environmental Reviews*. 2016;24(2):164-186. doi:10.1139/ER-2015-0072

197. Namroud MC, Beaulieu J, Juge N, Laroche J, Bousquet J. Scanning the genome for gene single nucleotide polymorphisms involved in adaptive population differentiation in white spruce. *Molecular Ecology*. 2008;17(16):3599-3613. doi:10.1111/J.1365-294X.2008.03840.X

198. Eckert AJ, Bower AD, Wegrzyn JL, et al. Association Genetics of Coastal Douglas Fir (*Pseudotsuga menziesii* var. *menziesii*, Pinaceae). I. Cold-Hardiness Related Traits. *Genetics*. 2009;182(4):1289-1302. doi:10.1534/GENETICS.109.102350

199. Hornoy B, Pavy N, Gérardi S, Beaulieu J, Bousquet J. Genetic Adaptation to Climate in White Spruce Involves Small to Moderate Allele Frequency Shifts in Functionally Diverse Genes. *Genome Biology and Evolution*. 2015;7(12):3269-3285. doi:10.1093/GBE/EVV218

200. Prunier J, Verta JP, Mackay JJ. Conifer genomics and adaptation: At the crossroads of genetic diversity and genome function. *New Phytologist*. 2016;209(1):44-62. doi:10.1111/nph.13565

201. Csilléry K, Rodríguez-Verdugo A, Rellstab C, Guillaume F. Detecting the genomic signal of polygenic adaptation and the role of epistasis in evolution. *Molecular Ecology*. 2018;27(3):606-612. doi:10.1111/MEC.14499

202. Depardieu C, Gérardi S, Nadeau S, et al. Connecting tree-ring phenotypes, genetic associations and transcriptomics to decipher the genomic architecture of drought adaptation in a widespread conifer. *Molecular Ecology*. 2021;30(16):3898-3917. doi:10.1111/MEC.15846

203. Holliday JA, Wang T, Aitken S. Predicting adaptive phenotypes from multilocus genotypes in sitka spruce (*Picea sitchensis*) using random forest. *G3: Genes, Genomes, Genetics*. 2012;2(9):1085-1093. doi:10.1534/G3.112.002733/-/DC1

204. St Clair JB, Howe GT. Genetic maladaptation of coastal Douglas-fir seedlings to future climates. *Global Change Biology*. 2007;13(7):1441-1454. doi:10.1111/J.1365-2486.2007.01385.X

205. Frank A, Howe GT, Sperisen C, et al. Risk of genetic maladaptation due to climate change in three major European tree species. *Global Change Biology*. 2017;23(12):5358-5371. doi:10.1111/GCB.13802

206. Isaac-Renton M, Montwé D, Hamann A, Spiecker H, Cherubini P, Treydte K. Northern Forest tree populations are physiologically maladapted to drought. *Nature Communications*. 2018;9(1):1-9. doi:10.1038/s41467-018-07701-0

207. Bisbing SM, Urza AK, Buma BJ, Cooper DJ, Matocq M, Angert AL. Can long-lived species keep pace with climate change? Evidence of local persistence potential in a widespread conifer. *Diversity and Distributions*. 2021;27(2):296-312. doi:10.1111/DDI.13191

208. Follieri M. Conifer extinction in Quaternary Italian records. *Quaternary International*. 2010;225(1):37-43. doi:10.1016/J.QUAINT.2010.02.001

209. Crisp MD, Cook LG. Cenozoic extinctions account for the low diversity of extant gymnosperms compared with angiosperms. *New Phytologist*. 2011;192(4):997-1009. doi:10.1111/J.1469-8137.2011.03862.X

210. Mellick R, Lowe A, Allen C, Hill RS, Rossetto M. Palaeodistribution modelling and genetic evidence highlight differential post-glacial range shifts of a rain forest conifer distributed across a latitudinal gradient. *J Biogeogr*. 2012;39(12):2292-2302. doi:10.1111/J.1365-2699.2012.02747.X

211. Leslie AB, Beaulieu JM, Rai HS, Crane PR, Donoghue MJ, Mathews S. Hemisphere-scale differences in conifer evolutionary dynamics. *Proceedings of the National Academy of Sciences*. 2012;109(40):16217-16221. doi:10.1073/PNAS.1213621109

212. Magri D, di Rita F, Aranbarri J, Fletcher W, González-Sampériz P. Quaternary disappearance of tree taxa from Southern Europe: Timing and trends. *Quaternary Science Reviews*. 2017;163:23-55. doi:10.1016/J.QUASCIREV.2017.02.014

213. Magri D, Parra I, di Rita F, Ni J, Shichi K, Worth JRP. Linking worldwide past and present conifer vulnerability. *Quaternary Science Reviews*. 2020;250:106640. doi:10.1016/J.QUASCIREV.2020.106640

214. Gonzalez P, Neilson RP, Lenihan JM, Drapek RJ. Global patterns in the vulnerability of ecosystems to vegetation shifts due to climate change. *Global Ecology and Biogeography*. 2010;19(6):755-768. doi:10.1111/J.1466-8238.2010.00558.X

215. Shuman JK, Shugart HH, O'Halloran TL. Sensitivity of Siberian larch forests to climate change. *Global Change Biology*. 2011;17(7):2370-2384. doi:10.1111/J.1365-2486.2011.02417.X

216. Brummitt NA, Bachman SP, Griffiths-Lee J, et al. Green Plants in the Red: A Baseline Global Assessment for the IUCN Sampled Red List Index for Plants. *PLoS One*. 2015;10(8):e0135152. doi:10.1371/JOURNAL.PONE.0135152

217. McDowell NG, Williams AP, Xu C, et al. Multi-scale predictions of massive conifer mortality due to chronic temperature rise. *Nature Climate Change*. 2015;6(3):295-300. doi:10.1038/nclimate2873

218. Sáenz-Romero C, Kremer A, Nagy L, et al. Common Garden comparisons confirm inherited differences in sensitivity to climate change between forest tree species. *PeerJ*. 2019;7(1). doi:10.7717/PEERJ.6213

219. Xie D, Du H, Xu WH, Ran JH, Wang XQ. Effects of climate change on richness distribution patterns of threatened conifers endemic to China. *Ecological Indicators*. 2022;136:108594. doi:10.1016/J.ECOLIND.2022.108594

220. Barber VA, Juday GP, Finney BP. Reduced growth of Alaskan white spruce in the twentieth century from temperature-induced drought stress. *Nature*. 2000;405(6787):668-673. doi:10.1038/35015049

221. Andalo C, Beaulieu J, Bousquet J. The impact of climate change on growth of local white spruce populations in Québec, Canada. *Forest Ecology and Management*. 2005;205(1-3):169-182. doi:10.1016/J.FORECO.2004.10.045
222. Hamann A, Wang T. Potential effects of climate change on ecosystem and tree species distribution in british columbia. *Ecology*. 2006;87(11):2773-2786. doi:10.1890/0012-9658
223. Russell JH, Krakowski J. Geographic variation and adaptation to current and future climates of Callitropsis nootkatensis populations. *Canadian Journal of Forest Research*. 2012;42(12):2118-2129. doi:10.1139/CJFR-2012-0240
224. Chen HYH, Luo Y. Net aboveground biomass declines of four major forest types with forest ageing and climate change in western Canada's boreal forests. *Global Change Biology*. 2015;21(10):3675-3684. doi:10.1111/GCB.12994
225. Charney ND, Babst F, Poulter B, et al. Observed Forest sensitivity to climate implies large changes in 21st century North American forest growth. *Ecology Letters*. 2016;19(9):1119-1128. doi:10.1111/ELE.12650
226. Seidl R, Thom D, Kautz M, et al. Forest disturbances under climate change. *Nature Climate.* 2017;7(6):395-402. doi:10.1038/nclimate3303
227. Bell DM, Pabst RJ, Shaw DC. Tree growth declines and mortality were associated with a parasitic plant during warm and dry climatic conditions in a temperate coniferous forest ecosystem. *Global Change Biology*. 2020;26(3):1714-1724. doi:10.1111/GCB.14834
228. Rajora OP, Mann IK, Shi YZ. Genetic diversity and population structure of boreal white spruce (*Picea glauca*) in pristine conifer-dominated and mixedwood forest stands. *Canadian Journal of Botany*. 2005;83(9):1096-1105. doi:10.1139/B05-083
229. Shalev TJ, El-Dien OG, Yuen MMS, et al. The western redcedar genome reveals low genetic diversity in a self-compatible conifer. *Genome Res*. 2022;32(10):1952-1964. doi:10.1101/GR.276358.121
230. Guillermo Gea-Izquierdo. The relationship between productivity and tree-ring growth in boreal coniferous forests. *Boreal Environment Research*. 2014; 19(5): 363–378.
231. Montwé D, Isaac-Renton M, Hamann A, Spiecker H. Drought tolerance and growth in populations of a wide-ranging tree species indicate climate change risks for the boreal north. *Global Change Biology*. 2016;22(2):806-815. doi:10.1111/GCB.13123
232. Sánchez-Gómez D, Velasco-Conde T, Cano-Martín FJ, Ángeles Guevara M, Teresa Cervera M, Aranda I. Inter-clonal variation in functional traits in response to drought for a genetically homogeneous Mediterranean conifer. *Environmental and Experimental Botany*. 2011;70(2-3):104-109. doi:10.1016/J.ENVEXPBOT.2010.08.007

233. de Miguel M, Cabezas JA, de María N, et al. Genetic control of functional traits related to photosynthesis and water use efficiency in Pinus pinaster Ait. drought response: Integration of genome annotation, allele association and QTL detection for candidate gene identification. *BMC Genomics*. 2014;15(1):1-19. doi:10.1186/1471-2164-15-464
234. Wei X, Benowicz A, Sebastian-Azcona J, Thomas BR. Genetic variation in leaf traits and gas exchange responses to vapour pressure deficit in contrasting conifer species. *Functional Ecology*. 2022;36(4):1036-1046. doi:10.1111/1365-2435.14007
235. Finkeldey R, Baldi P, Porta N la. Toward the Genetic Improvement of Drought Tolerance in Conifers: An Integrated Approach. *Forests*. 2022;13(12):2016. doi:10.3390/F13122016
236. Soudzilovskaia NA, Elumeeva TG, Onipchenko VG, et al. Functional traits predict relationship between plant abundance dynamic and long-term climate warming. *Proceedings of the National Academy of Sciences*. 2013;110(45):18180-18184. doi:10.1073/PNAS.1310700110
237. Choat B, Jansen S, Brodribb TJ, et al. Global convergence in the vulnerability of forests to drought. *Nature*. 2012;491(7426):752-755. doi:10.1038/nature11688
238. Sperry JS, Love DM. What plant hydraulics can tell us about responses to climate-change droughts. *New Phytologist*. 2015;207(1):14-27. doi:10.1111/NPH.13354
239. Anderegg WRL, Klein T, Bartlett M, et al. Meta-analysis reveals that hydraulic traits explain cross-species patterns of drought-induced tree mortality across the globe. *Proceedings of the National Academy of Sciences*. 2016;113(18):5024-5029. doi:10.1073/PNAS.1525678113
240. Arend M, Link RM, Patthey R, Hoch G, Schuldt B, Kahmen A. Rapid hydraulic collapse as cause of drought-induced mortality in conifers. *Proceedings of the National Academy of Sciences*. 2021;118(16):e2025251118. doi:10.1073/PNAS.2025251118
241. Sperry JS. Limitations on Stem Water Transport and Their Consequences. *Plant Stems.* 1995:105-124. doi:10.1016/B978-012276460-8/50007-2
242. Martin-StPaul N, Delzon S, Cochard H. Plant resistance to drought depends on timely stomatal closure. *Ecology Letters*. 2017;20(11):1437-1447. doi:10.1111/ELE.12851
243. Pivovaroff AL, Cook VMW, Santiago LS. Stomatal behaviour and stem xylem traits are coordinated for woody plant species under exceptional drought conditions. *Plant, Cell & Environment*. 2018;41(11):2617-2626. doi:10.1111/PCE.13367
244. Martínez-Vilalta J, Poyatos R, Aguadé D, Retana J, Mencuccini M. A new look at water transport regulation in plants. *New Phytologist*. 2014;204(1):105-115. doi:10.1111/NPH.12912
245. Skelton RP, West AG, Dawson TE. Predicting plant vulnerability to drought in biodiverse regions using functional traits. *Proceedings of the National Academy of Sciences*. 2015;112(18):5744-5749. doi:10.1073/PNAS.1503376112

246. Meinzer FC, Woodruff DR, Marias DE, et al. Mapping 'hydroscapes' along the iso- to anisohydric continuum of stomatal regulation of plant water status. *Ecology Letters*. 2016;19(11):1343-1352. doi:10.1111/ele.12670

247. Novick KA, Konings AG, Gentine P. Beyond soil water potential: An expanded view on isohydricity including land–atmosphere interactions and phenology. *Plant, Cell & Environment*. 2019;42(6):1802-1815. doi:10.1111/PCE.13517

248. Tardieu F, Simonneau T. Variability among species of stomatal control under fluctuating soil water status and evaporative demand: modelling isohydric and anisohydric behaviours. *Journal of Experimental Botany*. 1998;49(Special):419-432. doi:10.1093/jxb/49.Special_Issue.419

249. Klein T. The variability of stomatal sensitivity to leaf water potential across tree species indicates a continuum between isohydric and anisohydric behaviours. *Functional Ecology*. 2014;28(6):1313-1320. doi:10.1111/1365-2435.12289

250. Martínez-Vilalta J, Garcia-Forner N. Water potential regulation, stomatal behaviour and hydraulic transport under drought: deconstructing the iso/anisohydric concept. *Plant, Cell & Environment*. 2017;40(6):962-976. doi:10.1111/pce.12846

251. Fu X, Meinzer FC. Metrics and proxies for stringency of regulation of plant water status (iso/anisohydry): a global data set reveals coordination and trade-offs among water transport traits. *Tree Physiology*. 2019;39(1):122-134. doi:10.1093/TREEPHYS/TPY087

252. Hochberg U, Rockwell FE, Holbrook NM, Cochard H. Iso/Anisohydry: A Plant–Environment Interaction Rather Than a Simple Hydraulic Trait. *Trends in Plant Science*. 2018;23(2):112-120. doi:10.1016/J.TPLANTS.2017.11.002

253. Ratzmann G, Meinzer FC, Tietjen B. Iso/Anisohydry: Still a Useful Concept. *Trends in Plant Science*. 2019;24(3):191-194. doi:10.1016/J.TPLANTS.2019.01.001

254. Hartmann H, Link RM, Schuldt B. A whole-plant perspective of isohydry: stem-level support for leaf-level plant water regulation. *Tree Physiology*. 2021;41(6):901-905. doi:10.1093/TREEPHYS/TPAB011

255. Bartlett MK, Klein T, Jansen S, Choat B, Sack L. The correlations and sequence of plant stomatal, hydraulic, and wilting responses to drought. *Proceedings of the National Academy of Sciences*. 2016;113(46):13098-13103. doi:10.1073/pnas.1604088113

256. McCulloh KA, Domec JC, Johnson DM, Smith DD, Meinzer FC. A dynamic yet vulnerable pipeline: Integration and coordination of hydraulic traits across whole plants. *Plant, Cell & Environment*. 2019;42(10):2789-2807. doi:10.1111/PCE.13607

257. Dickman LT, Mcdowell NG, Sevanto S, Pangle RE, Pockman WT. Carbohydrate dynamics and mortality in a piñon-juniper woodland under three future precipitation scenarios. *Plant, Cell & Environment*. 2015;38(4):729-739. doi:10.1111/PCE.12441/

258. Meinzer FC, Woodruff DR, Marias DE, Mcculloh KA, Sevanto S. Dynamics of leaf water relations components in co-occurring iso- and anisohydric conifer species. *Plant, Cell & Environment*. 2014;37(11):2577-2586. doi:10.1111/PCE.12327/

259. Roman DT, Novick KA, Brzostek ER, Dragoni D, Rahman F, Phillips RP. The role of isohydric and anisohydric species in determining ecosystem-scale response to severe drought. *Oecologia*. 2015;179(3):641-654. doi:10.1007/s00442-015-3380-9

260. Jiang P, Meinzer FC, Fu X, Kou L, Dai X, Wang H. Trade-offs between xylem water and carbohydrate storage among 24 coexisting subtropical understory shrub species spanning a spectrum of isohydry. *Tree Physiology*. 2021;41(3):403-415. doi:10.1093/TREEPHYS/TPAA138

261. Benson MC, Oishi AC, Miniat C, Missik J, Novick KA. Anisohydric species have more vulnerable xylem than isohydric species in Eastern US forests. *Plant Cell and Environment.* 2022; 45(2): 329–346. doi: 10.1111/pce.14244

262. Benson MC, Miniat CF, Oishi AC, et al. The xylem of anisohydric Quercus alba L. is more vulnerable to embolism than isohydric codominants. *Plant, Cell & Environment*. 2022;45(2):329-346. doi:10.1111/PCE.14244

263. Gallé Á, Csiszár J, Benyó D, et al. Isohydric and anisohydric strategies of wheat genotypes under osmotic stress: Biosynthesis and function of ABA in stress responses. *Journal of Plant Physiology* 2013;170(16):1389-1399. doi:10.1016/J.JPLPH.2013.04.010

264. Coupel-Ledru A, Lebon É, Christophe A, et al. Genetic variation in a grapevine progeny (Vitis vinifera L. cvs Grenache×Syrah) reveals inconsistencies between maintenance of daytime leaf water potential and response of transpiration rate under drought. *Journal of Experimental Botany*. 2014;65(21):6205-6218. doi:10.1093/JXB/ERU228

265. Dal Santo S, Palliotti A, Zenoni S, et al. Distinct transcriptome responses to water limitation in isohydric and anisohydric grapevine cultivars. *BMC Genomics*. 2016;17(1):1-19. doi:10.1186/S12864-016-3136-X

266. Shelden MC, Vandeleur R, Kaiser BN, Tyerman SD. A comparison of petiole hydraulics and aquaporin expression in an anisohydric and isohydric cultivar of grapevine in response to water-stress induced cavitation. *Frontiers in Plant Science*. 2017;8:1893. doi:10.3389/FPLS.2017.01893/

267. Pashkovskiy PP, Vankova R, Zlobin IE, et al. Comparative analysis of abscisic acid levels and expression of abscisic acid-related genes in Scots pine and Norway spruce seedlings under water deficit. *Plant Physiology and Biochemistry*. 2019;140:105-112. doi:10.1016/J.PLAPHY.2019.04.037

268. Plaut JA, Yepez EA, Hill J, et al. Hydraulic limits preceding mortality in a piñon–juniper woodland under experimental drought. *Plant, Cell & Environment*. 2012;35(9):1601-1617. doi:10.1111/J.1365-3040.2012.02512.X

269. Woodruff DR, Meinzer FC, Marias DE, Sevanto S, Jenkins MW, Mcdowell NG. Linking nonstructural carbohydrate dynamics to gas exchange and leaf hydraulic behavior *in Pinus edulis* and *Juniperus monosperma*. *New Phytologist*. 2015;206(1):411-421. doi:10.1111/NPH.13170

270. Gu L, Pallardy SG, Hosman KP, Sun Y. Predictors and mechanisms of mortality of tree species Predictors and mechanisms of the drought-influenced mortality of tree species along the isohydric to anisohydic continuum in a decade-long study of a central US temperate forest Predictors and mechanisms of mortality of tree species. *Biogeosciences Discussions*. 2015;12:1285-1325. doi:10.5194/bgd-12-1285-2015

271. Nolan RH, Tarin T, Santini NS, McAdam SAM, Ruman R, Eamus D. Differences in osmotic adjustment, foliar abscisic acid dynamics, and stomatal regulation between an isohydric and anisohydric woody angiosperm during drought. *Plant, Cell & Environment*. 2017;40(12):3122-3134. doi:10.1111/PCE.13077

272. Hemberg T. Growth-Inhibiting Substances in Terminal Buds of Fraxinus. *Physiologia Plantarum*. 1949;2(1):37-44. doi:10.1111/J.1399-3054.1949.TB07646.X

273. Hemberg T. Significance of Growth-Inhibiting Substances and Auxins for the Rest-Period of the Potato Tuber. *Physiologia Plantarum*. 1949;2(1):24-36. doi:10.1111/J.1399-3054.1949.TB07645.X

274. Eagles CF, Wareing PF. Dormancy Regulators in Woody Plants: Experimental Induction of Dormancy in Betula pubescens. *Nature*. 1963;199(4896):874-875. doi:10.1038/199874a0

275. Ohkuma K, Lyon JL, Addicott FT, Smith OE. Abscisin II, an Abscission-Accelerating Substance from Young Cotton Fruit. *Science*. 1963;142(3599):1592-1593. doi:10.1126/SCIENCE.142.3599.1592

276. Cornforth JW, Milborrow B v., Ryback G, Wareing PF. Chemistry and Physiology of 'Dormins' In Sycamore: Identity of Sycamore 'Dormin' with Abscisin II. *Nature.* 1965;205(4978):1269-1270. doi:10.1038/2051269b0

277. Addicott FT, Lyon JL, Ohkuma K, et al. Abscisic Acid: A New Name for Abscisin II (Dormin). *Science*. 1968;159(3822):1493-1493. doi:10.1126/SCIENCE.159.3822.1493.B
278. Wright STC, Hiron RWP, Wright STC, Hiron RWP. (+)-Abscisic Acid, the Growth Inhibitor induced in Detached Wheat Leaves by a Period of Wilting. *Nature*. 1969;224(5220):719-720. doi:10.1038/224719A0
279. Mittelheuser CJ, van Steveninck RFM. Stomatal Closure and Inhibition of Transpiration induced by (RS)-Abscisic Acid. *Nature.* 1969;221(5177):281-282. doi:10.1038/221281a0
280. Jones RJ, Mansfield TA. Suppression of Stomatal Opening in Leaves Treated with Abscisic Acid. *Journal of Experimental Botany*. 1970;21(3):714-719. doi:10.1093/JXB/21.3.714
281. Taylor IB, Linforth RST, Al-Naieb RJ, Bowman WR, Marples BA. The wilty tomato mutants flacca and sitiens are impaired in the oxidation of ABA-aldehyde to ABA. *Plant, Cell & Environment*. 1988;11(8):739-745. doi:10.1111/J.1365-3040.1988.TB01158.X
282. Duckham SC, Taylor IB, Linforth RST, Al-Naieb RJ, Marples BA, Bowman WR. The Metabolism of cis ABA-aldehyde by the Wilty Mutants of Potato, Pea and Arabidopsis thaliana. *Journal of Experimental Botany*. 1989;40(8):901-905. doi:10.1093/JXB/40.8.901
283. Walker-Simmons M, Kudrna DA, Warner RL. Reduced Accumulation of ABA during Water Stress in a Molybdenum Cofactor Mutant of Barley. *Plant Physiology* 1989;90(2):728-733. doi:10.1104/PP.90.2.728
284. Mccarty DR, Carson CB, Stinard PS, Robertsonb DS. Molecular Analysis of viviparous-1: An Abscisic Acid-Insensitive Mutant of Maize. *Plant Cell*. 1989;1(5):523-532. doi:10.1105/TPC.1.5.523
285. Rock CD, Zeevaart JAD. The aba mutant of *Arabidopsis thaliana* is impaired in epoxy-carotenoid biosynthesis. *Proceedings of the National Academy of Sciences*. 1991;88(17):7496-7499. doi:10.1073/PNAS.88.17.7496
286. Koornneef M, Reuling G, Karssen CM. The isolation and characterization of abscisic acid-insensitive mutants of Arabidopsis thaliana. *Physiologia Plantarum*. 1984;61(3):377-383. doi:10.1111/J.1399-3054.1984.TB06343.X
287. Neill SJ, Horgan R. Abscisic Acid Production and Water Relations in Wilty Tomato Mutants Subjected to Water Deficiency. *Journal of Experimental Botany*. 1985;36(8):1222-1231. doi:10.1093/JXB/36.8.1222
288. Yoshida T, Fujita Y, Sayama H, et al. AREB1, AREB2, and ABF3 are master transcription factors that cooperatively regulate ABRE-dependent ABA signaling involved in drought stress tolerance and require ABA for full activation. *The Plant Journal*. 2010;61(4):672-685. doi:10.1111/J.1365-313X.2009.04092.X

289. Koornneef M, Jorna ML, Brinkhorst-van der Swan DLC, Karssen CM. The isolation of abscisic acid (ABA) deficient mutants by selection of induced revertants in non-germinating gibberellin sensitive lines of Arabidopsis thaliana (L.) heynh. *Theoretical and Applied Genetics*. 1982;61(4):385-393. doi:10.1007/BF00272861

290. Koornneef M, Hanhart CJ, Hilhorst HWM, Karssen CM. In Vivo Inhibition of Seed Development and Reserve Protein Accumulation in Recombinants of Abscisic Acid Biosynthesis and Responsiveness Mutants in Arabidopsis thaliana. *Plant Physiology* 1989;90(2):463-469. doi:10.1104/PP.90.2.463

291. Mccarty DR. Genetic control and integration of maturation and germination pathways in seed development. *Annu Rev Plant Physiologia Plantarum Mol Bioi*. 1995;46:71-93

292. Chater CCC, Oliver J, Casson S, Gray JE. Putting the brakes on: abscisic acid as a central environmental regulator of stomatal development. *New Phytologist*. 2014;202(2):376-391. doi:10.1111/NPH.12713

293. Nambara E, Marion-Poll A. Abscisic Acid Biosynthesis and Catabolism. *Annu Rev Plant Biology.* 2005;56(1):165-185. doi:10.1146/annurev.arplant.56.032604.144046

294. Hirai N, Yoshida R, Todoroki Y, Ohigashi H. Biosynthesis of Abscisic Acid by the Non-mevalonate Pathway in Plants, and by the Mevalonate Pathway in Fungi. *Bioscience, Biotechnology, and Biochemistry*. 2000;64(7):1448-1458. doi:10.1271/BBB.64.1448

295. Siewers V, Kokkelink L, Smedsgaard J, Tudzynski P. Identification of an abscisic acid gene cluster in the grey mold Botrytis cinerea. *Applied and Environmental Microbiology*. 2006;72(7):4619-4626. doi: 10.1128/AEM.02919-05

296. Spence CA, Lakshmanan V, Donofrio N, Bais HP. Crucial roles of abscisic acid biogenesis in virulence of rice blast fungus Magnaporthe oryzae. *Frontiers in Plant Science*. 2015;6(DEC):1082. doi:10.3389/FPLS.2015.01082/

297. Lievens L, Pollier J, Goossens A, Beyaert R, Staal J. Abscisic acid as pathogen effector and immune regulator. *Frontiers in Plant Science*. 2017;8:587. doi:10.3389/FPLS.2017.00587/

298. Izquierdo-Bueno I, González-Rodríguez VE, Simon A, et al. Biosynthesis of abscisic acid in fungi: identification of a sesquiterpene cyclase as the key enzyme in Botrytis cinerea. *Environmental Microbiology*. 2018;20(7):2469-2482. doi:10.1111/1462-2920.14258

299. Takino J, Kozaki T, Ozaki T, Liu C, Minami A, Oikawa H. Elucidation of biosynthetic pathway of a plant hormone abscisic acid in phytopathogenic fungi. *Bioscience, Biotechnology, and Biochemistry*. 2019;83(9):1642-1649. doi:10.1080/09168451.2019.1618700

300. Li HH, Hao RL, Wu SS, et al. Occurrence, function and potential medicinal applications of the phytohormone abscisic acid in animals and humans. *Biochemical Pharmacology*. 2011;82(7):701-712. doi:10.1016/J.BCP.2011.06.042
301. Takezawa D, Komatsu K, Sakata Y. ABA in bryophytes: How a universal growth regulator in life became a plant hormone? *Journal of Plant Research*. 2011;124(4):437-453. doi:10.1007/S10265-011-0410-5
302. Robertson DS. The Genetics of Vivipary in Maize. *Genetics*. 1955;40(5):745. doi:10.1093/GENETICS/40.5.745
303. Robichaud CS, Wong J, Sussex IM. Control of in vitro growth of viviparous embryo mutants of maize by abscisic acid. *Developmental Genetics*. 1979;1(4):325-330. doi:10.1002/DVG.1020010405
304. Robichaud C, Sussex IM. The Response of Viviparous-1 and Wild Type Embryos of *Zea mays* to Culture in the Presence of Abscisic Acid. *Journal of Plant Physiology* 1986;126(2-3):235-242. doi:10.1016/S0176-1617(86)80025-6
305. Ober ES, Setter TL. Water Deficit Induces Abscisic Acid Accumulation in Endosperm of Maize Viviparous Mutants. *Plant Physiology* 1992;98(1):353-356. doi:10.1104/PP.98.1.353
306. Wang Y, Zhang J, Sun M, et al. Multi-omics analyses reveal systemic insights into maize vivipary. *Plants*. 2021;10(11):2437. doi:10.3390/PLANTS10112437/S1
307. Chen K, Li GJ, Bressan RA, Song CP, Zhu JK, Zhao Y. Abscisic acid dynamics, signaling, and functions in plants. *Journal of Integrative Plant Biology.* 2020;62(1):25-54. doi:10.1111/JIPB.12899
308. Hsu PK, Dubeaux G, Takahashi Y, Schroeder JI. Signaling mechanisms in abscisic acid-mediated stomatal closure. *The Plant Journal*. 2021;105(2):307-321. doi:10.1111/TPJ.15067
309. Waadt R, Seller CA, Hsu PK, Takahashi Y, Munemasa S, Schroeder JI. Plant hormone regulation of abiotic stress responses. *Nature Reviews Molecular Cell Biology*. 2022;23(10):680-694. doi:10.1038/s41580-022-00479-6
310. Marin E, Nussaume L, Quesada A, et al. Molecular identification of zeaxanthin epoxidase of *Nicotiana plumbaginifolia*, a gene involved in abscisic acid biosynthesis and corresponding to the ABA locus of Arabidopsis thaliana. *EMBO J*. 1996;15(10):2331. doi:10.1002/j.1460-2075.1996.tb00589.x
311. Audran C, Borel C, Frey A, et al. Expression Studies of the Zeaxanthin Epoxidase Gene in *Nicotiana plumbaginifolia*. *Plant Physiology* 1998;118(3):1021. doi:10.1104/PP.118.3.1021

312. Audran C, Liotenberg S, Gonneau M, et al. Localisation and expression of zeaxanthin epoxidase mRNA in Arabidopsis in response to drought stress and during seed development. *Australian Journal of Plant Physiology* 2001;28(12):1161-1173. doi:10.1071/pp00134
313. Xiong L, Lee H, Ishitani M, Zhu JK. Regulation of osmotic stress-responsive gene expression by the LOS6/ABA1 locus in Arabidopsis. *Journal of Biological Chemistry*. 2002;277(10):8588-8596. doi:10.1074/jbc.M109275200
314. North HM, Almeida A de, Boutin JP, et al. The Arabidopsis ABA-deficient mutant aba4 demonstrates that the major route for stress-induced ABA accumulation is via neoxanthin isomers. *The Plant Journal*. 2007;50(5):810-824. doi:10.1111/J.1365-313X.2007.03094.X
315. Neuman H, Galpaz N, Cunningham FX, Zamir D, Hirschberg J. The tomato mutation nxd1 reveals a gene necessary for neoxanthin biosynthesis and demonstrates that violaxanthin is a sufficient precursor for abscisic acid biosynthesis. *The Plant Journal*. 2014;78(1):80-93. doi:10.1111/TPJ.12451
316. Qin X, Zeevaart JAD. The 9-cis-epoxycarotenoid cleavage reaction is the key regulatory step of abscisic acid biosynthesis in water-stressed bean. *Proceedings of the National Academy of Sciences*. 1999;96(26):15354-15361. doi:10.1073/pnas.96.26.15354
317. Iuchi S, Kobayashi M, Taji T, et al. Regulation of drought tolerance by gene manipulation of 9-cis-epoxycarotenoid dioxygenase, a key enzyme in abscisic acid biosynthesis in Arabidopsis. *The Plant Journal*. 2001;27(4):325-333. doi:10.1046/J.1365-313X.2001.01096.X
318. Schwartz SH, Tan BC, Gage DA, Zeevaart JAD, McCarty DR. Specific oxidative cleavage of carotenoids by VP14 of maize. *Science*. 1997;276(5320):1872-1874. doi:10.1126/science.276.5320.1872
319. Tan BC, Schwartz SH, Zeevaart JAD, Mccarty DR. Genetic control of abscisic acid biosynthesis in maize. *Proceedings of the National Academy of Sciences*. 1997;94(22):12235-12240. doi: 10.1073/PNAS.94.22.12235
320. Schwartz SH, Qin X, Zeevaart JAD. Elucidation of the Indirect Pathway of Abscisic Acid Biosynthesis by Mutants, Genes, and Enzymes. *Plant Physiology* 2003;131(4):1591-1601. doi:10.1104/PP.102.017921
321. Tan BC, Schwartz SH, Zeevaart JAD, McCarty DR. Genetic control of abscisic acid biosynthesis in maize. *Proceedings of the National Academy of Sciences*. 1997;94(22):12235-12240. doi:10.1073/pnas.94.22.12235
322. Burbidge A, Burbidge A, Grieve T, et al. Structure and expression of a cDNA encoding a putative neoxanthin cleavage enzyme (NCE), isolated from a wilt-related tomato

(*Lycopersicon esculentum* Mill.) library. *Journal of Experimental Botany*. 1997;48(314):2111-2112. doi:10.1093/jxb/48.12.2111

323. Chernys JT, Zeevaart JAD. Characterization of the 9-cis-epoxycarotenoid dioxygenase gene family and the regulation of abscisic acid biosynthesis in avocado. *Plant Physiology* 2000;124(1):343-353. doi:10.1104/PP.124.1.343
324. Tan BC, Joseph LM, Deng WT, et al. Molecular characterization of the Arabidopsis 9-cis epoxycarotenoid dioxygenase gene family. *The Plant Journal*. 2003;35(1):44-56. doi:10.1046/J.1365-313X.2003.01786.X
325. Auldridge ME, McCarty DR, Klee HJ. Plant carotenoid cleavage oxygenases and their apocarotenoid products. *Current Opinion in Plant Biology.* 2006;9(3):315-321. doi:10.1016/J.PBI.2006.03.005
326. Priya R, Siva R. Analysis of phylogenetic and functional diverge in plant nine-cis epoxycarotenoid dioxygenase gene family. *Journal of Plant Research*. 2015;128(4):519-534. doi:10.1007/s10265-015-0726-7
327. Cheng WH, Endo A, Zhou L, et al. A Unique Short-Chain Dehydrogenase/Reductase in Arabidopsis Glucose Signaling and Abscisic Acid Biosynthesis and Functions. *Plant Cell*. 2002;14(11):2723-2743. doi:10.1105/TPC.006494
328. González-Guzmán M, Apostolova N, Bellés JM, et al. The short-chain alcohol dehydrogenase ABA2 catalyzes the conversion of xanthoxin to abscisic aldehyde. *Plant Cell*. 2002;14(8):1833-1846. doi:10.1105/TPC.002477
329. Seo M, Peeters AJM, Koiwai H, et al. The Arabidopsis aldehyde oxidase 3 (AAO3) gene product catalyzes the final step in abscisic acid biosynthesis in leaves. *Proceedings of the National Academy of Sciences*. 2000;97(23):12908-12913. doi:10.1073/PNAS.220426197
330. Bittner F, Oreb M, Mendel RR. ABA3 Is a Molybdenum Cofactor Sulfurase Required for Activation of Aldehyde Oxidase and Xanthine Dehydrogenase in Arabidopsis thaliana. *Journal of Biological Chemistry*. 2001;276(44):40381-40384. doi:10.1074/JBC.C100472200
331. Dietz1 KJ, Sauter1 A, Wichert1 K, Messdaghi2 D, Hartung1 W. Extracellular b-glucosidase activity in barley involved in the hydrolysis of ABA glucose conjugate in leaves. *Journal of Experimental Botany*. 2000;51(346):937-944.
332. Lee KH, Piao HL, Kim HY, et al. Activation of Glucosidase via Stress-Induced Polymerization Rapidly Increases Active Pools of Abscisic Acid. *Cell*. 2006;126(6):1109-1120. doi:10.1016/J.CELL.2006.07.034

333. Xu ZY, Lee KH, Dong T, et al. A Vacuolar β-Glucosidase Homolog That Possesses Glucose-Conjugated Abscisic Acid Hydrolyzing Activity Plays an Important Role in Osmotic Stress Responses in Arabidopsis. *Plant Cell*. 2012;24(5):2184-2199. doi:10.1105/TPC.112.095935

334. Liu Z, Yan JP, Li DK, et al. UDP-Glucosyltransferase71C5, a Major Glucosyltransferase, Mediates Abscisic Acid Homeostasis in Arabidopsis. *Plant Physiology* 2015;167(4):1659-1670. doi:10.1104/PP.15.00053

335. Krochko JE, Abrams GD, Loewen MK, Abrams SR, Cutler AJ. (+)-Abscisic Acid 8′-Hydroxylase Is a Cytochrome P450 Monooxygenase. *Plant Physiology* 1998;118(3):849. doi:10.1104/PP.118.3.849

336. Cutler AJ, Krochko JE. Formation and breakdown of ABA. *Trends in Plant Science*. 1999;4(12):472-478. doi:10.1016/S1360-1385(99)01497-1

337. Kushiro T, Okamoto M, Nakabayashi K, et al. The Arabidopsis cytochrome P450 CYP707A encodes ABA 8'-hydroxylases: key enzymes in ABA catabolism. *EMBO J*. 2004;23(7):1647-1656. doi:10.1038/SJ.EMBOJ.7600121

338. Saito S, Hirai N, Matsumoto C, et al. Arabidopsis CYP707As encode (+)-abscisic acid 8'-hydroxylase, a key enzyme in the oxidative catabolism of abscisic acid. *Plant Physiology* 2004;134(4):1439-1449. doi:10.1104/PP.103.037614

339. Umezawa T, Okamoto M, Kushiro T, Nambara E, Oono Y, Seki M. CYP707A3 a major ABA 8'-hydroxylase involved in dehydration and rehydration response in *Arabidopsis thaliana*. *The Plant Journal*. 2006;46(2):171-82. doi: 10.1111/j.1365-313X.2006.02683.x.

340. Okamoto M, Tanaka Y, Abrams SR, Kamiya Y, Seki M, Nambara E. High Humidity Induces Abscisic Acid 8′-Hydroxylase in Stomata and Vasculature to Regulate Local and Systemic Abscisic Acid Responses in Arabidopsis. *Plant Physiology* 2009;149(2):825-834. doi:10.1104/PP.108.130823

341. Walton DC, Dorn B, Fey J. The isolation of an abscisic-acid metabolite, 4′-dihydrophaseic acid, from non-imbibed Phaseolus vulgaris seed. *Planta*. 1973;112(1):87-90. doi:10.1007/BF00386035

342. Milborrow B, Vaughan G. Characterization of Dihydrophaseic Acid 4′-O- β -D-Glucopyranoside as a Major Metabolite of Abscisic Acid. *Functional Plant Biology*. 1982;9(3):361-372. doi:10.1071/PP9820361

343. del Refugio Ramos M, Jerz G, Villanueva S, López-Dellamary F, Waibel R, Winterhalter P. Two glucosylated abscisic acid derivates from avocado seeds (Persea americana Mill. Lauraceae cv. Hass). *Phytochemistry*. 2004;65(7):955-962. doi:10.1016/J.PHYTOCHEM.2003.12.007

344. Cai L, Liu CS, Fu XW, et al. Two new glucosides from the pellicle of the walnut (*Juglans regia*). *Natural Products and Bioprospecting*. 2012;2(4):150-153. doi:10.1007/S13659-012-0009-0

345. Weng JK, Ye M, Li B, Noel JP. Co-evolution of Hormone Metabolism and Signaling Networks Expands Plant Adaptive Plasticity. *Cell*. 2016;166(4):881-893. doi:10.1016/J.CELL.2016.06.027

346. Wilkinson S, Davies WJ. Xylem Sap pH Increase: A Drought Signal Received at the Apoplastic Face of the Guard Cell That Involves the Suppression of Saturable Abscisic Acid Uptake by the Epidermal Symplast. *Plant Physiology* 1997;113(2):559-573. doi:10.1104/PP.113.2.559

347. Xie X, Wang Y, Williamson L, et al. The Identification of Genes Involved in the Stomatal Response to Reduced Atmospheric Relative Humidity. *Current Biology*. 2006;16(9):882-887. doi:10.1016/j.cub.2006.03.028

348. Park J, Lee Y, Martinoia E, Geisler M. Plant hormone transporters: what we know and what we would like to know. *BMC Biology*. 2017;15(1):1-15. doi:10.1186/S12915-017-0443-X

349. Kuromori T, Seo M, Shinozaki K. ABA Transport and Plant Water Stress Responses. *Trends in Plant Science*. 2018;23(6):513-522. doi:10.1016/J.TPLANTS.2018.04.001

350. Kuromori T, Miyaji T, Yabuuchi H, et al. ABC transporter AtABCG25 is involved in abscisic acid transport and responses. *Proceedings of the National Academy of Sciences*. 2010;107(5):2361-2366. doi:10.1073/PNAS.0912516107

351. Kuromori T, Sugimoto E, Shinozaki K. Arabidopsis mutants of AtABCG22, an ABC transporter gene, increase water transpiration and drought susceptibility. *The Plant Journal*. 2011;67(5):885-894. doi:10.1111/J.1365-313X.2011.04641.X

352. Kuromori T, Fujita M, Urano K, Tanabata T, Sugimoto E, Shinozaki K. Overexpression of AtABCG25 enhances the abscisic acid signal in guard cells and improves plant water use efficiency. *Plant Science*. 2016;251:75-81. doi:10.1016/J.PLANTSCI.2016.02.019

353. Park Y, Xu ZY, Kim SY, et al. Spatial Regulation of ABCG25, an ABA Exporter, Is an Important Component of the Mechanism Controlling Cellular ABA Levels. *Plant Cell*. 2016;28(10):2528-2544. doi:10.1105/TPC.16.00359

354. Kang J, Hwang JU, Lee M, et al. PDR-type ABC transporter mediates cellular uptake of the phytohormone abscisic acid. *Proceedings of the National Academy of Sciences*. 2010;107(5):2355-2360. doi:10.1073/PNAS.0909222107

355. Kang J, Yim S, Choi H, et al. Abscisic acid transporters cooperate to control seed germination. *Nature Communications*. 2015;6(1):1-10. doi:10.1038/ncomms9113

356. Kanno Y, Hanada A, Chiba Y, et al. Identification of an abscisic acid transporter by functional screening using the receptor complex as a sensor. *Proceedings of the National Academy of Sciences*. 2012;109(24):9653-9658. doi:10.1073/PNAS.1203567109

357. Zhang H, Zhu H, Pan Y, Yu Y, Luan S, Li L. A DTX/MATE-Type Transporter Facilitates Abscisic Acid Efflux and Modulates ABA Sensitivity and Drought Tolerance in Arabidopsis. *Molecular Plant*. 2014;7(10):1522-1532. doi:10.1093/MP/SSU063

358. Park SY, Fung P, Nishimura N, et al. Abscisic acid inhibits type 2C protein phosphatases via the PYR/PYL family of START proteins. *Science*. 2009;324(5930):1068-1071. doi:10.1126/SCIENCE.1173041

359. Ma Y, Szostkiewicz I, Korte A, et al. Regulators of PP2C phosphatase activity function as abscisic acid sensors. *Science*. 2009;324(5930):1064-1068. doi:10.1126/SCIENCE.1172408

360. Gonzalez-Guzman M, Pizzio GA, Antoni R, et al. Arabidopsis PYR/PYL/RCAR Receptors Play a Major Role in Quantitative Regulation of Stomatal Aperture and Transcriptional Response to Abscisic Acid. *Plant Cell*. 2012;24(6):2483-2496. doi:10.1105/TPC.112.098574

361. Tischer S v., Wunschel C, Papacek M, et al. Combinatorial interaction network of abscisic acid receptors and coreceptors from Arabidopsis thaliana. *Proceedings of the National Academy of Sciences*. 2017;114(38):10280-10285. doi:10.1073/PNAS.1706593114

362. Dittrich M, Mueller HM, Bauer H, et al. The role of Arabidopsis ABA receptors from the PYR/PYL/RCAR family in stomatal acclimation and closure signal integration. *Nature Plants*. 2019;5(9):1002-1011. doi:10.1038/s41477-019-0490-0

363. Fujii H, Chinnusamy V, Rodrigues A, et al. In vitro reconstitution of an abscisic acid signalling pathway. *Nature*. 2009;462(7273):660-664. doi:10.1038/nature08599

364. Rubio S, Rodrigues A, Saez A, et al. Triple Loss of Function of Protein Phosphatases Type 2C Leads to Partial Constitutive Response to Endogenous Abscisic Acid. *Plant Physiology* 2009;150(3):1345-1355. doi:10.1104/PP.109.137174

365. Vlad F, Rubio S, Rodrigues A, et al. Protein Phosphatases 2C Regulate the Activation of the Snf1-Related Kinase OST1 by Abscisic Acid in Arabidopsis. *Plant Cell*. 2009;21(10):3170-3184. doi:10.1105/TPC.109.069179

366. Umezawa T, Sugiyama N, Mizoguchi M, et al. Type 2C protein phosphatases directly regulate abscisic acid-activated protein kinases in Arabidopsis. *Proceedings of the National Academy of Sciences*. 2009;106(41):17588-17593. doi:10.1073/PNAS.0907095106

367. Boudsocq M, Droillard MJ, Barbier-Brygoo H, Laurière C. Different phosphorylation mechanisms are involved in the activation of sucrose non-fermenting 1 related protein kinases

2 by osmotic stresses and abscisic acid. *Plant Molecular Biology*. 2007;63(4):491-503. doi:10.1007/S11103-006-9103-1

368. Vlad F, Droillard MJ, Valot B, et al. Phospho-site mapping, genetic and in planta activation studies reveal key aspects of the different phosphorylation mechanisms involved in activation of SnRK2s. *The Plant Journal*. 2010;63(5):778-790. doi:10.1111/J.1365-313X.2010.04281.X
369. Ng LM, Soon FF, Zhou XE, et al. Structural basis for basal activity and autoactivation of abscisic acid (ABA) signaling SnRK2 kinases. *Proceedings of the National Academy of Sciences*. 2011;108(52):21259-21264. doi:10.1073/PNAS.1118651109
370. Nguyen QTC, Lee SJ, Choi SW, et al. Arabidopsis Raf-Like Kinase Raf10 Is a Regulatory Component of Core ABA Signaling. *Molecules and Cells*. 2019;42(9):646. doi:10.14348/MOLCELLS.2019.0173
371. Yoshida R, Hobo T, Ichimura K, et al. ABA-activated SnRK2 protein kinase is required for dehydration stress signaling in Arabidopsis. *Plant & Cell Physiology*. 2002;43(12):1473-1483. doi:10.1093/PCP/PCF188
372. Mustilli AC, Merlot S, Vavasseur A, Fenzi F, Giraudat J. Arabidopsis OST1 protein kinase mediates the regulation of stomatal aperture by abscisic acid and acts upstream of reactive oxygen species production. *Plant Cell*. 2002;14(12):3089-3099. doi:10.1105/TPC.007906
373. Geiger D, Scherzer S, Mumm P, et al. Activity of guard cell anion channel SLAC1 is controlled by drought-stress signaling kinase-phosphatase pair. *Proceedings of the National Academy of Sciences*. 2009;106(50):21425-21430. doi:10.1073/PNAS.0912021106
374. Lee SC, Lan W, Buchanan BB, Luan S. A protein kinase-phosphatase pair interacts with an ion channel to regulate ABA signaling in plant guard cells. *Proceedings of the National Academy of Sciences*. 2009;106(50):21419-21424. doi:10.1073/PNAS.0910601106
375. Brandt B, Brodsky DE, Xue S, et al. Reconstitution of abscisic acid activation of SLAC1 anion channel by CPK6 and OST1 kinases and branched ABI1 PP2C phosphatase action. *Proceedings of the National Academy of Sciences*. 2012;109(26):10593-10598. doi:10.1073/PNAS.1116590109
376. Wang P, Xue L, Batelli G, et al. Quantitative phosphoproteomics identifies SnRK2 protein kinase substrates and reveals the effectors of abscisic acid action. *Proceedings of the National Academy of Sciences*. 2013;110(27):11205-11210. doi:10.1073/PNAS.1308974110
377. Pei ZM, Murata Y, Benning G, et al. Calcium channels activated by hydrogen peroxide mediate abscisic acid signalling in guard cells. *Nature*. 2000;406(6797):731-734. doi:10.1038/35021067

378. Hamilton DWA, Hills A, Köhler B, Blatt MR. Ca2+ channels at the plasma membrane of stomatal guard cells are activated by hyperpolarization and abscisic acid. *Proceedings of the National Academy of Sciences*. 2000;97(9):4967-4972. doi:10.1073/PNAS.080068897

379. Zou JJ, Wei FJ, Wang C, et al. Arabidopsis Calcium-Dependent Protein Kinase CPK10 Functions in Abscisic Acid- and Ca2+-Mediated Stomatal Regulation in Response to Drought Stress. *Plant Physiology* 2010;154(3):1232-1243. doi:10.1104/PP.110.157545

380. Chater C, Gray JE, Beerling DJ. Early evolutionary acquisition of stomatal control and development gene signalling networks. *Current Opinion in Plant Biology.* 2013;16(5):638-646. doi:10.1016/J.PBI.2013.06.013

381. Cai S, Chen G, Wang Y, et al. Evolutionary Conservation of ABA Signaling for Stomatal Closure. *Plant Physiology* 2017;174(2):732-747. doi:10.1104/PP.16.01848

382. Brodribb TJ, Sussmilch F, McAdam SAM. From reproduction to production, stomata are the master regulators. *The Plant Journal*. 2020;101(4):756-767. doi:10.1111/TPJ.14561

383. Sun Y, Pri-Tal O, Michaeli D, Mosquna A. Evolution of Abscisic Acid Signaling Module and Its Perception. *Frontiers in Plant Science*. 2020;11. doi:10.3389/FPLS.2020.00934

384. Reynolds TL, Bewley JD. Characterization of Protein Synthetic Changes in a Desiccation-Tolerant Fern, Polypodium virginianum. Comparison of the Effects of Drying, Rehydration and Abscisic Acid. *Journal of Experimental Botany*. 1993;44(5):921-928. doi:10.1093/JXB/44.5.921

385. Oliver MJ, Velten J, Mishler BD. Desiccation Tolerance in Bryophytes: A Reflection of the Primitive Strategy for Plant Survival in Dehydrating Habitats? *Integrative and Comparative Biology*. 2005;45(5):788-799. doi:10.1093/ICB/45.5.788

386. Wang X, Chen S, Zhang H, et al. Desiccation tolerance mechanism in resurrection fern-ally Selaginella tamariscina revealed by physiological and proteomic analysis. *Journal of Proteome Research*. 2010;9(12):6561-6577. doi:10.1021/PR100767K

387. Xiao L, Yobi A, Koster KL, He Y, Oliver MJ. Desiccation tolerance in Physcomitrella patens: Rate of dehydration and the involvement of endogenous abscisic acid (ABA). *Plant, Cell & Environment*. 2018;41(1):275-284. doi:10.1111/PCE.13096

388. Eklund DM, Kanei M, Flores-Sandoval E, et al. An Evolutionarily Conserved Abscisic Acid Signaling Pathway Regulates Dormancy in the Liverwort *Marchantia polymorpha*. *Current Biology*. 2018;28(22):3691-3699.e3. doi:10.1016/J.CUB.2018.10.018

389. Jahan A, Komatsu K, Wakida-Sekiya M, et al. Archetypal Roles of an Abscisic Acid Receptor in Drought and Sugar Responses in Liverworts. *Plant Physiology* 2019;179(1):317-328. doi:10.1104/PP.18.00761

390. Lin BL, Yang WJ. Blue Light and Abscisic Acid Independently Induce Heterophyllous Switch in Marsilea quadrifolia. *Plant Physiology* 1999;119(2):429-434. doi:10.1104/PP.119.2.429
391. Lin BL, Wang HJ, Wang JS, Zaharia LI, Abrams SR. Abscisic acid regulation of heterophylly in Marsilea quadrifolia L.: effects of R-(−) and S-(+) isomers. *Journal of Experimental Botany*. 2005;56(421):2935-2948. doi:10.1093/JXB/ERI290
392. McAdam SAM, Brodribb TJ, Banks JA, et al. Abscisic acid controlled sex before transpiration in vascular plants. *Proceedings of the National Academy of Sciences*. 2016;113(45):12862-12867. doi:10.1073/PNAS.1606614113
393. Zhang Y, Mutailifu A, Zhang Y, Yang H, Zhang D. Detection of abscisic acid and relative transcript abundance in *Syntrichia caninervis* Mitt. 2021;43(4):376-383. doi:10.1080/03736687.2021.1989927
394. Takezawa D, Watanabe N, Ghosh TK, et al. Epoxycarotenoid-mediated synthesis of abscisic acid in Physcomitrella patens implicating conserved mechanisms for acclimation to hyperosmosis in embryophytes. *New Phytologist*. 2015;206(1):209-219. doi:10.1111/NPH.13231
395. Ae SR, Timmerhaus G, Daniel AE, et al. Microarray analysis of the moss P*hyscomitrella patens* reveals evolutionarily conserved transcriptional regulation of salt stress and abscisic acid signalling. *Plant Molecular Biology*. 2009;72(1):27-45. doi:10.1007/S11103-009-9550-6
396. Hanada K, Hase T, Toyoda T, Shinozaki K, Okamoto M. Origin and evolution of genes related to ABA metabolism and its signaling pathways. *Journal of Plant Research*. 2011;124(4):455-465. doi:10.1007/S10265-011-0431-0
397. Komatsu K, Nishikawa Y, Ohtsuka T, et al. Functional analyses of the ABI1-related protein phosphatase type 2C reveal evolutionarily conserved regulation of abscisic acid signaling between Arabidopsis and the moss *Physcomitrella patens*. *Plant Molecular Biology*. 2009;70(3):327-340. doi:10.1007/S11103-009-9476-Z
398. Chater C, Kamisugi Y, Movahedi M, et al. Regulatory Mechanism Controlling Stomatal Behavior Conserved across 400 Million Years of Land Plant Evolution. *Current Biology*. 2011;21(12):1025-1029. doi:10.1016/J.CUB.2011.04.032
399. Hauser F, Waadt R, Schroeder JI. Evolution of Abscisic Acid Synthesis and Signaling Mechanisms. *Current Biology*. 2011;21(9):R346-R355. doi:10.1016/J.CUB.2011.03.015
400. O'Donoghue MT, Chater C, Wallace S, Gray JE, Beerling DJ, Fleming AJ. Genome-wide transcriptomic analysis of the sporophyte of the moss *Physcomitrella patens*. *Journal of Experimental Botany*. 2013;64(12):3567-3581. doi:10.1093/JXB/ERT190

401. Komatsu K, Suzuki N, Kuwamura M, et al. Group A PP2Cs evolved in land plants as key regulators of intrinsic desiccation tolerance. *Nature Communications*. 2013;4(1):1-9. doi:10.1038/ncomms3219

402. Shinozawa A, Otake R, Takezawa D, et al. SnRK2 protein kinases represent an ancient system in plants for adaptation to a terrestrial environment. *Communications Biology*. 2019;2(1):1-13. doi:10.1038/s42003-019-0281-1

403. Cuming AC, Cho SH, Kamisugi Y, Graham H, Quatrano RS. Microarray analysis of transcriptional responses to abscisic acid and osmotic, salt, and drought stress in the moss, Physcomitrella patens. *New Phytologist*. 2007;176(2):275-287. doi:10.1111/J.1469-8137.2007.02187.X

404. Lind C, Dreyer I, López-Sanjurjo EJ, et al. Stomatal Guard Cells Co-opted an Ancient ABA-Dependent Desiccation Survival System to Regulate Stomatal Closure. *Current Biology*. 2015;25(7):928-935. doi:10.1016/J.CUB.2015.01.067

405. Renzaglia KS, Villarreal JC, Piatkowski BT, Lucas JR, Merced A. Hornwort Stomata: Architecture and Fate Shared with 400-Million-Year-Old Fossil Plants without Leaves. *Plant Physiology* 2017;174(2):788-797. doi:10.1104/PP.17.00156

406. Duckett JG, Pressel S. The evolution of the stomatal apparatus: intercellular spaces and sporophyte water relations in bryophytes—two ignored dimensions. *Philosophical Transactions of the Royal Society B: Biological Sciences*. 2018;373(1739). doi:10.1098/RSTB.2016.0498

407. Ruszala EM, Beerling DJ, Franks PJ, et al. Land Plants Acquired Active Stomatal Control Early in Their Evolutionary History. *Current Biology*. 2011;21(12):1030-1035. doi:10.1016/J.CUB.2011.04.044

408. Cardoso AA, McAdam SAM. Misleading conclusions from exogenous ABA application: a cautionary tale about the evolution of stomatal responses to changes in leaf water status. *Plant Signaling and Behavior.* 2019; 14(7) doi:10.1080/15592324.2019.1610307

409. Grantz DA, Linscheid BS, Grulke NE. Differential responses of stomatal kinetics and steady-state conductance to abscisic acid in a fern: comparison with a gymnosperm and an angiosperm. *New Phytologist*. 2019;222(4):1883-1892. doi:10.1111/NPH.15736

410. McAdam SAM, Brodribb TJ. Fern and Lycophyte Guard Cells Do Not Respond to Endogenous Abscisic Acid. *Plant Cell*. 2012;24(4):1510-1521. doi:10.1105/TPC.112.096404

411. Brodribb TJ, McAdam SAM. Passive origins of stomatal control in vascular plants. *Science*. 2011;331(6017):582-585. doi:10.1126/SCIENCE.1197985

412. McAdam SAM, Brodribb TJ. Separating Active and Passive Influences on Stomatal Control of Transpiration. *Plant Physiology* 2014;164(4):1578-1586. doi:10.1104/PP.113.231944
413. Hõrak H, Kollist H, Merilo E. Fern Stomatal Responses to ABA and CO_2 Depend on Species and Growth Conditions. *Plant Physiology* 2017;174(2):672-679. doi:10.1104/PP.17.00120
414. Sussmilch F, McAdam S. Surviving a Dry Future: Abscisic Acid (ABA)-Mediated Plant Mechanisms for Conserving Water under Low Humidity. *Plants*. 2017;6(4):54. doi:10.3390/plants6040054
415. Brodribb TJ, McAdam SAM, Jordan GJ, Feild TS. Evolution of stomatal responsiveness to CO_2 and optimization of water-use efficiency among land plants. *New Phytologist*. 2009;183(3):839-847. doi:10.1111/J.1469-8137.2009.02844.X
416. Buckley TN. Stomatal responses to humidity: has the 'black box' finally been opened? *Plant, Cell & Environment*. 2016;39(3):482-484. doi:10.1111/PCE.12651
417. Sussmilch FC, Brodribb TJ, McAdam SAM. Up-regulation of NCED3 and ABA biosynthesis occur within minutes of a decrease in leaf turgor but AHK1 is not required. *Journal of Experimental Botany*. 2017;68(11):2913-2918. doi:10.1093/JXB/ERX124
418. Qiu C, Ethier G, Pepin S, Dubé P, Desjardins Y, Gosselin A. Persistent negative temperature response of mesophyll conductance in red raspberry (Rubus idaeus L.) leaves under both high and low vapour pressure deficits: a role for abscisic acid? *Plant, Cell & Environment*. 2017;40(9):1940-1959. doi:10.1111/PCE.12997
419. Isik F. Genomic selection in forest tree breeding: The concept and an outlook to the future. *New Forests*. 2014;45(3):379-401. doi:10.1007/S11056-014-9422-Z
420. Deery DM, Jones HG. Field Phenomics: Will It Enable Crop Improvement? *Plant Phenomics*. 2021. doi:10.34133/2021/9871989
421. Lowe A, Harrison N, French AP. Hyperspectral image analysis techniques for the detection and classification of the early onset of plant disease and stress. *Plant Methods*. 2017;13(1). doi:10.1186/S13007-017-0233-Z
422. Yao J, Sun D, Cen H, et al. Phenotyping of Arabidopsis drought stress response using kinetic chlorophyll fluorescence and multicolor fluorescence imaging. *Frontiers in Plant Science*. 2018;9:603. doi:10.3389/FPLS.2018.00603/
423. Mertens S, Verbraeken L, Sprenger H, et al. Proximal Hyperspectral Imaging Detects Diurnal and Drought-Induced Changes in Maize Physiology. *Frontiers in Plant Science*. 2021;12:240. doi:10.3389/FPLS.2021.640914/

424. Ludovisi R, Tauro F, Salvati R, Khoury S, Mugnozza GS, Harfouche A. Uav-based thermal imaging for high-throughput field phenotyping of black poplar response to drought. *Frontiers in Plant Science*. 2017;8:1681. doi:10.3389/FPLS.2017.01681/

425. de Castro AI, Rallo P, Suárez MP, et al. High-Throughput System for the Early Quantification of Major Architectural Traits in Olive Breeding Trials Using UAV Images and OBIA Techniques. *Frontiers in Plant Science*. 2019;10:1472. doi:10.3389/FPLS.2019.01472/

426. Badenes ML, Fernández i Martí A, Ríos G, Rubio-Cabetas MJ. Application of genomic technologies to the breeding of trees. *Frontiers in Genetics*. 2016;7(NOV):198. doi:10.3389/FGENE.2016.00198/

427. Grattapaglia D, Silva-Junior OB, Resende RT, et al. Quantitative genetics and genomics converge to accelerate forest tree breeding. *Frontiers in Plant Science*. 2018;871:1693. doi:10.3389/FPLS.2018.01693/

428. Chen C, Mitchell SE, Elshire RJ, Buckler ES, El-Kassaby YA. Mining conifers' mega-genome using rapid and efficient multiplexed high-throughput genotyping-by-sequencing (GBS) SNP discovery platform. *Tree Genetics and Genomes*. 2013;9(6):1537-1544. doi:10.1007/S11295-013-0657-1

429. Gamal El-Dien O, Ratcliffe B, Klápště J, Chen C, Porth I, El-Kassaby YA. Prediction accuracies for growth and wood attributes of interior spruce in space using genotyping-by-sequencing. *BMC Genomics*. 2015;16(1):1-16. doi:10.1186/S12864-015-1597-Y

430. Ingvarsson PK, Street NR. Association genetics of complex traits in plants. *New Phytologist*. 2011;189(4):909-922. doi:10.1111/J.1469-8137.2010.03593.X

431. Muranty H, Jorge V, Bastien C, Lepoittevin C, Bouffier L, Sanchez L. Potential for marker-assisted selection for forest tree breeding: lessons from 20 years of MAS in crops. *Tree Genetics and Genomes*. 2014;10(6):1491-1510. doi:10.1007/S11295-014-0790-5

432. Lebedev VG, Lebedeva TN, Chernodubov AI, Shestibratov KA. Genomic Selection for Forest Tree Improvement: Methods, Achievements and Perspectives. *Forests 2020, Vol 11, Page 1190*. 2020;11(11):1190. doi:10.3390/F11111190

433. Zapata-Valenzuela J, Whetten RW, Neale D, McKeand S, Isik F. Genomic estimated breeding values using genomic relationship matrices in a cloned population of loblolly pine. *G3: Genes, Genomes, Genetics*. 2013;3(5):909-916. doi:10.1534/G3.113.005975/-/DC1

434. Thistlethwaite FR, Ratcliffe B, Klápště J, et al. Genomic selection of juvenile height across a single-generational gap in Douglas-fir. *Heredity.* 2019;122(6):848-863. doi:10.1038/s41437-018-0172-0

435. Cavers S, Cottrell JE. The basis of resilience in forest tree species and its use in adaptive forest management in Britain. *Forestry: An International Journal of Forest Research*. 2015;88(1):13-26. doi:10.1093/FORESTRY/CPU027

436. Messier C, Puettmann K, Chazdon R, et al. From Management to Stewardship: Viewing Forests As Complex Adaptive Systems in an Uncertain World. *Conservation Letters*. 2015;8(5):368-377. doi:10.1111/CONL.12156

437. Nagel LM, Palik BJ, Battaglia MA, et al. Adaptive Silviculture for Climate Change: A National Experiment in Manager-Scientist Partnerships to Apply an Adaptation Framework. *Journal of forestry*. 2017;115(3):167-178. doi:10.5849/JOF.16-039

438. D'Amato AW, Palik BJ. Building on the last "new" thing: Exploring the compatibility of ecological and adaptation silviculture. *Canadian Journal of Forest Research*. 2021;51(2):172-180. doi:10.1139/CJFR-2020-0306

439. Mori AS, Lertzman KP, Gustafsson L. Biodiversity and ecosystem services in forest ecosystems: a research agenda for applied forest ecology. *Journal of Applied Ecology*. 2017;54(1):12-27. doi:10.1111/1365-2664.12669

440. Clark PW, Freeman AJ, D'Amato AW, et al. Restoring a keystone tree species for the future: American chestnut assisted migration plantings in an adaptive silviculture experiment. *Forest Ecology and Management*. 2022;523:120505. doi:10.1016/J.FORECO.2022.120505

441. Vitt P, Havens K, Kramer AT, Sollenberger D, Yates E. Assisted migration of plants: Changes in latitudes, changes in attitudes. *Biological Conservation*. 2010;143(1):18-27. doi:10.1016/J.BIOCON.2009.08.015

442. Aubin I, Garbe CM, Colombo S, et al. Why we disagree about assisted migration: Ethical implications of a key debate regarding the future of Canada's forests. *The Forestry Chronicle*. 2011;87(6):755-765. doi:10.5558/TFC2011-092

443. Hewitt N, Klenk N, Smith AL, et al. Taking stock of the assisted migration debate. *Biological Conservation*. 2011;144(11):2560-2572. doi:10.1016/J.BIOCON.2011.04.031

444. Schwartz MW, Hellmann JJ, McLachlan JM, et al. Managed Relocation: Integrating the Scientific, Regulatory, and Ethical Challenges. *Bioscience*. 2012;62(8):732-743. doi:10.1525/BIO.2012.62.8.6

Chapter 1

NCEDs drive Rising but not Peaking abscisic acid profiles in conifer species

Graphical abstract

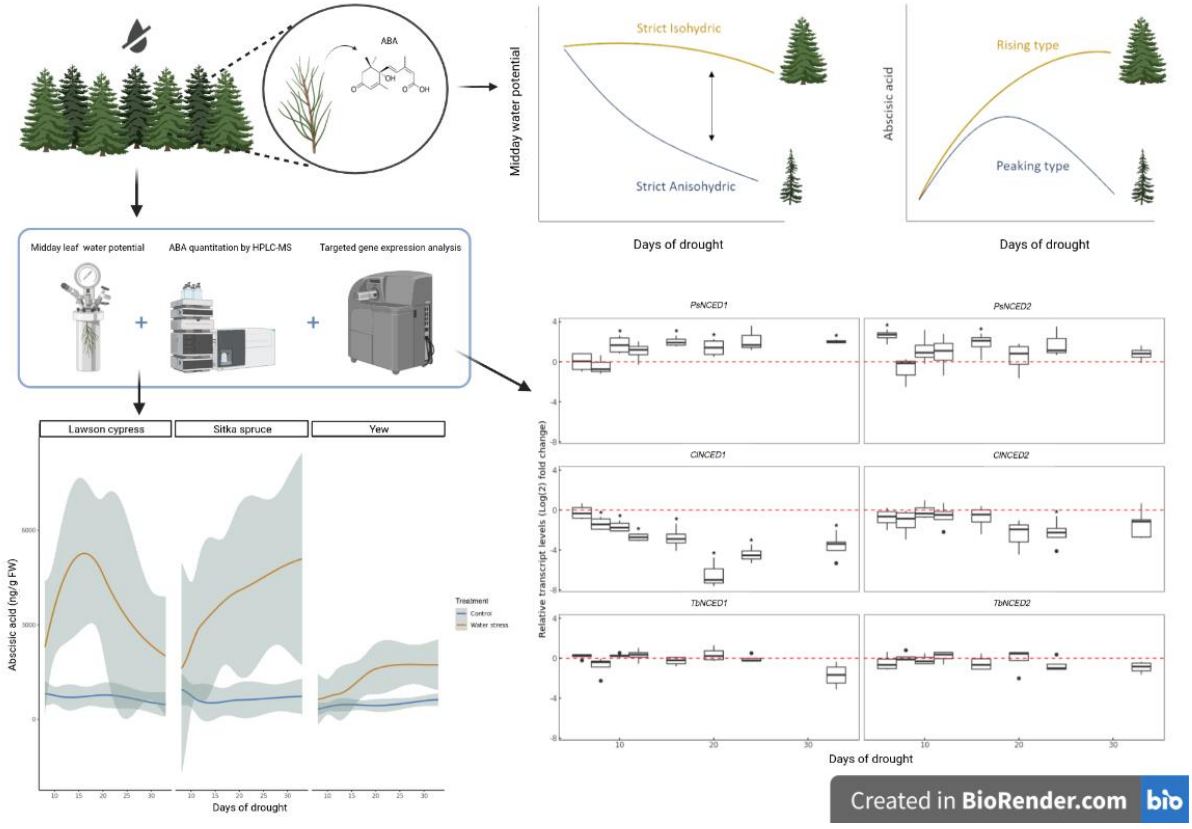

Abstract

Climate change poses one of the greatest threats to forest ecosystem integrity. Human societies widely rely on forests for their own development and well-being. It is crucial to find new ways of managing forests in the face of global warming and to do so we need to understand how trees respond to extreme

climatic events. In this work we investigate how conifer trees cope with drought and try to draw conclusions valid for the establishment of better forest regeneration practices. We look at the genetic mechanisms governing the production of the plant hormone abscisic acid (ABA), which safeguards plant's water status by the means of two divergent modes in conifers. To do this, we apply an interdisciplinary approach by using plant ecophysiology, biochemistry and genetic tools. In line with previous studies, we find that commercial conifer species from evolutionary ancient families adopt a conservative water strategy during drought by accumulating high levels of ABA in their leaves, while more derived species accumulate the hormone in a transient manner and allow for greater water loss. Moreover, we provide evidence that these contrasting strategies are controlled by divergent modes of differential expression of genes involved in the biosynthetic and catabolic pathways of ABA, adding more information for a clear definition of the iso/anisohydric paradigm. We believe that studying these and other related genes that regulate plant water status may help foresters develop and grow more resistant trees.

Introduction

Climate change represents a threat to forest ecosystems worldwide [1] as shown by phenomena such as drought-related forest die-off becoming more widespread [2,3]. Extreme droughts are increasing in frequency and duration and have the potential to alter forest structure and function in the next decades [2–6]. Research indicates that developing a better understanding of the mechanisms governing water and carbon exchange between plants and the environment is crucial to develop solutions through the choice of suitable species, knowledge of appropriate genetic markers and targeted breeding [7–11]. Studies of physiology, anatomy and genetics point to a major role of stomata as a regulatory point for the water and carbon balance in the evolutionary history of land plants [12–15]. Stomata are valve-like structures on the leaf surface, opening and closing in response to environmental cues such as light, CO_2 and water availability. The significant diversity observed in stomatal responses to water deficit among species and genotypes has led to a conceptual framework of contrasting responses known as isohydric and anisohydric [13,16]. Plants that apply a strict control on their water status through tight stomatal regulation are termed isohydric, whereas plants allowing a greater degree of water status variation under water deficit are anisohydric. These contrasting responses have distinct impacts on hydraulic function and carbon balance [17] and may help to explain the physiological bases of drought-induced tree mortality [16–18]. However, a quantitative definition encompassing plant forms and species is lacking [13,19,20] and there is a spectrum of responses observed [16,17,21,22]. Nonetheless, understanding

the regulation and signalling pathways involved in these processes is likely to be fundamental to identify or develop trees able to perform better under abiotic stress.

Abscisic acid (ABA) is a key molecule controlling plant processes involving changes in osmotic relations, such as growth, dormancy, and stress responses. A detailed understanding of how plants use ABA for controlling stomatal closure has developed from studies in model plant systems [23,24]. The concentration of ABA increases during water deficits (either soil water or air humidity) [20,25], triggering a complex signalling pathway that ultimately will induce the guard cells of the stomata to shrink and the stomatal pores to close [24,26]. One protein family has emerged for its regulatory role in the ABA biosynthetic pathway: NCEDs (9-cis-epoxycarotenoid dioxygenases). They are believed to be rate-limiting enzymes in the pathway, and represent the first committed step of ABA biosynthesis, i.e., cleavage of 9-cis-violaxanthin or 9-cis-neoxanthin to produce xanthoxin [27–32]. Over the course of plant evolution, NCEDs have duplicated and undergone functional diversification, producing organelle- and tissue-specific proteins, from algae, through *Physcomitrium patens (P. patens)* and the land plant phylogeny to *Arabidopsis thaliana (A. thaliana)* [32–35]. The chloroplast isoforms of NCED proteins were shown to be fast-responding to water deficit, being up-regulated within twenty minutes from the imposition of the stress in angiosperms [31,32,34,36]. The ABA metabolic pathway includes other enzymes that are also responsive to drought stress. The first enzyme in the pathway is the zeaxanthin epoxidase (ZEP), which in *A. thaliana* is encoded by *AtABA1* and is responsible for the epoxidation of zeaxanthin to all-trans-violaxanthin, then converted to neoxanthin and violaxanthin, the substrates of NCEDs [37–39]. The very last enzyme in the pathway is an abscisic acid aldehyde oxidase, encoded by *AtAAO3* in *A. thaliana*, which catalyses the oxidation of abscisic aldehyde to ABA [40,41].

Conifers represent an interesting but understudied system in which to examine the evolution and diversification of plant mechanisms to cope with drought, including the role of ABA. Our current understanding of conifer responses to drought stress is based on studies of plant hydraulics [25,42]. In contrast to angiosperms, conifers rely on ABA biosynthesis only for prolonged water deficit [43], whereas during mild water stress such as daily fluctuations in air humidity, stomatal closure is driven by passive changes in the leaf water status [43,44]. Moreover, conifers appear to be able to switch between these mechanisms of stomatal control, and this ability may be subject to natural selection. Basal conifer clades, such as Pinaceae, possess low cavitation-resistant xylem and respond to prolonged water stress by accumulating high levels of ABA in the leaves to induce tight closure of the stomatal pores (Rising-type response). In contrast, xylem in the more derived clades of Cupressaceae and Taxaceae is resistant to cavitation, and this allows them to switch from ABA-driven

to water potential dependent stomatal closure (Peaking-type response), allowing gas exchange to continue until the advanced stages of drought [45,46]. There is an apparent link between ABA-types and the iso/anisohydry paradigm. A typical Rising type accumulates and maintains high ABA levels and has tight stomatal closure as seen in the isohydric response to maintain a steady water status. A Peaking type would instead correspond to an anisohydric response, with ABA levels initially rising and then dropping and thus allowing stomata to stay relatively open (see Figure 1 for a schematic representation of contrasting behaviours).

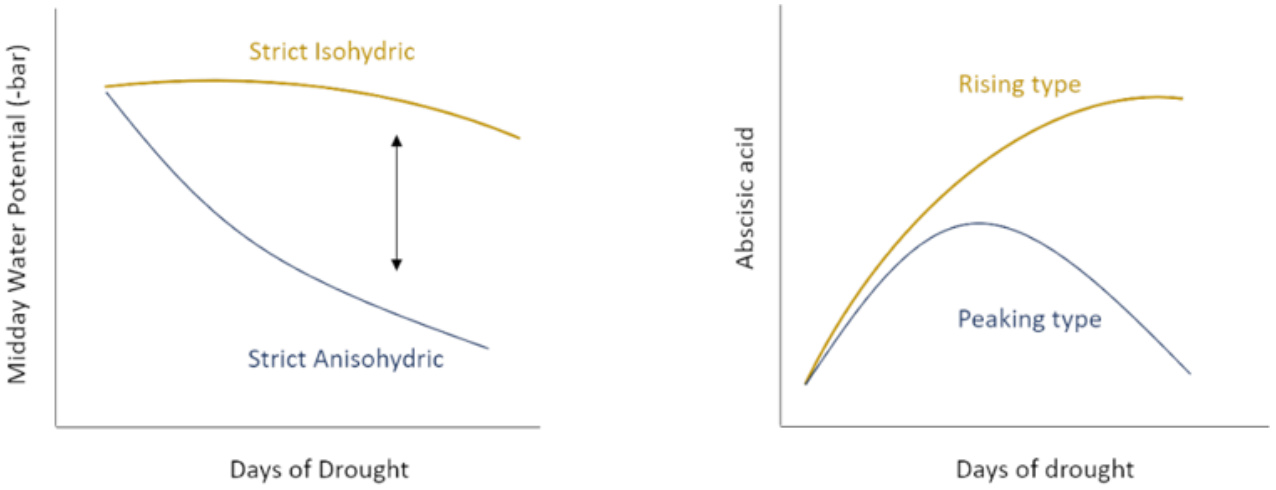

Figure 1. Schematic representation of iso/anisohydric and Rising/Peaking phenotypes observed in response to drought stress in conifer species.

The drought-responsive pathway from ABA production to stomatal control is relatively well understood in angiosperms but much less in gymnosperms [20] and the understanding of drought responses across conifers open the doors to functional studies of genes involved in ABA stomatal regulation for the first time.

This chapter has four objectives set out to fill this knowledge gap: 1) compare drought responses across several coniferous species and families by applying an artificial drought stress on potted seedlings and monitoring parameters related to the plant water status; 2) investigate the putative role of ABA along the spectrum of hydrosensitivity by modelling species-specific ABA profiles over the course of the drought, which should aid in the identification of Rising versus Peaking types in relation to water status, in our study species; 3) use gene sequence similarity analyses and phylogenetic reconstructions to identify putative *NCEDs* and other ABA-related gene sequences; 4) test the

responsiveness of these candidate genes to drought stress and relate these gene expression profiles to abscisic acid and water potential profiles.

We hypothesise that one or more *NCED* genes may be responsible for regulating ABA profiles in conifers and that a better understanding of their role may help to elucidate the differential isohydric and anisohydric responses observed across major conifer families. We expect that NCEDs enzymes will have a conserved role across conifers as drought-responsive, rate-limiting enzymes in ABA biosynthesis. We predict that variations in the transcriptional regulation of genes encoding NCEDs enzymes represents a major control point for ABA accumulation and are key to P/R (Peaking/Rising) types. In other words, *NCED* expression may increase in all species at least initially, and only show a downregulation in species with P-type ABA profiles but not in R-type species. This hypothesis assumes that ABA turnover is constitutive or enhanced during drought, as already reported [47]; therefore, the proposed regulation mechanism alone could actively control foliage ABA levels.

Materials and methods

Plant material and experimental design

One- to two-year-old conifer seedlings (15-40 cm tall) were obtained from Maelor forest nurseries Ltd (Ellesmere Rd, Whitchurch SY13 3HZ) and Alba Trees Nurseries (Lower, Winton Way, Tranent EH33 2AL) between January and August 2019 (see Supplementary table 1 for species identity, provenance, and provider) and stored in a cold room in dark plastic bags until potting. Species included were*: Chamaecyparis lawsoniana* (*C. lawsoniana)*, *Juniper communis* (*J. communis*), *Picea sitchensis* (*P. sitchensis)*, *Picea sitchensis x Picea glauca* (*P. sitchensis x P. glauca), Taxus baccata (T. baccata), Larix eurolepis (L. eurolepis), (Pseudotsuga menziesii (P. menziesii), Tsuga heterophylla (T. heterophylla), Sequoia sempervirens (S. sempervirens).* Trees were potted in 3 litres square pots using a homogenous 3:1 volumetric mix of potting compost (M2, ICL, Everris ltd, 4190 CA Geldermalsen, The Netherlands) and horticultural grit sand (Bathgate horticulture, Vale Park, Evesham, Worcestershire WR11 1GP). Once potted, trees were acclimatised for 4-6 weeks in a greenhouse with natural light supplemented to achieve a photoperiod of 16h/8h day/night and temperature set to 24/16 °C (day/night). Cooling and humidity control was achieved through venting via roof windows.

Three different drought experiments were run between March and October 2019 including eight different conifer species and one hybrid (see Table 1, for species and treatment durations). Each experiment used a complete randomised split-plot block design, in which the split-plots were the drought stress treatment and well-watered controls. The drought treatment consisted of completely withholding watering. Experiment 2 was slightly shorter due to higher temperatures, which exceeded the cooling capacity of the greenhouse. The details and overlap in species between experiment 1 and 2 was as shown in Table 1.

Table 1. Summary table of drought experiments. ***Experiment****: first, second and third;* ***Species****: conifer species tested in each of the three experiments;* ***Duration****: number of days of experimental drought;* ***Time points****: number of time points for sample collection in each experiment;* ***Sampling days****: time points for sample collection since water withheld.*

Experiment	**Species**	**Duration (days)**	**Time points**	**Sampling days**
1	*C. lawsoniana*, *J. communis*, *P. sitchensis*, *P. sitchensis x P. glauca,* *T. baccata*	34	8	6, 8, 10, 12, 16, 20, 24, 33
2	*C. lawsoniana*, *P. sitchensis*, *P. sitchensi x P. glauca,* *T. baccata,* *L. eurolepis,* *P. menziesii*	25	4	6, 9, 16, 24
3	*T. heterophylla,* *S. sempervirens*	35	5	6, 12, 18, 26, 34

Sampling and Tree Physiologyogy measurements

Samples were collected for experimental measurements between 11 am and 2 pm from randomly selected plants across all plots and blocks, i.e., either four (experiments 1 and 2) or six (experiment 3) of both the well-watered and drought-stressed trees at each time point. The volumetric Soil Water Content (SWC) was recorded in individual pots at the time of sample collection by completely

inserting a soil moisture probe (ML3 ThetaProbe Soil Moisture Sensor, Delta-T Devices, 130 Low Rd, Burwell, Cambridge CB25 0EJ) in the potting mix at root depth. The probe was used with default calibration for organic mix and measurements were recorded in a hand-held device (HH2 Soil Moisture Meter, Delta-T Devices). A single data point per pot was taken, as readings were consistent across the pot's surface (data not shown). Twigs were excised from each tree using a razor blade for water potential measurements and stored in moist sealable plastic bags kept in the dark in a cold transport box until measurements. Shoot tips with newly formed foliage were also collected for molecular analyses and these were snap-frozen in 15 mL falcon tubes by complete immersion in liquid N and stored in -80 °C until analysis. Midday Shoot Water Potential (MWP) was measured by using a Scholander-type digital pressure chamber (SKPM 1400/80**,** Skye instruments, Unit 21, Ddole Enterprise Park, Llandrindod Wells LD1 6DF). Pressure readings (bar) were recorded at the first appearance of xylem sap from the cut surface with the help of a hand-held lens. When no sap appeared, samples were considered damaged or dead and not included in any analyses.

Abscisic acid extraction and quantification

Abscisic acid (ABA) was extracted according to [45]. All procedures were performed under dim light to minimise ABA isomerisation. Briefly, 50 mg of frozen leaf tissue were weighed in 2 mL tubes containing stainless steel beads using an analytical balance. Tubes were filled with cold 80% Methanol (Sigma-Aldrich, catalog number 34860) in water with added BHT (2,6-Di-tert-butyl-4-methylphenol, Sigma-Aldrich, catalog number B1378) and then stored at -20 °C overnight. Samples were then homogenised using a mixer mill for less than 2 minutes to minimise overheating and 15 ng of deuterated [2H6] (+)-cis, trans-abscisic acid (d6-ABA) were added. Samples were incubated overnight at 4 °C to allow for extraction of ABA by passive diffusion and then centrifuged at 13,000 x g to pellet debris. A 1 mL aliquot was recovered and dried under vacuum using a SpeedVac vacuum concentrator (Thermo Scientific), with temperature control to avoid overheating and shielding from light by using aluminium foil. The residue was resuspended in 500 µL of 2% acetic acid in water, transferred to a new tube and partitioned with 300 µL of diethyl ether by short centrifugation at 13,000 x g. The upper polar phase (diethyl ether) was collected and transferred to a new tube. Phase separation was repeated, fractions pooled and then dried down in a heating block at 40 °C. Finally, samples were resuspended in 150 µL of 5% MeOH in 2% acetic acid, centrifuged and a 50 µL aliquot was transferred to a glass micro-vial for HPLC (High Performance Liquid Chromatography) analysis.

HPLC analysis was carried out on a Waters Acquity H-class separation module. Separation was achieved on an ACE C18, 3 µm, 150 x 3 column (Hichrom, UK) maintained at 45 °C. Samples were eluted in A: 0.1 % acetic acid, B: acetonitrile with a flow rate of 0.25 ml/min, a linear gradient of 20-95 % B in 5 min, and a total run time 8 min. Analytes were measured by mass spectrometry with a Waters Acquity TQD detector with electrospray ionisation in a negative ionisation mode. ABA was detected at multiple reaction monitoring (MRM) of 262.8 > 152.7 and D6-ABA was detected at MRM of 268.8 > 158.7, retention time 3.9 min for both. A calibration curve was run in the system and then spiked with the same concentration of internal standard (d6-ABA). The calibration curve was then plotted as peak area for ABA/peak area for IS against ABA concentration (see Supplementary figure 7 for an example chromatogram for ABA and calibration curve).

Gene sequence analyses

Sequence searches were conducted using conifer transcriptomes developed from previous studies within our group – *C. lawsoniana*, *Larix laricina (L. laricina)*, *Picea glauca (P. glauca)*, *P. sitchensis*, *T. baccata, Thuja occidentalis (T. occidentalis)* – and a transcriptome of ancient gymnosperm *Ginkgo biloba (G. biloba)*. Protein sequences of model plant species stored at NCBI were included in the analysis, nominally: *Amborella trichopoda (A. trichopoda)*, *A. thaliana*, *Marchantia polymorpha (M. polymorpha)*, *Oryza sativa (O. sativa)*, *P. patens* and *Selaginella moellendorffii (S. moellendorffii)*. RNA sequences were translated to amino acid sequences using VirtualRibosome – 2.0 (DTU Health Tech) and clustered on CD-HIT, 97% identity threshold to filter highly similar sequences out. Sequences shorter than 200 amino acids were removed to improve phylogenetic outputs. Putative ortholog sequence detection was then conducted with Orthofinder – 2.3.1 [48]. *A. thaliana* TAIR accessions for selected candidate genes from the ABA biosynthetic and catabolic pathways (*ABA1*, *AAO3*, *CYP707A3* and *NCED3*) were used as references for conifer ortholog identification within orthogroups (see table 2 for gene IDs). Orthogroup sequences clustered by the Orthofinder algorithm were used for further phylogenetic analyses through MEGA (Molecular Evolutionary Genetics Analysis). First, a new MSA (Multiple Sequence Alignment) was generated in MAFFT [49] with 1000 iterations. This MSA was used for phylogenetic tree inference in MEGA. A Maximum Likelihood tree was inferred using JTT (Jones-Taylor-Thornton) substitution model and node support values were obtained by using 1000 bootstrap replicates. A distance matrix was computed for between-groups estimates of evolutionary divergence of taxa by calculating the number of average amino acid substitutions on MEGA. The same approach was adopted for computing an identity matrix comparing gene sequences.

*Table 2. Candidate gene (**Conifer ID**), with relative forward and reverse primers (**Forward** and **Reverse sequence**) reference gene (**Model Name** and **Model ID**) and housekeeping (bold characters) gene sequence and primer information.*

Model Name	Model ID	Conifer ID	Forward sequence	Reverse sequence	Gene
NCED	AT3G14440	PSIR_DN33063_c0_g1	cagatcccggccttcacac	ggggatactcctcggcatc	*9-cis-epoxycarotenoid dioxygenase*
NCED	AT3G14440	PSIR_DN39298_c0_g1	cgtcgtaggcataggggttc	tcggaggacacaccatttg	*9-cis-epoxycarotenoid dioxygenase*
CYP707A3	AT5G45340	PSIR_DN32321_c0_g1	tgttggtaggaagcacgatacac	tcctcaatcaccttcggttatg	*Cytochrome P450, family 707*
CYP707A3	AT5G45340	PSIR_DN32134_c0_g1	aacgttaataatggccctggtg	tcctgaatgatcacgacaactc	*Cytochrome P450, family 707*
AAO3	AT2G27150	PSIR_DN38520_c0_g1	gtgcgagacatgccgtaag	gccacactttgcctgtaagc	*aldehyde oxidase 3*
ABA1	AT5G67030	PSIR_DN41411_c0_g1	tgcgtacagaggtccaatcc	cgccagtaatgcaaccattctcc	*zeaxanthin epoxidase (ZEP)*
mRNA capping enzyme family protein	AT3G09100	PSIR_DN38225_c0_g2	tttccttgtcagctgtgatgc	ttccattcgtaccagcatcc	**HOUSEKEEPING**
NCED	AT3G14440	CLAR_DN53708_c0_g1	gcaaatgcacaaggattgc	aagcaacggattggactcg	*9-cis-epoxycarotenoid dioxygenase*
NCED	AT3G14440	CLAR_DN53708_c0_g5	ggcgaggatgaggagattg	cttcttttgctctctcctgtcg	*9-cis-epoxycarotenoid dioxygenase*
CYP707A3	AT5G45340	CLAR_DN44841_c0_g1	ctcagtaggaaatgtgggtcttg	gcataacttcatcctcggaag	*Cytochrome P450, family 707*
CYP707A3	AT5G45340	CLAR_DN43170_c0_g2	ccccagataagtcaaaacatcg	tggctatcaacgtcgcatc	*Cytochrome P450, family 707*
CYP707A3	AT5G45340	CLAR_DN43349_c0_g1	ttgtctcttacgctgtgtcatcg	tgtgggaagaaggcggtttatg	*Cytochrome P450, family 707*
CYP707A3	AT5G45340	CLAR_DN44491_c1_g1	gatgcctccaaagcctaacag	gtggtggatcaggacgagtatc	*Cytochrome P450, family 707*
AAO3	AT2G27150	CLAR_DN54372_c1_g1	aagtgtggctgttgggtttc	tggtttacagggccatttctc	*aldehyde oxidase 3*
ABA1	AT5G67030	CLAR_DN50982_c0_g1_B	ggctgaacgaagcgacatactc	cactcccagcaggttcattgtg	*zeaxanthin epoxidase (ZEP)*
LisH dimerisation motif	AT4G32551	CLAR_DN46563_c1_g1	ggaagttgggacgataaaagc	cggtaatcaaatggttgtgc	**HOUSEKEEPING**
NCED	AT3G14440	TBAR_DN117190_c1_g5	gcctctcttctcgctatgtcc	caaaccctcgtgccgtctatc	*9-cis-epoxycarotenoid dioxygenase*
NCED	AT3G14440	TBAR_DN105025_c1_g1	tagttgacggaggatggagtg	cgacagaggacgctgcttttc	*9-cis-epoxycarotenoid dioxygenase*
CYP707A3	AT5G45340	TBAR_DN122486_c1_g3_B	cagctcaagatacaccgcc	gttctgtcgtgacagcctgg	*Cytochrome P450, family 707*
CYP707A3	AT5G45340	TBAR_DN113007_c0_g2	aggtgtcaaatggtgcttgg	atcccctccctcgtctctg	*Cytochrome P450, family 707*
AAO3	AT2G27150	TBAR_DN123260_c4_g3	agtctacagctcaagccagaacc	gacgcttcagcttgtatgcag	*aldehyde oxidase 3*
ABA1	AT5G67030	TBAR_DN109993_c1_g1	tcgtcaatgcctggttcaatc	ccttccgaccaacttgtactg	*zeaxanthin epoxidase (ZEP)*
LisH dimerisation motif	AT4G32551	TBAR_DN113162_c2_g5_B	tccgctactcttcagcaggttc	gcctctgaggtaccagatcgac	**HOUSEKEEPING**

RNA isolation, primer design and PCR

Total RNA was isolated from 30 to 90 mg of frozen leaf tissue samples from *C. lawsoniana*, *P. sitchensis* and *T. baccata* from experiment 1 using all sampling time points. The tissue was ground to a powder in 2 mL tubes containing stainless steel beads and using a mixer mill with blocks frozen in liquid N to prevent defrosting. Sample powder was either directly used in downstream extraction protocols or pre-washed with a sorbitol solution for difficult samples yielding low quality RNA (i.e., low spectrometric absorbance values).

Further RNA extraction and purification steps were performed according to the Monarch Total RNA Miniprep kit (NEB #T2010, Ipswich, Massachusetts 01938, USA). RNA was quantified both with a NanoDrop One/OneC Microvolume UV-Vis Spectrophotometer (Thermo Fisher, Waltham, Massachusetts, USA) and a Qubit 4 Fluorometer (Thermo Fisher), but since readings were consistent across the two instruments (data not shown) the NanoDrop was preferred for ease of use. Sample RNA yield ranged from 20 ng/µL to 300 ng/µL. The RNA sample quality was determined based on UV absorbance ratios by using a threshold set to minimum 260/280 ~ 1.8-2 and 260/230 ~ 1.7-2 values. RNA integrity was assessed using a Bioanalyzer system (Agilent, Santa Clara, California, USA) and only samples with a RIN (RNA Integrity Number) ~ 7 or above were used in downstream analyses. Complementary DNA (cDNA) was synthesised from ~160 ng of total RNA using a Reverse Transcription Master Mix provided by Fluidigm (South San Francisco, California, USA) according to manufacturer's instructions.

Primers were selected using PrimerIdent online tool [50] for multi-gene families or PrimerBlast (see table 2 for primer details). Selected primers were tested *in silico* for tertiary and quaternary structures with the Multiple Primer Analyzer from Thermo Fisher and OligoEvaluator from Sigma-Aldrich. Primers were obtained from Sigma and resuspended in TE buffer (Tris 10 mM, EDTA 1 mM), pH 8.0 (Teknova, #T0225, Hollister, California, USA) and tested by PCR amplification for specificity, visualised by gel electrophoresis and confirmed by Sanger sequencing. Newly synthesised cDNA was purified, diluted, and used as template in a pre-amplification reaction according to the Delta Gene Assays protocol (Fluidigm, South San Francisco, California, USA). Three master mixes were prepared containing species-specific primers for the three test species (*C. lawsoniana*, *P. sitchensis* and *T. baccata*). Reverse-transcription quantitative PCRs (RT-qPCRs) were set up by using microfluidic 192.24 IFC (Integrated Fluid Circuits) plates on Juno system (Fluidigm) and then run using a Biomark HD system (Fluidigm) equipped with a high sensitivity laser imaging system. Rt-

qPCR cycle threshold (Ct) values were normalised against well-watered control samples and housekeeping genes and used to calculate gene expression fold-change across time points. These values were then log2-transformed.

Reference genes for RT-qPCR calculations

Candidate reference genes were identified from previous RNA-seq experiments in *C. lawsoniana*, *P. sitchensis* and *T. baccata* including several tissues and drought treatments similar to those used here. The FPKM (Fragments Per Kilobase Million) data were analysed with a script pipeline created in R with three criteria for the identification of suitable reference genes:

1. Expression in all tissues and treatments.
2. Low variance in expression levels (log2(fold-change) between 0 and 1)
3. Medium to high expression levels (log2(mean(FPKM)) between 5 and 7)

Sequences with an FPKM < 1 were not considered as they were considered too low to accurately predict gene expression levels. A reasonable threshold area that met the criteria was visually identified by plotting the log2 fold-change of the mean FPKM against the log2 mean FPKM values. Candidate gene sequences were then selected based on their presence/absence across all species data sets and based on GO (Gene Ontology) terms annotations. This sequence search produced a total of three candidate housekeeping genes shared by our study species according to TAIR annotations: mRNA capping enzyme family protein [51], LisH dimerisation motif [52], RING/U-box superfamily protein [53]. Only the first two were used in downstream applications, as RING/U-box superfamily protein did not amplify reliably in our study species.

Statistics and data analysis

All data analyses were performed in R environment. SWC and MWP readings were tested for normality and homogeneity of variance considering treated and control trees as separate groups. Differences in mean SWC between well-watered control and drought-treated pots were assessed with a Student's t-test ($P < 0.05$). Differences between mean SWC among species and experiments were tested with a One-Way Anova followed by a Tukey HSD (Honestly Significant Difference) post-hoc test (adjusted P value < 0.05), considering control and drought stress as separate groups.

Differences in mean MWP between treated and control trees were first assessed with a Student's t-test ($P < 0.05$). Differences in mean MWP between species were assessed with ANOVA followed by a Tukey HSD (Honestly Significant Difference) post-hoc test (adjusted P value < 0.05), considering control and drought stress as separate groups.

The relationship between MWP and SWC was curvilinear and varied between species. Second order polynomial equations were fit to these data to attempt to model the different relationships. The slope σ of the linear regression between MWP and SWC was instead chosen to represent the degree of iso to anisohydric response, in a way similar to previous work [54]. A Tukey HSD post-hoc test was implemented using the *cld* (compact letter display) function in the lsmeans package in R to assess all pairwise comparisons among treatment means, hence the difference between slopes. The grouping pattern for all pairwise comparisons was used as a means of assigning species to drought sensitivity responses (i.e., degree of iso to anisohydry). A third (visual) method to display varying degrees of drought sensitivity was plotting the linear regression between intercept and slopes estimates of the linear model fit to SWC and MWP.

The response of MWP to SWC was further inspected by fitting a linear mixed model (estimated using *lmer* function in REML package and "*nloptwrap*" optimizer) to predict MWP with Species, Time and Treatment (formula: MWP ~ Species * Time * Treatment). The model included Block as random effect (formula: ~1 | Block) in order to account for random distribution across the greenhouse.

Differences in ABA levels between well-watered control and drought-treated trees were assessed with a Student's t-test ($P < 0.05$). Abscisic acid time series were analysed by fitting a smoothing curve to data across 4 to 8 time points and calculating its 95% confidence interval. When ABA records reached approximately the same levels as the starting record, the trend was a P-type, otherwise R-type.

A one-sample T test was implemented to compare the gene transcript levels detected for each target gene to a zero-fold-change baseline at each time point (no change in gene expression, $P < 0.05$)

Results

Soil drought progression and shoot water potential

We sought to monitor soil drought progression by measuring SWC and assess its effect on plant water status by measuring changes in MWP. We did this in three different experiments from spring to autumn 2019, including several conifer species representing three phylogenetic families. Some species were included in both experiment 1 and 2, to validate findings from our first experiment (see Table 1). The drought treatment in experiments 1-3 led to a decrease in SWC as shown by the significant difference between drought treated pots and control pots for all species (Student's t-test, $P < 0.05$, see Figure 2). Well-watered pots maintained a mean SWC of ~40%, whereas drought-treated pots dropped below 10%. There were also significant differences in the mean SWC in the drought-stressed plants among the study species (Table 3). C. *lawsoniana* differed from most species as it reached the lowest mean SWC, followed by *J. communis* and *S. sempervirens*.

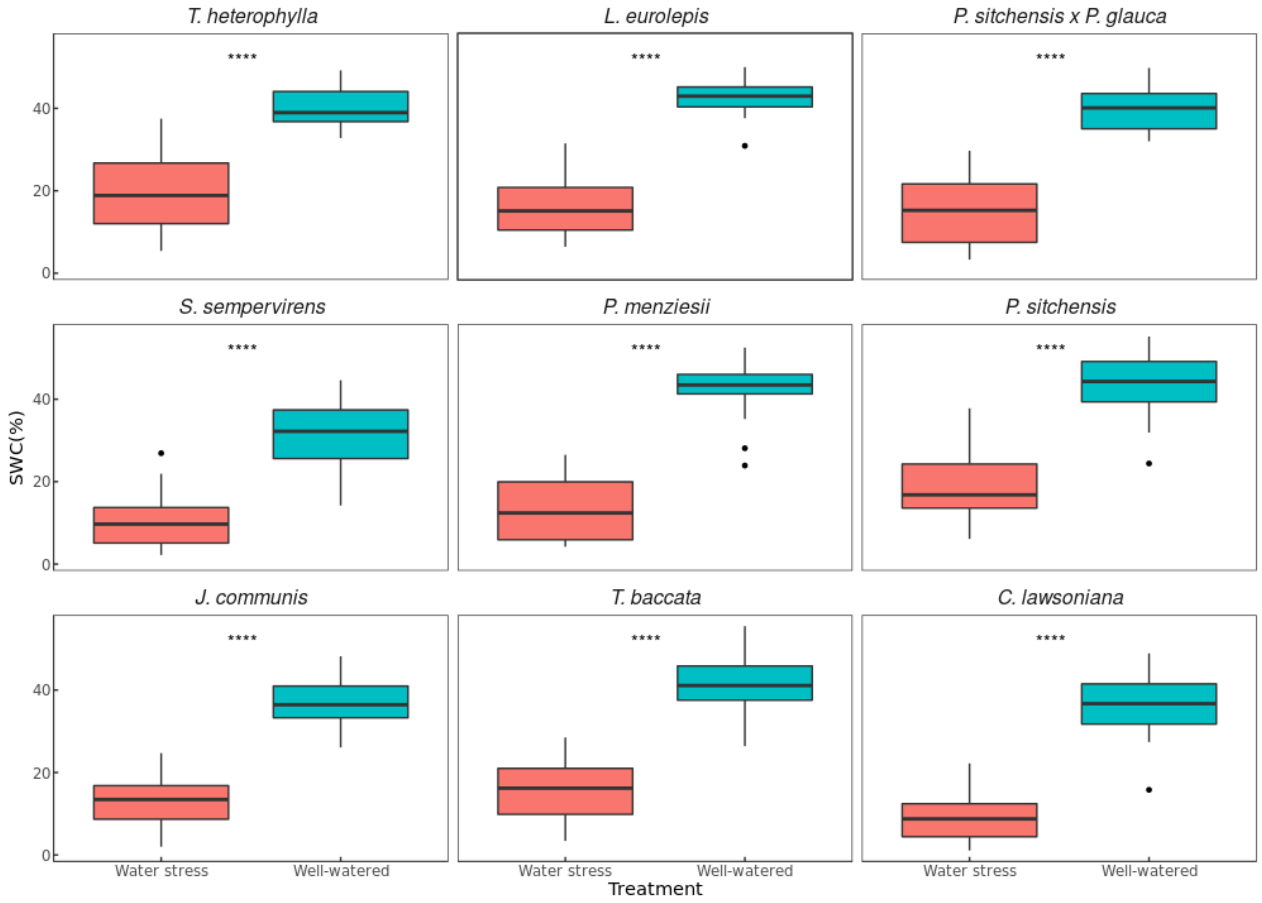

Figure 2. Mean SWC in pots of droughted and well-watered plants. ***Red****: drought-treated trees, N = 16-32, depending on experimental design;* ***Blue****: well-watered control trees, N = 16-32, depending*

on experimental design. ***Asterisks:*** *significant differences between treated and control trees;* ***dots*** *represent potential outliers.* ***Bars*** *indicate maximum and minimum values. Student's t-test (P value < 0.05).*

The MWP (midday leaf water potential) decreased with drought progression for all study species (Figure 3) to as low as –38.50 bar at 34 days of water stress for *J. communis*. In *L. eurolepis* and *T. heterophylla* the mean MWP showed a smaller, less significant decrease compared to controls and a significant difference from all other species under drought stress (Supplementary figure 1, figure 3 and table 4). We found high variation in MWP of treated *P. sitchensis* trees and no significant difference in mean MWP between treatment and control.

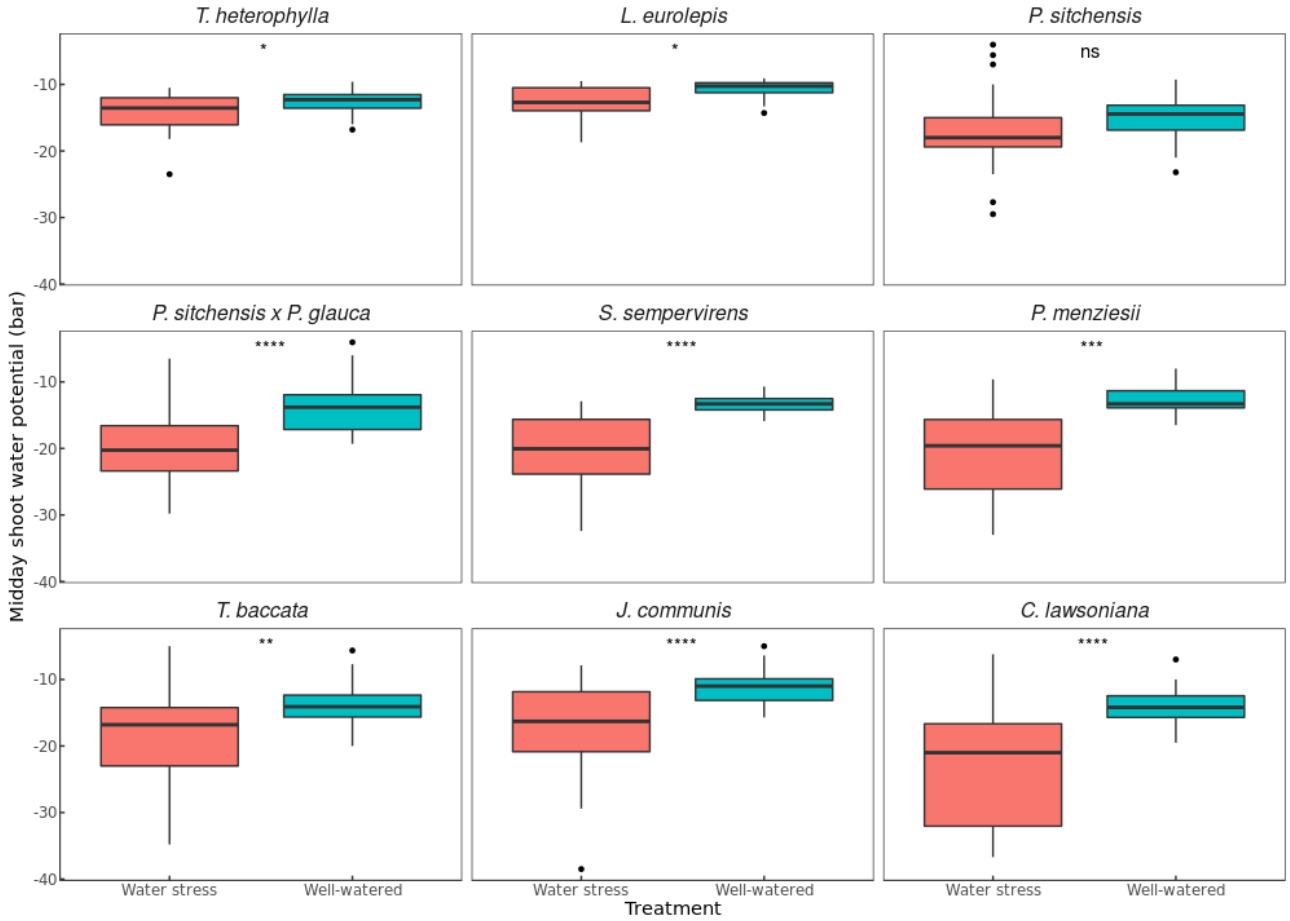

Figure 3. MWP change between drought treatments. ***Red****: drought-treated trees, N = 16-32, depending on experimental design;* ***Blue****: well-watered control trees, N = 16-32, depending on experimental design.* ***Asterisks:*** *significant differences between treated and control trees;* ***dots*** *represent potential outliers.* ***Bars*** *indicate maximum and minimum values. Student's t-test (P value < 0.05).*

Table 3. Tukey HSD post-hoc test summary of differences in SWC among species. Only significant contrasts for treated pots are shown (adjusted P value < 0.05). ***term****: regression term;* ***contrast****: pairwise comparison levels;* ***null.value****: value to which the estimate is compared;* ***estimate****: estimated value of the regression term,* ***conf.low****: lower confidence interval limit;* ***conf.high****: upper confidence interval limit;* ***adj.p.value****: p-value adjusted for multiple comparisons.*

term	contrast	null.value	estimate	conf.low	conf.high	adj.p.value
Species	*S. sempervirens-T. heterophylla*	0	-9.067	-14.993	-3.14	0
Species	*J. communis-T. heterophylla*	0	-6.539	-12.372	-0.706	0.015
Species	*C. lawsoniana-T. heterophylla*	0	-10.464	-16.297	-4.631	0
Species	*C. lawsoniana-L. eurolepis*	0	-7.347	-14.374	-0.319	0.033
Species	*S. sempervirens-P. sitchensis*	0	-8.43	-14.356	-2.504	0
Species	*J. communis-P. sitchensis*	0	-5.903	-11.736	-0.07	0.045
Species	*C. lawsoniana-P. sitchensis*	0	-9.828	-15.661	-3.995	0
Species	*C. lawsoniana-P. sitchensis x P. glauca*	0	-6.409	-12.147	-0.671	0.016
Species	*C. lawsoniana-T. baccata*	0	-6.252	-12.036	-0.468	0.023

The mixed model's total explanatory power was substantial (conditional R^2 = 0.71), and the part related to the fixed effects alone (marginal R^2) was of 0.71. The model's intercept, corresponding to Species = *T. heterophylla*, Time = 0 and Treatment = Well-watered, was at -11.71 (95% CI [-14.16, -9.26], t(448) = -9.39, p < .001). Within the model the interaction effect of water stress on species with time was statistically significant for all study species except for *L. eurolepis* and *T. heterophylla* (see mixed model summary in Supplementary table 2).

We fitted an ordinary least square regression to predict MWP with Species and SWC (formula: MWP ~ Species * SWC). The model explains a statistically significant and substantial proportion of the variance (R2 = 0.72, F(17, 221) = 33.44, p < .001, adj. R2 = 0.70). The model's intercept, corresponding to Species = *T. heterophylla* and SWC = 0, was at - 17.57 (95% CI [-20.80, -14.34], t(221) = -10.73, p < .001). The model confirmed a statistically significant effect of Species on MWP. The overall effect of SWC was small but statistically significant (p = 0.025). The interaction effect of

SWC on Species was significant for all species but *T. heterophylla* and *L. eurolepis,* which did not differ from each other (see supplementary table 3).

We used the slope of the linear model estimated by OLS (Ordinary Least-Squares) on treated trees to quantify species-specific responses to drought stress. We found that *T. heterophylla* had the smallest slope ($\sigma = 0.17$), while *C. lawsoniana* had the highest ($\sigma = 1.59$). The other species had slopes situated between these two extremes (see Figure 4) - i.e., overall showing a range of decreasing stomatal sensitivity to soil water depletion (decreasing SWC). The Tukey HSD test only found a significant difference for the two most extreme species, confirming the continuous range of responses in between. *T. heterophylla* response to SWC was significantly different from seven other species and not from *L. eurolepis* and *P. sitchensis* (see table 3). *J. communis, T. baccata* and *P. menziesii* were significantly different from *L. eurolepis* and *P. sitchensis* and from *C. lawsoniana*, while the latter was significantly different from all species.

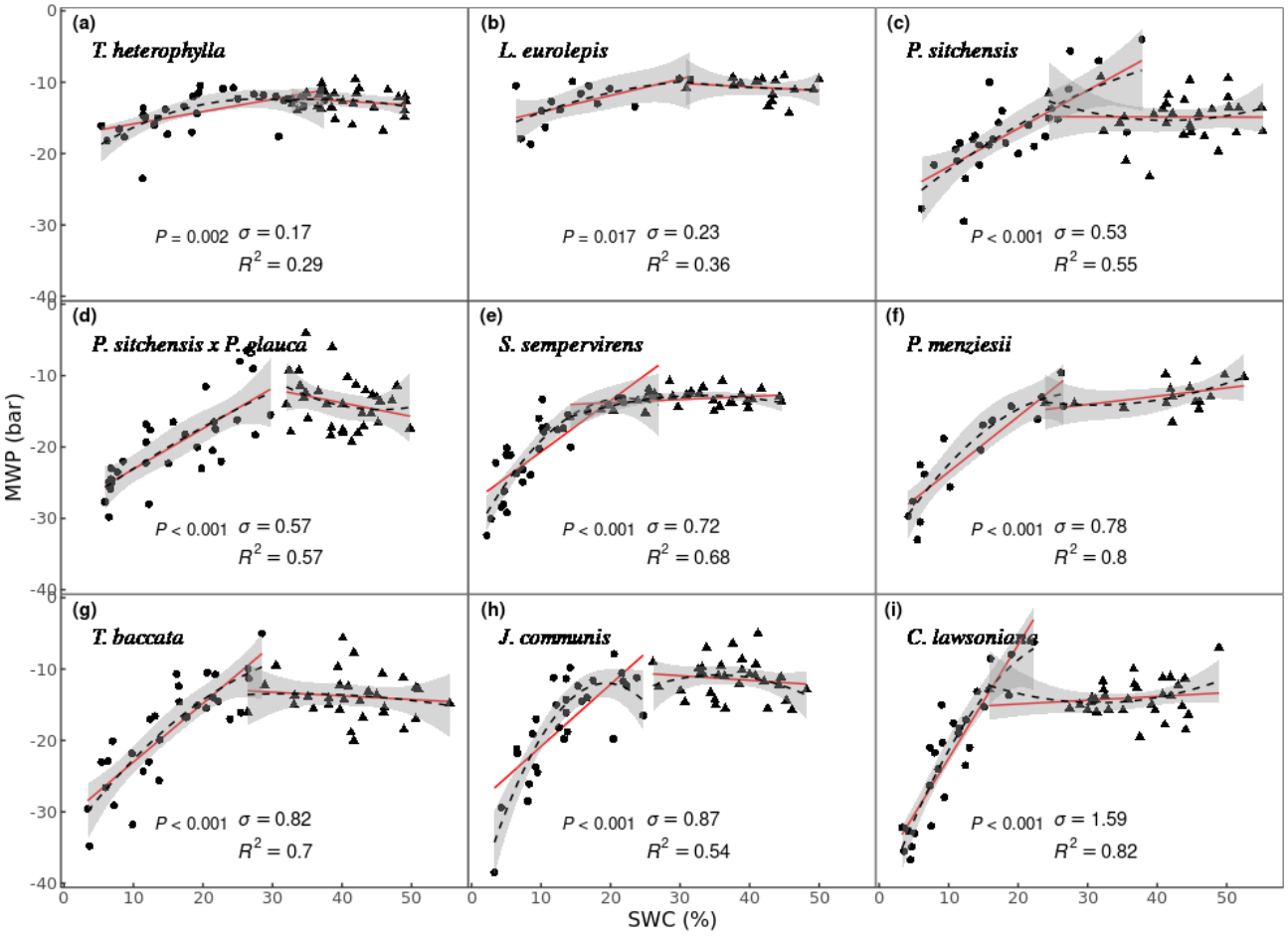

Figure 4. Curvilinear and linear relationships between MWP and SWC. ***Triangles****: well-watered controls, N = 16-32;* ***Circles****: drought-treated trees, N = 16-32.* ***Red line****: Linear regression model of*

MWP against % SWC. ***Black dashed line****: second order polynomial regression.* R^2*, P-values and slope for the ordinary linear model for drought-treated trees are shown.* ***Grey*** *areas are 95% confidence intervals.*

Table 4. Tukey HSD post-hoc test summary of differences in MWP among species. Only significant contrasts for treated pots are shown (adjusted P value < 0.05). ***term****: regression term;* ***contrast****: pairwise comparison levels;* ***null.value****: value to which the estimate is compared;* ***estimate****: estimated value of the regression term,* ***conf.low****: lower confidence interval limit;* ***conf.high****: upper confidence interval limit;* ***adj.p.value****: p-value adjusted for multiple comparisons.*

term	contrast	null.value	estimate	conf.low	conf.high	adj.p.value
Species	*P. sitchensis x P. glauca-T. heterophylla*	0	0.636	0.035	1.236	0.029
Species	*S. sempervirens-T. heterophylla*	0	0.713	0.113	1.314	0.008
Species	*P. menziesii-T. heterophylla*	0	0.746	0.026	1.466	0.036
Species	*C. lawsoniana-T. heterophylla*	0	0.875	0.264	1.486	0.000
Species	*P. sitchensis x P. glauca-L. eurolepis*	0	0.829	0.109	1.548	0.011
Species	*S. sempervirens-L. eurolepis*	0	0.906	0.186	1.626	0.003
Species	*P. menziesii-L. eurolepis*	0	0.939	0.116	1.761	0.012
Species	*T. baccata-L. eurolepis*	0	0.746	0.034	1.458	0.032
Species	*C. lawsoniana-L. eurolepis*	0	1.068	0.339	1.797	0.000

When plotting the intercept estimated by the linear model for treated trees against its the slope value, a phylogenetic signal appeared that was consistent with the work from Brodribb and collaborators [45] in the distribution of conifer families across the iso/anisohydric spectrum (see Figure 5 and table 5). The derived Cuprassaceae *C. lawsoniana* partitioned at the extreme anisohydric end of the spectrum; the derived Cupressaceae *J. communis* and Taxaceae *T. baccata* grouped together in the anisohydric part, followed by Pinaceae *P. menziesii*; the basal cupressaceae *S. sempervirens* and Pinaceae *P. sitchensis* and *P. sitchensis x P. glauca* occupied a more isohydric portion of the spectrum, followed by Pinaceae, *L. eurolepis* and *T. heterophylla* in the isohydric and strict isohydric end.

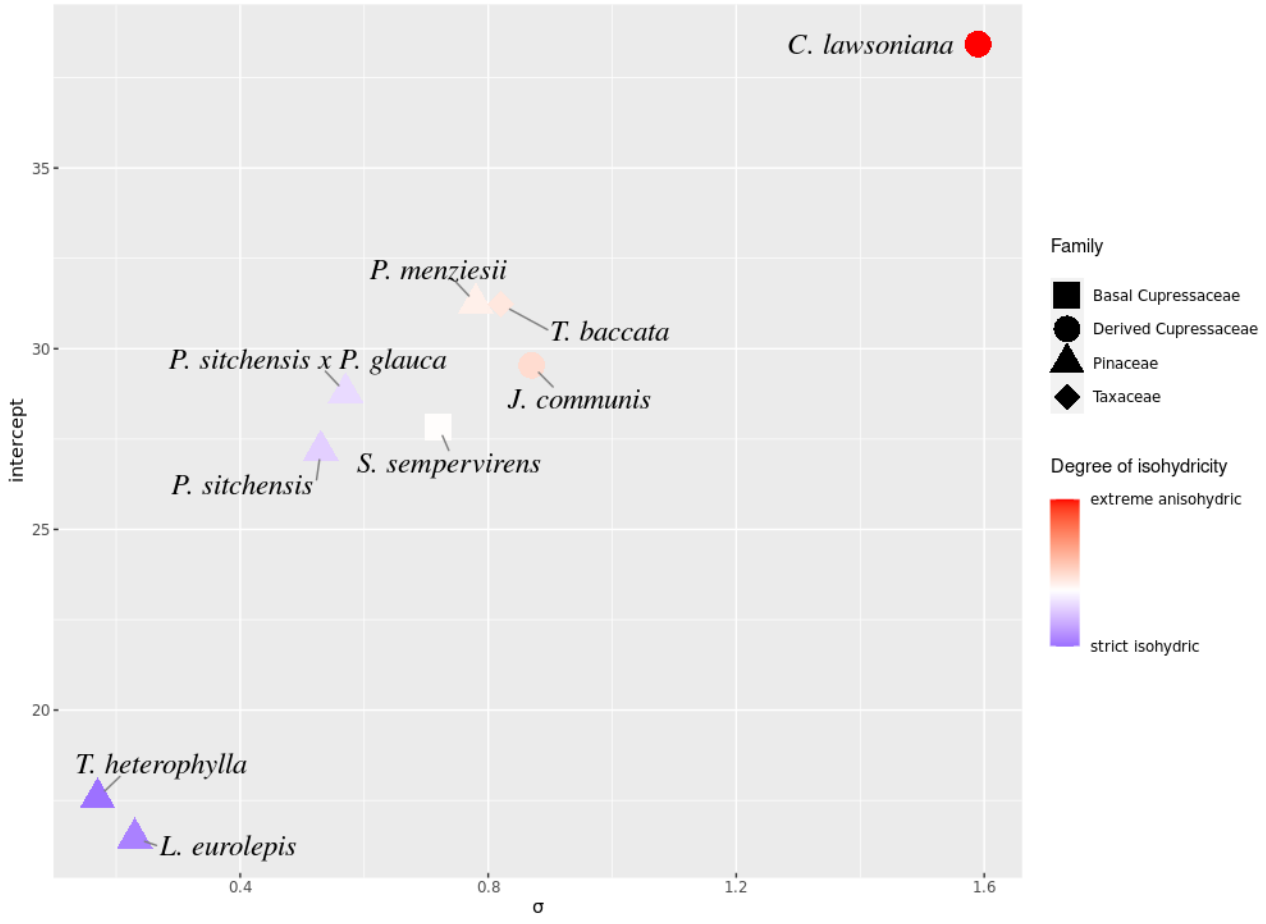

Figure 5. *Two-dimensional spectrum of iso/anisohydric responses across conifer families. Intercept values (**intercept**) were regressed against slope values (**σ**) of the same linear model to obtain a visual cue of the isohydry space. Values transition from more (**purple**) to less (**red**) isohydric.*

Table 5. Compact letters display of Tukey HSD post-hoc test summary of MWP versus SWC. Means that do not share any letter are significantly different at the 5% level of significance. ***Species****: species name;* ***SWC.trend****: slope values of the MWP~SWC relationship;* ***SE****: standard error;* ***df****: degrees of freedom;* ***lower.CL****: lower confidence interval limit;* ***upper.CL****: upper confidence interval limit;* ***group****: groups based on mean comparisons.*

Species	SWC.trend	SE	df	lower.CL	upper.CL	group
T. heterophylla	0.172	0.076	221	-0.04	0.385	a
L. eurolepis	0.23	0.128	221	-0.126	0.586	ab
P. sitchensis	0.535	0.088	221	0.29	0.78	abc
P. sitchensis x P. glauca	0.568	0.089	221	0.321	0.816	bc
S. sempervirens	0.717	0.105	221	0.424	1.01	bc
P. menziesii	0.776	0.118	221	0.446	1.106	c
T. baccata	0.821	0.092	221	0.563	1.079	c
J. communis	0.87	0.117	221	0.544	1.197	c
C. lawsoniana	1.592	0.141	221	1.199	1.985	d

Reproducibility

Consistency in ranking the responses was examined by comparing results from experiments 1 and 2, which had four species in common (see Table 1). In both cases, *C. lawsoniana* showed the most anisohydric response with a negative slope of -2 in Experiment 2. In the same experiment, towards a more isohydric part of the spectrum we found *P. sitchensis x P. glauca* and *P. sitchensis* (σ = - 0.53 and σ = - 0.27 respectively). *T. baccata* was positioned between these two, with a slope of - 0.45 (Supplementary figure 2).

Abscisic acid dynamics

The level of ABA determined in all species at 4 time points showed large differences between well-watered controls and drought treated plants, with the only exception of *J. communis*, where no significant difference was observed (Figure 6). The controls had ABA levels ranging from 100 to 500 ng/g FW, which changed very little over the course of the study. In contrast, the drought stressed plants in all species had major increases in ABA accumulation levels, but the accumulation profiles appeared very different among species relative to time point and midday leaf water potential (MWP) (see Figure 7 and 8). The derived Cupressaceae *C. lawsoniana* accumulated high ABA levels after a few days of treatment, reaching a peak of almost 10000 ng of ABA within the second week of drought

stress and then returned to moderate levels close to 2000 ng by the end, even though MWP continued to become more negative. This ABA profile observed in *C. lawsoniana* is similar to a peaking type, as described by Brodribb and collaborators [45]. *J. communis* followed a similar profile but had a less pronounced peak ~2000 ng of ABA in some individuals and overall, it showed low levels of endogenous ABA. *T. baccata* showed a somewhat weak ABA accumulation profile, reaching as high as 3000 ng of abscisic acid and then decreasing slowly to ~500 ng. We classified these three species as peaking types based on the observation of decreasing ABA levels despite intensifying drought conditions. In contrast, Pinaceae species accumulated abscisic acid throughout the drought experiment reaching or approaching a plateau without decreasing, with each species varying compared to others. Several plants had ABA levels in the range of 1000 ng to 2000 ng, with the exceptions of *L. eurolepis* (~5000 ng) and remarkably *P. sitchensis* (~9,000 ng). These species display profiles consistent with rising type similar to those from Brodribb and collaborators [45]. The basal Cupressaceae *S. sempervirens* had an unclear ABA profile, not rising enough to be clearly assigned to a peaking or rising type.

Based on the above results, we decided to focus the molecular investigation of *NCED* gene sequences and their expression in C. *lawsoniana*, *P. sitchensis* and *T. baccata* due to the range of drought responses and ABA accumulation profiles that we observed among them.

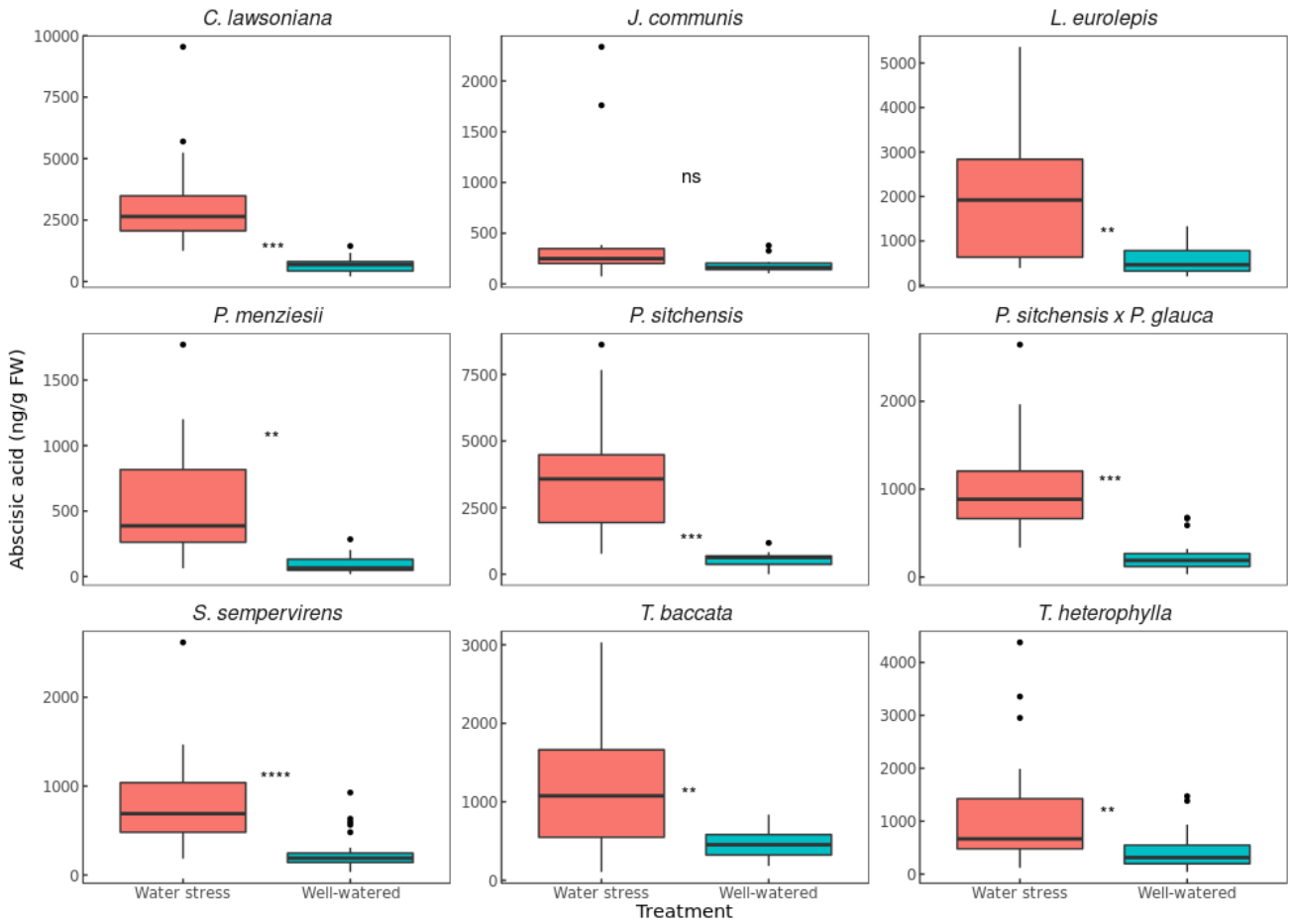

Figure 6. *Mean abscisic acid change between drought treatments.* ***Red****: drought-treated trees, N = 12-30;* ***Blue****: well-watered control trees, N = 12-30.* ***Asterisks*** *represent significant differences between treated and control trees; Tukey HSD (Honestly Significant Difference) post-hoc test (adjusted P value < 0.05).* ***Bars*** *indicate standard deviation.* ***Dots*** *represent potential outliers.*

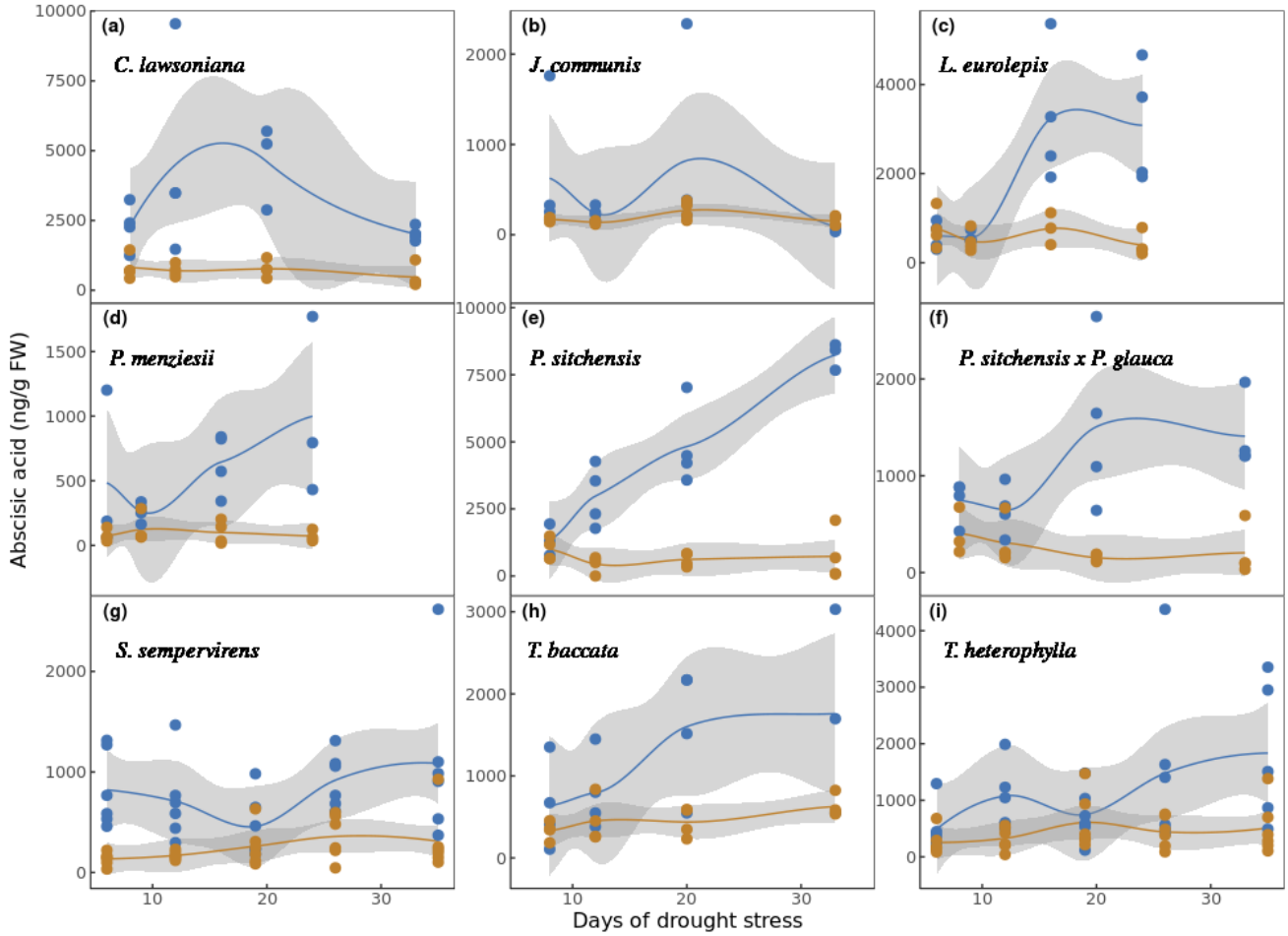

Figure 7. Abscisic acid time trends across conifer species. "Loess" formula was fit to ABA readings normalised against fresh foliage weight. ***Blue*** *dots and lines: drought-treated trees, N = 3-6 per time point.* ***Orange*** *dots and lines: well-watered trees, N = 3-6 per time point.* ***Grey shaded area****: 95% confidence interval.*

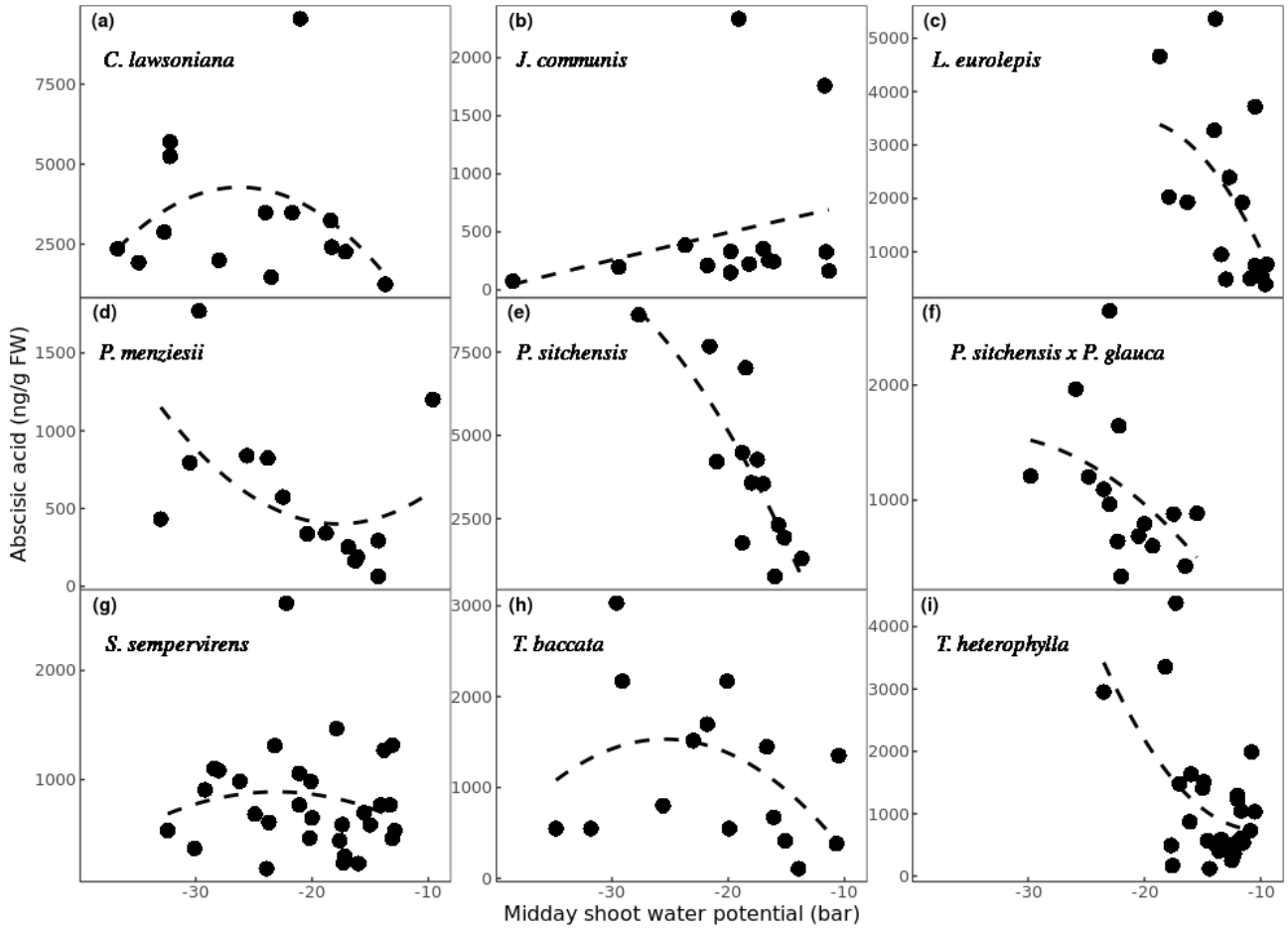

Figure 8. *Abscisic acid accumulation in relation to MWP. A second order polynomial function was fit to the data (**dashed line**). Species showing decreasing ABA levels as MWP became more negative were considered Peaking types, and species with increasing ABA levels as MWP became more negative were considered Rising type. N = 16-32.*

Candidate gene analyses

We conducted sequence similarity searches on our conifer transcriptomes using *A. thaliana* protein accessions as reference sequences. The analysis returned two putative *NCED* sequences for each of the three study species (*C. lawsoniana*, *P. sitchensis* and *T. baccata),* two sequences for *T. occidentalis* and three sequences for *L. laricina* and *P. glauca*. These putative *NCED* genes form two distinguished groups comprising conifer sequences only – with a 53% bootstrap support value at the branch node (see Figure 9) - here named 1 and 2. Since these groups separated from the whole angiosperm reference group (i.e., *A. thaliana*), we named the conifer sequences *NCED1* to *NCED3*. A distance matrix was computed for between-groups estimates of evolutionary divergence. The number of average amino acid substitutions for conifer group 1 compared to model angiosperms (*O. Sativa* and *A. thaliana*) was 0.49, while for conifer group 2 this was 0.53 (Supplementary table 4).

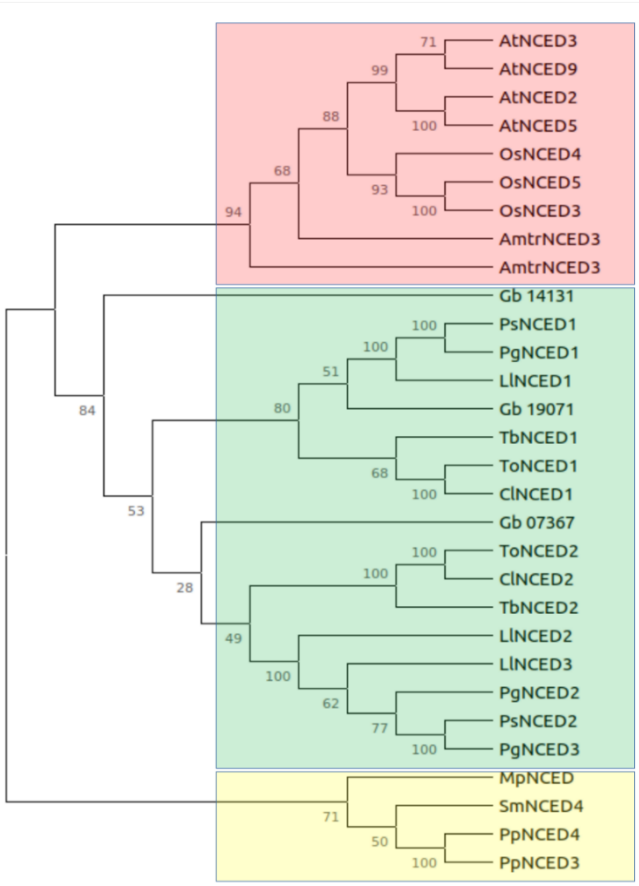

Figure 9. Putative NCED orthologs ML phylogenetic tree. Support bootstrap values (1000 replicates) are shown on the nodes. ***Red****: angiosperms;* ***Green****: gymnosperms;* ***Yellow****: seedless plants. Amtr: A. trichopoda; At: A. thaliana; Cl: C. lawsoniana; Gb: G. biloba; Ll: L. laricina; Mp: M. polymorpha; Os: O. sativa; Pg: P. glauca; Ps: P. sitchensis; Sm: S. moellendorffii; To: T. occidentalis.*

Table 6. Identity matrix of putative NCED ortholog protein sequences calculated based on pairwise comparisons withing a multiple sequence alignment.

%	AtNCED2	AtNCED3	AtNCED5	AtNCED9	PsNCED1	PsNCED2	ClNCED1	ClNCED2	TbNCED1	TbNCED2
AtNCED2	/									
AtNCED3	70.2	/								
AtNCED5	73.4	69.5	/							
AtNCED9	70.7	71.8	71.8	/						
PsNCED1	61.8	67.9	66.4	66.6	/					
PsNCED2	57.7	63.1	60.6	61.5	75.8	/				
ClNCED1	63.7	68.9	67.7	64.5	77	76.8	/			
ClNCED2	61.4	66.3	63.7	62.6	73.3	71.2	75	/		
TbNCED1	62.9	67	65.5	65.9	80.9	77.8	82.9	73.5	/	
TbNCED2	60.2	64.9	63.3	62	72.8	74.4	74.5	78.1	74.8	/

The multiple sequence alignment (MSA) of all protein sequences showed that they were highly conserved from residue 98 to 609, with a global similarity score above 0.7 spanning the main catalytic domain with no aa substitutions observed in the key histidine residues that coordinate the catalytic site (Supplementary figure 3). Pairwise comparisons of whole sequences within the MSA returned sequence identities for the putative conifer NCEDs (Table 6). *Ps*NCED1 and *Ps*NCED2 were 75.8% identical with each other, and 67.9% and 63.1% identical to *At*NCED3 and only 61.8% and 57.7% identical to *At*NCED2. *Cl*NCED1 and *Cl*NCED2 were 75% identical to each other and they were 68.9 and 66.3 identical to *At*NCED3 and only 63.7% and 61.4% identical to *At*NCED2. *Tb*NCED1 and *Tb*NCED2 were 74.8% identical to each other and they were 67% and 64.9% identical to *At*NCED3 and only 62% and 60.2% identical to *At*NCED2. These observations indicated an overall similarity of the discovered conifer NCEDs to *At*NCED3, which is linked to ABA biosynthesis, compared to *At*NCED2, which is not linked to ABA biosynthesis.

The search for candidate genes included two other genes encoding ABA biosynthesis enzymes, ABA1 (zeaxanthin epoxidase) and AAO3 (abscisic aldehyde oxidase). We found one putative ABA1 protein sequence based on homology to the *A. thaliana* gene for each of the study conifer species and *T. occidentalis*, and two homologous sequences for *L. laricina* and *P. glauca*. These sequences were named ABA1 to ABA2 (Figure 10). The sequences were highly conserved (> 0.7 similarity global score) from residue 91 to 659, including the characteristic FAD (flavin-adenine dinucleotide) binding domain and the FHA domain (forkhead-associated domain) (Supplementary figure 4). We also found one putative ortholog sequence of *At*AAO3 for each of the three study species, two for *L. laricina* and *T. occidentalis,* so these sequences were named AAO1 to AAO2 (Figure 11). We found less conservation among these sequences, especially within the Aldehyde oxidase and xanthine dehydrogenase, a/b hammerhead domain (Ald_Xan_dh_C, residues 579 to 688). There was a higher degree of variation within the Molybdopterin cofactor-binding domain (residues 977 to 1239). The *P. sitchensis* sequence *(Ps*AAO) was truncated, lacking the residues preceding the Ald_Xan_dh_C, but was nonetheless retained as it was the only representative sequence for *P. sitchensis* (Supplementary figure 5).

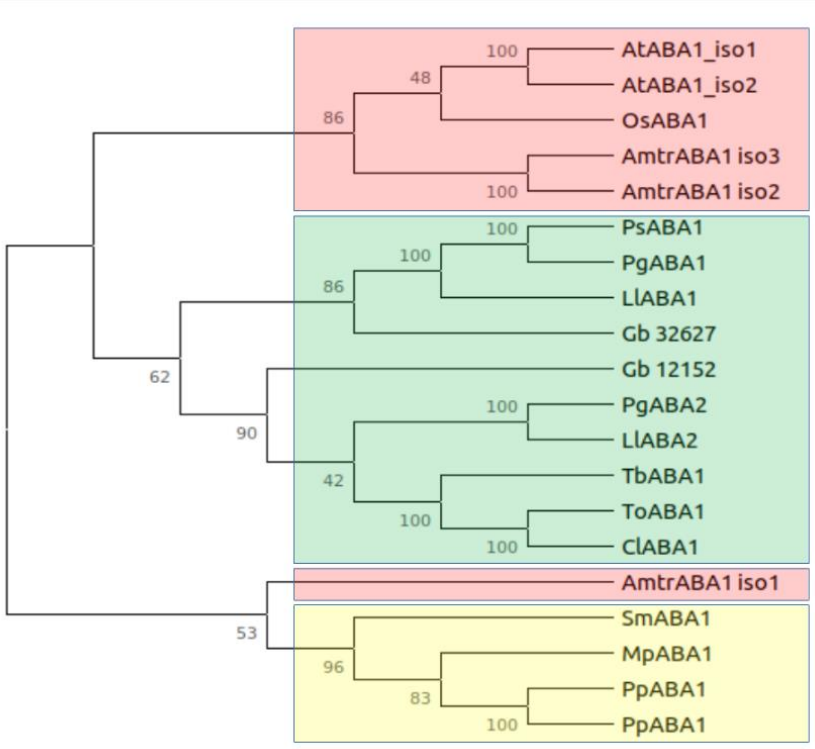

Figure 10. Putative ABA1 orthologs ML phylogenetic tree. Support bootstrap values (1000 replicates) are shown on the nodes. ***Red****: angiosperms;* ***Green****: gymnosperms;* ***Yellow****: seedless plants. Amtr: A. trichopoda; At: A. thaliana; Cl: C. lawsoniana; Gb: G. biloba; Ll: L. laricina; Mp: M. polymorpha; Os: O. sativa; Pg: P. glauca; Ps: P. sitchensis; Sm: S. moellendorffii; To: T. occidentalis.*

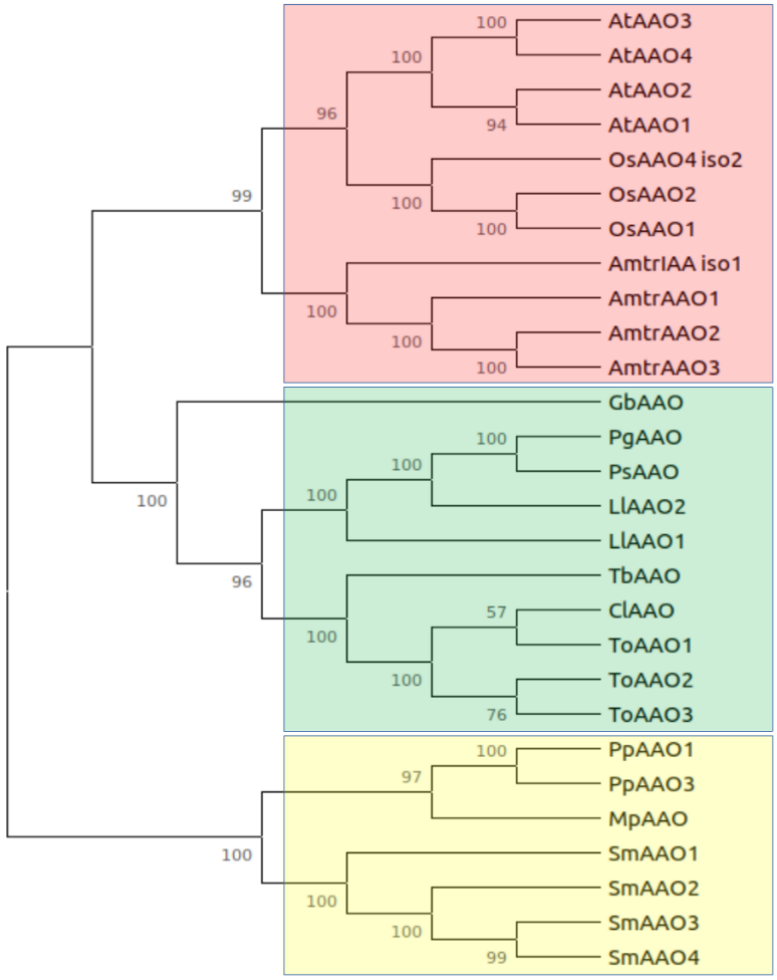

Figure 11. Putative AAO3 orthologs ML phylogenetic tree. Support bootstrap values (1000 replicates) are shown on the nodes. ***Red****: angiosperms;* ***Green****: gymnosperms;* ***Yellow****: seedless plants. Amtr: A. trichopoda; At: A. thaliana; Cl: C. lawsoniana; Gb: G. biloba; Ll: L. laricina; Mp: M. polymorpha; Os: O. sativa; Pg: P. glauca; Ps: P. sitchensis; Sm: S. moellendorffii; To: T. occidentalis.*

Our search for genes encoding enzymes in ABA catabolism focused on the *CYP707A* genes, specifically the *CYP707A3* subclass, as they have been shown to control the main catabolic pathway of ABA [47]. We found four putative CYP707A protein sequences for *C. lawsoniana,* three for *L. laricina,* two for *P. sitchensis* and only one for *P. glauca, T. occidentalis* and *T. baccata* (Figure 12). The phylogenetic reconstruction indicated that the protein sequences formed two separate groups: group 1 containing ClCYP707A1, PsCYP707A1 and TbCYP707A1 and group 2 containing ClCYP707A2, ClCYP707A3 and ClCYP707A4. ClCYP707A2 and ClCYP707A3 further diverged from ClCYP707A4. Group 1 was more closely related to AtCYP707A1 and AtCYP707A3, while group 2 was more closely related to AtCYP707A2. Overall, we observed a high degree of sequence similarity among taxa (Supplementary figure 6).

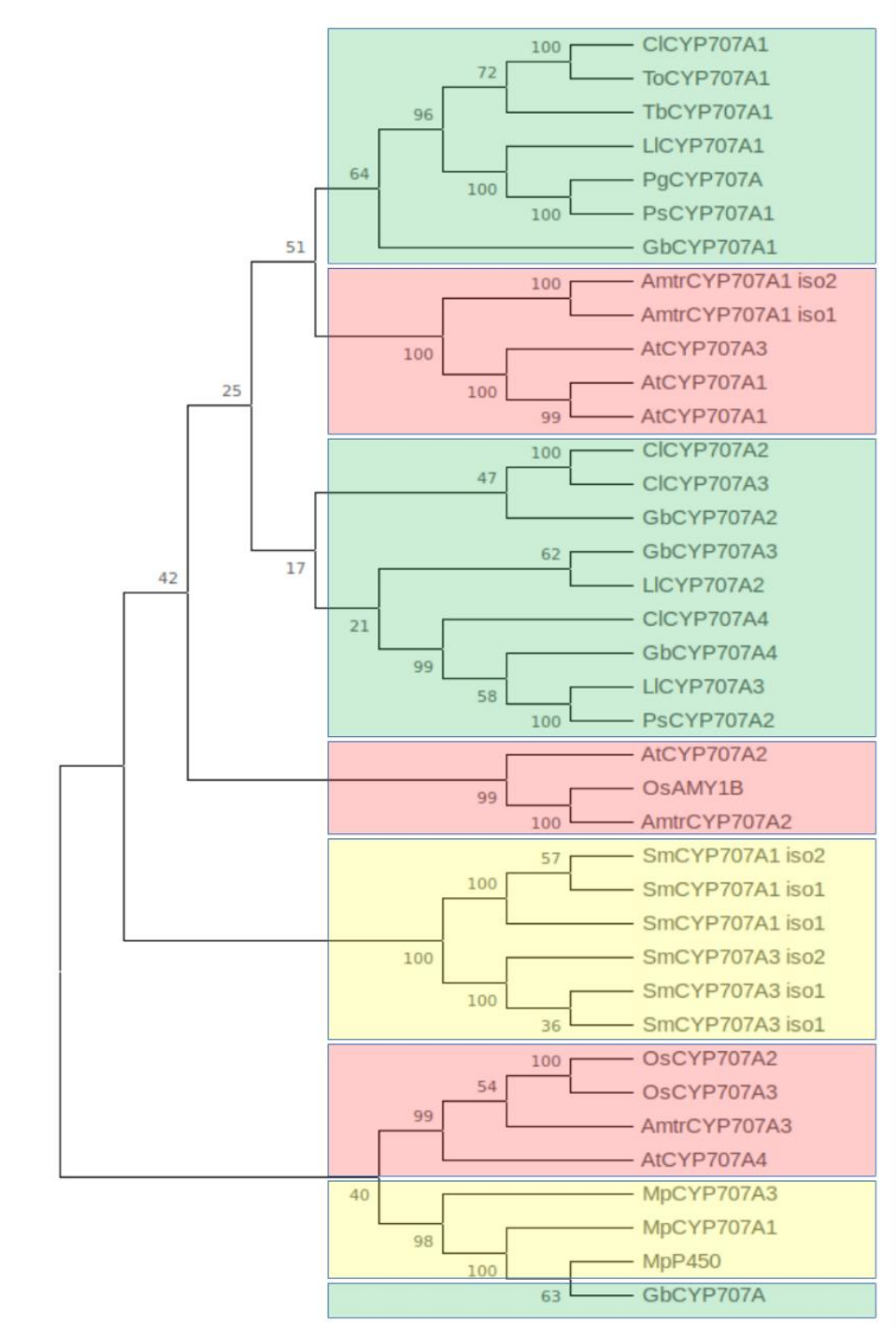

Figure 12. Putative CYP707A orthologs ML phylogenetic tree. Support bootstrap values (1000 replicates) are shown on the nodes. ***Red****: angiosperms;* ***Green****: gymnosperms;* ***Yellow****: seedless plants. Amtr: A. trichopoda; At: A. thaliana; Cl: C. lawsoniana; Gb: G. biloba; Ll: L. laricina; Mp: M. polymorpha; Os: O. sativa; Pg: P. glauca; Ps: P. sitchensis; Sm: S. moellendorffii; To: T. occidentalis.*

Gene expression

A main hypothesis of our research is that *NCED* gene expression levels underpin the accumulation of ABA in conifers responding to drought. Changes in *NCED* transcript levels relative to controls were determined in *C. lawsoniana*, *P. sitchensis* and *T. baccata* as they represented a range of MWP (midday leaf water potential) and ABA responses. Foliage samples from experiment 1 were analysed by RT-qPCR with gene-specific primers targeting two distinct *NCED* gene sequences identified in each species as the close homologs to *NCEDs* in *A. thaliana*. The data showed a 4 to 8-fold (2 to 3 in Log_2) increase in *NCED* gene expression in *P. sitchensis*, starting from 10 days of drought (Figure 13). The increase was more consistently detected in *PsNCED1* than in *PsNCED2*. On the contrary the *C. lawsoniana* sequence *ClNCED1* was clearly down-regulated from 8 days of drought, going as low as a 100-fold (Log_2 fold change of -7) decrease. *ClNCED2* expression decreased later and more variably from 20 to 33 days. There was no significant differential expression for *T. baccata NCED* genes.

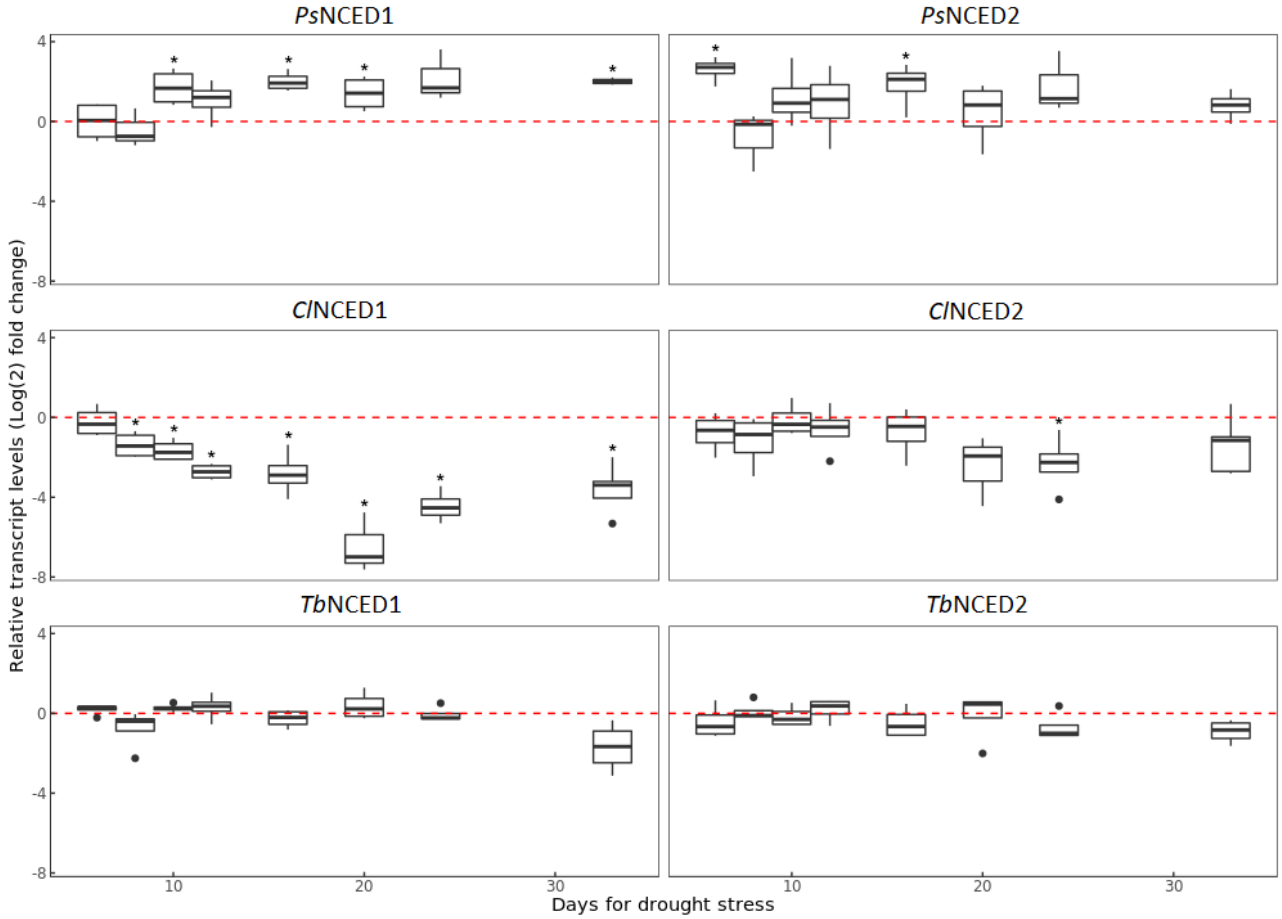

Figure 13. *Relative transcript levels at 8 time points during the imposed drought stress for each of the putative ortholog NCED sequences identified. Raw Ct values were normalised against well-*

watered controls and reference genes to obtain ΔΔCt values. ***Asterisks*** *represent significant differences between treated trees and the zero-fold-change baseline (****dashed red line****); Tukey HSD (Honestly Significant Difference) post-hoc test (adjusted P value < 0.05).* ***Dots*** *represent potential outliers. N = 4.*

Single homolog sequences of *AAO3* and *ABA1* were analysed using the same methodology. In *P. sitchensis, PsABA1* was significantly overexpressed relative to controls at 12, 20 and 24 days of drought, showing a 2 to 4-fold increase in transcripts abundance. *PsAAO* was significantly overexpressed at about the same level at only 12 days of drought stress and decreased afterwards producing variable, non-significant, assay results (Figure 14). *ClAAO* was weakly but significantly overexpressed at 8 days but downregulated at 16 days of drought. *ClABA1* appear to follow the same pattern as *ClAAO*, but globally did not appear to be differentially expressed (Figure 14). In *T. baccata,* the data indicated variable levels of gene expression, with weak but significant down-regulation of *TbAAO* only at 24 days and *TbABA1* at 33 days of drought, while no clear signal was detected for other days.

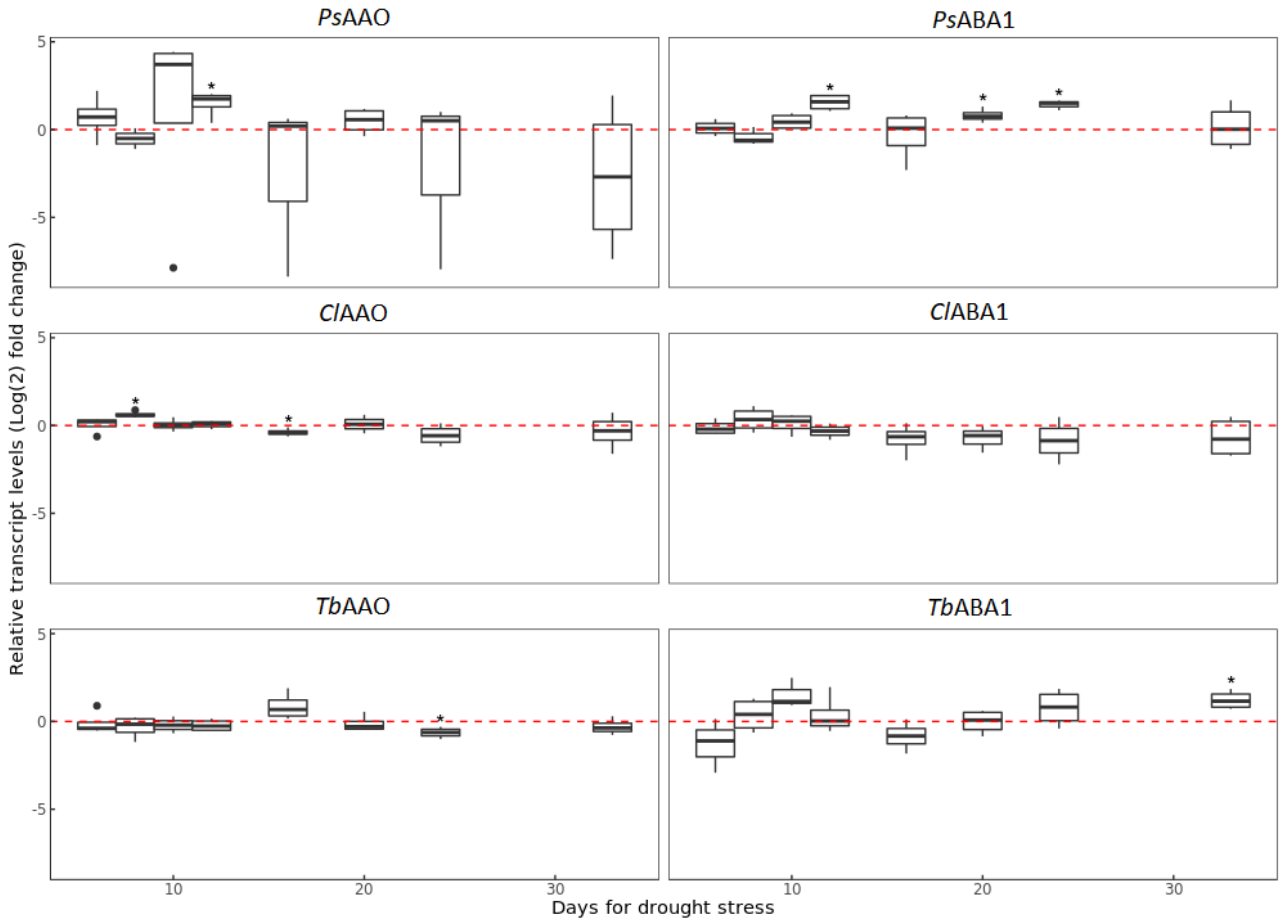

Figure 14. *Relative transcript levels at 8 time points during the imposed drought stress for each of the putative ortholog ABA1 and AAO sequences identified. Raw Ct values were normalised against well-watered controls and reference genes to obtain ΔΔ*Ct values.* ***Asterisks*** *represent significant differences between treated and the zero-fold-change baseline (****dashed red line****); Tukey HSD (Honestly Significant Difference) post-hoc test (adjusted P value < 0.05).* ***Dots*** *represent potential outliers. N = 4*

We investigated the expression of putative catabolic *CYP707A* genes, responsible for the breakdown of ABA (Figure 15). *ClCYP707A4* was significantly overexpressed up to 64-fold starting from 12 days of drought stress. On the contrary, *C. lawsoniana ClCYP707A1* and *ClCYP707A2* were strongly downregulated from 10 and 8 days of drought respectively reaching as low as 1000-fold decrease. *ClCYP707A3* appeared to be downregulated, but this change was not statistically significant. *T. baccata TbCYP707A1* expression was significantly downregulated at three time points (12, 24 and 34 days of drought) with its lowest negative fold change at 34 days of drought stress (5 to 6-fold). *TbCYP707A2* appeared to vary its expression from significantly up- to down-regulated between the second week and third week of drought, being weakly differentially expressed at 12, 16 and 24 days. In contrast, there was no significant change in the expression levels of *PsCYP707A1s* in *P. sitchensis*.

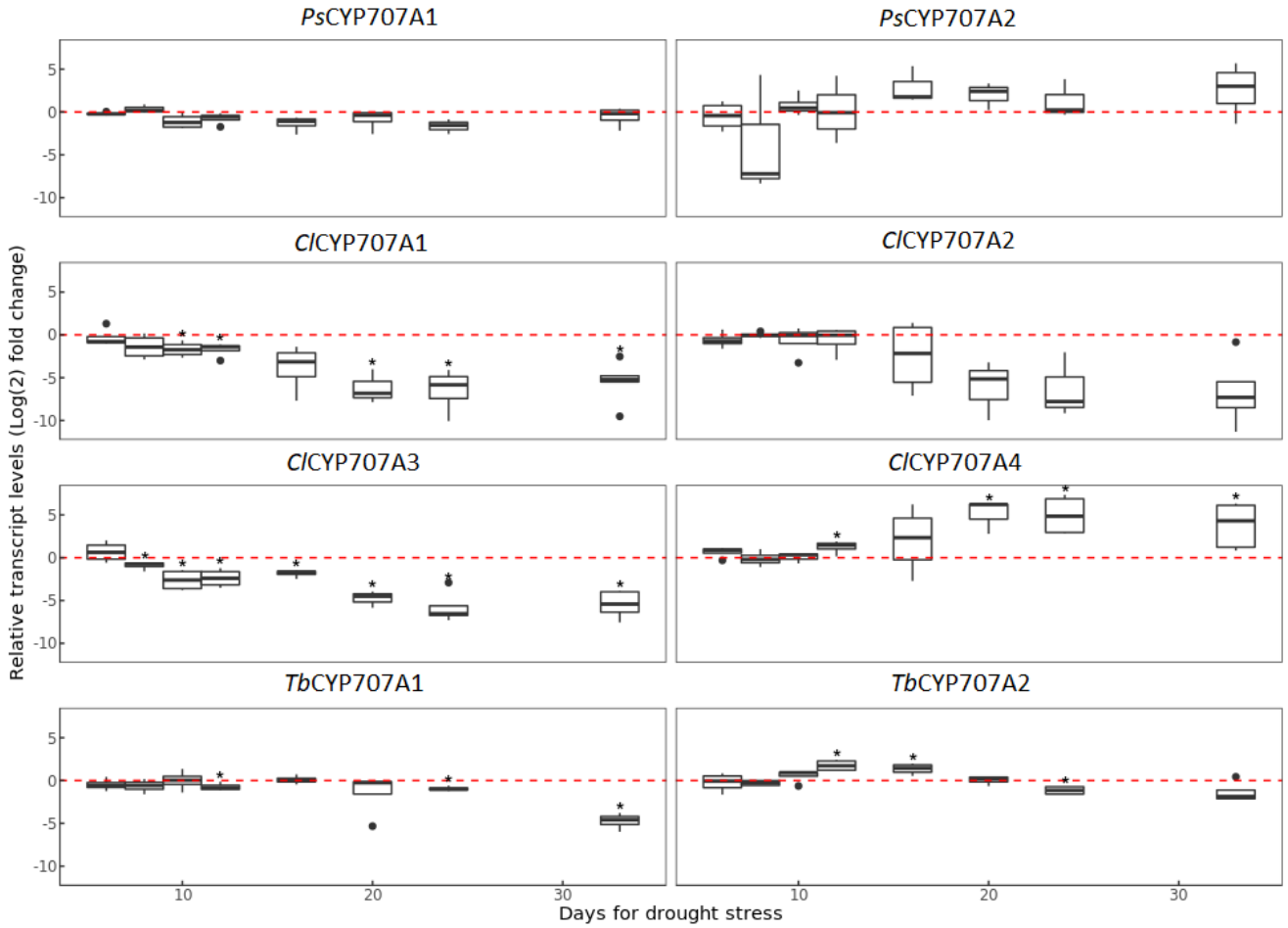

Figure 15. *Relative transcript levels at 8 time points during the imposed drought stress for each of the putative ortholog CYP707A sequences identified. Raw Ct values were normalised against well-watered controls and reference genes to obtain* $\Delta\Delta Ct$ *values.* ***Asterisks*** *represent significant differences between treated and the zero-fold-change baseline (****dashed red line****); Tukey HSD (Honestly Significant Difference) post-hoc test (adjusted P value < 0.05).* ***Dots*** *represent potential outliers. N = 4.*

Discussion

Our study explored a genetic mechanism hypothesised to underpin contrasting water relations and ABA accumulation profiles in species spanning three families of conifers. We used physiological data in response to a drought treatment to classify species along the iso/anisohydry spectrum. Our classification system allowed us to discern a degree of drought sensitivity from more to less conservative, in good agreement with previous studies. Our study species diverged in their ABA accumulation ranging from P- to R- type profiles corresponding to drought response strategies. Here, we discuss how ABA-related gene expression results may help to explain the observed drought response phenotypes. Changes in gene expression indicate that *NCED* may regulate ABA accumulation in the R-type *P. sitchensis*, but not in P-type *C. lawsoniana*.

Tree Physiologyogy under drought conditions

We imposed a drought treatment on nine conifer species in three separate experiments. Water status varied significantly across the study species. We observed a significant decrease in the mean MWP between water-stressed and control trees in all species, but the difference was small in *L. eurolepis* and *T. heterophylla* and even non-significant in *P. sitchensis*. In contrast, members of Cupressaceae *C. lawsoniana, J. communis* and *S. sempervirens* as well as *T. baccata* (Taxaceae) reached a more negative shoot water potential under drought stress. The observations indicated a range of responses from conservative to more permissive strategies adopted across species, based on the relationship between MWP and SWC. Changes along the iso- to anisohydry spectrum are often reported by measuring stomatal or midday leaf water potential to soil water potential or pre-dawn leaf water potential [6,22,55–57], which are proxies of soil water availability to the root system. Here we used volumetric SWC to model the response of shoot water potential to drought stress, but this approach has been reported elsewhere [58,59]. Volumetric SWC was an overall good predictor for shoot MWP and allowed us to classify species along the iso/anisohydry spectrum similar to that of [54].

We used the slope (σ) of the drought-stress regression line to classify our study plants as follows: *L. eurolepis* and *T. heterophylla* (σ = -0.17 and -0.23, respectively) as strict isohydric; *P. sitchensis*, *P. sitchensis x P. glauca* and *S. sempervirens* (σ ranging from -0.53 to -0.72) as relative isohydric and occupying the middle of the range; *P. menziesii*, *J. communis* and *T. baccata* (σ = -0.78, -0.82, and -0.87, respectively) as more anisohydric; and *C. lawsonia*na (σ = -1.59) as extreme anisohydric.

We explored the statistical meaning of this distribution along a continuum to better understand the position of each species relative to another. The trend can also be visualised by plotting the coordinates of the intercept and slope of the linear regression between MWP and SWC for each species. As indicated, we found that species in the Pinaceae were strict to relative isohydric, compared to derived Cupressaceae or Taxaceae, which were more anisohydric. There was a further distinction between derived and basal Cupressaceae, with *S. sempervirens* – basal clade – clustering together with the more conservative Pinaceae. Although we did not quantify this phylogenetic signal, these results are clearly consistent with previous research showing the adaptive significance of variation in water relations across the conifer phylogeny and especially resistance to embolism [45,59–62]. The minimum xylem water potential that a plant can withstand depends on anatomical and structural constraints such us vessel architecture and rooting depth, but ultimately it will depend on intrinsic xylem resistance to embolism [62–64]. Our observations are consistent with reports of P50 values (the water potential at which 50% of the xylem conductivity is lost) reported for these species' groups [45,65] and with the evolutionary history of water relations in conifers.

Abscisic acid profiles

Studies on ABA accumulation in response to drought stress have shown that tree species produce Rising (R) or Peaking (P) types [44,45]. While R-types rely on the maintenance of accumulated ABA levels to control leaf water status and to prevent vessel embolism, P-type trees switch from ABA-driven to turgor-driven stomatal closure, characterised by a drop in ABA levels, and keep transpiring for longer into a drought event. These contrasting types have been observed in both conifers and angiosperm species [44,66–69]. While angiosperms can adopt both types within the same genus [67,68], Brodribb and collaborators [45] proposed that ABA types initially evolved in the conifer phylogeny under different climatic conditions so that the most ancient conifer families display a Rising type, while more derived (recently evolved) Cupressaceae and Taxaceae adopted a Peaking type. Species-specific abscisic acid profiles found in our study were in general agreement with previous reports. Peaking type profiles were found in extreme anisohydric *C. laswoniana* and anisohydric *J. communis* and *T. baccata*.

For ABA accumulation to stop, leaf water potential must surpass the leaf turgor loss point, which can be as low as -40 bar [44,66–69]. At this point, leaf water status is low enough to cause passive stomatal closure and a peaking type may be observed. We found high variation in abscisic acid levels within our study species. This, combined with a relatively short drought, probably contributed to somewhat

weak or incomplete Peaking profiles, such as those found in *J. communis* and *T. baccata*. Basal Cupressaceae *S. sempervirens* eluded our classification method, as it did not clearly display a rising nor peaking accumulation profile. On the contrary, all the Pinaceae included in the study were classified as Rising types. This is coherent with the strict to relatively isohydric responses we observed in these species since constant accumulation of ABA is needed for a conservative strategy to prevent excessive water loss through stomatal leakage and to avoid embolism.

ABA-related genes and their expression

Genetic control of drought responses and ABA accumulation has been studied in detail in model angiosperms but has received less attention in conifers [70]. Most of the studies addressing the genetics of drought responses in conifers have made use of transcriptome analyses [70–73], while a few have identified candidate genes by use of expression studies [74,75]. Our sequence similarity searchers were successful at identifying candidate ABA-related genes using previously generated transcriptomes from a range of conifer species. We investigated changes in the expression of these candidate genes over the course of a simulated drought. While genes involved in abscisic acid accumulation and signalling may be conserved across the land plant phylogeny [76,77], our observations suggest that their regulation and functional specialization in conifers may differ from model angiosperms. *NCED* genes are widely recognised as key regulators of drought responses for fine-tuning fast ABA biosynthesis in model plants [29,78]. We found two sequence clusters of putative *NCED* genes in our study species, which we named *NCED1* and *NCED2*. These sequences were highly conserved, and the sub-groups were both sister to angiosperm *NCEDs*, although group 1 was more closely related to the *NCED3* which has been linked to ABA in *A. thaliana* (0.49 average amino acid substitutions). The expression of *NCED* was clearly drought responsive but the observed changes in expression varied substantially among conifer species and families. Furthermore, our data suggest a potentially divergent regulation of gene expression of *NCEDs* in group 1 and 2.

In *P. sitchensis* (Pinaceae family), increased *NCED* gene expression was observed for *PsNCED1* starting from day 10 of drought until the end of the drought experiment, although the level was variable. A non-consistent trend was observed for *PsNCED2*, which was significantly overexpressed at only two time points and most significantly after 6 days of drought, before changes in *PsNCED1* were detected.

The overall changes in *NCED* transcript levels observed in *P. sitchensis* are in line with the ABA accumulation profile during drought. The *PsNCED2* transcript level changes differed from those of *PsNCED1*, suggesting that they may have partly complimentary roles, having potentially arisen through duplication and followed by partial functional divergence. Alternatively, *PsNCED2* may be more active in other tissues, developmental stages or under other kinds of stress and only marginally involved in the drought response, as is observed with the extensive diversification reported in angiosperm *NCEDs* [35,79]. Based on our data, *PsNCED1* could be the main biosynthetic gene controlling ABA levels in *P. sitchensis* and, as such, it may be sufficient to explain the rising ABA type observed in *P. sitchensis*.

We hypothesised that a Peaking type would result from the downregulation of *NCEDs*. In line with our hypothesis, we observed reduced NCED gene expression in *C. lawsoniana*. At least *ClNCED1* was clearly and progressively downregulated. Here again, we could not establish a clear pattern for the group 2 sequence *ClNCED2,* as it was significantly downregulated at only one time point, and it had highly variable expression levels. Nonetheless, *ClNCED1* reached its lowest expression at 20 days of drought stress, about the same time *ClNCED2* reached its only significant downregulation (24 days). Therefore, we propose *ClNCED1* may be the main candidate for the role of rate-limiting enzyme in *C. lawsoniana*, and downregulation happened before the peak of abscisic acid was observed during the first two weeks of drought. One possibility is that ABA accumulated due to early overexpression of *ClNCEDs*, which we didn't capture in our sampling. Alternatively, the peak in ABA levels could be due to overexpression of other biosynthetic genes, implying that expression of *ClNCEDs* is not rate-limiting for accumulation. Another explanation is that ABA could come from other sources, such as ABA-GE stores 64,70, while import from roots or different tissues has been ruled out in other conifer studies [80–83]. As suggested in *P. sitchensis, ClNCED2* may be weakly responsive to drought stress or may be involved in other processes and tissues.

We also explored *ABA1* and *AAO3* gene sequence phylogenies and found one sequence for each of our study species, although there were duplications in the other conifer species. We observed a high degree of similarity between taxa, suggesting that these genes are highly conserved across the land plants phylogeny. *ABA1* and *AAO3* can support ABA biosynthesis at lower expression levels compared to key *NCEDs* under drought stress in model plants [37,38,41,84,85].

In our study, *AAO3* and *ABA1* did not show substantial changes in expression levels, with few exceptions. *P. sitchensis* showed high variability in *PsAAO3* expression and no significant trend, but *PsABA1* seemed to partially mirror *NCED* overexpression with some level of upregulation, which was significant at three time points. In *C. lawsoniana ClABA1* and *ClAAO3* expression results suggest they do not contribute to peaking ABA levels; in fact, they appeared to switch from being weakly upregulated to being weakly downregulated, although the changes were not statistically significant. Overall, our observations suggest that changes in *AAO3* and *ABA1* expression may have a minor role, if any at all depending on the species, in driving changes in ABA levels. If *ClABA1* and *ClAAO3* are not limiting in *C. lawsoniana* for *de novo* synthesis of ABA, it is not surprising that they are not differentially expressed or are even downregulated to drive decreases in ABA accumulation. On the other hand, the minor upregulation of *PsABA1* in *P. sitchensis* may complement the strong upregulation of *PsNCED1* and thus support increased ABA biosynthesis.

In *A. thaliana, CYP707A1-A4* genes encode 8′-hydroxylases that have a role in controlling cellular ABA levels through catabolism, being upregulated upon re-hydration and oxidising ABA to phaseic acid [47,86,87]. We found two homologous sequences of *AtCYP707As* in *P. sitchensis* and *T. baccata,* while *C. lawsoniana* had four. We also found that *L. laricina CYP707A* have undergone multiple duplications events. It was possible to distinguish between two groups of conifer *CYP707As*. Group 1 included sequences that were more closely related to *A. thaliana CYP707A1* and *CYP707A3*, known for functioning in leaf drought responses in *A. thaliana* [87]. Group 2 was more closely related to *A. thaliana CYP707A2*, a gene that is involved in seed dormancy in model plants [47,88,89], and was the most diversified with multiple putative paralogs in *C. lawsoniana* and *L. laricina*. In *C. lawsoniana* three *CYP707A* sequences were downregulated, and one was upregulated. It is possible that the four paralogues co-operate in fine tuning ABA accumulation, although functional analyses are needed to establish the role of each of them. We can speculate that downregulation of one or more sequences among *ClCYP707A1*, *2* and *3* at the early stages of drought may contribute to raise the levels of abscisic acid, potentially coming from ABA-GE stores in the vacuole based on our expression data for biosynthetic genes. On the other hand, upregulation of *ClCYP707A4* may counteract this process

and remove ABA starting from the second week of drought to produce the typical peaking type we have observed. However, recent evidence suggests that Peaking-types are not produced by ABA degradation to PA, but by conjugation into ABA-GE 64. Since we didn't measure either PA or ABA-GE, we can only speculate as to the role of *CYP707As* in fine-tuning ABA levels in Peaking-type conifers. In contrast, we didn't find any significant change in *P. sitchensis* orthologs *PsCYP707A1* and *PsCYP707A2,* meaning that the ABA catabolic function is either maintained at constitutive levels or not required. This supports our interpretation of a key role for *PsNCED1* and perhaps also *PsABA1* in leading the steady accumulation of abscisic acid in *P. sitchensis* and production of the rising ABA profile.

Finally, to our surprise, *T. baccata* didn't seem to differentially express *NCED* genes despite increased levels of ABA in response to drought. *TbAAO* and *TbABA1* appeared to be weakly differentially expressed at only one time point each, but no clear signal was detected for other time points. The only genes that were differentially expressed were *TbCYP707As*. We observed that *TbCYP707A1* was weakly but significantly downregulated, except for the last day of drought, were a 32-fold decrease in expression was found. TbCYP707A2 on the contrary switched from up to downregulation, suggesting that *TbCYP707As* may be downregulated to allow ABA accumulation despite biosynthetic functions not being differentially regulated.

Conclusions

We investigated the possible genetic mechanisms underpinning contrasting drought responses among conifer species. We confirmed that different conifer families can adopt diverging strategies to cope with drought and accumulate ABA following typical Rising or Peaking phenotypes. While the more conservative Pinaceae and basal Cupressaceae tend to rely on constant accumulation of ABA, the more risk-taking derived Cupressaceae may produce Peaking profiles. We observed a clearly drought-responsive expression in *NCED* genes that is consistent with a role in controlling such ABA levels in Rising-type *P. sitchensis*. Based on our data, *PsNCED1* could be the main biosynthetic gene controlling ABA levels in *P. sitchensis* and, as such, it may be sufficient to explain the rising ABA type observed in *P. sitchensis*. In contrast, there was no clear contribution of putative *NCEDs* in ABA accumulation in Peaking-type *C. lawsoniana*. Expression of other biosynthetic genes suggests they may complement *NCED* function and mirror to some extent *NCED* expression. A contribution of putative catabolic *CYP707As* to ABA profiles was less clear based on transcript levels, although it

seems they could cooperate with *NCED* genes in fine-tuning abscisic acid accumulation at least in *C. lawsoniana*. More work is needed to clarify these roles, and our data suggest that the role of ABA-GE stores and related genes in producing such phenotypes may be a fruitful area of study in future. *T. baccata* gene expression responses remained elusive, and more work is needed to establish a clear drought response strategy. In practice, understanding and characterising these responses may inform species choice and adaptive tree breeding faced with changing climates.

Literature cited

1. Masson-Delmotte V, Zhai P, Pörtner HO, et al. Global warming of 1.5°C An IPCC Special Report on the impacts of global warming of 1.5°C above pre-industrial levels and related global greenhouse gas emission pathways, in the context of strengthening the global response to the threat of climate change, sustainable development, and efforts to eradicate poverty Edited by Science Officer Science Assistant Graphics Officer Working Group I Technical Support Unit 2019.
2. Allen CD, Macalady AK, Chenchouni H, et al. A global overview of drought and heat-induced tree mortality reveals emerging climate change risks for forests. Forest Ecology and Management. 2010;259(4):660-684. doi:10.1016/j.foreco.2009.09.001
3. McDowell NG, Williams AP, Xu C, et al. Multi-scale predictions of massive conifer mortality due to chronic temperature rise. Nature Climate Change. 2016;6(3):295-300. doi:10.1038/nclimate2873
4. Allen CD, Breshears DD, McDowell NG. On underestimation of global vulnerability to tree mortality and forest die-off from hotter drought in the Anthropocene. Ecosphere. 2015;6(8):1-55. doi:10.1890/ES15-00203.1
5. Williams AP, Allen CD, Macalady AK, et al. drought stress and tree mortality. Nature Climate Change. 2012;3(3):292-297. doi:10.1038/nclimate1693
6. Roman DT, Novick KA, Brzostek ER, Dragoni D, Rahman F, Phillips RP. The role of isohydric and anisohydric species in determining ecosystem-scale response to severe drought. Oecologia. 2015;179(3):641-654. doi:10.1007/s00442-015-3380-9
7. McAusland L, Vialet-Chabrand S, Davey P, Baker NR, Brendel O, Lawson T. Effects of kinetics of light-induced stomatal responses on photosynthesis and water-use efficiency. New Phytologist. 2016;211(4):1209-1220. doi:10.1111/NPH.14000
8. Dunn J, Hunt L, Afsharinafar M, et al. Reduced stomatal density in bread wheat leads to increased water-use efficiency. Journal of Experimental Botany. 2019;70(18):4737. doi:10.1093/JXB/ERZ248

9. Papanatsiou M, Petersen J, Henderson L, Wang Y, Christie JM, Blatt MR. Optogenetic manipulation of stomatal kinetics improves carbon assimilation,water use, and growth. Science. 2019;363(6434):1456-1459. doi:10.1126/SCIENCE.AAW0046/
10. Matallana-Ramirez LP, Whetten RW, Sanchez GM, Payn KG. Breeding for Climate Change Resilience: A Case Study of Loblolly Pine (*Pinus taeda* L.) in North America. Frontiers in Plant Science. 2021;12:790. doi:10.3389/FPLS.2021.606908/
11. Miedaner T, Juroszek P. Climate change will influence disease resistance breeding in wheat in Northwestern Europe. Theoretical and Applied Genetics. 2021;134(6):1771-1785. doi:10.1007/S00122-021-03807-0/
12. Cowan IR, Farquhar GD. Stomatal function in relation to leaf metabolism and environment. Symposia of the Society for Experimental Biology. 1977;31:471-505. PMID: 756635
13. Tardieu F, Simonneau T. Variability among species of stomatal control under fluctuating soil water status and evaporative demand: modelling isohydric and anisohydric behaviours. Journal of Experimental Botany. 1998;49(Special):419-432. doi:10.1093/jxb/49.Special_Issue.419
14. McAdam SAM, Brodribb TJ. Linking Turgor with ABA Biosynthesis: Implications for Stomatal Responses to Vapor Pressure Deficit across Land Plants. Plant Physiology. 2016;171(3):2008-2016. doi:10.1104/pp.16.00380
15. Yang YJ, Bi MH, Nie ZF, et al. Evolution of stomatal closure to optimize water-use efficiency in response to dehydration in ferns and seed plants. New Phytologist. 2021;230(5):2001-2010. doi:10.1111/NPH.17278
16. Skelton RP, West AG, Dawson TE. Predicting plant vulnerability to drought in biodiverse regions using functional traits. Proceedings of the National Academy of Sciences. 2015;112(18):5744-5749. doi:10.1073/pnas.1503376112
17. Klein T. The variability of stomatal sensitivity to leaf water potential across tree species indicates a continuum between isohydric and anisohydric behaviours. Functional Ecology. 2014;28(6):1313-1320. doi:10.1111/1365-2435.12289
18. McDowell NG, Allen CD. Darcy's law predicts widespread forest mortality under climate warming. Nature Climate Change. 2015;5(7):669-672. doi:10.1038/nclimate2641
19. Deans RM, Brodribb TJ, McAdam SAM. An Integrated Hydraulic-Hormonal Model of Conifer Stomata Predicts Water Stress Dynamics. Plant Physiology. 2017;174(2):478-486. doi:10.1104/pp.17.00150
20. Tardieu F, Davies WJ. Integration of hydraulic and chemical signalling in the control of stomatal conductance and water status of droughted plants. Plant Cell and Environment. 1993;16(4):341-349. doi:10.1111/j.1365-3040.1993.tb00880.x
21. Ratzmann G, Meinzer FC, Tietjen B. Iso/Anisohydry: Still a Useful Concept. Trends in Plant Science. 2019;24(3):191-194. doi:10.1016/J.TPLANTS.2019.01.001

22. Hartmann H, Link RM, Schuldt B. A whole-plant perspective of isohydry: stem-level support for leaf-level plant water regulation. Tree Physiology. 2021;41(6):901-905. doi:10.1093/TREEPHYS/TPAB011
23. Seo M, Marion-Poll A. Abscisic acid metabolism and transport. Advances in Botanical Research. 2019;92:1-49. doi:10.1016/bs.abr.2019.04.004
24. Hsu PK, Dubeaux G, Takahashi Y, Schroeder JI. Signaling mechanisms in abscisic acid-mediated stomatal closure. Plant Journal. 2021;105(2):307-321. doi:10.1111/tpj.15067
25. Sussmilch FC, Brodribb TJ, McAdam SAM. What are the evolutionary origins of stomatal responses to abscisic acid in land plants? Journal of Integrative Biology. 2017;59(4):240-260. doi:10.1111/jipb.12523
26. Kollist H, Nuhkat M, Roelfsema MRG. Closing gaps: Linking elements that control stomatal movement. New Phytologist. 2014;203(1):44-62. doi:10.1111/nph.12832
27. Tan BC, Schwartz SH, Zeevaart JAD, Mccarty DR. Genetic control of abscisic acid biosynthesis in maize. Proceedings of the National Academy of Sciences U S A. 1997;94(22):12235-12240. doi:10.1073/pnas.94.22.12235
28. Schwartz SH, Tan BC, Gage DA, Zeevaart JAD, McCarty DR. Specific oxidative cleavage of carotenoids by VP14 of maize. Science. 1997;276(5320):1872-1874. doi:10.1126/science.276.5320.1872
29. Qin X, Zeevaart JAD. The 9-cis-epoxycarotenoid cleavage reaction is the key regulatory step of abscisic acid biosynthesis in water-stressed bean Proceedings of the National Academy of Sciences U S A. 1999;96(26):15354-15361. doi:10.1073/pnas.96.26.15354
30. Iuchi S, Kobayashi M, Taji T, et al. Regulation of drought tolerance by gene manipulation of 9-cis-epoxycarotenoid dioxygenase, a key enzyme in abscisic acid biosynthesis in Arabidopsis. Plant Journal. 2001;27(4):325-333. doi:10.1046/J.1365-313X.2001.01096.X
31. Tan BC, Cline K, McCarty DR. Localization and targeting of the VP14 epoxy-carotenoid dioxygenase to chloroplast membranes. Plant Journal. 2001;27(5):373-382. doi:10.1046/j.1365-313X.2001.01102.x
32. Burbidge A, Burbidge A, Grieve T, et al. Structure and expression of a cDNA encoding a putative neoxanthin cleavage enzyme (NCE), isolated from a wilt-related tomato (*Lycopersicon esculentum* Mill.) library. Journal of Experimental Botany. 1997;48(314):2111-2112. doi:10.1093/jxb/48.12.2111
33. Chernys JT, Zeevaart JAD. Characterization of the 9-Cis-Epoxycarotenoid Dioxygenase Gene Family and the Regulation of Abscisic Acid Biosynthesis in Avocado. Plant Physiology. 2000;124(1):343-354. doi:10.1104/pp.124.1.343
34. Hauser F, Waadt R, Schroeder JI. Evolution of abscisic acid synthesis and signaling mechanisms. Current Biology. 2011;21(9):R346-R355. doi:10.1016/j.cub.2011.03.015
35. Priya R, Siva R. Analysis of phylogenetic and functional diverge in plant nine-cis epoxycarotenoid dioxygenase gene family. Journal of Plant Research. 2015;128(4):519-534. doi:10.1007/s10265-015-0726-7

36. Hanada K, Hase T, Toyoda T, Shinozaki K, Okamoto M. Origin and evolution of genes related to ABA metabolism and its signaling pathways. Journal of Plant Research. 2011;124(4):455-465. doi:10.1007/s10265-011-0431-0
37. Marin E, Nussaume L, Quesada A, et al. Molecular identification of zeaxanthin epoxidase of Nicotiana plumbaginifolia, a gene involved in abscisic acid biosynthesis and corresponding to the ABA locus of *Arabidopsis thaliana*. EMBO Journal. 1996;15(10):2331-2342. doi:10.1002/j.1460-2075.1996.tb00589.x
38. Audran C, Borel C, Frey A, et al. Expression studies of the zeaxanthin epoxidase gene in Nicotiana plumbaginifolia. Plant Physiology. 1998;118(3):1021-1028. doi:10.1104/pp.118.3.1021
39. Audran C, Liotenberg S, Gonneau M, et al. Localisation and expression of zeaxanthin epoxidase mRNA in Arabidopsis in response to drought stress and during seed development. Australian Journal of Plant Physiology. 2001;28(12):1161-1173. doi:10.1071/pp00134
40. Seo M, Peeters AJM, Koiwai H, et al. The Arabidopsis aldehyde oxidase 3 (AAO3) gene product catalyzes the final step in abscisic acid biosynthesis in leaves. Proceedings of the National Academy of Sciences. 2000;97(23):12908-12913. doi:10.1073/PNAS.220426197
41. Koiwai H, Nakaminami K, Seo M, Mitsuhashi W. Tissue-Specific Localization of an Abscisic Acid. Enzyme. 2004;134(4):1697-1707. doi:10.1104/pp.103.036970.1
42. McAdam SAM, Brodribb TJ. Separating Active and Passive Influences on Stomatal Control of Transpiration. Plant Physiology. 2014;164(4):1578-1586. doi:10.1104/pp.113.231944
43. McAdam SAM, Brodribb TJ. The Evolution of Mechanisms Driving the Stomatal Response to Vapor Pressure Deficit. Plant Physiology. 2015;167(3):833-843. doi:10.1104/pp.114.252940
44. Brodribb TJ, McAdam SAM. Abscisic Acid Mediates a Divergence in the Drought Response of Two Conifers. Plant Physiology. 2013;162(3):1370-1377. doi:10.1104/pp.113.217877
45. Brodribb TJ, McAdam SAM, Jordan GJ, Martins SCV. Conifer species adapt to low-rainfall climates by following one of two divergent pathways. Proceedings of the National Academy of Sciences. 2014;111(40):14489-14493. doi:10.1073/pnas.1407930111
46. Harfouche A, Meilan R, Altman A. Molecular and physiological responses to abiotic stress in forest trees and their relevance to tree improvement. Tree Physiology. 2014;34(11):1181-1198. doi:10.1093/treephys/tpu012
47. Kushiro T, Okamoto M, Nakabayashi K, et al. The Arabidopsis cytochrome *P450 CYP707A* encodes ABA 8 0-hydroxylases: key enzymes in ABA catabolism. EMBO Journal. 2004;23:1647-1656. doi:10.1038/sj.emboj.7600121
48. Emms DM, Kelly S. OrthoFinder: phylogenetic orthology inference for comparative genomics. Genome Biology. 2019; 20(1):238. doi: 10.1186/s13059-019-1832-y.
49. Katoh K, Misawa K, Kuma KI, Miyata T. MAFFT: a novel method for rapid multiple sequence alignment based on fast Fourier transform. Nucleic Acids Research. 2002;30(14):3059. doi:10.1093/NAR/GKF436

50. Pessoa AM, Pereira S, Teixeira J. PrimerIdent: A web based tool for conserved primer design. Bioinformation. 2010;5(2):52-54. doi: 10.6026/97320630005052
51. Lee S, Doxey AC, McConkey BJ, Moffatt BA. Nuclear Targeting of Methyl-Recycling Enzymes in Arabidopsis thaliana Is Mediated by Specific Protein Interactions. Molecular Plant. 2012;5(1):231-248. doi:10.1093/mp/ssr083
52. Liu Z, Meyerowitz EM. LEUNIG regulates AGAMOUS expression in arabidopsis flowers. Development. 1995;121(4):975-991. doi:10.1242/dev.121.4.975
53. Kosarev P, Mayer KF, Hardtke CS. Evaluation and classification of RING-finger domains encoded by the Arabidopsis genome. Genome Biolog. 2002;3(4):0016.1. doi:10.1186/gb-2002-3-4-research0016
54. Martnez-Vilalta J, Poyatos R, Aguade D, Retana J, Mencuccini M. A new look at water transport regulation in plants. New Phytologist. 2014;204(1):105-115. doi:10.1111/nph.12912
55. Martínez-Vilalta J, Garcia-Forner N. Water potential regulation, stomatal behaviour and hydraulic transport under drought: deconstructing the iso/anisohydric concept. Plant Cell and Environment. 2017;40(6):962-976. doi:10.1111/pce.12846
56. Meinzer FC, Woodruff DR, Marias DE, et al. Mapping 'hydroscapes' along the iso- to anisohydric continuum of stomatal regulation of plant water status. Ecology Letters. 2016;19(11):1343-1352. doi:10.1111/ele.12670
57. Hochberg U, Rockwell FE, Holbrook NM, Cochard H. Iso/Anisohydry: A Plant-Environment Interaction Rather Than a Simple Hydraulic Trait. Trends in Plant Science. 2018;23(2):112-120. doi:10.1016/j.tplants.2017.11.002
58. Attia Z, Domec JC, Oren R, Way DA, Moshelion M. Growth and physiological responses of isohydric and anisohydric poplars to drought. Journal of Experimental Botany. 2015;66(14):4373-4381. doi:10.1093/jxb/erv195
59. Bayar E, Deligöz A. Impacts of precommercial thinning on gas exchange, midday water potential, and chlorophyll content in *Pinus nigra subsp. pallasiana* stand from the semiarid region. Trees - Structure and Function. 2020;34(5):1169-1181. doi:10.1007/s00468-020-01989-6
60. Jacobsen Al, Agenbag L, Esler Kj, Pratt Rb, Ewers Fw, Davis Sd. Xylem density, biomechanics and anatomical traits correlate with water stress in 17 evergreen shrub species of the Mediterranean-type climate region of South Africa. Journal of Ecology. 2007;95(1):171-183. doi:10.1111/j.1365-2745.2006.01186.x
61. Willson CJ, Manos PS, Jackson RB. Hydraulic traits are influenced by phylogenetic history in the drought-resistant, invasive genus Juniperus (Cupressaceae). American Journal of Botany. 2008;95(3):299-314. doi:10.3732/ajb.95.3.299
62. Choat B, Jansen S, Brodribb TJ, et al. Global convergence in the vulnerability of forests to drought. Nature. 2012;491(7426):752-755. doi:10.1038/nature11688
63. Brodribb TJ, Cochard H. Hydraulic Failure Defines the Recovery and Point of Death in Water-Stressed Conifers. Plant Physiology. 2009;149(1):575-584. doi:10.1104/pp.108.129783

64. Urli M, Porte AJ, Cochard H, Guengant Y, Burlett R, Delzon S. Xylem embolism threshold for catastrophic hydraulic failure in angiosperm trees. Tree Physiology. 2013;33(7):672-683. doi:10.1093/treephys/tpt030

65. Maherali H, Pockman WT, Jackson RB. Adaptive variation in the vulnerability of woody plants to xylem cavitation. Ecology. 2004;85(8):2184-2199. doi:10.1890/02-0538

66. Nolan RH, Tarin T, Santini NS, McAdam SAM, Ruman R, Eamus D. Differences in osmotic adjustment, foliar abscisic acid dynamics, and stomatal regulation between an isohydric and anisohydric woody angiosperm during drought. Plant Cell and Environment. 2017;40(12):3122-3134. doi:10.1111/pce.13077

67. Yao GQ, Nie ZF, Turner NC, et al. Combined high leaf hydraulic safety and efficiency provides drought tolerance in Caragana species adapted to low mean annual precipitation. New Phytologist. 2021;229(1):230-244. doi:10.1111/NPH.16845

68. Yao GQ, Li FP, Nie ZF, et al. Ethylene, not ABA, is closely linked to the recovery of gas exchange after drought in four Caragana species. Plant Cell Environment. 2021;44(2):399-411. doi:10.1111/PCE.13934

69. Mercado-Reyes JA, McAdam S. Extreme drought deactivates ABA biosynthesis. Authorea Preprints. March 31, 2022. doi:10.22541/AU.164873604.42418092/V1

70. Moran E, Lauder J, Musser C, Stathos A, Shu M. The genetics of drought tolerance in conifers. New Phytologist. 2017;216(4):1034-1048. doi:10.1111/NPH.14774

71. Fox H, Doron-Faigenboim A, Kelly G, et al. Transcriptome analysis of *Pinus halepensis* under drought stress and during recovery. Tree Physiology. 2018;38(3):423-441. doi:10.1093/TREEPHYS/TPX137

72. Lu M, Seeve CM, Loopstra CA, Krutovsky K v. Exploring the genetic basis of gene transcript abundance and metabolite levels in loblolly pine (*Pinus taeda* L.) using association mapping and network construction. BMC Genetics. 2018;19(1):1-13. doi:10.1186/S12863-018-0687-7

73. de María N, Guevara MÁ, Perdiguero P, et al. Molecular study of drought response in the Mediterranean conifer Pinus pinaster Ait.: Differential transcriptomic profiling reveals constitutive water deficit-independent drought tolerance mechanisms. Ecology and Evolution. 2020;10(18):9788-9807. doi:10.1002/ECE3.6613

74. van Ghelder C, Parent GJ, Rigault P, et al. The large repertoire of conifer NLR resistance genes includes drought responsive and highly diversified RNLs. Scientific Reports 2019 9:1. 2019;9(1):1-13. doi:10.1038/s41598-019-47950-7

75. Pashkovskiy PP, Vankova R, Zlobin IE, et al. Comparative analysis of abscisic acid levels and expression of abscisic acid-related genes in Scots pine and Norway spruce seedlings under water deficit. Plant Physiology and Biochemistry. 2019;140:105-112. doi:10.1016/J.PLAPHY.2019.04.037

76. Sussmilch FC, Brodribb TJ, McAdam SAM. Up-regulation of NCED3 and ABA biosynthesis occur within minutes of a decrease in leaf turgor but AHK1 is not required. Journal of Experimental Botany. 2017;68(11):2913-2918. doi:10.1093/JXB/ERX124

77. McAdam SAM, Sussmilch FC. The evolving role of abscisic acid in cell function and plant development over geological time. Seminars in Cell and Developmental Biology. 2021;109:39-45. doi:10.1016/J.SEMCDB.2020.06.006

78. S H Schwartz 1, B C Tan, D A Gage, J A Zeevaart, D R McCarty. Specific Oxidative Cleavage of Carotenoids by VP14 of Maize. Science. 1997; 20;276(5320):1872-4. doi: 10.1126/science.276.5320.1872.

79. Frey A, Effroy D, Lefebvre V, et al. Epoxycarotenoid cleavage by NCED5 fine-tunes ABA accumulation and affects seed dormancy and drought tolerance with other NCED family members. The Plant Journal. 2012;70(3):501-512. doi:10.1111/j.1365-313X.2011.04887.x

80. Manzi M, Lado J, Rodrigo MJ, Zacarías L, Arbona V, Gómez-Cadenas A. Root ABA Accumulation in Long-Term Water-Stressed Plants is Sustained by Hormone Transport from Aerial Organs. Plant & Cell Physiology. 2015;56(12):2457-2466. doi:10.1093/pcp/pcv161

81. McAdam SAM, Brodribb TJ, Ross JJ. Shoot-derived abscisic acid promotes root growth. Plant Cell and Environment. 2016;39(3):652-659. doi:10.1111/pce.12669

82. McAdam SAM, Brodribb TJ. Mesophyll cells are the main site of abscisic acid biosynthesis in water-stressed leaves. Plant Physiology. 2018:pp.01829.2017. doi:10.1104/pp.17.01829

83. Sack L, John GP, Buckley TN. ABA accumulation in dehydrating leaves is associated with decline in cell volume not turgor pressure. Plant Physiology. 2017;176(1):pp.01097.2017. doi:10.1104/pp.17.01097

84. Seo M, Peeters AJM, Koiwai H, et al. The Arabidopsis aldehyde oxidase 3 (AAO3) gene product catalyzes the final step in abscisic acid biosynthesis in leaves. Proceedings of the National Academy of Sciences. 2000;97(23):12908-12913. doi:10.1073/pnas.220426197

85. Barrero JM, Rodríguez PL, Quesada V, Piqueras P, Ponce MR, Micol JL. Both abscisic acid (ABA)-dependent and ABA-independent pathways govern the induction of NCED3, AAO3 and ABA1 in response to salt stress. Plant Cell and Environment. 2006;29(10):2000-2008. doi:10.1111/J.1365-3040.2006.01576.X

86. Saito S, Hirai N, Matsumoto C, et al. Arabidopsis *CYP707As* encode (+)-abscisic acid 8′-hydroxylase, a key enzyme in the oxidative catabolism of abscisic acid. Plant Physiology. 2004;134(4):1439-1449. doi:10.1104/PP.103.037614

87. Okamoto M, Tanaka Y, Abrams SR, Kamiya Y, Seki M, Nambara E. High humidity induces abscisic acid 8′-hydroxylase in stomata and vasculature to regulate local and systemic abscisic acid responses in Arabidopsis. Plant Physiology. 2009;149(2):825-834. doi:10.1104/PP.108.130823

88. Matakiadis T, Alboresi A, Jikumaru Y, et al. The Arabidopsis abscisic acid catabolic gene CYP707A2 plays a key role in nitrate control of seed dormancy. Plant Physiology. 2009;149(2):949-960. doi:10.1104/pp.108.126938

89. Zhu G, Liu Y, Ye N, Liu R, Zhang J. Involvement of the abscisic acid catabolic gene CYP707A2 in the glucose-induced delay in seed germination and post-germination growth of Arabidopsis. Physiol Plant. 2011;143(4):375-384. doi:10.1111/j.1399-3054.2011.01510.x

Supplementary material

Tables

Supplementary table 1. Study species and essential information. ***Age****: years in seedbed + years after transplant to open field or pot.* ***Provenance****: Country of origin of the material.* ***Type of material****: trees from Seed Orchard progeny, Germplasm, field stand or planting stock.* ***Provider****: company providing the material.*

Species name	**Size (cm)**	**Age (years)**	**Provenance**	**Type of material**	**Provider**
P. sitchensis	20-50	2+1	Denmark	Orchard	Maelor
P. sitchensis x P. glauca	20-50	1+1	UK	Orchard	Maelor
Larix eurolepis	20-40	1+1	Denmark	Seed	Maelor
Tsuga heterophylla	30-40	1U1	USA	Seed	Maelor
Pseudotsuga menziesii	20-40	1+1	France	Orchard	Maelor
C. lawsoniana	20-40	1.5	UK	Stand	Alba
Juniper communis	20-40	1.5	UK	Planting stock	Alba
T. baccata	20-40	2	UK	Planting stock	Alba

Supplementary table 2. Summary of the mixed linear model of MWP (Midday Water Potential) with Time and Treatment. Blocks were considered as random factor. Fixed part of the model includes: ***Estimate*** *= Slope estimate,* ***CI*** *= Confidence interval,* ***p*** *= p-value; Random effect part includes:* $\boldsymbol{\sigma}$ *= total variance within blocks,* $\boldsymbol{\tau 00}$ *= random intercept variance between blocks,* ***ICC*** *= inter-class correlation coefficient,* $\boldsymbol{N_{block}}$ *= number of experimental blocks.*

		MWP	
Predictors	Estimates	CI	p
(Intercept)	-11.71	-14.16 – -9.26	<0.001
Species [L. eurolepis]	1.14	-3.07 – 5.34	0.595
Species [*P. sitchensis*]	-3.46	-6.93 – 0.01	0.051
Species [*P. sitchensis* x P. glauca]	-2.12	-5.50 – 1.25	0.217
Species [S. sempervirens]	-1.60	-5.07 – 1.86	0.363
Species [P. menziesii]	1.33	-2.88 – 5.53	0.536
Species [T. baccata]	-1.23	-4.64 – 2.18	0.478
Species [J. communis]	-0.44	-3.86 – 2.98	0.800
Species [C. lawsoniana]	-2.03	-5.47 – 1.41	0.246
Time	-0.05	-0.16 – 0.06	0.397
Treatment [Water stress]	1.00	-2.47 – 4.46	0.572
Species [L. eurolepis] * Time	0.03	-0.22 – 0.28	0.789
Species [*P. sitchensis*] * Time	0.07	-0.11 – 0.25	0.454
Species [*P. sitchensis* x P. glauca] * Time	0.05	-0.12 – 0.22	0.556
Species [S. sempervirens] * Time	0.05	-0.11 – 0.21	0.529
Species [P. menziesii] * Time	-0.11	-0.36 – 0.13	0.368
Species [T. baccata] * Time	-0.01	-0.18 – 0.17	0.954
Species [J. communis] *	0.09	-0.08 – 0.27	0.280

Time			
Species [C. lawsoniana] * Time	0.03	-0.14 – 0.20	0.719
Species [L. eurolepis] * Treatment [Water stress]	0.90	-5.20 – 6.99	0.772
Species [*P. sitchensis*] * Treatment [Water stress]	5.92	0.96 – 10.88	0.019
Species [*P. sitchensis* x P. glauca] * Treatment [Water stress]	2.16	-2.67 – 6.99	0.381
Species [S. sempervirens] * Treatment [Water stress]	1.92	-2.98 – 6.82	0.442
Species [P. menziesii] * Treatment [Water stress]	1.26	-4.69 – 7.21	0.678
Species [T. baccata] * Treatment [Water stress]	4.10	-0.73 – 8.94	0.096
Species [J. communis] * Treatment [Water stress]	5.10	0.21 – 10.00	0.041
Species [C. lawsoniana] * Treatment [Water stress]	3.02	-1.85 – 7.88	0.223
Time * Treatment [Water stress]	-0.13	-0.29 – 0.03	0.106
(Species [L. eurolepis] * Time) * Treatment [Water stress]	-0.14	-0.50 – 0.22	0.432
(Species [*P. sitchensis*] * Time) * Treatment [Water stress]	-0.46	-0.72 – -0.20	0.001
(Species [*P. sitchensis* x P. glauca] * Time) * Treatment [Water stress]	-0.44	-0.69 – -0.20	<0.001
(Species [S. sempervirens] * Time) *	-0.39	-0.61 – -0.16	0.001

Treatment [Water stress]			
(Species [P. menziesii] * Time) * Treatment [Water stress]	-0.62	-0.98 – -0.27	0.001
(Species [T. baccata] * Time) * Treatment [Water stress]	-0.50	-0.75 – -0.26	<0.001
(Species [J. communis] * Time) * Treatment [Water stress]	-0.68	-0.93 – -0.43	<0.001
(Species [C. lawsoniana] * Time) * Treatment [Water stress]	-0.70	-0.95 – -0.45	<0.001

Random Effects

σ^2	9.83
$\tau_{00\ Block}$	0.00
ICC	0.00
N_{Block}	8
Observations	486
Marginal R^2 / Conditional R^2	0.706 / 0.706

Supplementary table 3. Summary of the linear model of MWP with SWC. Blocks were considered as random factor. Fixed part of the model includes: ***Estimate*** *= Slope estimate,* ***CI*** *= Confidence interval,* ***p*** *= p-value.*

	MWP		
Predictors	Estimates	CI	p
(Intercept)	-17.57	-20.80 – -14.34	<0.001
Species [L. eurolepis]	1.11	-4.34 – 6.56	0.688
Species [*P. sitchensis*]	-9.62	-14.42 – -4.82	<0.001
Species [*P. sitchensis* x P. glauca]	-11.21	-15.67 – -6.75	<0.001
Species [S. sempervirens]	-10.27	-14.38 – -6.16	<0.001
Species [P. menziesii]	-13.69	-18.55 – -8.83	<0.001
Species [T. baccata]	-13.66	-18.12 – -9.20	<0.001
Species [J. communis]	-11.97	-16.69 – -7.26	<0.001
Species [C. lawsoniana]	-20.86	-25.35 – -16.36	<0.001
SWC	0.17	0.02 – 0.32	0.025
Species [L. eurolepis] * SWC	0.06	-0.24 – 0.35	0.699
Species [*P. sitchensis*] * SWC	0.36	0.13 – 0.59	0.002
Species [*P. sitchensis* x P. glauca] * SWC	0.40	0.17 – 0.63	0.001
Species [S. sempervirens] * SWC	0.54	0.29 – 0.80	<0.001
Species [P. menziesii] * SWC	0.60	0.33 – 0.88	<0.001
Species [T. baccata] * SWC	0.65	0.41 – 0.88	<0.001
Species [J. communis] * SWC	0.70	0.42 – 0.97	<0.001
Species [C. lawsoniana] *	1.42	1.10 – 1.73	<0.001

SWC	
Observations	239
R^2 / R^2 adjusted	0.720 / 0.699

Supplementary table 4. % Similarity matrix for groups of putative NCED ortholog sequences. ***Conifers1*** *= including NCED group 1;* ***Conifers2*** *= including NCED group 2.*

%	**Angiosperms**	**Conifers1**	**Conifers2**	**Ginkgo**	**Seedless**
Angiosperms					
Conifers1	0.49				
Conifers2	0.532	0.375			
Ginkgo	0.533	0.37	0.387		
Seedless	0.626	0.546	0.563	0.579	

Figures

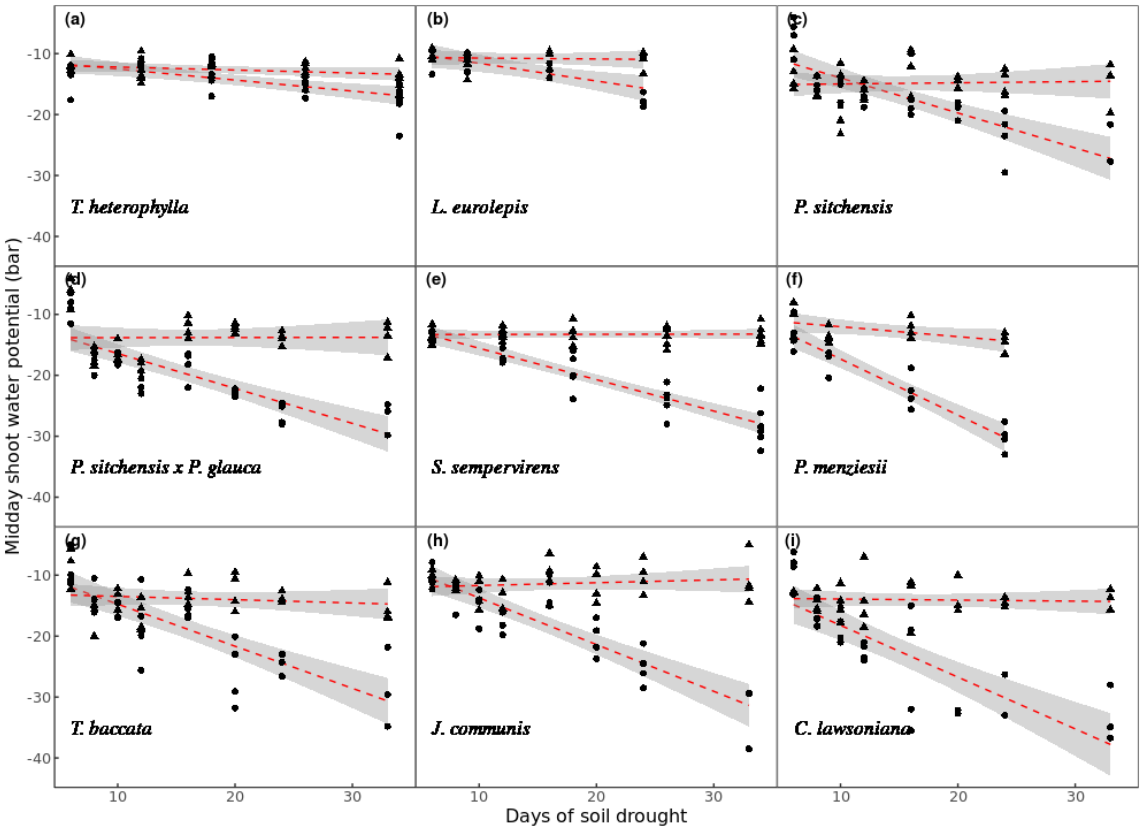

Supplementary figure 1. Midday Shoot Water Potential (MWP) progression during experimental drought. ***Triangles****: well-watered controls, N = 2-6 per time point.* ***Circles****: drought-treated trees, N = 2-6 per time point.* ***Red line****: Linear regression of MWP against days since withholding water.* ***Black dashed line****: second order polynomial regression. R^2, P-values and slope for the ordinary linear model are shown.* ***Grey shaded area****: 95% confidence interval.*

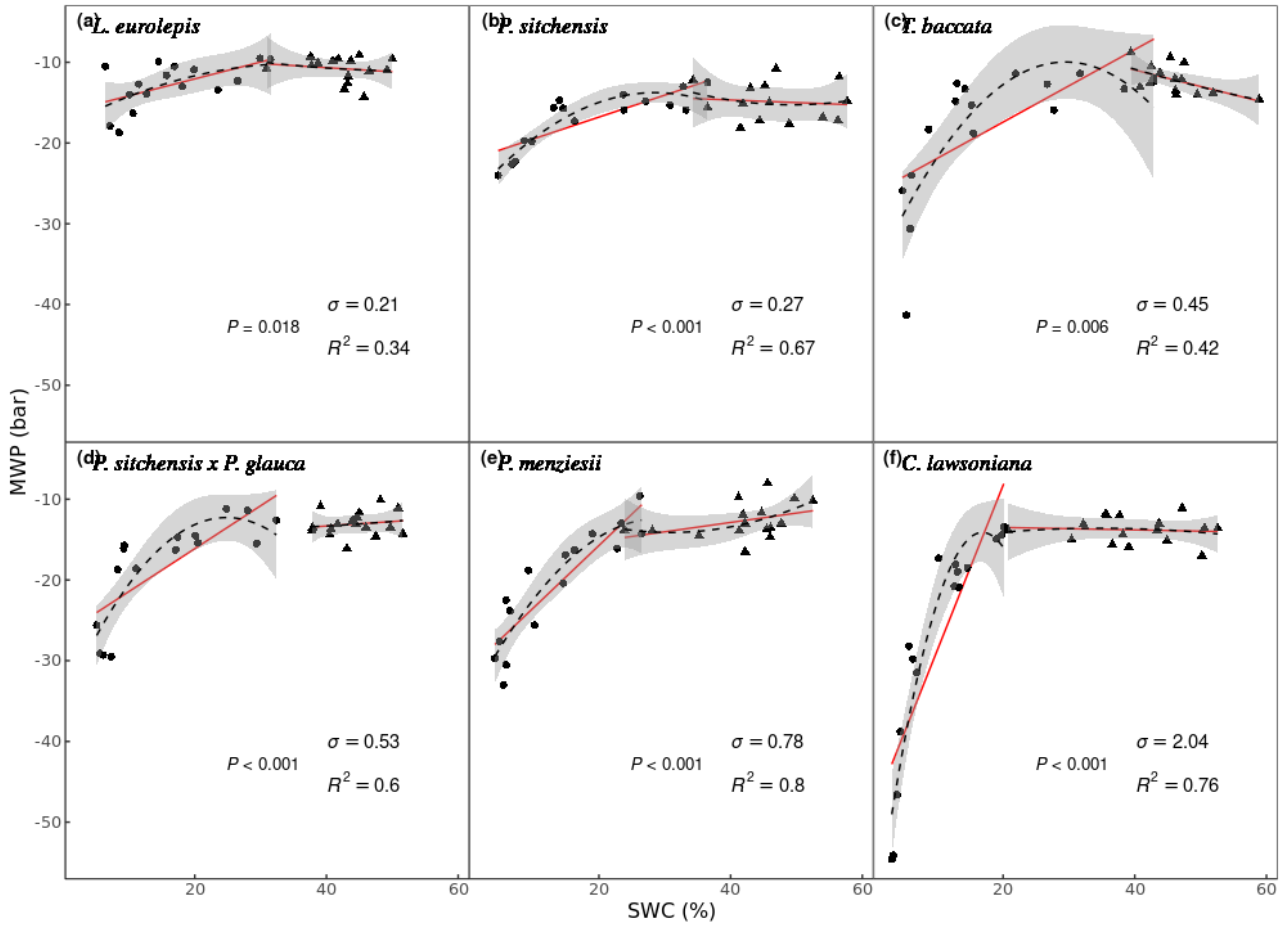

Supplementary figure 2. Curvilinear and linear relationships between MWP and SWC. ***Triangles****: well-watered controls, N = 16.* ***Circles****: drought-treated trees, N = 16.* ***Red line****: Linear regression model of Midday Shoot Water Potential (MWP) against % volumetric soil water content (SWC).* ***Black dashed line****: second order polynomial regression. R^2, P-values and slope for the ordinary linear model are shown.* ***Grey shaded area****: 95% confidence interval.*

"NCED_alignment_supplemental.pdf"

Supplementary figure 3. MAFFT multiple sequence alignment (MSA) of putative and model NCED protein sequences. Amtr: A. trichopoda; At: A. thaliana; Cl: C. lawsoniana; Gb: G. biloba; Ll: L. laricina; Mp: M. polymorpha; Os: O. sativa; Pg: P. glauca; Ps: P. sitchensis; Sm: S. moellendorffii; To: T. occidentalis. Residues with similarity scores above the 0.7 similarity cut-off value are shown in red on white background. Columns that are strictly conserved are shown in white on red background..

"ABA1_alignment_supplemental.pdf"

Supplementary figure 4. MAFFT multiple sequence alignment (MSA) of putative and model ABA1 protein sequences. Amtr: A. trichopoda; At: A. thaliana; Cl: C. lawsoniana; Gb: G. biloba; Ll: L. laricina; Mp: M. polymorpha; Os: O. sativa; Pg: P. glauca; Ps: P. sitchensis; Sm: S. moellendorffii; To: T. occidentalis. Residues with similarity scores above the 0.7 similarity cut-off value are shown in red on white background. Columns that are strictly conserved are shown in white on red background.

"AAO3_alignment_supplemental.pdf"

Supplementary figure 5. MAFFT multiple sequence alignment (MSA) of putative and model AAO protein sequences. Amtr: A. trichopoda; At: A. thaliana; Cl: C. lawsoniana; Gb: G. biloba; Ll: L. laricina; Mp: M. polymorpha; Os: O. sativa; Pg: P. glauca; Ps: P. sitchensis; Sm: S. moellendorffii; To: T. occidentalis. Residues with similarity scores above the 0.7 similarity cut-off value are shown in red on white background. Columns that are strictly conserved are shown in white on red background.

"CYP707A_alignment_supplemental.pdf"

Supplementary figure 6. MAFFT multiple sequence alignment (MSA) of putative and model CYP707A protein sequences. Amtr: A. trichopoda; At: A. thaliana; Cl: C. lawsoniana; Gb: G. biloba; Ll: L. laricina; Mp: M. polymorpha; Os: O. sativa; Pg: P. glauca; Ps: P. sitchensis; Sm: S. moellendorffii; To: T. occidentalis. Residues with similarity scores above the 0.7 similarity cut-off value are shown in red on white background. Columns that are strictly conserved are shown in white on red background.

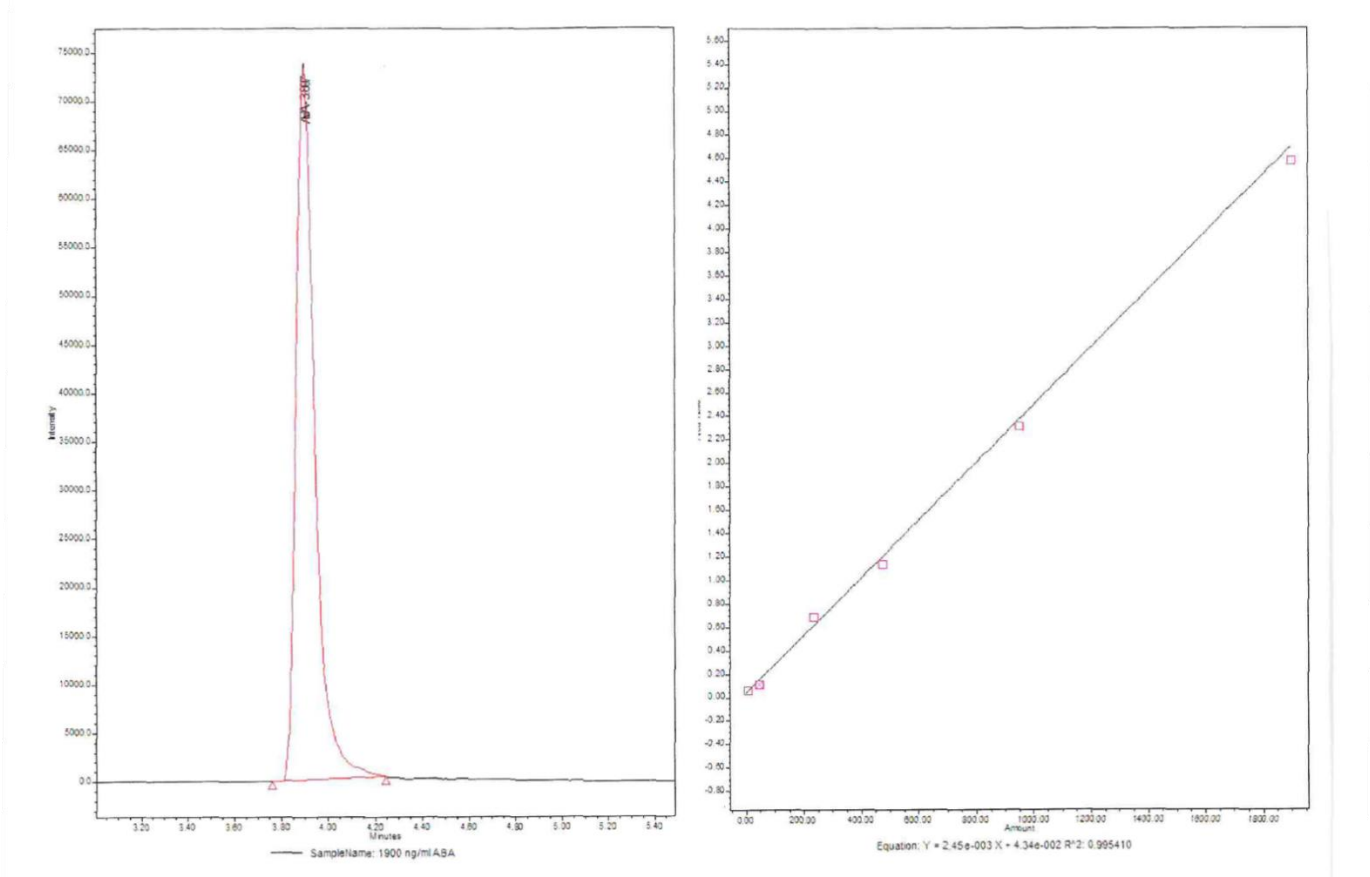

Supplementary figure 7. ABA peak as detected by LC-MS and standard curve.

Chapter 2

Characterisation of six putative NCED proteins in three conifer species

Graphical abstract

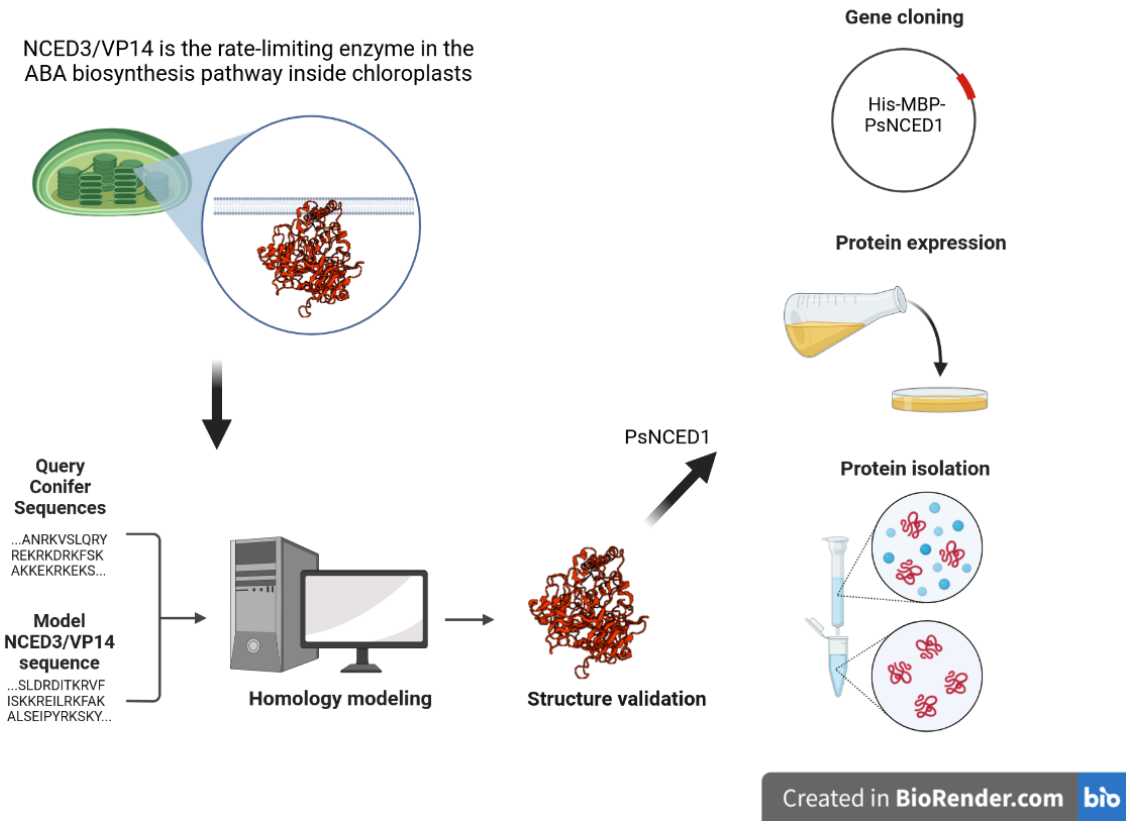

Abstract

Carotenoid cleavage dioxygenases (CCDs) are a large protein family contributing to carotenoid turnover inside the plant cell. They catalyse the oxidative cleavage of alkene bonds in the carotenoid polyene chain, through a non-heme Fe^{II} co-factor. Nine-*cis*-epoxycarotenoid dioxygenases (NCEDs)

are a sub-family known for their ability to selectively break the 11-12 double bond of neoxanthin and violaxanthin, in what has been recognised as the first committed step in the biosynthesis of abscisic acid. NCEDs have been characterised in detail in angiosperm systems, but studies in other taxa are poor. In this chapter, we characterise six conifer NCEDs identified in chapter 1, through *in silico* studies. We then attempt to clone, purify and test one selected NCED from *Picea sitchensis*. Although non-conclusive, we provide evidence for the conserved function of some of the candidate NCEDs and set a solid basis for further functional studies by isolating PsNCED1.

Introduction

Carotenoids

Carotenoids are naturally occurring pigments, which are synthesised by all photosynthetic organisms on Earth and have been extensively reviewed [1–3]. They are C_{40} isoprenoid compounds, typically alternating double and single bonds in the polyene chain. Around 600 different structures are known nowadays, all generated by isomerisation around the C=C double bond, and each with a particular reactivity. Each carotenoid can adopt a *trans* or *cis* configuration, in which the polyene chain will extend in a linear conformation to reach its low-energy state. Overall, these are highly hydrophobic molecules mostly associated with all plastid membranes, where they seem to be synthetised by enzyme complexes called metabolons [4,5]. Carotenoids are precursor molecules found in some of the most important metabolic pathways in the plant cell, being converted into pigments operating in plant interactions with pollinators, photoprotection of the antenna systems, photosynthesis or phytohormones involved in responses to environmental cues. Importantly, one of such phytohormones is abscisic acid (ABA), an isoprenoid molecule implicated in fine-tuning a wide range of plant responses to biotic and abiotic stresses.

Carotenoid dioxygenases

While carotenoids are important molecules regulating plant growth, development and many more functions, they must be metabolised to keep a constant turnover and generate apocarotenoids [6,7]. These are regulatory molecules, such as hormones and signalling molecules, produced *in vivo* by the activity of carotenoid cleavage dioxygenases (CCDs) [8–10]. The typical reaction catalysed by this large

enzyme family is the oxidative cleavage of specific alkene bonds within the carotenoid polyene chain, through a non-heme Fe^{II} co-factor. A key characteristic of CCDs, highly conserved from bacteria to plants, is the presence of four His residues coordinating the iron centre (Figure 1). Several CCDs have been discovered with preference for cleavage of one specific bond or a few bonds, generating a great variety of interactions and apocarotenoid compounds. All these reactions have in common the substrate (a C_{40} carotenoid) and the fact that the first product is an aldehyde (Figure 1 in General Introduction).

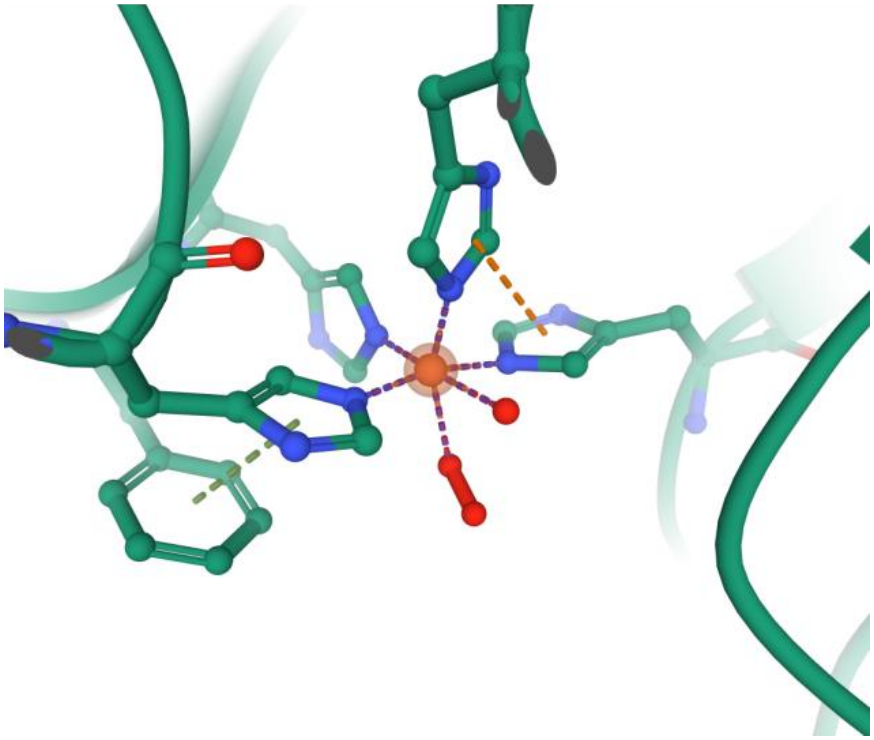

*Figure 1. Detail of the CCD/NCED catalytic centre. Four histidine residues (nitrogen atoms shown in **blue**) bind octahedrally a FeII ion (**orange sphere**) in cooperation with a dioxygen and a water molecule (oxygen atoms shown in **red**).*

Zea mays VP14

The first CCD to be structurally resolved and functionally characterised was *Zea mays* (*Z. mays*) VIVIPAROUS-14 (VP14), which is one of a few proteins that hold substrate specificity to catalyse the cleavage of the 11-12 double bond in the 9-*cis* isoform of neoxanthin and violaxanthin, producing xanthoxin and a C_{25} epoxy apo-aldehyde, which are precursors of ABA [11-14]. First identified during a genetic screening of viviparous seeds, the gene coding for VP14 was observed to be responsive to

water stress and was proposed to be associated with ABA biosynthesis [11]. Sequence homology analyses revealed a significant similarity to lignostilbene dioxygenases (LSDs), which catalyse a double bond oxidative cleavage. Recombinant VP14 was then isolated and tested *in vitro* for cleavage activity [12,13]. The crystal structure of VP14 was ultimately resolved [14] and homology comparisons to *Z. mays* CCD1, together with mutational studies, allowed the identification of the amino acid residues conferring substrate specificity and bond selectivity. VP14 appeared as a seven-bladed β-propeller capped by an α-helical domain (Figure 2). The tunnel crossing the β-propeller hosts the catalytic iron centre, octahedrally bound by four His residues (His-590 in blade 1, His-298 in blade 3, His-347 in blade 4, and His-412 in blade 5). A highly reactive dioxygen molecule coordinates to the Fe ion and is needed for catalysing the cleavage. Both the β-propeller and α-helices 1 and 3 present several hydrophobic residues that allow docking of the ligand and penetration of the thylakoid membrane respectively. VP14 is thought to anchor to the thylakoid membrane, where it can easily access its substrates [15].

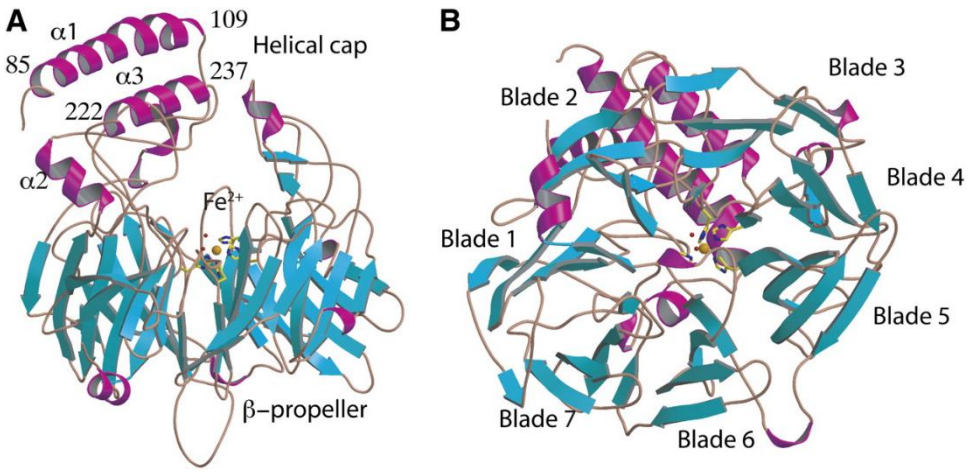

*Figure 2. Z. mays VP14 3D structure. **A** and **B**: Side view of ZmVP14 showing the α-helices and top view of the β-strands of the seven-bladed β-propeller. Figure adapted from Messing et al, 2010 [14].*

Other NCEDs

Several CCDs with specificity for the 11-12 double bond of 9-*cis*-neoxanthin and 9-*cis*-violaxanthin have been characterised since VP14 was discovered in *Z. mays*. These sequences have been grouped into a sub-family of enzymes named NCEDs (9-cis-epoxycarotenoid dioxygenases) and are widely represented in plant genomes. Examples are found in tomato, bean and avocado [16–18], but they have been especially well characterised in *Arabidopsis thaliana (A. thaliana),* where they have undergone

multiple duplications followed by functional diversification [19–21]. NCED sequences have also been identified in non-angiosperm species, mainly through gene expression studies, including mosses [22], lycophytes [23] and conifers [24,25]. No functional studies of NCED proteins have been undertaken in non-angiosperm species, to our knowledge.

Here, we want to address this knowledge gap to confirm the role of NCED enzymes in ABA biosynthesis in conifers on drought response. We selected six putative NCED sequences from three species belonging to the conifer families of the northern hemisphere (Pinaceae, Cupressaceae, Taxaceae) that we studied in a previous drought experiment. First, we applied *in silico* modelling methods to assess their structural features. We then chose one sequence, based on its responsiveness to drought for molecular cloning and protein expression. Finally, we tested the recombinant protein *in vitro* for its catalytic activity towards neoxanthin and violaxanthin.

Materials and methods

Protein sequences and alignment

Protein sequences for 9-*cis*-epoxycarotenoid dioxygenases (NCEDs) and carotenoid-cleavage dioxygenases (CCDs) of *Z. mays* and *A. thaliana* were obtained from UniProt database (https://www.uniprot.org/). Protein sequences of conifer NCED putative homologs were identified in chapter 1; here, we analyse NCED1 and NCED2 of *Chamaecyparis lawsoniana* (*C. lawsoniana* - ClNCEDs), *Picea sitchensis* (*P. sitchensis* - PsNCEDs) and *Taxus baccata* (*T. baccata* - TbNCEDs), obtained from transcriptomes developed from previous studies and analysed according to the previous chapter. MAFFT (Multiple Alignment using Fast Fourier Transform) [26] server (https://mafft.cbrc.jp/alignment/server/) was used for multiple protein sequence alignment – version 7, L-INS-i iterative refinement method, 1e-10 threshold.

Phylogenetic tree construction

A Maximum Likelihood phylogenetic tree of the amino acid sequences was inferred using MEGA X (Molecular Evolutionary Genetics Analysis) [27]. Amino acid distances were computed using JTT

(Jones-Taylor-Thornton) matrix-based model. Node support values in the bootstrap consensus tree were inferred from 1000 replicates.

In silico structural analyses

Physical and chemical parameters of selected protein sequences were computed using ExPASy's ProtParam tool (https://www.expasy.org/resources/protparam) [28]. The following parameters were considered: molecular weight (MW), isoelectric point (pI), number of positive and negative residues (+R and -R), instability index (Ii), aliphatic index (Ai), grand average hydropathy (GRAVY). Motif analysis was conducted on MEME (Multiple Em for Motif Elicitation) [29] server (https://meme-suite.org/meme/). BLAST [30] (https://blast.ncbi.nlm.nih.gov/Blast.cgi?PAGE=Proteins) and Interproscan [31] (http://www.ebi.ac.uk/interpro/search/sequence/) were used for motif identification.

Sequence similarities, amino acid substitutions and secondary structure information from aligned sequences were obtained from Espript 3.0 [32] (Easy Sequencing in PostScript) server (https://espript.ibcp.fr/ESPript/ESPript/). A similarity global score with a cut-off of 0.7 was calculated for each possible residue pair in each column. Residues with similarity scores above the cut-off value are shown in cyan blue on black background. Columns that are strictly conserved are shown in black on cyan blue background.

3D models for putative conifer NCED proteins were created with both *ab initio* and comparative modelling strategies using four different platforms: AlphaFold2 colab notebook [33] (ab initio, https://colab.research.google.com/), Modeller [34] (https://salilab.org/modeller/), ProMod3 3.2.1 [35] at SwissModel [36] (https://swissmodel.expasy.org/) and Phyre2 Protein Fold Recognition Server [37] (http://www.sbg.bio.ic.ac.uk/~phyre2/html/page.cgi?id=index) (comparative). All models were structurally compared with *Z. mays* VP14 using TM-align [38] (https://zhanggroup.org/TM-align/) and the best scoring model was selected based on the root mean square deviation between corresponding residues (RMSD) and TM-score values. Further quality checks on the best scoring model were performed with ProSa [39] (https://prosa.services.came.sbg.ac.at/prosa.ph), Errat [40] and Verify3D [41,42] through SAVES v6.0 web server (https://saves.mbi.ucla.edu/), whereas QMEANDisCo Global score and Ramachandran plots were assessed using ModBase [43] at Expasy's SwissModel [36] structure assessment web page (https://swissmodel.expasy.org/assess).

Presence/absence prediction of N-terminal pre-sequences was computed using TargetP-2.0 [44] webserver (https://services.healthtech.dtu.dk/service.php?TargetP). Membrane topology was modelled using MEMEMBED [45] through PSIPRED workbench [46] (http://bioinf.cs.ucl.ac.uk/psipred/). Protein-ligand interactions were predicted through SwissDock [47,48] (http://www.swissdock.ch/) and molecular graphics and analyses performed with UCSF Chimera [49] using Viewdock tool – the lowest energy interaction was chosen as the best fit.

The following procedures apply to the Picea sitchensis NCED1 only, which was chosen as representative homolog sequence for conifer NCEDs.

cDNA sequence synthesis

A synthetic gene sequence, coding for a truncated version of NCED33063 from *Picea sitchensis*, was obtained by Thermo Fisher Scientific (Waltham, Massachusetts, USA) through the GeneArt Strings service. The sequence included the alpha helices, the catalytic domain and C-terminus. The putative chloroplast signal peptide and the C-terminal UTR (untranslated region) were not included, as they were not necessary for our *in vitro* assay. The sequence was also optimised for expression in *Escherichia coli* (*E. coli)*, prior to synthesis. Two different restriction sites were added at the N- and C-termini of the sequence: a BamHI and a EcorRI site respectively; these were extended with four random nucleotides to improve restriction efficiency and stability of the sequence. The total length of the sequence was 1580 bp. 1250 ng of synthetic product were suspended in 10 mM Tris pH 8.5 buffer, delivered dried and subsequently resuspended in 10 microliters of nuclease-free water.

Sequence cloning

A pMAL-c6-T plasmid vector containing a N-terminal Maltose Binding Protein (MBP) tag (New England Biolabs) was transformed (1 µL) into DH-5 alpha competent *E. coli* cells through heat-shock. The malE gene sequence coding for the MBP tag is positioned between the 6X Histidine tag coding sequence and the multiple cloning site, to improve target protein solubility and can be cleaved with a TEV reaction upon protein purification. Briefly, the cells were thawed on ice and 50 µL of cell suspension were added to the plasmid vector. The mixture was incubated on ice for 30 minutes. Heat-shock was applied for 45 seconds at 42 °C in a PCR machine and returning the cells on ice for 2 minutes. Competent cells were then recovered in 100 µL of LB (Luria Broth) liquid media for 45-60 minutes at 37 °C. The liquid culture was finally plated on LB-Agar plates supplemented with 100

μg/ml ampicillin and grown at 37 °C overnight. One colony was picked, inoculated on 5-10 ml of liquid LB media supplemented with 100 μg/ml ampicillin and grown overnight at 37 °C. Plasmid DNA was then extracted and purified from the bacterial liquid culture using a Nucleospin plasmid Quick Pure purification kit (Macherey-Nagel™, Düren, Germany). Total DNA was quantified with the Nanodrop One/OneC Microvolume UV-Vis Spectrophotometer (Thermo Fisher, Waltham, Massachusetts, USA) to 120 ng/μL.

The synthetic fragment and the acceptor plasmid were digested using 0.25 μL BamHI and 0.25 μL of EcoRI restriction enzymes, with 0.5 μL of CutSmart buffer. Reactions were incubated at 37 °C for 1h, 65 °C for 5 min, 80 °C for 5 min. Subsequently, the reaction products were combined and 0.5 μL of Ligase T4 and 1 μL of Ligase Buffer were added. The mix was incubated 37 °C for 2h, 65 °C for 5 min, 80 °C for 5 min. The restriction/ligation product and the control empty plasmid were then transformed into DH-5 alpha competent *E. coli* cells by heat-shock and grown overnight on LB-agar ampicillin-enriched media. 20 colonies were selected for screening by PCR and grown overnight in liquid LB medium before DNA isolation.

Cell transformation

The purified vector was transformed into NEBExpress Competent *E. coli* cells (New England Biolabs). 1-5 μL of the cell mixture were thawed on ice. The tube was gently flicked 4-5 times and the mixture was incubated on ice for 30 minutes. Heat shock was then applied at 42°C for 20 seconds. The tube was incubated on ice for 5 minutes, then 950 μL of room temperature SOC were pipetted into the mixture followed by incubation at 37°C for 60 minutes with vigorous agitation (250 rpm). Afterwards the cell suspension was mixed by flicking the tube and diluted with several 10-fold serial dilutions in SOC. 50-100 μL of cell suspension were spread on warm selection plates and incubated overnight at 37°C.

Protein expression

5-10 ml LB liquid media with ampicillin were inoculated with a single colony and the culture was incubated at 37°C overnight. This starter culture was then used to inoculate 1 L of LB liquid medium enriched with antibiotic, 440 mM sorbitol (Fisher Scientific, # 11357868) and 2.5 mM betaine (Merck, # 61962-50G). The scaled-up culture was incubated at 37°C until OD600 reached 0.4 - 0.6 and induced with filtered IPTG (Merck, # I6758-1G) to 0.4 mM, for 5 hours at 25°C.

Protein expression was verified by Coomassie stain and His-tag stain (InVision His-tag In-gel staining, Invitrogen) following separation on SDS- polyacrylamide gel (Bolt 12%, Bis-Tris, 1.0 mm, Mini Protein Gel, Thermo Fisher). Cells were harvested from the liquid culture by centrifugation of multiple aliquots at 10,000 × g for 10 min using 500 ml centrifuge bottles. The pellet was resuspended in a few ml of sterile LB media, pooled together and centrifuged again. Finally, the supernatant was discarded by decantation and the pellet stored at -80°C until needed. Before use, the pellet was thawed on ice and weighed on an analytical balance. A modified protocol from Massiah and collaborators [50] involving the use of Sarkosyl detergent (N-Lauroylsarcosine, Sigma Aldrich, no. 61739) was implemented to solubilise as much protein as possible, due to its tendency to form a thick insoluble pellet. 5 ml of room temperature BugBuster Protein Extraction Reagent (Novagen, Madison, Wisconsin 53719, USA) per gram of wet pellet were used to resuspend the cells, by both pipetting and vortexing. The suspension was incubated on a rotating mixer for 20 minutes at room temperature. At this point, 30% Sarkosyl stock solution was added to 10% (v/v) final concentration and the emulsion was incubated at room temperature overnight. The next morning, the cell debris was centrifuged for 20 minutes at 20,000 x g and the supernatant was transferred to a clean 15 ml tube and stored at 4°C.

Protein purification

Protein purification was obtained by using a Novagen HIS-bind kit. 2 ml of Ni^{2+}-NTA agarose resin (1 ml bed volume) were added into a plastic column (7 ml volume). The column was then washed with 20 ml of milliQ water to remove excess ethanol and equilibrated with 20 ml binding buffer (50 mM Tris·Cl pH 7.5, 200 mM NaCl, pH 7.4-7.5). The protein extract was diluted with binding buffer such that the concentration of Sarkosyl was reduced to 1% and was then loaded onto the pre-equilibrated Ni^{2+}-NTA column and allowed to flow through. The column was then washed with 20 ml binding buffer containing 25-50 mM imidazole (Merck, # I202-100G) to remove any unbound protein; the HIS-tagged NCED protein was then eluted in 5 fractions of 1 ml each with buffer containing 300 mM imidazole. Samples were analysed by SDS-PAGE gel to check for protein purity.

Elution fractions containing the His-NCED were pooled together and loaded onto an Amicon Ultra-15 Centrifugal Filter tube (Millipore, # UFC9010). Several washes with 50 mM Tris·Cl pH 7.5 (4,000 × g at room temperature) were applied to remove excess salt and finally concentrate the purified

protein. The His-tag MBP-bound protein was quantified at the NanoDrop (Protein A280 method, absorbance at 280 nm) to ≈ 1.5 mg/ml. Protein samples were stored in aliquots at -80°C.

Although we attempted to cleave the MBP tag using a TEV protease (New England Biolabs, # P8112S) and purify the cleaved protein product using an amylose resin (NEB, # E8021S) in combination with a Maltose solution (NEB, # 63423) according to manufacturer instructions, this did not produce a detectable cleaved protein.

Enzymatic assay

Experimental procedures followed Sergeant et al. 2009 [51] *with some modifications.*

Twenty µL from stock purified MBP-psiNCED1 (≈ 30 µg) were incubated with 1 µL of 20mM Iron Sulfate, 1 µL of 20mM Ascorbate and 32 µL H_2O, on ice for 10 minutes. This aliquot was added to the reaction mix, containing: 15 µL 1M TRIS-HCl (50mM final conc.), 1 µL 0.005% V/V TRITON X-100 (0.0003% final conc.), 75 µL Catalase (2mg/mL stock), 5 µL 9-cis-neoxanthin (1 mg/mL stock, Merck, # 72994) or all-trans-violaxanthin (1 mg/mL stock, Toronto Research Chamicals, # V634510) ≈ 5 µg. One Maltose Binding Protein (MBP)-only control and one control with no enzyme were run in parallel to the reaction. All reactions were incubated in the dark for 0, 10, 20, 40 and 60 minutes (15 minutes should suffice to observe product [51]) and stopped by adding 700 µL of milliQ water. Products were extracted 3 times with 700 µL of ethyl acetate by vortexing. The solvent was then removed under vacuum overnight at -80°C in the dark.

Liquid Chromatography-Mass Spectroscopy

Reaction products were analysed by LC-MS on a Xevo G2-oligo spectrometer system coupled to an Acquity UHPLC system (Waters Corporation, Milford, USA), using a C18 column (Kinetex, 5 µm C18 100Å LC column, 100 x 2.1 mm). The mobile phases were **A** water acidified with 0.1% formic acid and **B** acetonitrile with 0.1% formic acid. The linear gradient used started with 20% B, at 2 min was 30% B, at 6 min was 38% B, at 8 min was 50% B, at 10 min was 70% B, at 12 min was 20% B, and ended at 15 min with 20% B. Flow rate was 0.2 mL min^{-1}. Column temperature was maintained at 40 °C. The mass spectrometer was operated in the negative ionization mode, with spectra acquired over a mass range of 50 to 1200 m/z.

Results

Physical parameters, multiple sequence alignment and motif analysis

Physico-chemical properties of each conifer protein, *A. thaliana* NCED3 and maize VP14 are shown in Table 1. The interpretation of the scoring values is based on the work of Walker and colleagues [28] and references therein. Protein length varied substantially among conifers between 513 amino acids (*Tb*NCED1) and 631 (*Cl*NCED1 and *Ps*NCED1), with predicted molecular weight between 57 and 70.4 kDa. All proteins scored an instability index (Ii) above 40, except for AtNCED3, indicating that they may be unstable under *in vitro* conditions. On the other hand, the aliphatic index (Ai) was rather high, scoring ≈ 80 for all proteins, suggestive of high thermostability. Grand average hydropathy (GRAVY) scores were negative, which may indicate a globular hydrophilic nature of the protein, rather than a hydrophobic one.

Table 1. ProtParam summary table of angiosperm and putative conifer NCED protein chemico-physical parameters. ***MW****: Molecular Weight;* ***pI****: Isoelectric point;* ***+R/-R****: number of positive/negative residues;* ***Ii****: Instability index;* ***Ai****: Aliphatic index;* ***GRAVY****: GRand AVerage hydropathY.*

ID	Length	MW (kDa)	pI	-R	+R	Ii	Ai	GRAVY
ZmVP14	604	65.4	5.68	76	59	44.46	80.48	-0.183
AtNCED3	599	65.8	5.9	71	59	39.2	79.58	-0.283
PsNCED1	631	70.2	6.25	81	75	46.95	80.98	-0.331
PsNCED2	611	67.5	5.97	70	61	42.99	84.08	-0.235
ClNCED1	631	70.4	6.08	81	73	50.68	77.58	-0.336
ClNCED2	603	67	5.68	84	70	40.47	85.52	-0.302
TbNCED1	513	57	6.19	66	58	45.06	83.45	-0.267
TbNCED2	590	66.1	5.91	77	66	55.44	84.92	-0.29

A MSA (Multiple Sequence Alignment) revealed high evolutionary conservation among the putative conifer NCED protein sequences when compared to the angiosperm reference sequence *Zm*VP14 (see Supplementary Figure 1). The highest sequence identity was found between *Tb*NCED1 and reference sequence *Zm*VP14 (60.69%, see Table 2). This result was based on a reduced coverage and shorter sequence length of *Tb*NCED1 compared to the second-best scoring sequence - *At*NCED3 - which had

an identity score of 60.64%. All conifer putative ortholog sequences followed, with identity scores between 56% and 51%. In contrast, *At*CCD4 was only 35.04% identical to *Zm*VP14. Similarly, *Zm*CCD1 was 32.04% identical.

*Table 2. MSA details table, showing sequence IDs (**ID**), alignment length (**Length (aa)**), alignment coverage (**Coverage (%)**) and sequence identity (**Identity to anchor sequence (%)**), using ZmVP14 as reference anchor sequence.*

ID	Length (aa)	Coverage (%)	Identity to anchor sequence (%)
ZmVP14	604	100	100
TbNCED1	510	83.28	60.69
AtNCED3	599	95.7	60.64
TbNCED2	590	91.56	55.89
PsNCED1	631	96.03	55.45
ClNCED1	631	96.85	55.38
ClNCED2	600	91.72	52
PsNCED2	610	93.21	51.47
AtCCD4	595	94.7	35.04
ZmCCD1	539	85.43	32.06

Motif conservation was investigated by uploading protein sequences on MEME web server [29]. Motif analysis showed that angiosperm and putative conifer NCEDs shared 10 motifs enriched across the whole protein sequence and conserved in the same order, whereas other carotenoid cleavage dioxygenases lacked from 3 to 4 of these motifs (motifs 2, 5, 6, 10 in Figure 3). *At*CCD4 lacked motif 2, which in *Zm*VP14 covers a portion of the hydrophobic pocket inside the β-propeller including important residues Val-315 and Met-345 and form non-specific interactions with the ligand. *At*CCD4 had respectively a proline and a phenylalanine in place of these amino acids. Both *At*CCD4 and *Zm*CCD1 lacked motif 5, 6 and 10. Motif 5 in *Zm*VP14 includes Leu-218 and Leu-227, again in the same hydrophobic patch, and several hydrophobic residues in the α3-helix - Ile-224, Ala-225, Ala-228, Leu-229, Tyr-231, Ala-232, Ala-234, Ala-235, and Gly-237 – needed for membrane penetration. Motif 6 includes a Met-432 next to the 9-cis bond of the ligand molecule, while motif 10 spans a region between the α1-helix and a β-strand.

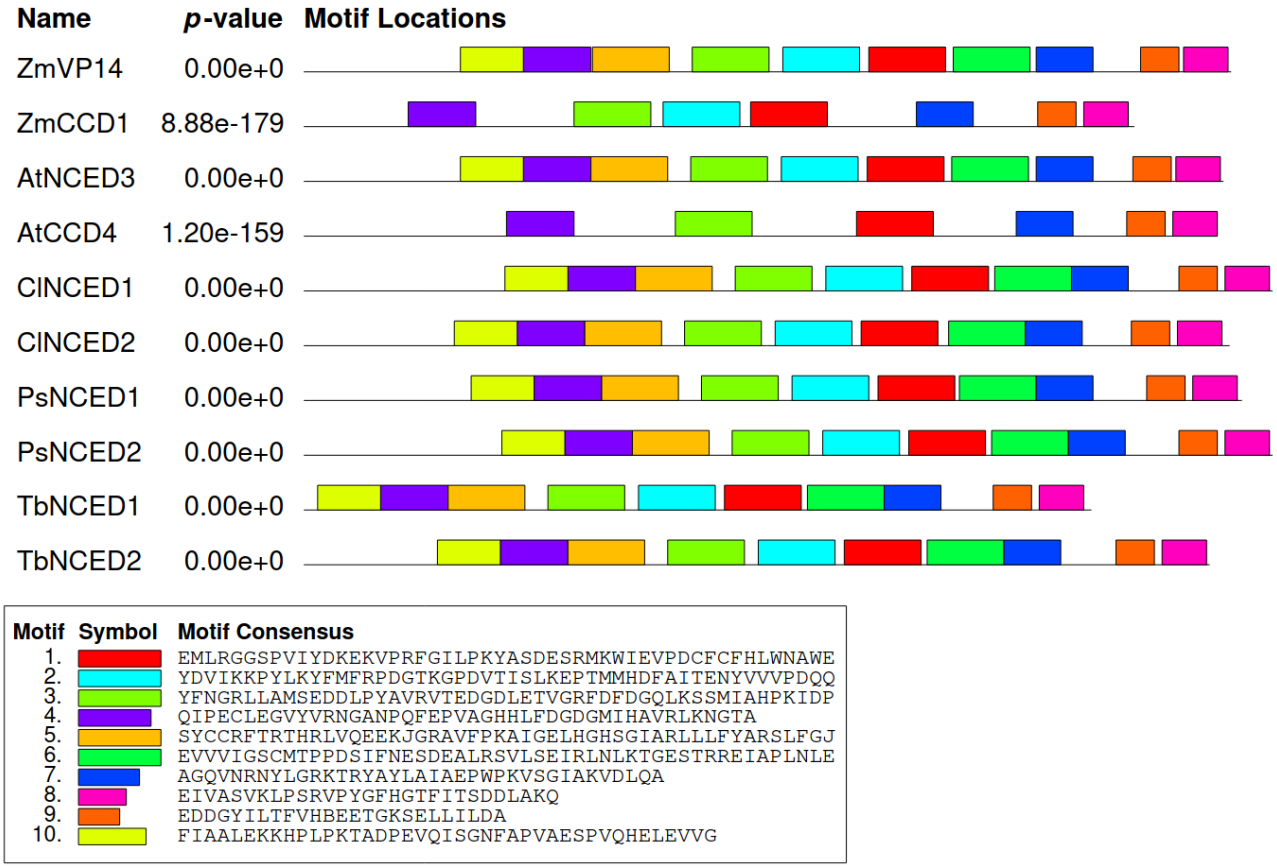

Figure 3. *MEME (Multiple Em for Motif Elicitation) results. Sequence motifs enriched in the set of study proteins are shown with different colours and are supported by a combined match* ***p-value****.* ***Consensus sequences*** *for each motif are shown in the legend box.*

Amino acid sequence variation

A closer inspection of the protein sequence alignment allowed us to identify which key residues were conserved between 9-cis-epoxycarotenoid dioxygenases and carotenoid cleavage dioxygenases, and between angiosperm and conifer proteins. Conifer and angiosperm NCEDs shared most of amino acids conferring ligand stereoselectivity, including the four key His residues, with some exceptions. A first set of important substitutions was found between residues 214 and 265 (Figure 4). Within the substrate pocket, *Ps*NCED2 changed Ala-214 for a Proline and *Zm*CCD1 had a deletion. Ile-215 was highly conserved but was changed for a non-equivalent Phe in *Zm*CCD1. Leu-218 and Leu-227 were conserved among *Zm*VP14, *At*NCED3 and all conifer candidate sequences. *At*CCD4 had non-conservative substitutions at both positions, having a Phe and Gly respectively. Asp-265 was highly conserved among angiosperm and conifer NCEDs but was substituted by a Ser in *At*CCD4 and an Ala in *Zm*CCD1.

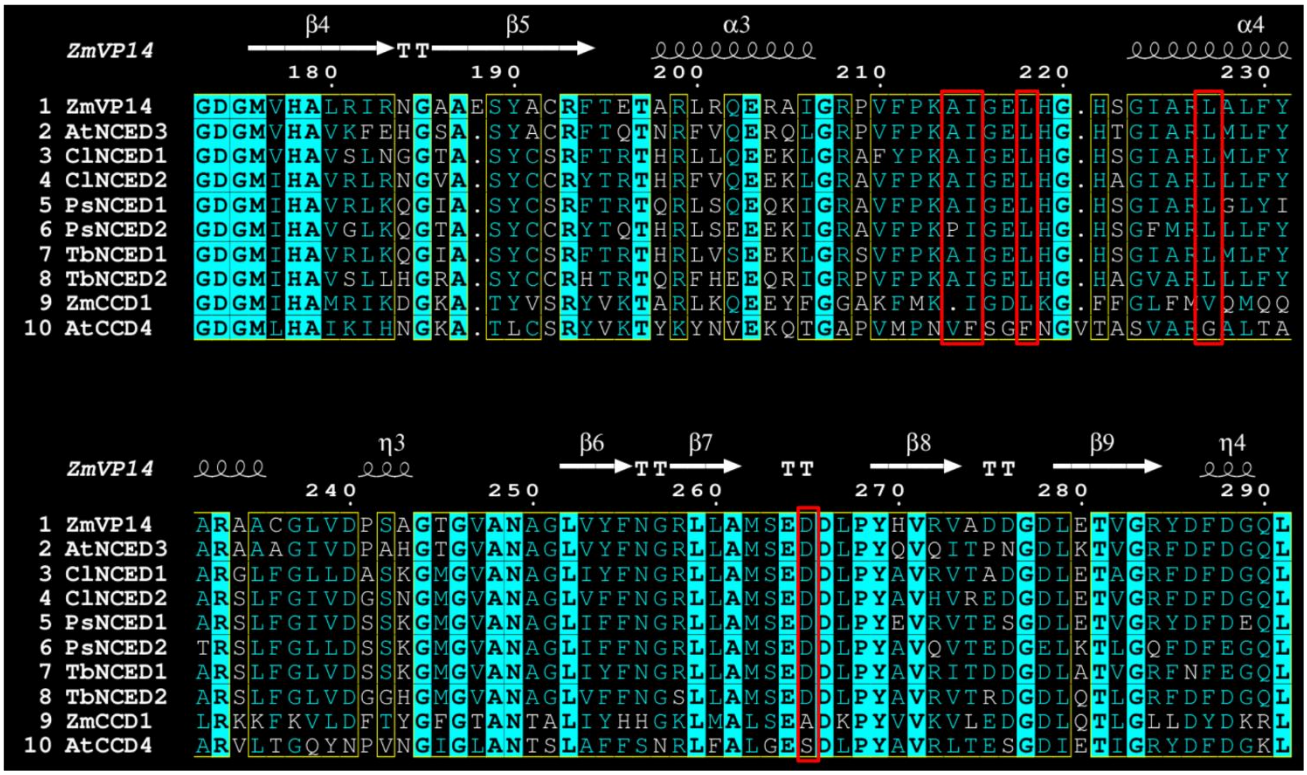

Figure 4. MSA showing structural features based on reference sequence of Z. mays VP14. Target region comprising residues between position 214 and 265. Residues with similarity scores above the 0.7 similarity cut-off value are shown in cyan blue on black background. Columns that are strictly conserved are shown in black on cyan blue background. Sequence regions harboring amino acid substitutions relevant to protein function are highlighted with red boxes. At = A. thaliana, Cl = C. lawsoniana, Ps = P. sitchensis, Tb = T. baccata, Zm = Z. mays.

Between residues 300 and 400 (Figure 5), Val-315 was conserved among angiosperm and several conifer NCEDs, although *Ps*NCED1 and *Tb*NCED1 swapped it for an equivalent Isoleucine residue. *Zm*CCD1 and *At*CCD4 had non-conservative substitutions at this position – His and Pro respectively. Ile-316 was conserved, although *Zm*CCD1 had a deletion at this position. *At*CCD4 swapped Met-345 for a Phe. Phe-365 was changed for a Val in *Ps*NCED2 and a Met in *At*CCD4. Leu-367 was conserved except for a non-equivalent substitution with Proline in *Ps*NCED2 and *Zm*CCD1.

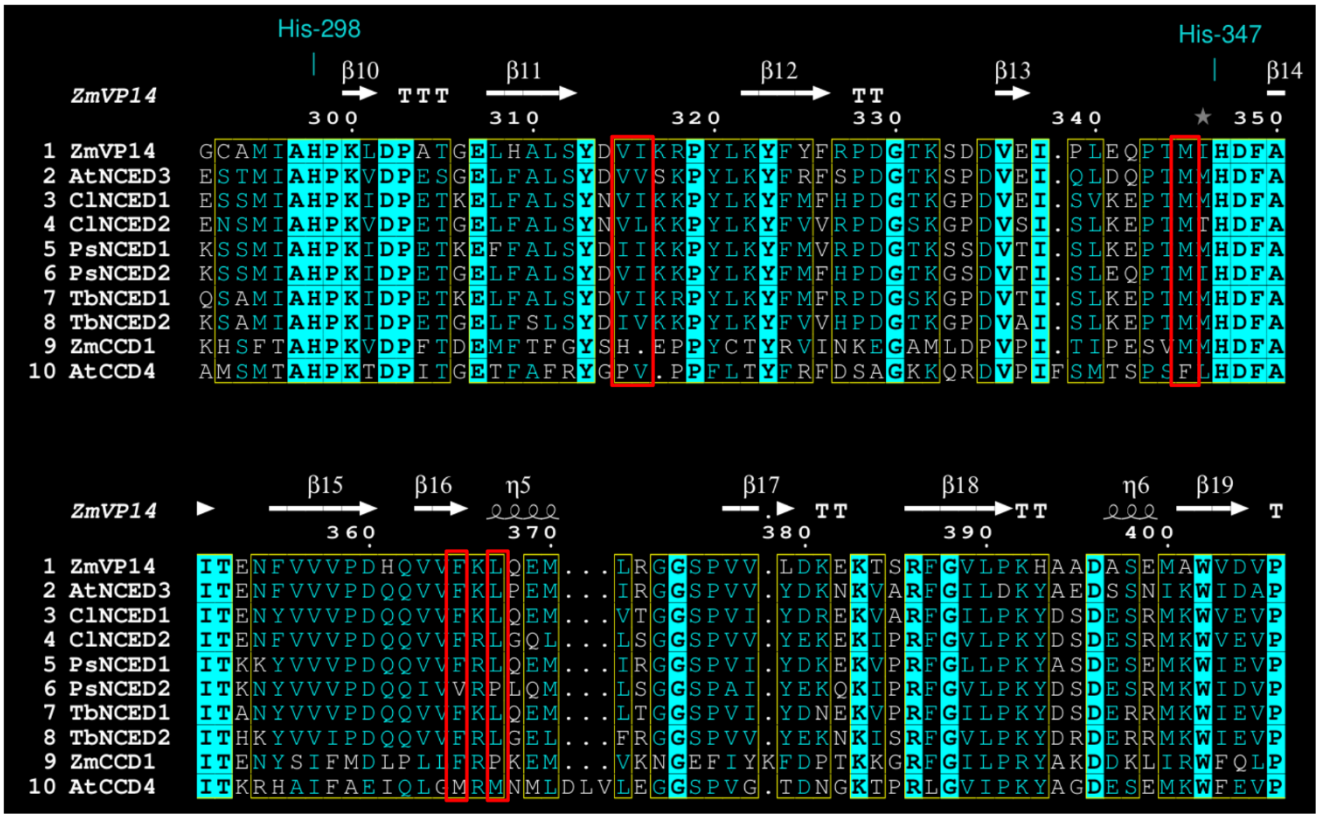

Figure 5. *MSA showing structural features based on reference sequence of Z. mays VP14. Target region comprising residues between position 300 and 400. Residues with similarity scores above the 0.7 similarity cut-off value are shown in cyan blue on black background. Columns that are strictly conserved are shown in black on cyan blue background. Sequence regions harboring amino acid substitutions relevant to protein function are highlighted with red boxes. At = A. thaliana, Cl = C. lawsoniana, Ps = P. sitchensis, Tb = T. baccata, Zm = Z. mays.*

Towards the C-terminal part of the proteins (Figure 6) three Phe residues - Phe-411, Phe-171, and Phe-589 hold in position the substrate's carbon 9 to carbon 15, which include the 9-*cis* bond of the carotenoid molecule. These three Phe residues are well-conserved except for *At*CCD4, which lacks Phe-411, having an Ile in its place. Other important residues surrounding the same 9-cis bond are: Phe-127, Leu-170, Met-432, Val-478, Trp-501, and Pro-502. Leu-170 was highly variable, being substituted by an aromatic residue - either a Phe or a Trp – in *At*NCED3, *Cl*NCED1 and *Cl*NCED2, and *Zm*CCD1. Val-478 was overall conserved by substitutions with another aromatic residue, Ala, but *At*CCD4 and *Zm*CCD1 showed a Phe in this position. Trp-501 was highly conserved, and only changed in *At*CCD4 and *Zm*CCD1 for aliphatic Met or Ile residues respectively. Pro-502 only changed in *Zm*CCD1 for an Ala.

Another relevant portion located inside the β-barrel is represented by residues 499-503 forming a loop that together with Leu-170 accommodates the carotenoid molecule (Figure 6 and Supplementary figure 2). This loop was conserved among angiosperm and conifer NCEDs, but not in *At*CCD4 and *Zm*CCD1.

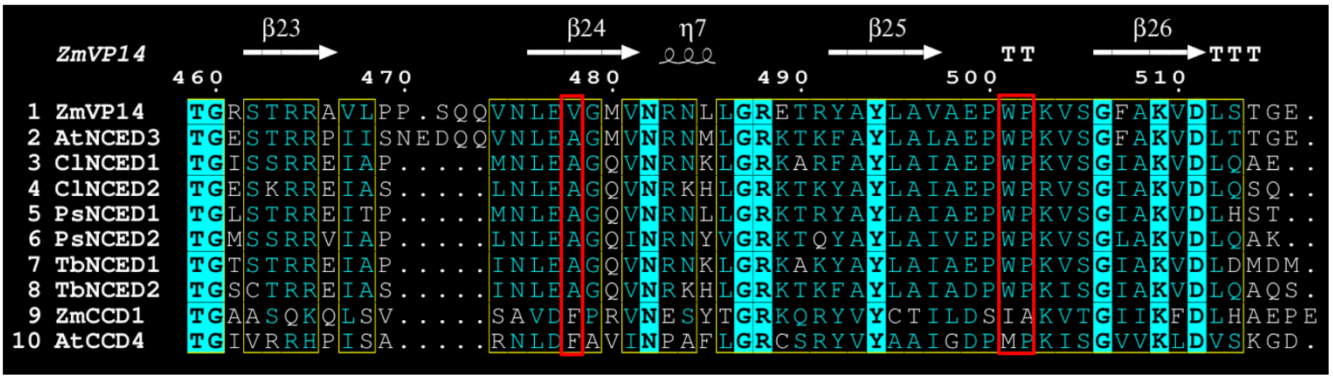

Figure 6. MSA showing structural features based on reference sequence of Z. mays VP14. Target region comprising residues between position 478 and 502. Residues with similarity scores above the 0.7 similarity cut-off value are shown in cyan blue on black background. Columns that are strictly conserved are shown in black on cyan blue background. Sequence regions harboring amino acid substitutions relevant to protein function are highlighted with red boxes. At = A. thaliana, Cl = C. lawsoniana, Ps = P. sitchensis, Tb = T. baccata, Zm = Z. mays.

Structure modelling

The 3D protein structures of putative conifer NCEDs were modelled using both *ab initio* and homology methods. Phyre2, Modeller and Swiss-Model were used with the 9-*cis*-epoxycarotenoid dioxygenase crystallographic structure of *Z. mays* VP14 in complex with oxygen obtained by Messing et al. 2010 [14], built on residues 84 to 604, as a template for model prediction. The *ab initio* model generated by AlphaFold2 fit the same structure but included an unresolved stretch of residues at the N-terminus of the protein, including the highly variable regions that precede the alpha helices (Supplementary figure 3).

The 3D models were structurally aligned to ZmVP14 using TM-align web server. Root mean square deviation (RMSD) and TM-score were used to evaluate equivalence and superimposition of the residues in the alignment. RMSD values below 2 Å represent good models. TM-scores below 0.2 indicate unrelated protein structures, while values above 0.5 indicate good matching. Modeller structures consistently showed the best scores, although all homology modelling tools generated accurate models compared to ZmVP14 crystallographic structure (see Tables 3 and 4). AlphaFold2 performed consistently more poorly both in terms of RMSD and TM-score, probably because of difficult N-terminus pre-sequences. Homology models generated by Modeller were hence preferred for structure validation and downstream analyses.

Table 3. Root mean square deviation (RMSD) between corresponding residues computed by TM-align web server. Each RMSD value refers to one structural model inferred by one modelling algorithm.

Modelling algorithm	**PsNCED1**	**PsNCED2**	**ClNCED1**	**ClNCED2**	**TbNCED1**	**TbNCED2**
Swiss-Model	0.52	0.44	0.51	0.41	0.45	0.45
Modeller	0.32	0.4	0.28	0.4	0.31	0.42
Phyre2	0.82	0.86	0.85	0.82	0.81	0.81
AlphaFold	1.61	1.58	1.64	1.59	1.64	1.67

Table 4. TM-score computed by TM-align web server. Each TM- score value refer to one structural model inferred by one modelling algorithm.

Modelling algorithm	**PsNCED1**	**PsNCED2**	**ClNCED1**	**ClNCED2**	**TbNCED1**	**TbNCED2**
Swiss-Model	0.97	0.97	0.97	0.97	0.95	0.98
Modeller	0.97	0.97	0.98	0.97	0.96	0.98
Phyre2	0.97	0.97	0.97	0.98	0.95	0.97
AlphaFold	0.95	0.95	0.95	0.96	0.93	0.95

Validation of Modeller structures was conducted through quality scores and energy plots. All modelled conifer protein structures uploaded on ProSa web server showed local quality scores below zero (positive scores indicating problematic parts of the structure) (see Supplementary Figure 4), except for a C-terminal stretch of residues, positioning above the zero line. ProSa also computes Z-scores indicating overall model quality. All conifer models had Z-scores between –8 and –9, positioning in the range of experimentally known native crystal structures (Supplementary Figure 5). Compatibility between tertiary structure and its amino acid sequence was assessed by Verify-3D through comparison with known good structures. All modelled structures showed a 3D-1D compatibility score above the 0.2 acceptance threshold for more than 80% of the residues (see Table 5). Modelled protein structures were further inspected by their QMEANDisCo Global scores and Ramachandran plots obtained from ModBase at SwissModel (Table 5 and Supplementary figure 7). QMEANDisCo is a scoring function used to obtain both global (structure) and local (residue) quality estimates. All QMEANDisCo Global scores were above 0.8, indicating good agreement with experimental structures. Ramachandran plots did not show substantial deviations of Phi/Psi angles from allowed regions; the proportion of residues falling in the favoured regions of the plot and that of outliers are reported in Table 5.

Table 5. Summary table of quality scores for predicted models. ***3D-1D*** *= Verify3D score indicating the proportion of residues passing the quality threshold of 0.2,* ***Favoured*** *= the proportion of residues falling in favoured regions of the Ramachandran plot,* ***Outliers*** *= the proportion of outlier residues in the Ramachandran plot.*

ID	3D-1D ≥ 0.2 (%)	QMEANDisCo	Favoured (%)	Outliers (%)
PsNCED1	83.2	0.84	92.44	1.74
PsNCED2	86.07	0.82	93.2	0.78
ClNCED1	86.63	0.83	94.16	0.97
ClNCED2	85.49	0.8	93.2	1.36
TbNCED1	87.8	0.81	92.89	2.37
TbNCED2	80.04	0.82	91.91	1.35

Membrane and ligand interactions

The presence of N-terminal chloroplast transit peptides is predicted by TargetP-2.0 for AtCCD4, AtNCED3, ZmVP14, PsNCED2, ClNCED1, but not for ZmCCD1, PsNCED1, ClNCD2, TbNCED1 and TbNCED2 (see Supplementary table). Memembed was used to predict the orientation of the proteins on the thylakoid membrane (see Figure 7). All proteins were predicted to penetrate the lipid bilayer to some extent by using their helices. An example of docking simulation results (protein in complex with 9-*cis*-neoxanthin) is shown for PsNCED1 (Figure 8; Supplementary figure 6 for others). Among the possible protein-ligand interactions, the most favoured were the ones allowing the carotenoid molecule to fit in the tunnel beneath the α-helices and inside the β-propeller in their extended form, thus positioning the 9-cis double bond next to the catalytic iron (Figure 8). The only two exceptions were represented by *Tb*NCED1 and *Tb*NCED2, which did not show a protein-ligand conformational state favourable to stretch the polyene chain in its linear shape nor to fit the carotenoid molecule in the catalytic pocket.

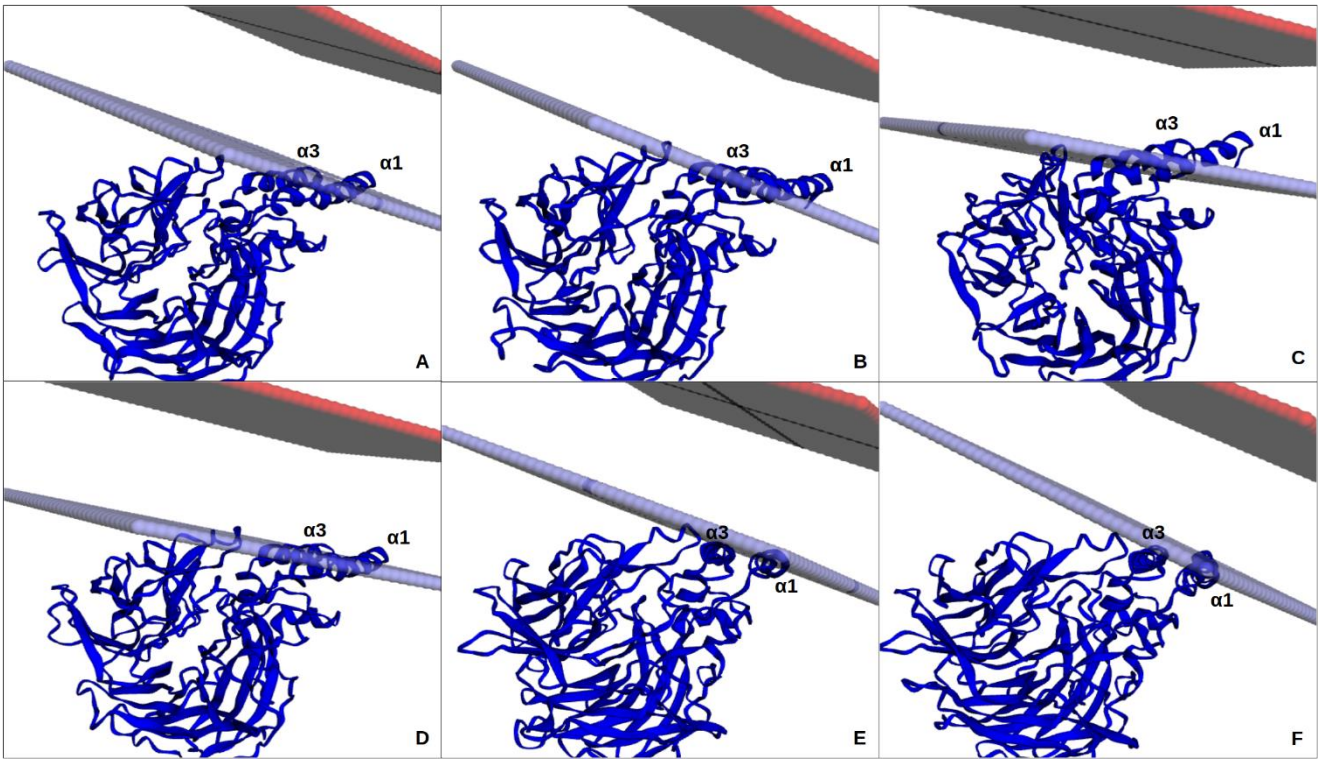

Figure 7. Protein-membrane interaction simulations for putative conifer NCED structures. A generic lipidic bilayer is show in red and blue. ***A*** *= PsNCED1,* ***B*** *= PsNCED2,* ***C*** *= ClNCED1,* ***D*** *= ClNCED2,* ***E*** *= TbNCED1,* ***F*** *= TbNCED2.*

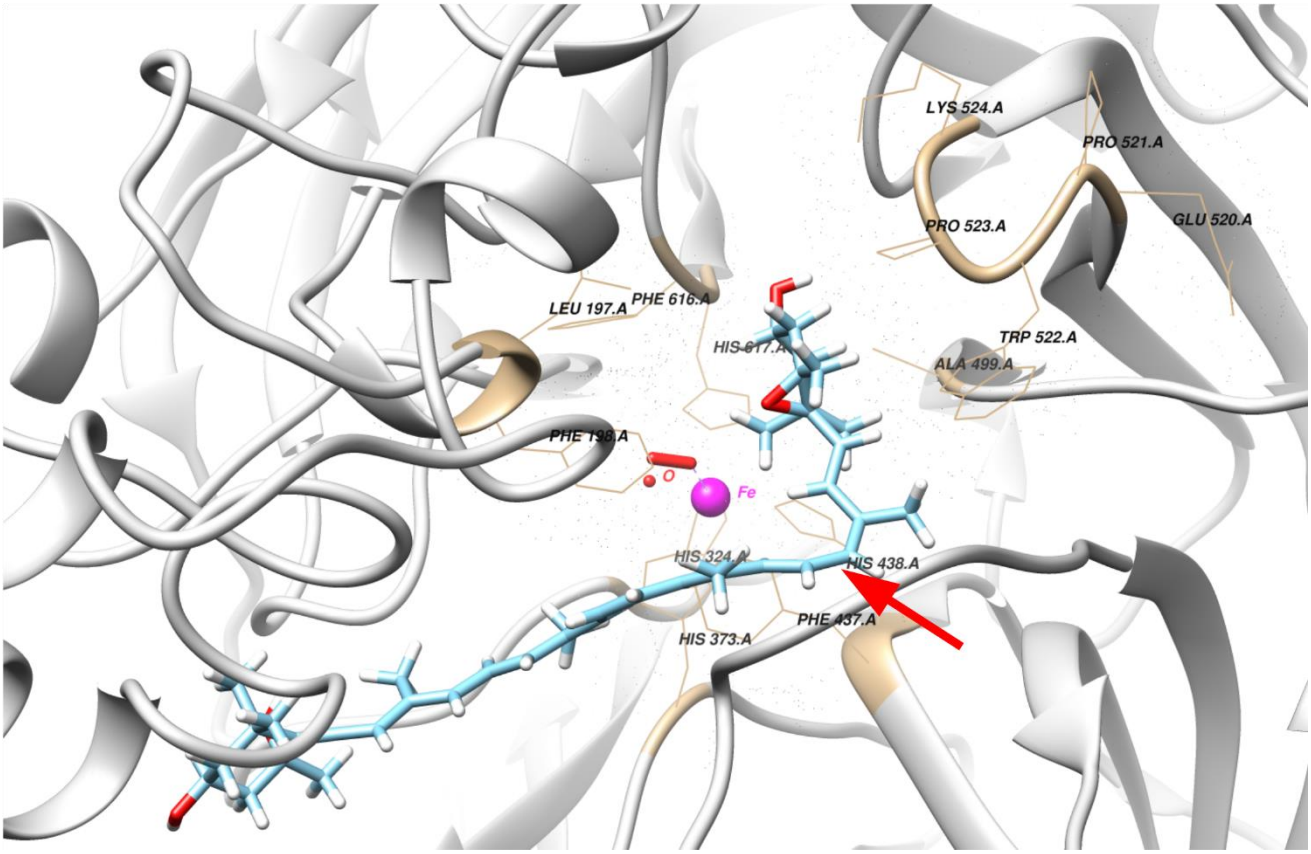

Figure 8. *Close-up of the ligand docking simulation run by Swiss-dock web server and visualised on CHIMERA viewdock tool. PsNCED1 structure (**grey ribbons**) is shown in complex with FeII (**purple sphere**) and 9-cis-neoxanthin (**cyan blue**). Key residues in the catalytic pocket are indicated by **black labels**. **Red arrow** points at cleavage site.*

Protein cloning and isolation

The *P. sitchensis* NCED1 was chosen for *in vitro* testing because of its drought responsiveness in previous gene expression studies and expressed as an His-MBP-tagged protein. The expressed protein proved rather insoluble and formed inclusion bodies (IB) upon cell lysis that appeared in the Coomassie-stained SDS page gel as irregular bands (see Figure 9). In order to improve sample solubility, the protein was expressed in a modified LB liquid media containing sorbitol and betaine at 25°C for 5-6 hours, which resulted in the best trade-off between protein yield and IB formation.

Protein purification steps included the addition of Sarkosyl to the cell lysis buffer. Sarkosyl is a mild non anionic detergent that has been shown to improve protein solubility with no denaturing effects [50]. Although Sarkosyl disrupted the protein pellet, it also rendered the cell extract somewhat viscous, hampering thorough clean-up of the protein upon on-column purification. Nevertheless, it was

possible, using sarkosyl at 1%, to extract soluble recombinant protein which could be purified to a reasonable degree. The isolated uncleaved protein appeared as a band of about 96 kDa on Coomassie-stained SDS gel (Figure 10). The difference in size between the recombinant NCED protein and the empty vector protein supports correct protein production and isolation, so this was used in functional testing of enzymatic activity.

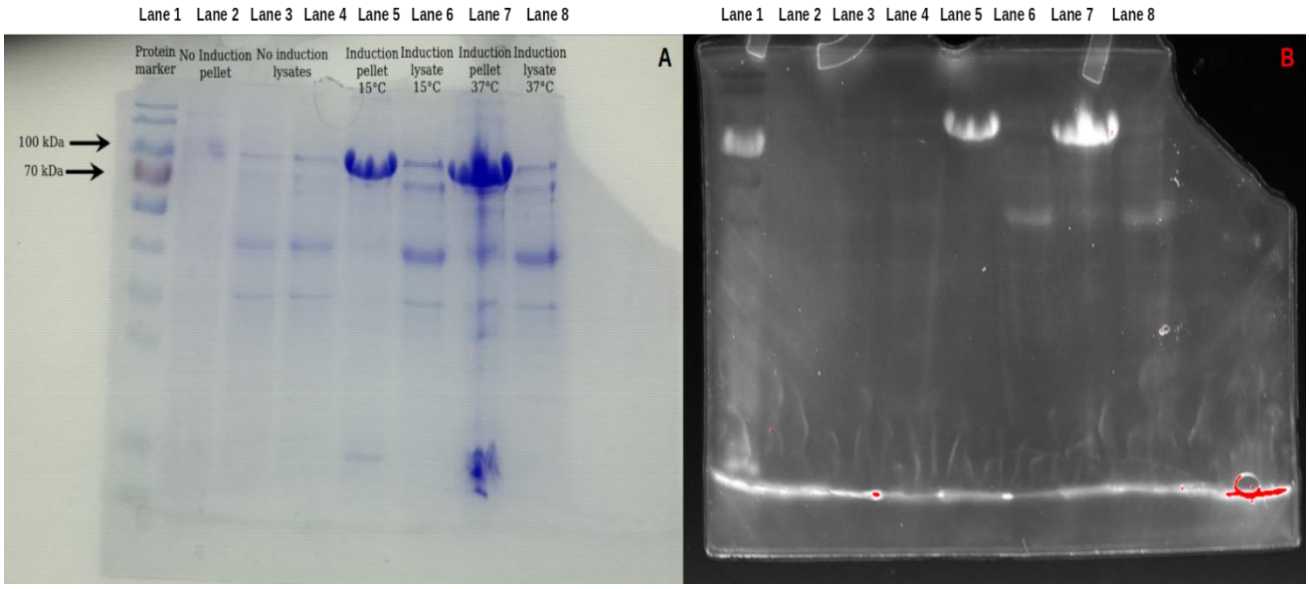

Figure 9. ***A****: Coomassie-stained SDS-PAGE gel, showing expressed recombinant protein segregation between extraction pellet and lysate.* ***Blue smeared bands*** *about 100 kDa are recombinant His-MBP-PsNCED1.* ***Lane 1****: protein marker. No-induction controls are shown in* ***lanes 2-4****. Protein expression in* ***lanes 5-8****.* ***B****: His-stained version of the same SDS page gel, confirming the presence of an His-tagged protein.*

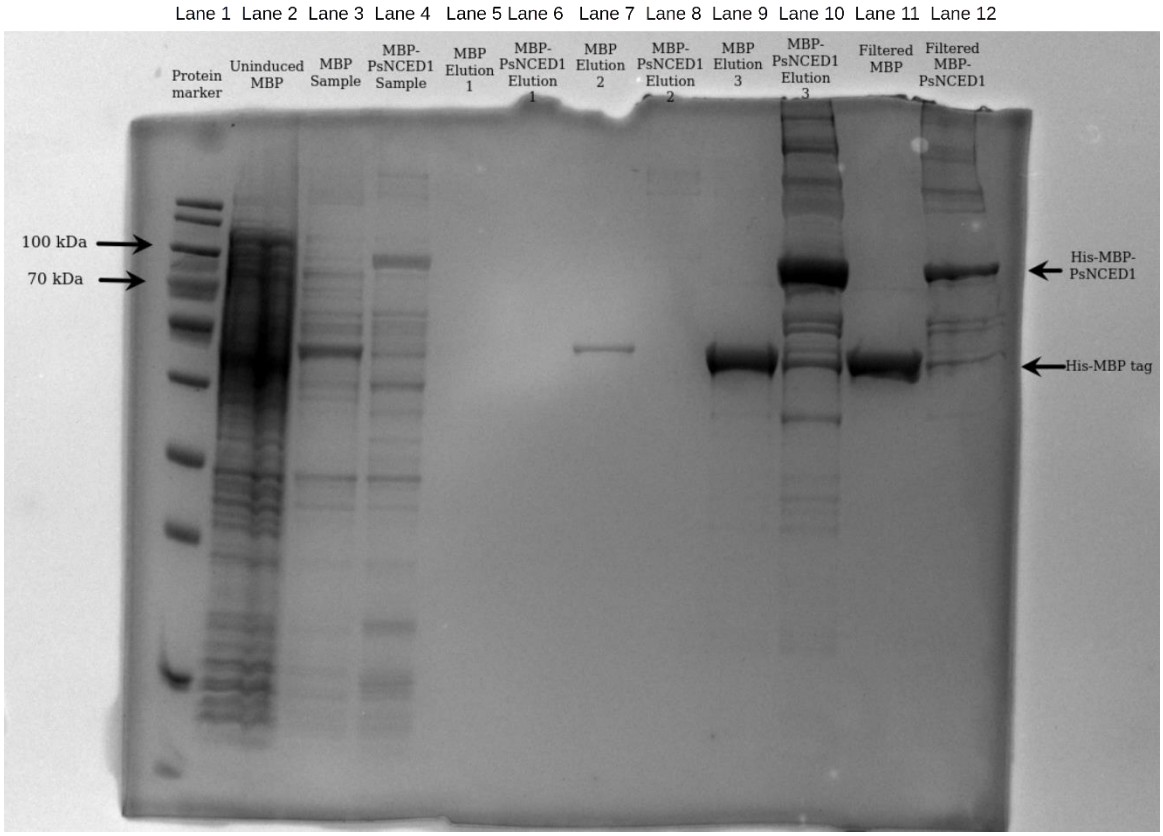

Figure 10. Coomassie-stained SDS-PAGE gel, showing recombinant His-MBP-PsNCED1 and control His-MBP tag extraction and purification steps. ***Lane 1****: protein marker,* ***lane 2****: control LB culture sample before addition of IPTG,* ***lane 3****: control sample from induced culture,* ***lane 4****: IPTG-induced sample of PsNCED1 recombinant protein,* ***lane 5-10****: elution fractions for both MBP control and recombinant protein.* ***Lane 11-12****: MBP control isolated from empty vector expression and His-MBP-PsNCED1 respectively, after filtration through size-exclusion column.*

Enzymatic assay

We tested the purified *Ps*NCED1 protein *in vitro*, to confirm its catalytic action and cleavage specificity towards 9-cis epoxycarotenoids neoxanthin and violaxanthin, using a mass spectrometry-based assay modified from Sergeant and collaborators [51]. The enzyme assay did not appear to be successful as upon analysis no peak was observed in the chromatogram, nor any species observed in the mass spectrum, which corresponded to the product (although the ABA standard was detectable). However, under the conditions it was not possible to observe the substrate in either the enzyme assays or the negative controls. This might have been caused by substrate degradation during the preparation of the reaction mix, as neoxanthin and violaxanthin are highly sensitive to light and oxygen.

Discussion

Carotenoid cleavage dioxygenases are a large protein family responsible for the biosynthesis of apocarotenoids in plants. NCEDs are a subset of these proteins which have the substrate specificity to catalyse the cleavage of the 11-12 bond of 9-cis-neoxanthin and 9-cis-violaxanthin, to produce xanthoxin – the precursor of ABA. Here, we aimed to characterise putative 9-*cis*-epoxycarotenoid dioxygenases, which we hypothesise to be involved in ABA production in conifer species. The sequences targeted for investigations were identified based on previous phylogenetic analysis and gene expression studies that showed their conservation and responsiveness to drought stress. We showed they had a high degree of similarity to the reference NCED sequences in model angiosperm species. We then modelled the corresponding protein structures using several *in silico* methods, providing substantial evidence supporting their identity and predicted function, as a pre-requisite to select the best candidate for protein cloning and testing.

Physical parameters and comparative sequence analysis

We compared amino acid sequences of our conifer candidates to *Z. mays* VP14 and *A. thaliana* NCED3, the former being the first NCED to be structurally and functionally characterised [12,14] and the latter being one of the most studied NCEDs among plants [52–54]. Our analysis also included sequences of *Z. mays* CCD1 and *A. thaliana* CCD4, which are not stereoselective in their cleavage activity and hence are not involved in ABA biosynthesis [55–58].

Protein sequence and structural alignments allowed to establish the degree of similarity between model angiosperm species and conifers, but also between CCDs and NCEDs. Overall, conifer sequences were more homologous to the reference *Zm*VP14 sequence than those of the CCDs, with an identity between 50% and 60% (Table 1). Identity scores should be carefully interpreted because they are influenced by sequence coverage. As a rule of thumb 30% coverage is considered a good threshold for inferring protein homology [59]. In our case, sequence coverage ranged between 83% (*Tb*NCED1) and 97% (*Cl*NCED1), making their identity scores reliable.

We further inspected protein sequence alignments through a motif search (Figure 3). Protein sequence motifs are conserved amino acid blocks bearing enough information to make them signatures of a protein family – and hence protein function [60–62]. They are often useful to reduce the complexity of

sequence alignments. Here we found 10 shared motifs across the alignment, although only 6 were conserved in all sequences. The known NCED references *Zm*VP14, *At*NCED3 and conifer putative NCEDs shared all 10 motifs and signatures of protein function in the same order, in agreement with sequence identity estimates. All motifs were related to the carotenoid oxidoreductase activity with CCDs significantly missing 3-4 of them. Importantly, the missing motifs contain residues that have hydrophobic interactions with the ligand in the substrate tunnel, contributing to the stereoselectivity by positioning the 11-12 bond of 9-*cis*-violaxanthin and 9-*cis*-neoxanthin next to the catalytic iron [14].

Important residues identified during the structural and functional study of *Zm*VP14 [14] were well-conserved between angiosperm and conifer NCEDs, with some exceptions. *Ps*NCED2 had 3 non-conservative substitutions at residue positions inside the hydrophobic tunnel: Ala-214, Phe-365 and Leu-367; these amino acids are among those thought to hold the carotenoid molecule in place through non-specific interactions. Interestingly, *Zm*CCD1 and *At*CCD4 either lacked the same amino acids or had substitutions at the same positions. While substitution of Phe-365 didn't affect VP14 function in mutational studies [14], the effect of the other substitutions is not known. We can argue that *Ps*NCED2 may have reduced affinity for the substrate of interest to some extent, as observed in docking simulations (Supplementary figure 6) and may be consistent with its reduced gene expression responsiveness to drought compared to *Ps*NCED1 (chapter 1).

The highest variability in important and key amino acid composition was observed in both *Zm*CCD1 and *At*CCD4, which had 9 relevant substitutions in the hydrophobic tunnel alone, including Phe-411, Val-478, Trp-501 and Pro-502. These residues are directly involved in positioning the 11-12 bond of the carotenoid molecule over the catalytic iron and the oxygen. *Zm*CCD1 and *At*CCD4 lacked another key region, a loop forming a pocket in association with Leu-170 in *Zm*VP14, which accommodates the second ring of the carotenoid molecule. Finally, *At*CCD4 lacked key Phe-411, which again participates in locking the substrate over the iron molecule. In contrast, these residues were conserved in all conifer sequences (in agreement with the motif analysis), indicating they are likely to have stereospecific cleavage activity of the 9-*cis* form of neoxanthin and violaxanthin, even though *P. sitchensis* NCED2 and *T. baccata* sequences presented some substitutions in the catalytic pocket, which may again affect the overall strength or affinity of the protein-ligand interaction.

Protein structure modelling

We used *in silico* 3D modelling to predict protein folding, based on both *ab initio* and homology methods [63]. *In silico* protein modelling is a fast and inexpensive way of obtaining valuable information about protein structure and function, where experimental methods fail or are unavailable [63,64]. Different algorithms returned the same model based on *Zm*VP14 crystal structure and identified all conifer proteins as monomeric epoxycarotenoid dioxygenases in complex with Fe^{II} and oxygen with a high degree of confidence. We found that the structure predicted by AlphaFold colab tool was less accurate, but this was expected as comparative methods remain more robust than others [65]. It is noteworthy that the *ab initio* algorithm reached the same model outcome as homology-based modelling. Agreement between different prediction methods is a good indicator of model accuracy, but quality checks and model validation are still needed to know which structure is best [66] fit for downstream applications [66]. Several algorithms and quality score systems have been developed. TM-align compares structural alignments residue-by-residue, providing an accuracy measure for residue matching in the form of RMSD score of superimpositions, and a combined measure of structural quality in the form of TM-score, which is more sensitive to global topology and less dependent on sequence coverage [38]. Based on these local and global scores, we were able to select the best performing modelling tool and the model that was closest to *Zm*VP14, our structural reference for NCEDs. Modeller performed consistently better, so its predicted structures were chosen for further quality checks. ProSa uses the known structures in the Protein Data Bank (PDB) to return local and global quality scores for the protein of interest [39]. Local quality scores are based on residue energy calculations across the length of the protein and positive scores correspond to problematic parts of the structure.

The predicted conifer NCED structures were in the range of native crystal structures for model quality given by Z-scores (Supplementary figure 4), although they did show some difficult (poorly resolved) regions towards the C-terminal portion of the protein (Supplementary figure 3). These were mainly loops between secondary structures (see Supplementary figure 7), which are often difficult to predict as they may exist in different conformational states [67–70]. To further validate the accuracy of the predicted protein structures, we used Verify-3D. Its algorithm assesses the compatibility of the amino acid sequence with the atomic positioning of each residue in the 3D protein environment [41,42] and confirmed that the modelled structures were compatible with their sequences (Figure 7). We also used a newly developed algorithm, QMEANDisCo, to obtain an estimate of local and global quality of the model. QMEANDisCo derives from the combination of QMEAN – a scoring function for the degree

of ”nativeness” of a structure [71] - and DisCo, which computes pairwise distances between a model and an ensemble of constraints derived from homologous experimental protein structures [72]. All models obtained a score above 0.8 and were hence comparable to known native experimental structures. Finally, we investigated the stereochemistry of the models by producing Ramachandran plots. More than 90% of the residues fell in the favoured regions of the plot, suggesting general stability for the predicted protein structures (see Table 5 and Supplementary figure 7).

In silico functional study

Functional analyses in this study included signal peptide prediction, membrane interaction simulations and ligand docking. *Zm*VP14 has been previously shown to be targeted to the chloroplast by a transit peptide located at the N-terminal, which is cleaved after import is completed [15]. An amphipathic sequence of 160 residues in the α-helices is responsible for thylakoid membrane targeting, together with a part of the β-propeller, so that the tertiary structure might be involved in membrane interaction [15]. Membrane localization seems to be a conserved feature of NCEDs in *A. thaliana* and *P. vulgaris* [20]. TargetP-2.0 predicted a chloroplast transit peptide in *Zm*VP14, *At*NCED3 and *At*CCD4 as expected [20]. The same signal was identified in *Ps*NCED2, *Cl*NCED1, but not *Zm*CCD1 and intriguingly not in the remaining six conifer sequences. This is not conclusive evidence of the absence of interaction of these conifer NCED sequences with thylakoid membranes, as signal and transit peptide can be highly variable and their identification difficult or uncertain.

In contrast, all putative conifer NCEDs were predicted to have the capacity of membrane binding, by interacting with a lipidic bilayer in our simulation (see Figure 7). This may indicate that conifer NCEDs could be localised either on the intern or the outer membrane of chloroplasts, not requiring import inside the organelle. Although most of the carotenoids are stored on the thylakoid membranes, some others including violaxanthin can be found on the chloroplast envelope [73,74], so they may be accessible to cytoplasmic CCDs and NCEDs.

When running docking simulations we chose the lowest energy state for the protein-ligand interaction. The carotenoid molecule stretched in its linear form inside the hydrophobic pocket, with its 11,12 double bond next to the catalytic iron. This positioning has been already observed in *Zm*VP14 and it is not possible in *Zm*CCD1 [14]. Surprisingly, *Tb*NCED1 and *Tb*NCED2 did not show such an arrangement, but instead they accommodated the ligand molecule in a state that did not allow it to reach the catalytic pocket. This evidence is consistent with gene expression studies, where the two *T.*

baccata sequences didn't seem to respond to drought stress. *Tb*NCED1 and *Tb*NCED2 may therefore be involved in the cleavage of similar but different substrates analyses by use of recombinant protein analysis to verify catalytic activity of the PsNCED1 enzyme are presented below. In addition, complementation studies in *A. thaliana* are ongoing to confirm the identity and catalytic activity of studied enzymes each of the species investigated here.

Protein isolation

PsNCED1 was selected as representative sequence for conifer NCEDs and expressed as an His-MBP-tagged protein. The MBP tag has been observed to improve protein solubility and foldability of difficult samples [75,76]. However, the expressed protein was insoluble and formed inclusion bodies during cell lysis procedures (see Figure 10). In order to improve sample solubility and increase the chances of isolating a folded structure, the protein was expressed in an improved LB liquid media containing sorbitol and betaine [50] at 25°C for 5-6 hours, which resulted in the best trade-off between protein yield and IB formation. Protein purification steps included the addition of Sarkosyl to the cell lysis buffer. This is an anionic detergent known for aiding correct protein folding and isolation under difficult conditions, such as IB formation [50]. Although Sarkosyl did disrupt the protein pellet, it also rendered the cell extract somewhat viscous, hampering thorough clean-up of the protein upon on-column purification (see Figure 11). To cleave the MBP tag, a standard cleavage procedure including the use of TEV protease was applied according to manufactured instructions. Although the reaction did work with a 48h incubation or longer on small samples, on-column purification using an amylose resin did not yield a cleaved pure product, therefore the uncleaved protein had to be used in downstream applications.

Enzymatic assay

Finally, we attempted at testing the isolated protein *in vitro*, but it was not possible to obtain any reaction product according to LC-MS analysis. This could be due to the lability of the substrates, which are sensitive to light and oxygen, so that they may have been degraded during reaction preparation. The fact that we were not able to detect the product nor the substrate of the reaction using LC-MS points in this direction. Another possibility is that the MBP tag may have been affecting the protein activity. This is less likely compared to the first option since previous studies used an uncleaved VP14 protein during *in vitro* testing [51].

Conclusions

In this work we collected several lines of evidence suggesting that the six selected conifer CCD sequences are indeed NCEDs. Sequence and structure similarities to reference protein of *Z. mays* VP14 and *A. thaliana* NCED3 point at functional homology. *In silico* analyses conducted in this study and previous experimental work suggest that our candidate NCEDs are likely to cleave 9-*cis*-neoxanthin and 9-*cis*-violaxanthin as part of the ABA biosynthesis pathway. This validates the importance of monitoring these candidate sequences in gene expression studies in response to drought or other stress factors that trigger ABA production in conifers. Further direct evidence is needed to confirm the cleavage stereospecificity of our candidate proteins, especially for TbNCEDs. *In vitro* and *in vivo* assays are ongoing to confirm the candidate protein's function.

Literature cited

1. Britton G. Structure and properties of carotenoids in relation to function. *The FASEB Journal*. 1995;9(15):1551-1558. doi:10.1096/FASEBJ.9.15.8529834
2. Vershinin A. Mini-review Biological functions of carotenoids-diversity and evolution. *BioFactors*. 1999;10:99-104.
3. Nisar N, Li L, Lu S, Khin NC, Pogson BJ. Carotenoid metabolism in plants. *Molecular Plant*. 2015;8(1):68-82. doi:10.1016/J.MOLP.2014.12.007
4. Cunningham FX, Gantt E. Genes and enzymes of carotenoid biosynthesis in plants. *Annual Review of Plant Physiology and Plant Molecular Biology*. 1998;49:557-583.
5. Enrique Lopez-Juez, Kevin A Pyke. Plastids unleashed: their development and their integration in plant development. *The International Journal of Developmental Biology*. 2005;49(5-6):557-77.doi:10.1387/ijdb.051997el.
6. Hannoufa A, Hossain Z. Regulation of carotenoid accumulation in plants. *Biocatalysis and Agricultural Biotechnology*. 2012;1(3):198-202. doi:10.1016/J.BCAB.2012.03.004
7. Li L, Yuan H. Chromoplast biogenesis and carotenoid accumulation. *Archives of Biochemistry and Biophysics*. 2013;539(2):102-109. doi:10.1016/J.ABB.2013.07.002
8. Giuliano G, Al-Babili S, von Lintig J. Carotenoid oxygenases: cleave it or leave it. *Trends in Plant Science*. 2003;8(4):145-149. doi:10.1016/S1360-1385(03)00053-0

9. Auldridge ME, McCarty DR, Klee HJ. Plant carotenoid cleavage oxygenases and their apocarotenoid products. *Current Opinion in Plant Biology.* 2006;9(3):315-321. doi:10.1016/J.PBI.2006.03.005
10. Daruwalla A, Kiser PD. Structural and mechanistic aspects of carotenoid cleavage dioxygenases (CCDs). *Biochimica et Biophysica Acta - Molecular and Cell Biology of Lipids*. 2020;1865(11). doi:10.1016/J.BBALIP.2019.158590
11. Tan BC, Schwartz SH, Zeevaart JAD, Mccarty DR. Genetic control of abscisic acid biosynthesis in maize. *Proceedings of the National Academy of Sciences*. 1997;94(22):12235-12240. doi:10.1073/PNAS.94.22.12235
12. Sh S, Bc T, Da G, et al. Specific Oxidative Cleavage of Carotenoids by VP14 of Maize. 1997;276(8):1872-1874. doi:10.1126/science.276.5320.1872
13. Schwartz SH, Tan BC, McCarty DR, Welch W, Zeevaart JAD. Substrate specificity and kinetics for VP14, a carotenoid cleavage dioxygenase in the ABA biosynthetic pathway. *Biochimica et Biophysica Acta - General Subjects*. 2003;1619(1):9-14. doi:10.1016/S0304-4165(02)00422-1
14. Messing SAJ, Mario Amzel L, Gabelli SB, et al. Structural insights into maize viviparous14, a key enzyme in the biosynthesis of the phytohormone abscisic acid. *Plant Cell*. 2010;22(9):2970-2980. doi:10.1105/tpc.110.074815
15. Tan BC, Cline K, McCarty DR. Localization and targeting of the VP14 epoxy-carotenoid dioxygenase to chloroplast membranes. *The Plant Journal*. 2001;27(5):373-382. doi:10.1046/j.1365-313X.2001.01102.x
16. Burbidge A, Burbidge A, Grieve T, et al. Structure and expression of a cDNA encoding a putative neoxanthin cleavage enzyme (NCE), isolated from a wilt-related tomato (*Lycopersicon esculentum* Mill.) library. *Journal of Experimental Botany*. 1997;48(314):2111-2112. doi:10.1093/jxb/48.12.2111
17. Qin X, Zeevaart JAD. The 9-cis-epoxycarotenoid cleavage reaction is the key regulatory step of abscisic acid biosynthesis in water-stressed bean. *Proceedings of the National Academy of Sciences*. 1999;96(26):15354-15361. doi:10.1073/pnas.96.26.15354
18. Chernys JT, Zeevaart JAD. Characterization of the 9-Cis-Epoxycarotenoid Dioxygenase Gene Family and the Regulation of Abscisic Acid Biosynthesis in Avocado. *Plant Physiology* 2000;124(1):343-354. doi:10.1104/pp.124.1.343
19. Iuchi S, Kobayashi M, Taji T, et al. Regulation of drought tolerance by gene manipulation of 9-cis-epoxycarotenoid dioxygenase, a key enzyme in abscisic acid biosynthesis in Arabidopsis. *The Plant Journal*. 2001;27(4):325-333. doi:10.1046/J.1365-313X.2001.01096.X

20. Tan BC, Joseph LM, Deng WT, et al. Molecular characterization of the Arabidopsis 9-cis epoxycarotenoid dioxygenase gene family. *The Plant Journal*. 2003;35(1):44-56. doi:10.1046/J.1365-313X.2003.01786.X
21. Auldridge ME, Block A, Vogel JT, et al. Characterization of three members of the Arabidopsis carotenoid cleavage dioxygenase family demonstrates the divergent roles of this multifunctional enzyme family. *The Plant Journal*. 2006;45(6):982-993. doi:10.1111/J.1365-313X.2006.02666.X
22. Cuming AC, Cho SH, Kamisugi Y, Graham H, Quatrano RS. Microarray analysis of transcriptional responses to abscisic acid and osmotic, salt, and drought stress in the moss, Physcomitrella patens. *New Phytologist*. 2007;176(2):275-287. doi:10.1111/j.1469-8137.2007.02187.x
23. Xu Z, Xin T, Bartels D, et al. Genome Analysis of the Ancient Tracheophyte *Selaginella tamariscina* Reveals Evolutionary Features Relevant to the Acquisition of Desiccation Tolerance. *Molecular Plant*. 2018;11(7):983-994. doi:10.1016/J.MOLP.2018.05.003
24. Lorenz WW, Alba R, Yu YS, Bordeaux JM, Simões M, Dean JFD. Microarray analysis and scale-free gene networks identify candidate regulators in drought-stressed roots of loblolly pine (P. taeda L.). *BMC Genomics*. 2011;12. doi:10.1186/1471-2164-12-264
25. Pashkovskiy PP, Vankova R, Zlobin IE, et al. Comparative analysis of abscisic acid levels and expression of abscisic acid-related genes in Scots pine and Norway spruce seedlings under water deficit. *Plant Physiology and Biochemistry*. 2019;140:105-112. doi:10.1016/J.PLAPHY.2019.04.037
26. Katoh K, Misawa K, Kuma KI, Miyata T. MAFFT: a novel method for rapid multiple sequence alignment based on fast Fourier transform. *Nucleic Acids Research*. 2002;30(14):3059. doi:10.1093/NAR/GKF436
27. Kumar S, Stecher G, Li M, Knyaz C, Tamura K. MEGA X: Molecular Evolutionary Genetics Analysis across Computing Platforms. *Molecular Biology and Evolution*. 2018;35(6):1547-1549. doi:10.1093/MOLBEV/MSY096
28. Walker JM, Gasteiger E, Hoogland C, et al. Protein Identification and Analysis Tools on the ExPASy Server. *The Proteomics Protocols Handbook*. 1999;112:571-607. doi:10.1385/1-59259-890-0:571
29. Bailey TL, Johnson J, Grant CE, Noble WS. The MEME Suite. *Nucleic Acids Research*. 2015;43(W1):W39-W49. doi:10.1093/NAR/GKV416
30. Altschul SF, Gish W, Miller W, Myers EW, Lipman DJ. Basic local alignment search tool. *Journal of Molecular Biology*. 1990;215(3):403-410. doi:10.1016/S0022-2836(05)80360-2

31. Jones P, Binns D, Chang HY, et al. InterProScan 5: genome-scale protein function classification. *Bioinformatics*. 2014;30(9):1236-1240. doi:10.1093/bioinformatics/btu031
32. Gouet P, Courcelle E, Stuart DI, Métoz F. ESPript: analysis of multiple sequence alignments in PostScript. *Bioinformatics*. 1999;15(4):305-308. doi:10.1093/bioinformatics/15.4.305
33. Jumper J, Evans R, Pritzel A, et al. Highly accurate protein structure prediction with AlphaFold. *Nature. 2021*; 596(7873):583-589. doi:10.1038/s41586-021-03819-2
34. Eswar N, Webb B, Marti-Renom MA, et al. Comparative protein structure modeling using Modeller. *Current Protocols in Bioinformatics*. 2006; 5(1). doi:10.1002/0471250953.BI0506S15
35. Studer G, Tauriello G, Bienert S, Biasini M, Johner N, Schwede T. ProMod3-A versatile homology modelling toolbox. *PLOS Computational Biology*. 2021;17(1). doi:10.1371/JOURNAL.PCBI.1008667
36. Waterhouse A, Bertoni M, Bienert S, et al. SWISS-MODEL: homology modelling of protein structures and complexes. *Nucleic Acids Research*. 2018;46(1): W296-W303. doi:10.1093/NAR/GKY427
37. Kelley LA, Mezulis S, Yates CM, Wass MN, Sternberg MJE. The Phyre2 web portal for protein modeling, prediction and analysis. *Nature Protocols*. 2015;10(6):845-858. doi:10.1038/nprot.2015.053
38. Zhang Y, Skolnick J. TM-align: a protein structure alignment algorithm based on the TM-score. *Nucleic Acids Research*. 2005;33(7):2302-2309. doi:10.1093/NAR/GKI524
39. Wiederstein M, Sippl MJ. ProSA-web: interactive web service for the recognition of errors in three-dimensional structures of proteins. *Nucleic Acids Research*. 2007;35(2):W407-W410. doi:10.1093/NAR/GKM290
40. Colovos C, Yeates TO. Verification of protein structures: Patterns of nonbonded atomic interactions. *Protein Science*. 1993;2(9):1511-1519. doi:10.1002/PRO.5560020916
41. Bowie JU, Lüthy R, Eisenberg D. A method to identify protein sequences that fold into a known three-dimensional structure. *Science*. 1991;253(5016):164-170. doi:10.1126/SCIENCE.1853201
42. Lüthy R, Bowie JU, Eisenberg D. Assessment of protein models with three-dimensional profiles. *Nature*. 1992;356(6364):83-85. doi:10.1038/356083A0
43. Pieper U, Webb BM, Barkan DT, et al. ModBase, a database of annotated comparative protein structure models, and associated resources. *Nucleic Acids Research*. 2011;39:D465. doi:10.1093/NAR/GKQ1091

44. Armenteros JJA, Salvatore M, Emanuelsson O, et al. Detecting sequence signals in targeting peptides using deep learning. *Life Science Alliance*. 2019;2(5). doi:10.26508/LSA.201900429
45. Nugent T, Jones DT. Membrane protein orientation and refinement using a knowledge-based statistical potential. *BMC Bioinformatics*. 2013;14(1):1-10. doi:10.1186/1471-2105-14-276
46. Buchan DWA, Jones DT. The PSIPRED Protein Analysis Workbench: 20 years on. *Nucleic Acids Research*. 2019;47(W1):W402-W407. doi:10.1093/NAR/GKZ297
47. Grosdidier A, Zoete V, Michielin O. SwissDock, a protein-small molecule docking web service based on EADock DSS. *Nucleic Acids Research*. 2011;39. doi:10.1093/NAR/GKR366
48. Grosdidier A, Zoete V, Michielin O. Fast docking using the CHARMM force field with EADock DSS. *Journal of Computational Chemistry*. 2011;32(10):2149-2159. doi:10.1002/JCC.21797
49. Pettersen EF, Goddard TD, Huang CC, et al. UCSF Chimera--a visualization system for exploratory research and analysis. *Journal of Computational Chemistry*. 2004;25(13):1605-1612. doi:10.1002/JCC.20084
50. Massiah MA, Wright KM, Du H. Obtaining Soluble Folded Proteins from Inclusion Bodies Using Sarkosyl, Triton X-100, and CHAPS: Application to LB and M9 Minimal Media. *Current Protocols in Protein Science*. 2016; 84:6.13.1-6.13.24. doi:10.1002/0471140864.PS0613S84
51. Sergeant MJ, Li JJ, Fox C, et al. Selective Inhibition of Carotenoid Cleavage Dioxygenases: phenotypic effects on shoot branching. *Journal of Biological Chemistry*. 2009;284(8):5257-5264. doi:10.1074/JBC.M805453200
52. Endo A, Sawada Y, Takahashi H, et al. Drought induction of Arabidopsis 9-cis-epoxycarotenoid dioxygenase occurs in vascular parenchyma cells. *Plant Physiology* 2008;147(4):1984-1993. doi:10.1104/PP.108.116632
53. Ikegami K, Okamoto M, Seo M, Koshiba T. Activation of abscisic acid biosynthesis in the leaves of A. thaliana in response to water deficit. *Journal of Plant Research*. 2009;122(2):235-243. doi:10.1007/S10265-008-0201-9
54. Ma Y, Cao J, He J, Chen Q, Li X, Yang Y. Molecular Mechanism for the Regulation of ABA Homeostasis During Plant Development and Stress Responses. *International Journal of Molecular Sciences*. 2018;19(11):3643. doi:10.3390/ijms19113643
55. Vogel JT, Tan BC, McCarty DR, Klee HJ. The carotenoid cleavage dioxygenase 1 enzyme has broad substrate specificity, cleaving multiple carotenoids at two different bond positions. *Journal of Biological Chemistry*. 2008;283(17):11364-11373. doi:10.1074/jbc.M710106200

56. Sun Z, Hans J, Walter MH, et al. Cloning and characterisation of a maize carotenoid cleavage dioxygenase (ZmCCD1) and its involvement in the biosynthesis of apocarotenoids with various roles in mutualistic and parasitic interactions. *Planta*. 2008;228(5):789-801. doi:10.1007/S00425-008-0781-6

57. Huang FC, Molnár P, Schwab W. Cloning and functional characterization of carotenoid cleavage dioxygenase 4 genes. *Journal of Experimental Botany*. 2009;60(11):3011-3022. doi:10.1093/JXB/ERP137

58. Bruno M, Koschmieder J, Wuest F, et al. Enzymatic study on AtCCD4 and AtCCD7 and their potential to form acyclic regulatory metabolites. *Journal of Experimental Botany*. 2016;67(21):5993. doi:10.1093/JXB/ERW356

59. Pearson WR. An Introduction to Sequence Similarity ("Homology") Searching. *Current protocols in bioinformatics*. 2013;0 3(SUPPL.42). doi:10.1002/0471250953.BI0301S42

60. Bork P. Mobile modules and motifs. *Current Opinion in Structural Biology*. 1992;2(3):413-421. doi:10.1016/0959-440X(92)90233-W

61. Bork P, Koonin E v. Protein sequence motifs. *Current Opinion in Structural Biology*. 1996;6(3):366-376. doi:10.1016/S0959-440X(96)80057-1

62. Bork P, Gibson TJ. [11] Applying motif and profile searches. *Methods in Enzymology*. 1996;266:162-184. doi:10.1016/S0076-6879(96)66013-3

63. Dorn M, E Silva MB, Buriol LS, Lamb LC. Three-dimensional protein structure prediction: Methods and computational strategies. *Computational Biology and Chemistry*. 2014;53(PB):251-276. doi:10.1016/J.COMPBIOLCHEM.2014.10.001

64. Singh N, Upadhyay S, Jaiswar A. In silico Analysis of Protein. 2016;1(2):1-7.

65. Khan FI, Wei DQ, Gu KR, Hassan MI, Tabrez S. Current updates on computer aided protein modeling and designing. *International Journal of Biological Macromolecules*. 2016;85:48-62. doi:10.1016/J.IJBIOMAC.2015.12.072

66. Schwede T. Protein Modeling: What Happened to the "Protein Structure Gap"? *Structure*. 2013;21(9):1531-1540. doi:10.1016/J.STR.2013.08.007

67. Sippl MJ. Calculation of conformational ensembles from potentials of mena force: An approach to the knowledge-based prediction of local structures in globular proteins. *Journal of Molecular Biology*. 1990;213(4):859-883. doi:10.1016/S0022-2836(05)80269-4

68. Ring CS, Kneller DG, Langridge R, Cohen FE. Taxonomy and conformational analysis of loops in proteins. *Journal of Molecular Biology*. 1992;224(3):685-699. doi:10.1016/0022-2836(92)90553-V

69. Rufino SD, Donate LE, Canard LHJ, Blundell TL. Predicting the conformational class of short and medium size loops connecting regular secondary structures: application to comparative modelling. *Journal of Molecular Biology*. 1997;267(2):352-367. doi:10.1006/JMBI.1996.0851
70. Wojcik J, Mornon JP, Chomilier J. New efficient statistical sequence-dependent structure prediction of short to medium-sized protein loops based on an exhaustive loop classification. *Journal of Molecular Biology*. 1999;289(5):1469-1490. doi:10.1006/JMBI.1999.2826
71. Benkert P, Biasini M, Schwede T. Toward the estimation of the absolute quality of individual protein structure models. *Bioinformatics*. 2011;27(3):343-350. doi:10.1093/BIOINFORMATICS/BTQ662
72. Studer G, Rempfer C, Waterhouse AM, Gumienny R, Haas J, Schwede T. QMEANDisCo—distance constraints applied on model quality estimation. *Bioinformatics*. 2020;36(6):1765-1771. doi:10.1093/BIOINFORMATICS/BTZ828
73. Schwartz N, Armbruster U, Iven T, et al. Tissue-Specific Accumulation and Regulation of Zeaxanthin Epoxidase in Arabidopsis Reflect the Multiple Functions of the Enzyme in Plastids. *Plant & Cell Physiology*. 2015;56(2):346-357. doi:10.1093/PCP/PCU167
74. Sun T, Yuan H, Cao H, Yazdani M, Tadmor Y, Li L. Carotenoid Metabolism in Plants: The Role of Plastids. *Molecular Plant*. 2018;11(1):58-74. doi:10.1016/J.MOLP.2017.09.010
75. Nallamsetty S, Waugh DS. A generic protocol for the expression and purification of recombinant proteins in Escherichia coli using a combinatorial His6-maltose binding protein fusion tag. *Nature Protocols*. 2007;2(2):383-391. doi:10.1038/nprot.2007.50
76. Duong-Ly KC, Gabelli SB. Affinity Purification of a Recombinant Protein Expressed as a Fusion with the Maltose-Binding Protein (MBP) Tag. *Methods in Enzymology*. 2015;559:17. doi:10.1016/BS.MIE.2014.11.004

Supplementary material

Tables

Supplementary table 1. TargetP – 2.0 output table. ***CS position*** *= chloroplast signal position in the sequence,* ***SP*** *= signal peptide,* ***mTP*** *= mitochondrial transit peptide,* ***cTP*** *= chloroplast transit peptide,* ***lTP*** *= thylakoidal lumen composite transit peptide,* ***Other*** *= no targeting peptide.*

ID	Prediction	OTHER	SP	mTP	cTP	lTP	CS Position
ZmVP14	cTP	0.31	0	0.02	0.68	0	CS pos: 34-35. PRA-VS. Pr: 0.2976
ZmCCD1	OTHER	1	0	0	0	0	
AtNCED3	cTP	0.01	0	0	0.98	0.01	CS pos: 52-53. VSS-AL. Pr: 0.2114
AtCCD4	cTP	0.34	0	0.01	0.63	0.02	CS pos: 35-36. INS-AV. Pr: 0.4207
ClNCED1	cTP	0.25	0	0.01	0.73	0.02	CS pos: 58-59. RVQ-SV. Pr: 0.4809
ClNCED2	OTHER	0.87	0	0.03	0.1	0	
PsNCED1	OTHER	0.81	0	0.14	0.05	0	
PsNCED2	cTP	0.07	0	0.02	0.89	0.02	CS pos: 44-45. INA-HT. Pr: 0.2784
TbNCED1	OTHER	0.99	0	0.01	0	0	
TbNCED2	OTHER	0.77	0	0.17	0.06	0.01	

Figures

"Chapter 2 Supplemental alignment.pdf"

Supplementary figure 1. MAFFT multiple sequence alignment (MSA) of putative and model NCED and CCD protein sequences. At: A. thaliana; Cl: C. lawsoniana; Ps: P. sitchensis; Tb: T. baccata; Zm: Z. mays. Residues with similarity scores above the 0.7 similarity cut-off value are shown in red on white background. Columns that are strictly conserved are shown in white on red background. ZmVP14 was used as reference anchor sequence and its structural features from PDB file 3npe [14] are shown. Click on interactive element to visualise.

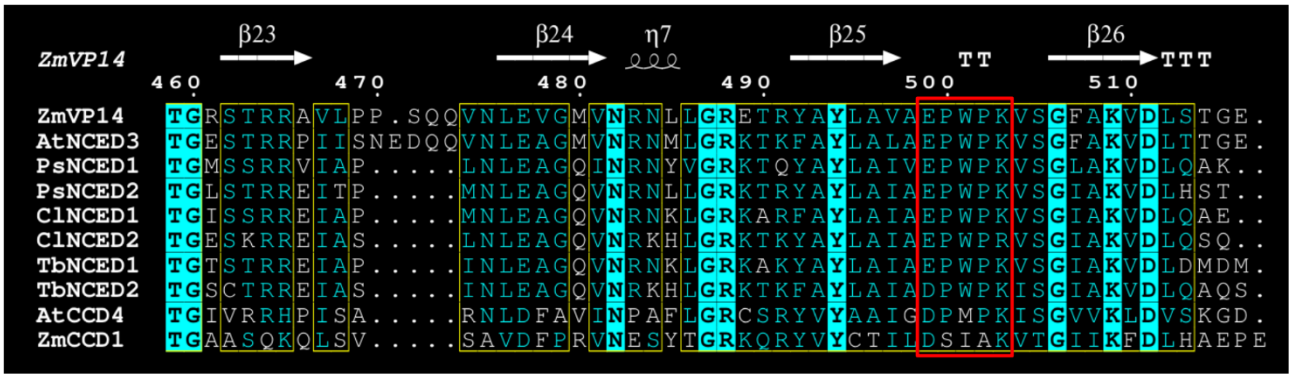

Supplementary figure 2. MSA showing structural features based on reference sequence of Z. mays VP14. Target region comprising residues between position 499 and 503. Residues with similarity scores above the 0.7 similarity cut-off value are shown in cyan blue on black background. Columns that are strictly conserved are shown in black on cyan blue background. Sequence regions harboring amino acid substitutions relevant to protein function are highlighted with red boxes. ZmVP14 was used as reference anchor sequence and its structural features from PDB file 3npe [14] are shown. At = A. thaliana, Cl = C. lawsoniana, Ps = P. sitchensis, Tb = T. baccata, Zm = Z. mays.

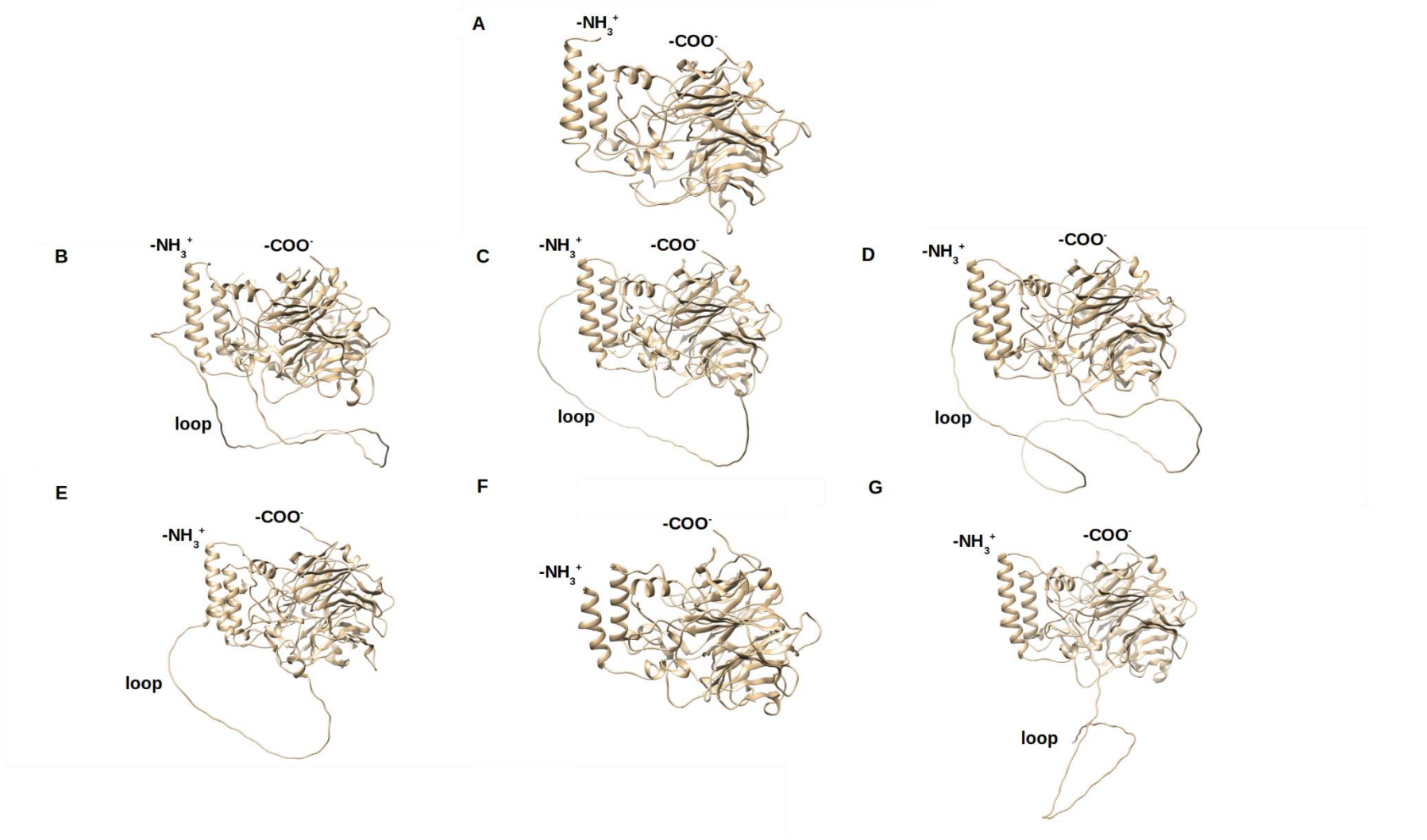

Supplementary figure 3. Reference ZmVP14 known crystal structure and Putative conifer NCED structures predicted by AlphaFold2 colab ab initio algorithm. ***A****: ZmVP14,* ***B****: PsNCED1,* ***C****: PsNCED2,* ***D****: ClNCED1,* ***E****: ClNDED2,* ***F****: TbNCED1,* ***G****: TbNCED2.*

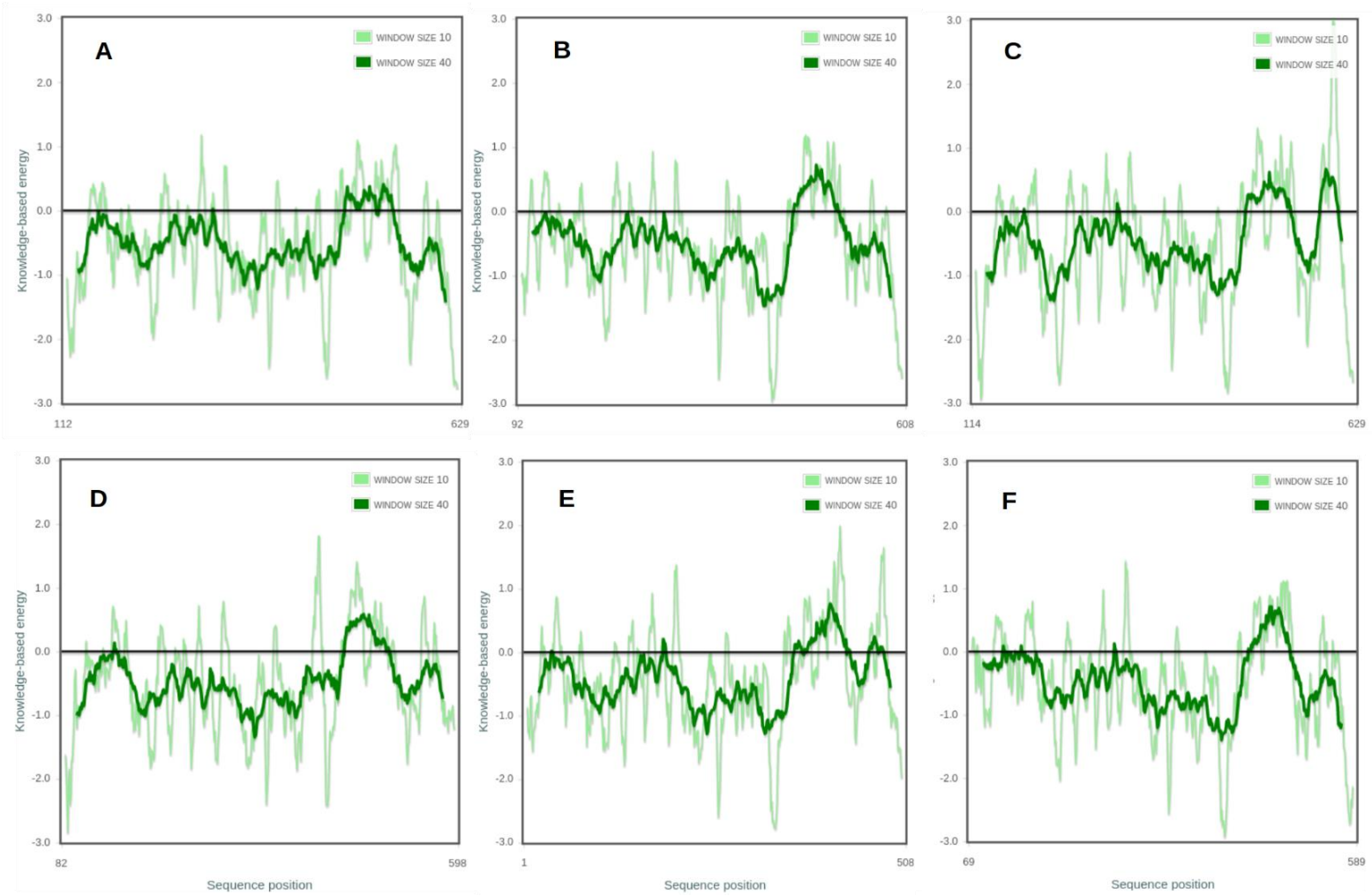

*Supplementary figure 4. ProSa web server model local quality estimates. Panels show energies as a function of amino acid sequence position. Positive values may correspond to unresolved parts of the structure. The plot is smoothed by calculating the average energy over 40-residue fragments (**dark green**). A second line with a window size of 10 residues is also shown (**light green**). **A**: PsNCED1, **B**: PsNCED2, **C**: ClNCED1, **D**: ClNDED2, **E**: TbNCED1, **F**: TbNCED2.*

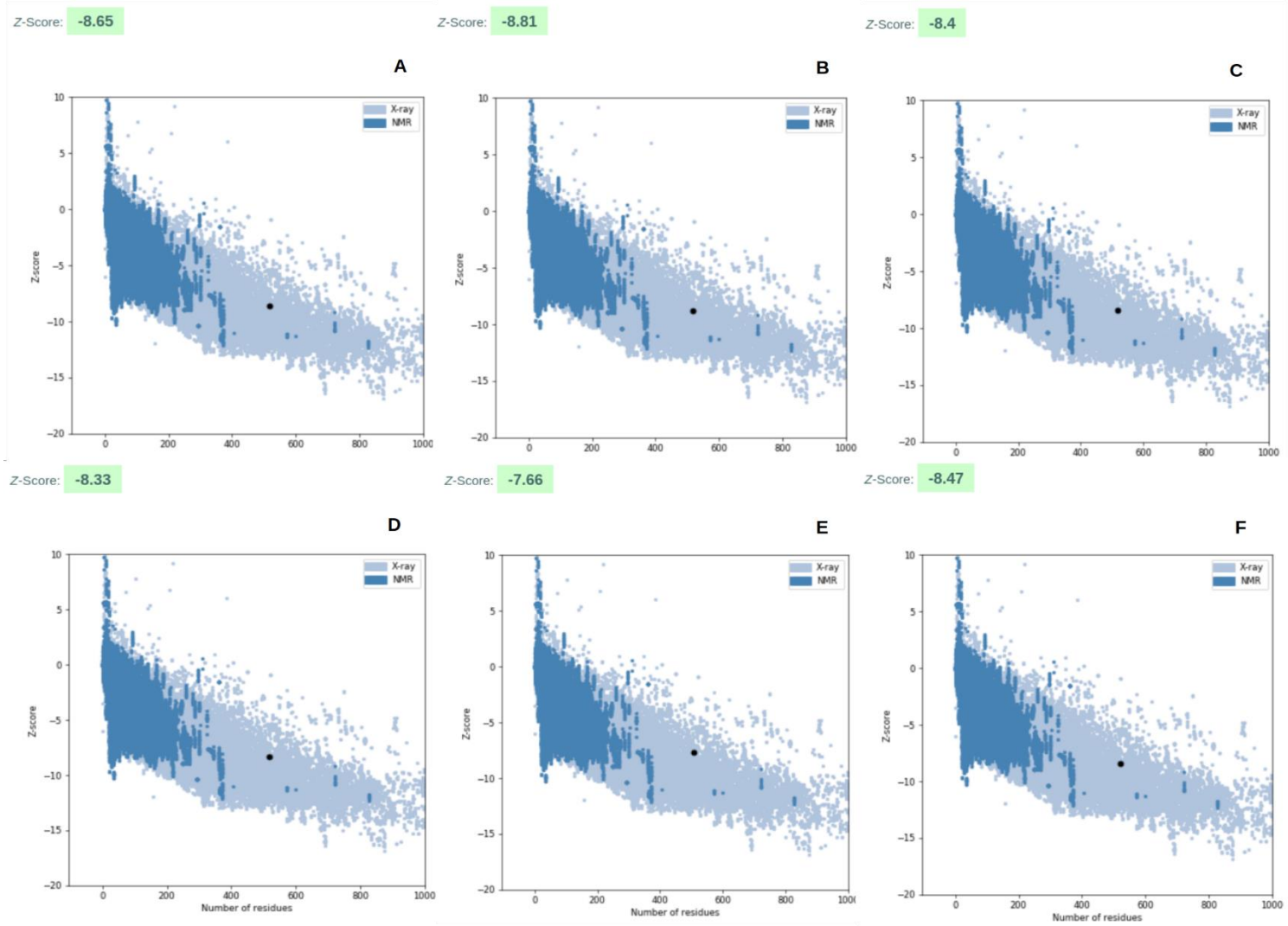

*Supplementary figure 5. ProSa web server model global quality estimates. Panels show Z-scores and predicted model position in a range of experimentally known protein structures in the Protein Data Bank (PDB), either NMR (**dark blue**) or X-ray quality (**light blue**). **A**: PsNCED1, **B**: PsNCED2, **C**: ClNCED1, **D**: ClNDED2, **E**: TbNCED1, **F**: TbNCED2.*

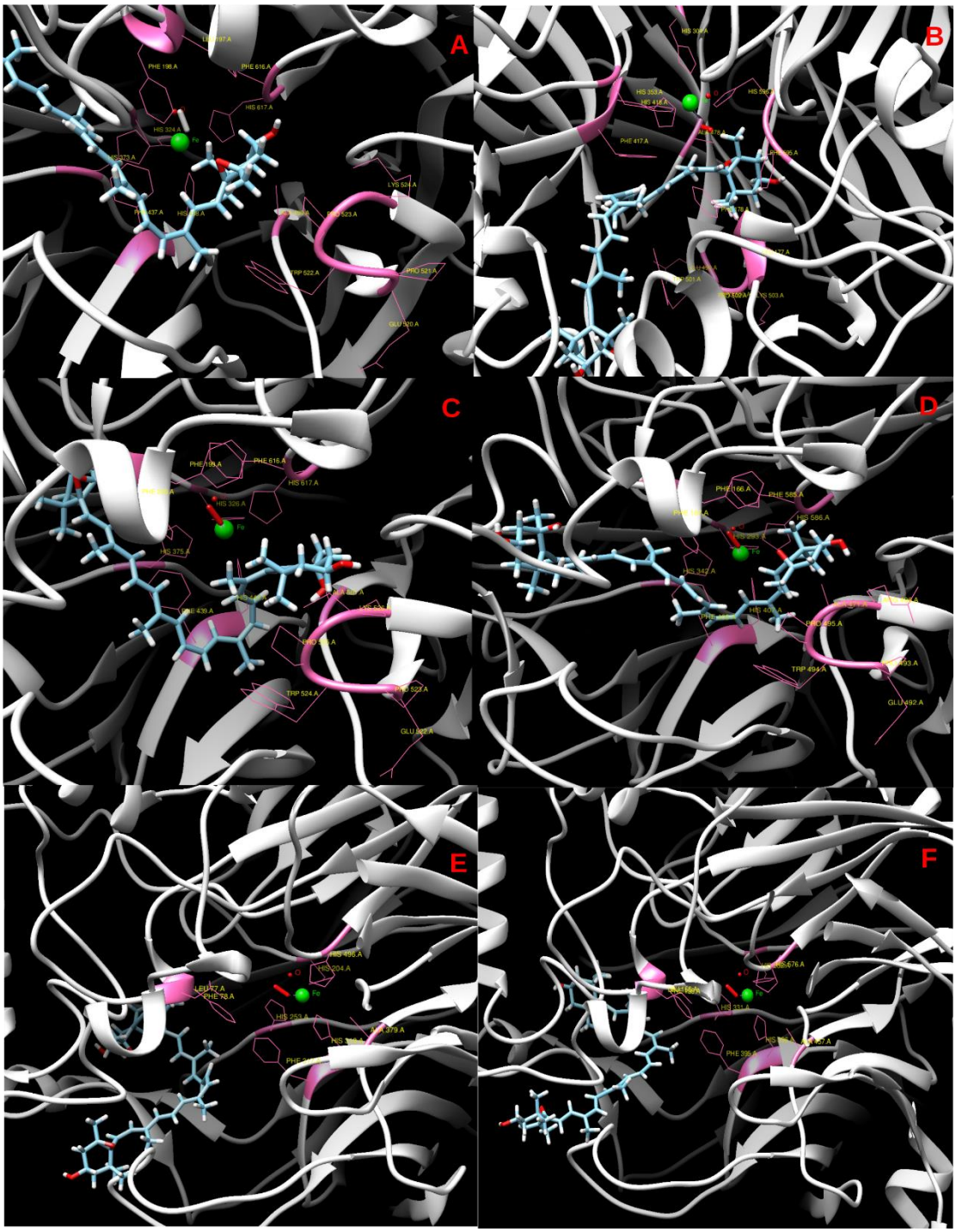

Supplementary figure 6. Close-up of ligand docking simulation based on modelling by Swiss-dock web server and visualised on CHIMERA viewdock tool. ***Protein structure*** *is shown in* ***white****, important residues that interact with the ligand are shown in* ***magenta*** *and* ***labelled****. Catalytic iron is shown as a* ***green sphere*** *and the water molecule + dioxygen is shown in* ***red****. Ligand is shown in* ***cyan blue****.* ***A****: PsNCED1,* ***B****: PsNCED2,* ***C****: ClNCED1,* ***D****: ClNDED2,* ***E****: TbNCED1,* ***F****: TbNCED2.*

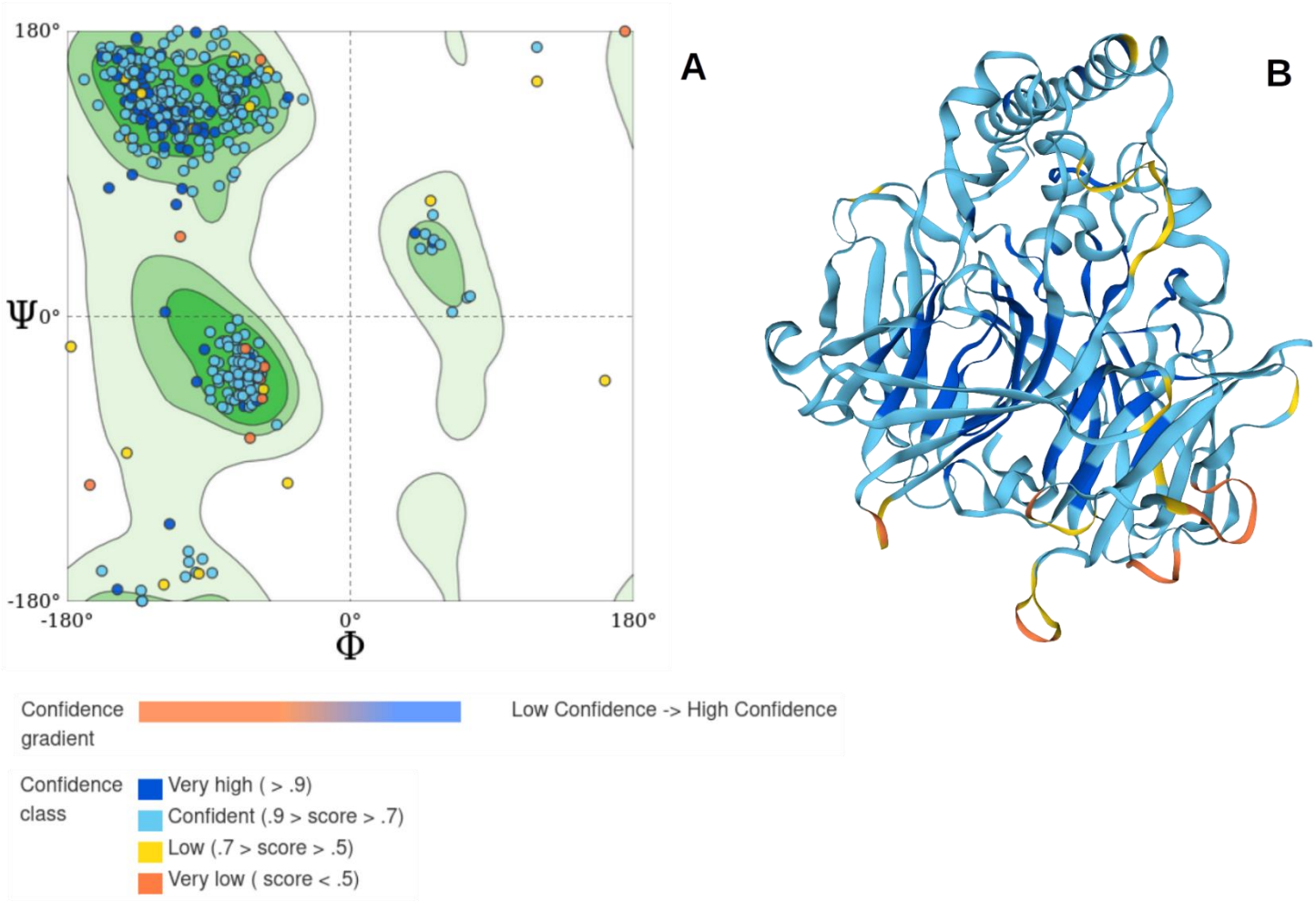

Supplementary figure 7. Structure quality summary of PsNCED1 as returned by SwissModel web server. ***A:*** *Ramachandran plot.* ***B:*** *Structure model. QMEANDisCO (range 0-1) is used to compute confidence gradient and class interpretation guides shown below.*

Chapter 3

Leaf-level gas conductance explains variation in water use among breeding families of *Picea sitchensis* and *Picea lutzii*

Graphical abstract

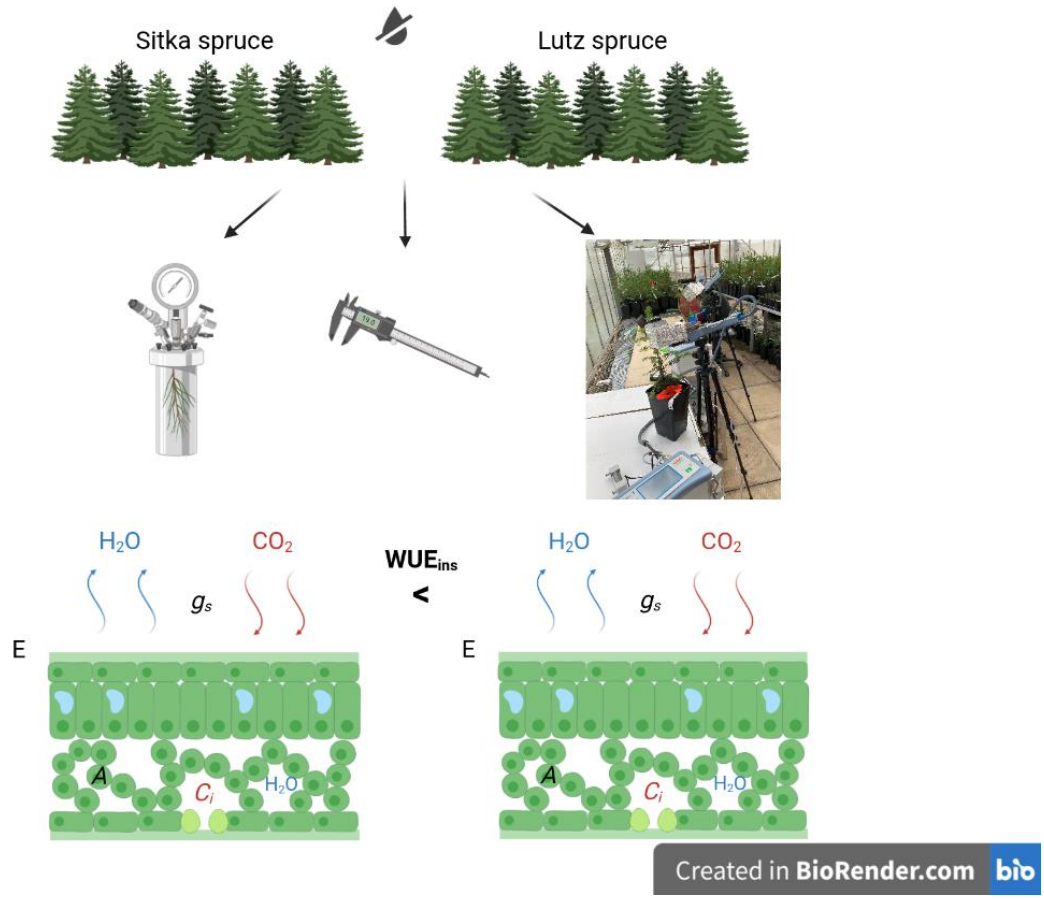

Abstract

Natural and planted forests are faced with new climatic challenges. Researchers and tree breeders have joined their efforts in the search of genotypes and phenotypic traits that may confer higher adaptability to future climate scenarios. Commercial tree species are some of the most studied systems in the field of forest research, but variation in physiological drought responses at the interspecific level is somewhat elusive. At the same time, recent interest has emerged around hybrids, which may retain traits of interest of both parental species. In this chapter, we explore variability in water and photosynthesis-related traits in response to an occasional drought in a set of Sitka (*Picea sitchensis)* and Lutz spruce (*Picea lutzii)* breeding families.

Introduction

Forest Research has estimated the UK woodland area to be 3.24 million hectares - 13% of the total land area in the UK (March 2022) - including commercial plantations. Of these, 51% is made up of conifers and half of this portion is represented by *Picea sitchensis* (*P. sitchensis*) [1], making it the principal tree species in the UK timber industry. *P. sitchensis* dominates the UK softwood timber market because of its high yields on diverse sites and viability under current climatic conditions [2]. However, it may suffer on dryer sites because it originates from the west coast of North America and is adapted to moist maritime climates. Indeed, *P. sitchensis* plantations tend to perform better in the wetter north-west of the UK, compared to the drier south-east [3–5].

Evidence suggests that the UK will follow the global trend of climate warming and its mean temperatures may increase even faster than in other regions [6]. Winters are expected to become warmer and wetter, and summers will get hotter and drier [6,7]. This change will likely exacerbate differences in regional weather patterns, with the north-west potentially becoming even more suitable for *P. sitchensis* plantations, and the south-east seeing a possible increase in drought cracks and diebacks [3,4]. Climate change will affect timber quality even when trees survive droughts [4].

Our knowledge of the UK forest resilience to climate change, and that of *P. sitchensis*, is limited and only a few reports have studied the responses of conifers grown in the UK to extreme weather events

[8,9]. Overall, *P. sitchensis* may be more sensitive to drought stress and more prone to xylem cavitation than other species [10–13]. Despite this, yield may remain high under future climate conditions and may even compensate for its drought susceptibility; therefore, it continues to be used as the dominant species in productive forestry [14]. The UK Government is setting out to increase afforestation rates to between 30,000 and 50,000 hectares per year, as part of the effort to increase forest land cover up to 17-19% and reach net-zero carbon emissions by 2050 [15]. While species richness has proven to increase forest resistance to abiotic and biotic disturbances and maintain interannual productivity [16–19], it is to be expected that a relevant part of the new planted forest will be made up of *P. sitchensis*.

In this context, it is crucial to advance our knowledge of the resilience of *P. sitchensis* to climate disturbances including drought, in order to inform on best practises in silviculture and tree breeding. Genetic selection of best performing *P. sitchensis* progenies has been ongoing since 1963 [20], by mainly looking at height, diameter, stem-straightness and wood density. As of today, more than 90% of the planted *P. sitchensis* in the UK is from improved planting stock, increasing the total timber yield by 29% [21,22]. Tree breeding for yield and form traits may carry some drawbacks such as the loss of genetic diversity associated with resistance traits, which can be overcome by crossing different provenances. Despite the obvious economic benefits of tree selection for improved timber yield and quality, it is unclear whether breeding practises can provide a solution to the threat posed by climate change. Recent studies on improved Sitka full-sibling families (i.e., both parents are known improved material) have highlighted homogeneous responses to drought both in terms of eco-physiological functional traits and biomass production, as well as in comparison to unimproved seed lots [12,23]. In the search for alternatives to dominant *P. sitchensis*, some interest has re-emerged around its natural occurring hybrid with *Picea glauca – Picea x lutzii* (*P. lutzii*) [24,25]. The hybrid is found both in the wet maritime zones of the native habitat occupied of *P. sitchensis* and in the drier inland areas growing together with *P. glauca*. Breeding efforts, such as those made by our partners at Maelor Forestry Nurseries ltd, are currently aiming at obtaining a tree that retains the high yield typical of *P. sitchensis* and site tolerance of *P. glauca* [21,24–27].

In this study, we used a controlled drought experiment comparing several seedlings from full-sibling families of *P. sitchensis* and *P. lutzii*. The objective was to assess the effects of acute short-term drought on the different families by 1) monitoring changes in water relations, 2) studying changes in photosynthesis-related traits expected to vary in response to drought and, 3) calculating water use efficiency. This experimental approach aimed to identify putative physiological markers of inter- and intra-specific diversity in closely related species that are highly important to the UK timber market.

Materials and methods

Plant material and experimental conditions

Two-year-old seedlings (30-50 cm tall) of *P. sitchensis* and *P. lutzii* were obtained from Maelor Forest Nurseries ltd (Fields Farm, Bronington, Wrexham, SY13 3HZ). Both species included five breeding families each, but only four were used due to space constraints and variation in plant vigour (see Table 1 for identifiers and origin). Trees were shipped with bare roots, in dark plastic bags and potted upon arrival into 3-litres square pots containing medium coarse potting compost (pH: 5.3 to 6.0, Levington®). Potted seedlings were allowed to acclimatise for 8 weeks in a greenhouse supplied with artificial lights (photoperiod 16h/8h - day/night). Temperature and relative air humidity were monitored by using a SKH 2065 - PT100 RH+ temperature probe fitted with a radiation screen (Skye instruments ltd, Ddole Enterprise Park, Llandrindod, Wells Powys LD1 6DF, UK). Oscillations in temperature and air humidity were buffered by automatic air ventilation through roof vents. Photosynthetically active radiation (PAR) was monitored by a QS5-15 PAR quantum sensor (Delta-T devices ltd, 130 Low Road, Burwell, Cambridge, CB25 0EJ, UK). All sensors were connected to a GP2 data logger (Delta-T devices ltd), and data recorded daily (8:00AM) (see figure 1). It must be noted that a heatwave caused high temperature conditions inside the greenhouse for the duration of the experiment, with peaks above 40°C, the ventilation and cooling systems being not sufficient to ameliorate them. Although we did not consider temperature as a factor in our experimental design, it could have been exacerbating tree stress to some extent. Implications are discussed.

Table 1. Provenance and type of material of the full-sibling families of Sitka and P. lutzii used in this experiment. Pl = Picea lutzii, Ps = Picea sitchensis. WSFN = P. glauca pollen from Canada. SS = Sitka spruce (P. sitchensis). Veg. Prop. = vegetative propagation. W+1 = 1 year grafted + 1 year in open field.

Species and provenance	**Parent ♀**	**Parent ♂ (pollen)**	**Propagation method**	**Type of crop**	**Batch no.**
Pl700	SS686	WSFN6055	Somatic embryogenesis -> veg. prop.	W+1	15100700/1
Pl701	SS1350	WSFN6121	Full sibling seed -> veg. prop.	W+1	16100701
Pl702	SS1494	WSFN6055	Full sibling seed -> veg. prop.	W+1	16100702
Pl703	SS390	WSFN6096	Somatic embryogenesis -> veg. prop.	W+1	15100703/1
Ps111	SS1492	SS1500	Full sibling seed -> veg. prop.	W+1	1990111
Ps112	SS1492	SS1583	Full sibling seed -> veg. prop.	W+1	1990112
Ps117	SS394	SS1583	Full sibling seed -> veg. prop.	W+1	1990117
PsA18			Seed orchard seed - open pollination	1+1	198202

Trees were organised in a design with 5 blocks distributed across the greenhouse, each block containing 14 trees of all breeding families. Pots were watered to full capacity until the drought treatment was started by completely withholding water. The drought treatment lasted for 25 days during July 2021, after which pots were re-watered to full capacity twice in August (04/08 and 06/08). All physiology measurements were collected from randomly selected trees. Once sampled for water

potential determinations (see details below), each tree was virtually removed from the experimental design, but physically maintained in its position.

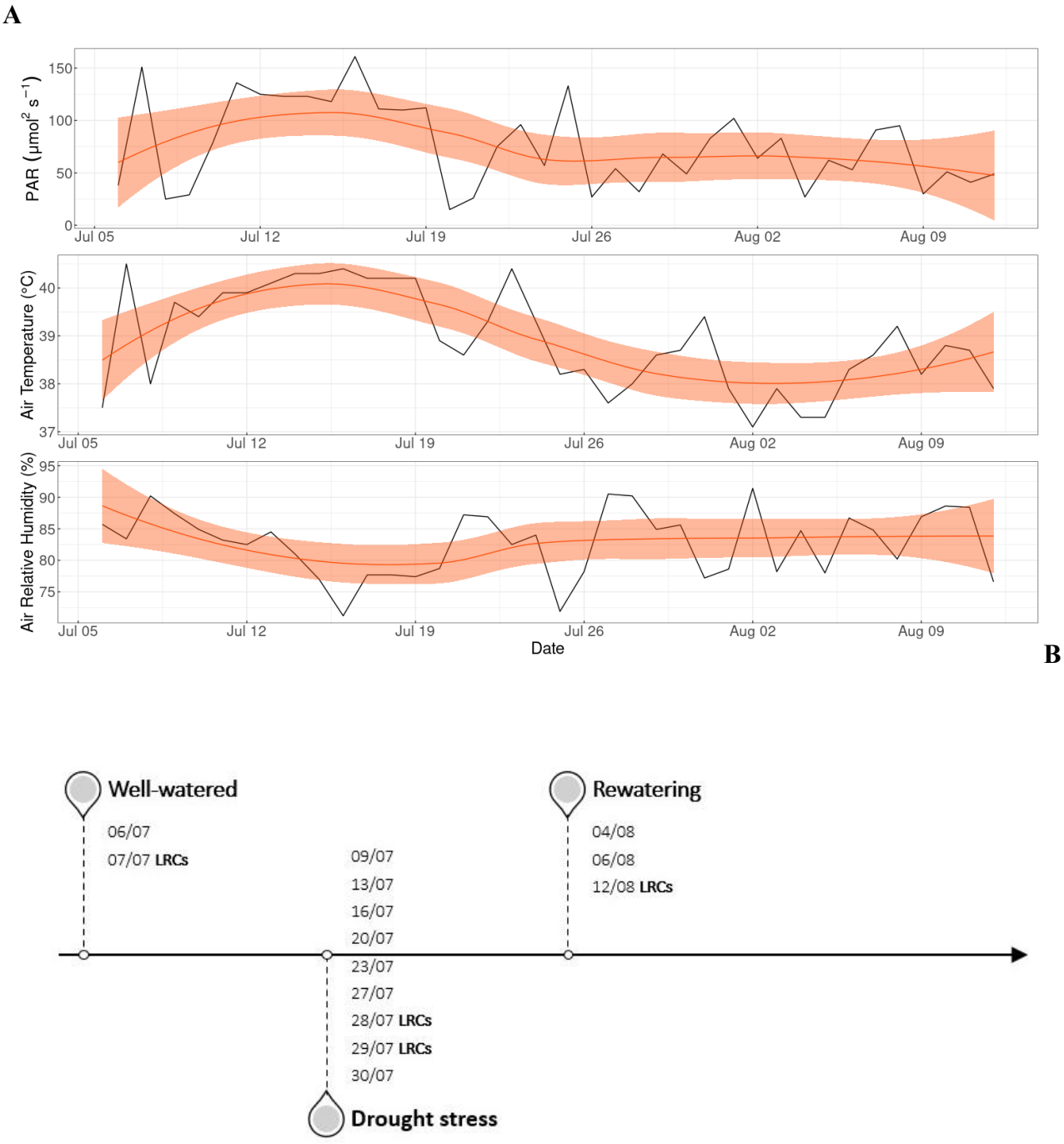

Figure 1. ***A****: Time course of experimental PAR (Photosynthetic Active Radiation), Air Temperature and Air Relative Humidity, measured daily at morning by greenhouse sensors. Smoothing line and 95% confidence interval are applied (orange line and shaded area, respectively).* ***B****: Experimental time windows (Well-watered, Drought stress and Rewatering) and sampling time points (dates); LRCs (Light Response Curves) measured on selected time points.*

Plant physiology measurements

Gas exchange measurements were performed using a LC-pro T IRGA (InfraRed Gas Analyser) device (ADC BioScientific ltd., Global House, Geddings Rd, Hoddesdon EN11 0NT, UK) at the following time points: 09/07, 13/07, 16/07, 20/07, 23/07, 27/07, 30/07, 04/08, 06/08 (2, 6, 9, 13, 16, 20, 23, 28 and 30 days since first withholding water). Needle-leaf area was measured with Easy Leaf Area software (Easlon and Bloom, 2014). Green and fully expanded twigs were selected, and then a photograph was taken with an iPhone SE camera and loaded onto the Easy Leaf Area dashboard. A white paper sheet with a reference red square of known area (3 x 3 cm) was used as a background. The estimated leaf area was recorded on the LC-pro T system and used to normalise gas exchange readings for every twig. Three twigs from each of four individual trees per family were sampled and the mean value was calculated. The IRGA operated in CO_2 ambient mode with a supplied air flowrate of 200 μmol s^{-1} and saturating PAR (see light response curves for saturating PAR estimation). A cylindrical conifer leaf chamber equipped with a LED white light was used, and complete insulation was achieved by applying a grease layer on the gasket and by sealing the chamber with tape to prevent air leakage. Three instant readings were recorded every 2-3 minutes after letting the twig acclimatising in the chamber – once sub-stomatal CO_2 and stomatal gas conductance had reached steady values. The following parameters were recorded: stomatal conductance of H_2O (g_s), leaf transpiration rate (E), instantaneous net leaf assimilation rate (A), sub-stomatal CO_2 (C_i), intrinsic water use efficiency (WUE_i) - calculated as the ratio of A/g_s - and instantaneous water use efficiency (WUE_{ins}) - calculated as the ratio of A/E.

Light response curves (LRCs) were obtained from a subset of three seedlings of each family at three time points: before starting the drought treatment (well-watered, 7th of July), at the end of the drought (drought, 28th and 29th of July), and after rewatering (rewatered, 12th of August). The same twigs of the same three seedlings from each breeding family were re-analysed at every time point. Data were collected by placing a single twig and in the conifer chamber letting it acclimatise at maximum PAR (1500 μmol m^{-2} s^{-1} - the chamber was wrapped in a black plastic sheet to minimise interference by environmental light). PAR was then reduced following a stepwise sequence: 1500, 1250, 1000, 800, 600, 400, 200, 150, 50, 30, 0 μmol m^{-2} s^{-1}; at intervals of 3 minutes and net photosynthetic assimilation (A) was recorded at each step. Light response curves were modelled by fitting a nonlinear least squares regression (non-rectangular hyperbola). Four parameters were estimated by the model: light saturated rate of photosynthesis (A_{sat}), dark respiration (R_d), apparent quantum yield (AQY), curvature parameter (theta). Light compensation point (LCP) and light saturation point (LSP) were obtained by

solving the model equation when A = 0 and 90% A_{sat} respectively. The highest light saturation points of each of the three seedlings from every family estimated for the well-watered subset of trees were used as saturating PAR in all subsequent IRGA measurements for trees belonging to the same family.

Volumetric soil water content (SWC) was measured in the pot of each seedling with a ML3 ThetaProbe soil moisture sensor (Delta-T devices) fully inserted below the soil line. Plant water status was assessed by measuring midday xylem water potential (MWP) between 11:00 and 14:00, using a Scholander-type pressure chamber (SKPM 1400/80**,** Skye instruments, Unit 21, Ddole Enterprise Park, Llandrindod Wells LD1 6DF). Three twigs from each individual tree were excised using a razor blade and immediately fitted in the chamber for measuring. Xylem sap extrusion was observed using a 10X illuminated magnifier. MWP readings from the 3 replicates were then averaged.

Tree height and diameter

Seedling growth was estimated on a subset of trees during the drought and recovery period by measuring stem height and diameter. Five seedlings per family were measured at each time point. Tree height was measured with a 2m metric ruler from the first node to the tip of the trunk. Stem diameter was measured with a 150mm digital calliper (0.01 mm resolution) at the first node next to the soil line.

Statistical analysis

All statistical analyses were performed in R environment. Data distribution and linear model residuals were checked for normality and homogeneity of variance using Shapiro-Wilk test and Bartlett test respectively. When linearity assumptions were violated, non-parametric Kruskal-Wallis test followed by post hoc Student's t-test were applied to compare means of photosynthesis parameters among species and breeding families, including both droughted and re-watered seedlings. One-sample ANOVA followed by Student's t-test were used to compare light response curves parameters. Comparisons of growth parameters between families were performed by ANOVA, while pairwise comparisons between first and last experimental day for each family were performed with T test. Relationships between plant water status (MWP), photosynthetic parameters (g_s, E, A, C_i, WUE_i, WUE_{ins}) and SWC are presented by fitting a simple linear regression or second order polynomial function, chosen accordingly to lowest significance p-value and highest r^2 coefficients. Time course of water status (MWP), photosynthetic parameters (g_s, E, A, C_i, WUE_i, WUE_{ins}) and SWC are

presented and multiple pairwise comparisons against a base-mean (all versus all) are computed using a Student's t-test. Correlation between tree water status and photosynthesis variables was assessed by applying a Spearman's correlation test. A PCA (Principal Component Analysis) was run on a scaled and standardised data matrix.

Results

The *P. sitchensis* and the hybrid *P. lutzii* seedlings exposed to drought for 25 days and rewatered remained healthy and increased their overall size over the course of the study. There were no significant differences in height and diameter between families at the beginning of the study nor were by the end of it (Supplementary figure 1 and supp. Table 1).

Changes in soil water content and water potential

The volumetric SWC progressively decreased with the drought for the duration of the experiment, from ≈ 50% to less than 10%. When rewatered at the end, pots showed a full recovery of SWC to pre-drought levels (Figure 2). The data indicated that the pot drying rate varied significantly between families, with some crossing the base-mean threshold later than others, such as families *Pl*700, indicating slower loss of water. Overall, pots reached below 30% SWC between 13 and 16 days after the start of the drought. MWP also decreased but to a lesser extent and did not show a clear trend across families relative to SWC. In fact, the average midday water potential changed less than expected, varying between –8 and –13 bars until rewatering, when an increase of 30-40% was observed compared to the initial values (Figure 2). Exceptions were noted in *Pl*701, *Pl*703 and *Ps*112, where a significant decrease in mean water potential was observed during the drought period, but it was not consistent for the entire duration of the experiment. In all cases a transient increase towards less negative water potential was observed after around 20 days of drought stress. g_s was relatively low when the first measurements were taken, being close to 0.1 mol m^{-2} s^{-1} and tended to further decrease between 13 and 23 days of drought stress. Changes in E were consistent with g_s, although the data were more variable, and differences were less significant. A clear increase in overall gas conductance was observed upon rewatering, up to 155% for family *Pl*700, although the increase was not significant compared to the base-mean value (Figure 2).

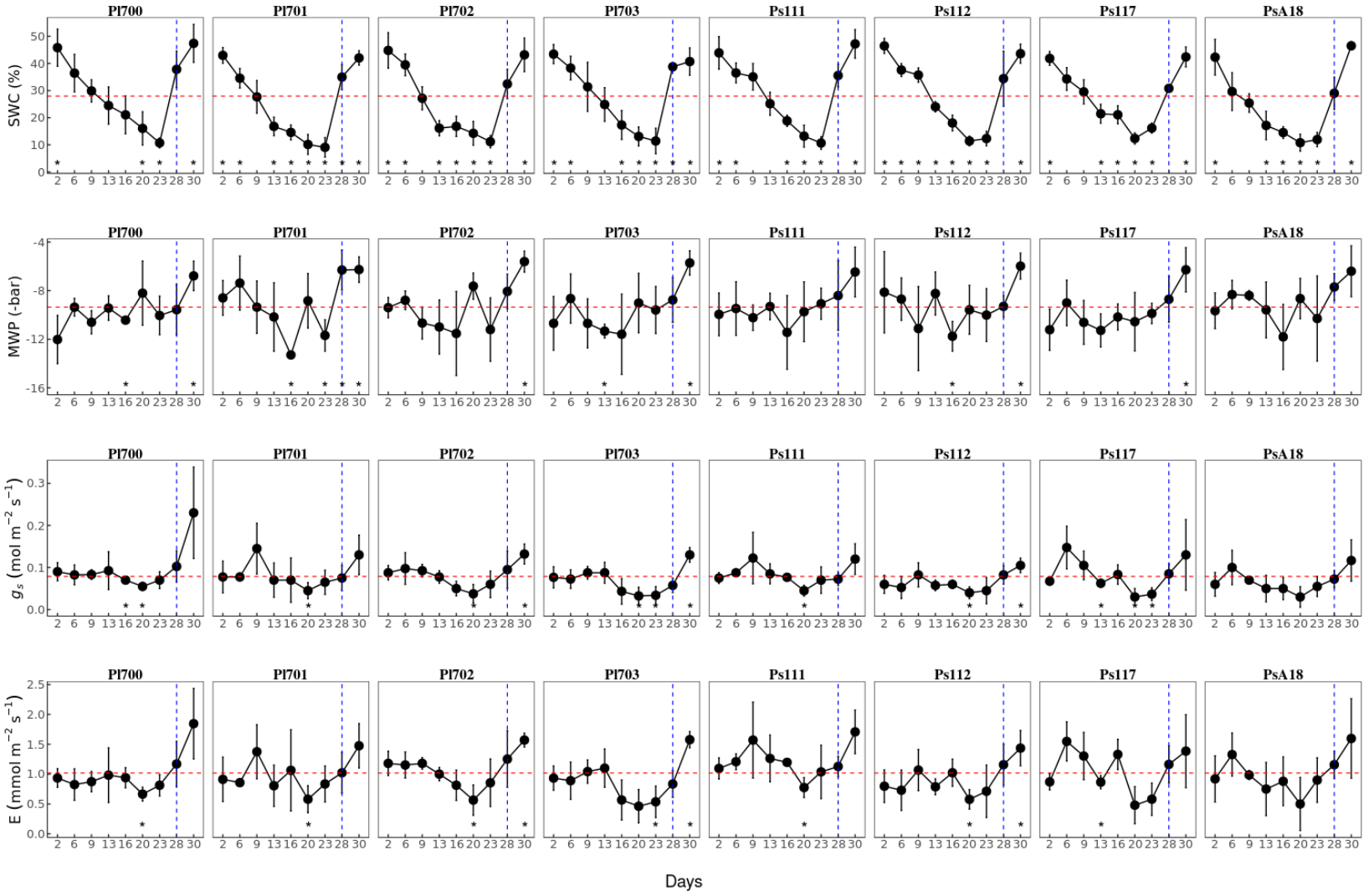

*Figure 2. Time course **SWC**, **MWP**, **g_s**) and **E** for P. sitchensis (Ps) and P. lutzii (Pl) upon drought treatment. Bars are standard deviation. Blue dashed line indicates beginning of rewatering, red dashed line indicates baseline mean of all values. **Days** = days from water withholding to rewatering. N = 4 per day, bars are standard deviations. Asterisks are significance p-values below 0.05 threshold.*

Determination of photosynthesis levels and water use efficiency

Mean *A* tended to increase slightly between day 9 and day 13 in all families up to ≈ 10 μmol m^{-2} s^{-1} before decreasing (Figure 3). Mean *A* decreases were significant in 3 of the *P. lutzii* families (*Pl*700, *Pl*702 and *Pl*703) and only between 20 and 23 days of drought stress. The increase in water availability after rewatering triggered a steep increase in photosynthetic carbon assimilation in all families to above 10 μmol m^{-2} s^{-1}. Although this change was significantly higher than base-mean only for families *Pl*701 and *Pl*702, it represented an increase of 50-120% compared to initial values for all families. Sub-stomatal CO_2 (C_i) showed a significant decrease only in families *Pl*701 and *Ps*117, and changes were consistently in the opposite direction compared to mean photosynthetic rate (Figure 3). WUE_i and WUE_{ins} followed similar trends and appeared to change in the opposite direction compared to ci. Mean water use efficiency increased transiently during drought treatment in families *Pl*701, *Pl*702 and *Ps*117 and most strikingly in family *Ps*A18. Family *Pl*701 showed ≈ 40-60% increases in WUE_{ins} at 13 and 23 days of drought, as well as after rewatering. *Pl*702 had a 50% increase in WUE_{ins} at 13 days only, while families *Ps*117 and *Ps*A18 increased their water use efficiency, but this was statistically significant only after rewatering.

The data indicated that *P. lutzii* had a significantly higher instantaneous water use efficiency compared to *P. sitchensis* (Kruskal-Wallis p-value < .05) (Table 2). There were significant differences in mean E, g_s and instantaneous water use efficiency (WUE_{ins}) between breeding families of both species across the entire duration of the drought and recovery experiment (Kruskal-Wallis p-value < .05, post hoc t-test p-value < .05) (Table 3). Mean instantaneous water use efficiency was highest in *Pl*700, *Pl*701 and *Ps*117 (6.31-7.50 μmol ~ $mmol^{-1}$) and was lowest in *Ps*111 and *Ps*A18 (5.50-5.68 μmol ~ $mmol^{-1}$). We found the highest mean E in *Ps*111, *Pl*702 and *Ps*117 (1.08-1.22 mmol m^{-2} s^{-1}) with *Ps*111 recording the highest mean E which was significantly different from all other families. The lowest mean E was found in *Ps*112 and *Pl*703 (0.86-0.92 mmol m-2 s-1). Gs to water vapour (gs) was highest in *Pl*700, *Ps*111 and *Pl*702 (0.08-0.1 mmol m^{-2} s^{-1}), while families *Pl*703 and *Ps*A18 had the lowest values (0.07 mmol m^{-2} s^{-1}). The other families showed a high degree of variability in their stomatal responses to experimental treatment.

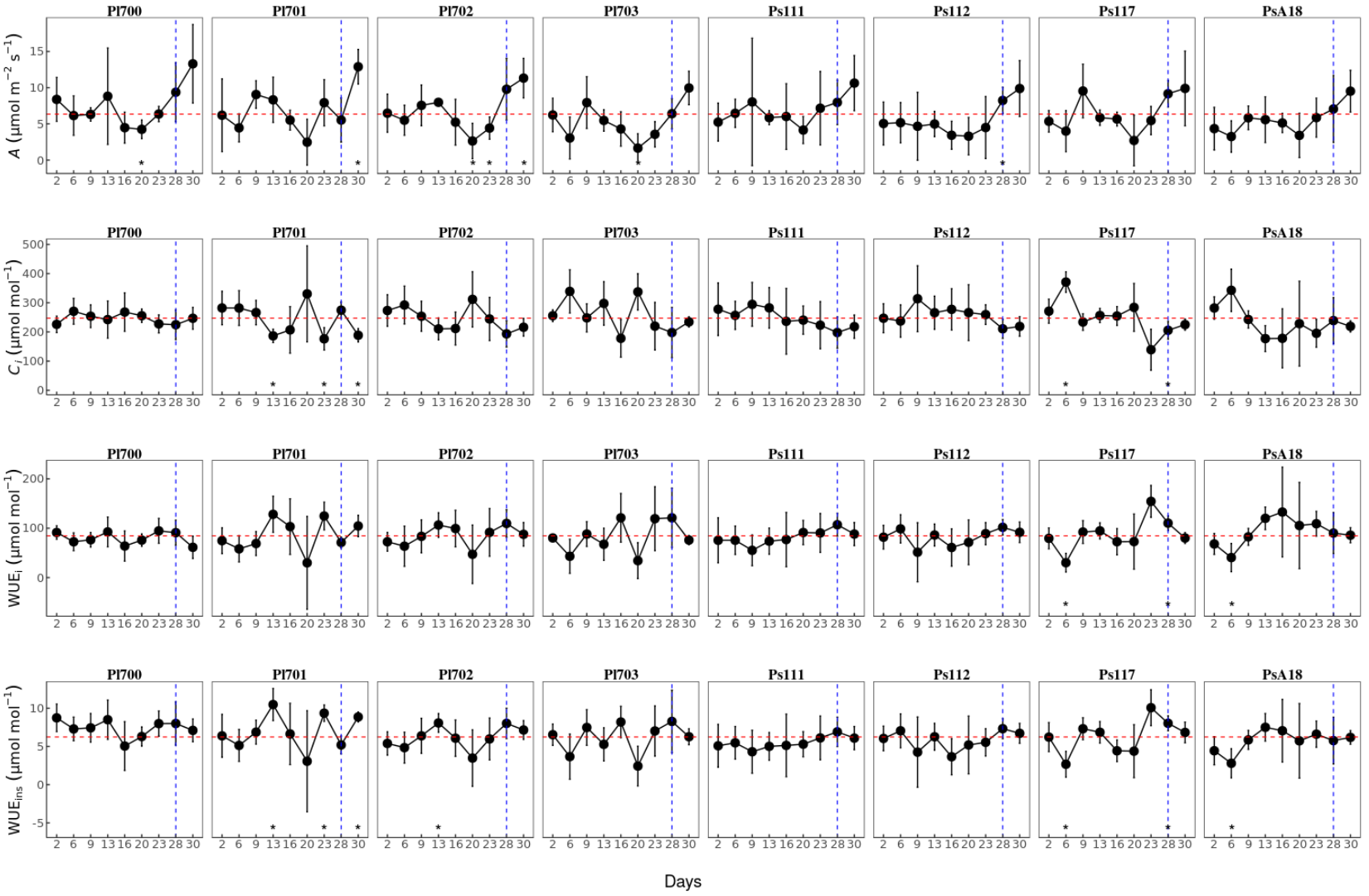

Figure 3. ***A*****,** ***C*****$_i$****,** ***WUE*****$_i$** *and* ***WUE*****$_{ins}$** *for P. sitchensis (Ps) and P. lutzii (Pl) upon drought treatment. Days = days from water withholding to rewatering. Bars are standard deviation. Blue dashed line indicates beginning of rewatering, red dashed line indicates baseline mean of all values. N = 4 per day, bars are standard deviations. Asterisks are significance p-values below 0.05 threshold.*

Table 2. Summary of non-parametric analysis of variance of P. lutzii (Picea lutzii) and P. sitchensis (Picea sitchensis) water status and photosynthesis parameters. ***MWP*** *(- bar),* g_s *(mol* m^{-2} s^{-1}*),* ***E*** *(mmol* m^{-2} s^{-1}*),* ***A*** *(µmol* m^{-2} s^{-1}*),* C_i *(µmol* mol^{-1}*),* WUE_i *(µmol* mol^{-1}*),* WUE_{ins} *(µmol* $mmol^{-1}$*). Mean = mean values, (SD) = Standard Deviation.*

Kruskal-Wallis test

Variable	N	*P. lutzii*, *n* = 138[1]	*P. sitchensis*, *n* = 139[1]	p-value[2]
MWP	275	-9.30 (2.41)	-9.27 (2.26)	>0.9
E	277	0.99 (0.41)	1.05 (0.43)	0.13
g_s	277	0.08 (0.05)	0.08 (0.04)	0.2
A	277	6.7 (3.8)	6.1 (3.6)	0.2
C_i	277	248 (69)	247 (71)	>0.9
WUE_i	277	84 (41)	85 (38)	0.6
WUE_{ins}	277	6.67 (2.83)	5.83 (2.50)	**0.005**

[1] Mean (SD)
[2] Kruskal-Wallis rank sum test

Table 3. Summary of non-parametric analysis of variance and post hoc multiple comparisons by Tukey test of P. lutzii (Picea lutzii) and P. sitchensis (Picea sitchensis) water status and photosynthesis parameters. ***MWP*** *(- bar),* g_s *(mol* m^{-2} s^{-1}*),* ***E*** *(mmol m-2 s-1),* ***A*** *(µmol* m^{-2} s^{-1}*),* C_i *(µmol* mol^{-1}*),* WUE_i *(µmol* mol^{-1}*),* WUE_{ins} *(µmol* $mmol^{-1}$*). Mean = mean values, (SD) = Standard Deviation. T test significant differences between groups are shown in compact letter display. Level of significance: p-value < 0.05.*

Kruskal-Wallis test

		P. lutzii				*P. sitchensis*				
Variable	**N**	*Pl700*, *n* = 32[1]	*Pl701*, *n* = 35[1]	*Pl702*, *n* = 36[1]	*Pl703*, *n* = 35[1]	*Ps111*, *n* = 35[1]	*Ps112*, *n* = 35[1]	*Ps117*, *n* = 34[1]	*PsA18*, *n* = 35[1]	**p-value**[2]
MWP	275	-9.51 (2.04)	-8.98 (2.72)	-9.16 (2.48)	-9.58 (2.38)	-9.28 (2.20)	-9.13 (2.49)	-9.70 (2.15)	-8.99 (2.21)	0.7
E	277	1.02 (0.45) **bc**	0.99 (0.42) **bc**	1.08 (0.37) **ab**	0.86 (0.39) **c**	1.22 (0.40) **a**	0.92 (0.37) **c**	1.08 (0.45) **abc**	0.99 (0.45) **bc**	**0.006**
g_s	277	0.10 (0.07) **a**	0.08 (0.05) **ab**	0.08 (0.04) **a**	0.07 (0.03) **b**	0.08 (0.03) **a**	0.07 (0.03) **b**	0.09 (0.05) **ab**	0.07 (0.04) **b**	**0.015**
A	277	7.7 (4.3)	7.0 (3.9)	6.9 (3.5)	5.3 (3.2)	6.9 (4.1)	5.5 (3.5)	6.6 (3.4)	5.4 (3.1)	0.13
C_i	277	245 (41)	245 (81)	245 (65)	255 (81)	248 (69)	254 (65)	251 (69)	237 (82)	>0.9
WUE_i	277	81 (22)	84 (49)	84 (38)	85 (49)	82 (33)	82 (33)	86 (37)	91 (48)	>0.9
WUE_{ins}	277	7.50 (2.01) **a**	6.89 (3.45) **ab**	6.18 (2.41) **bc**	6.17 (3.07) **bc**	5.50 (2.26) **c**	5.84 (2.51) **bc**	6.31 (2.55) **abc**	5.68 (2.69) **c**	**0.020**

[1] Mean (SD)
[2] Kruskal-Wallis rank sum test

Modelling relationships between physiological traits

We explored the relationships between gas exchange and plant water status variables by computing a correlation matrix (Figure 4 and 5). This showed that E and g_s were positively correlated with SWC across all families; however, MWP was not significantly correlated with SWC. *A* was highly correlated with E and g_s (Correlation coefficient ≈ 0.5-0.9) in most families (except Ps117, correlation coefficient ≈ 0.2). In contrast, *A* was not significantly correlated with MWP (p-value > 0.05) and gave low correlations with SWC in all families (≈ 0.2-0.4, but not significant for Ps117).

We observed higher and wider ranging correlations between *A* and water use efficiency in *P. sitchensis* compared to *P. lutzii*. Correlation between *A* and WUE_i was 0.3 - 0.5 in *P. lutzii*, compared to 0.3 - 0.8 in *P. sitchensis*. Similarly, the correlation between *A* and WUE_{ins} was 0.6 - 0.7 in *P. lutzii* and 0.5 - 0.8 in *P. sitchensis*. *A* was negatively correlated with C_i (Correlation coefficient ≈ 0.5-0.7), while C_i was negatively and highly correlated with water use efficiency (Correlation coefficient ≈ - 0.9). A PCA analysis of the above data across all families identified two principal components, the first explaining 47.5% of variability in the data and the second explaining 34.5% (Figure 6). Most of the variability along the main axis was driven by E and g_s, whereas MWP did not represent a major factor. Water use efficiency and C_i moved along the second axis, but in opposite directions, being inversely correlated. *A* positioned diagonally in between the main axes and represented a substantial portion of total variability. PCA analysis did not identify differences between study families.

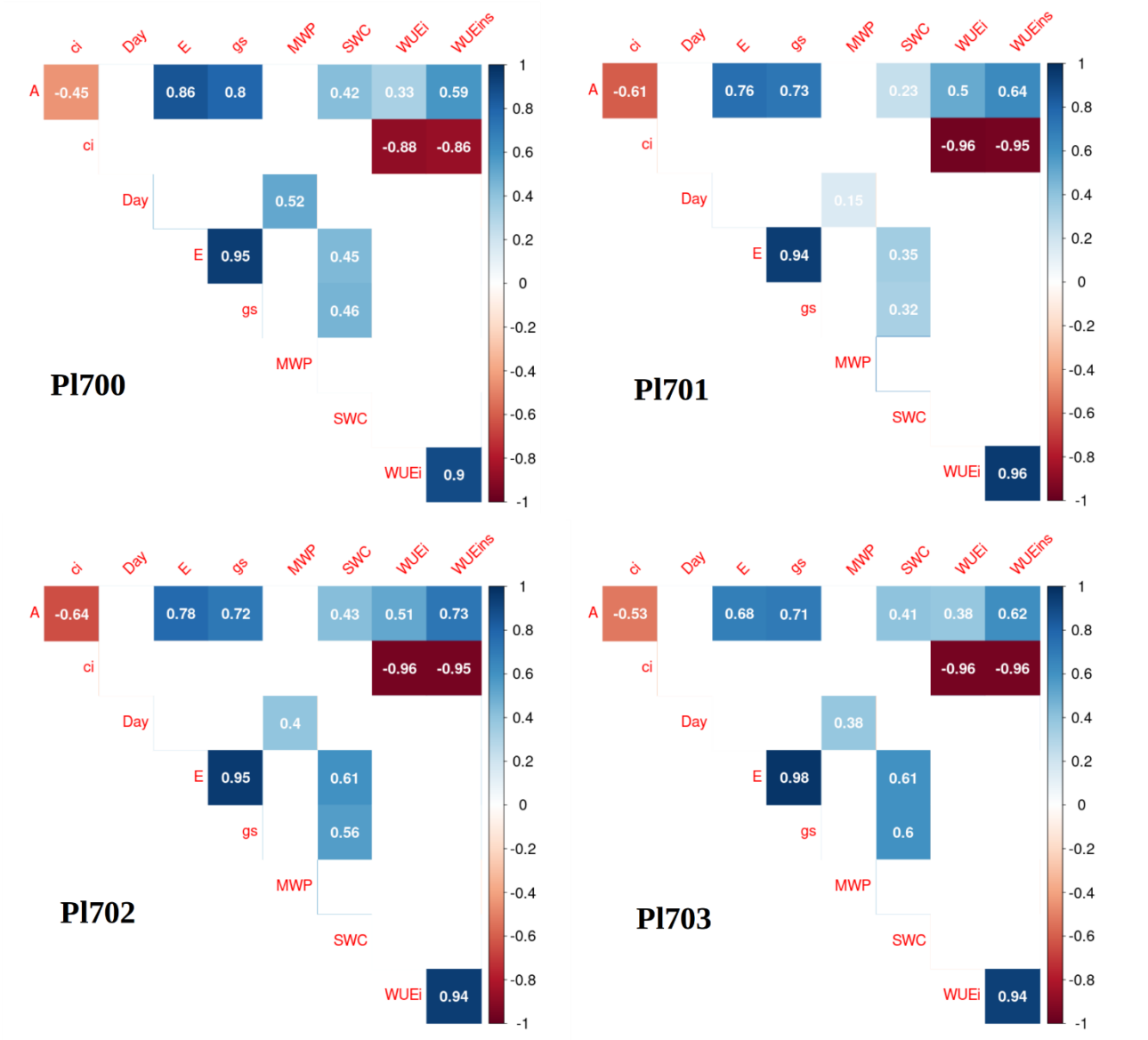

*Figure 4. Correlation matrix based on Spearman's correlation test for relationships between physiological responses following drought treatment in Picea lutzii hybrids. Colours indicate positive (**blue**) to negative (**red**) correlation. Correlation coefficients are shown in **white** inside each square. **Empty (white) squares** indicate absence of significant correlation (**p-value < 0.05**). N = 32-36.*

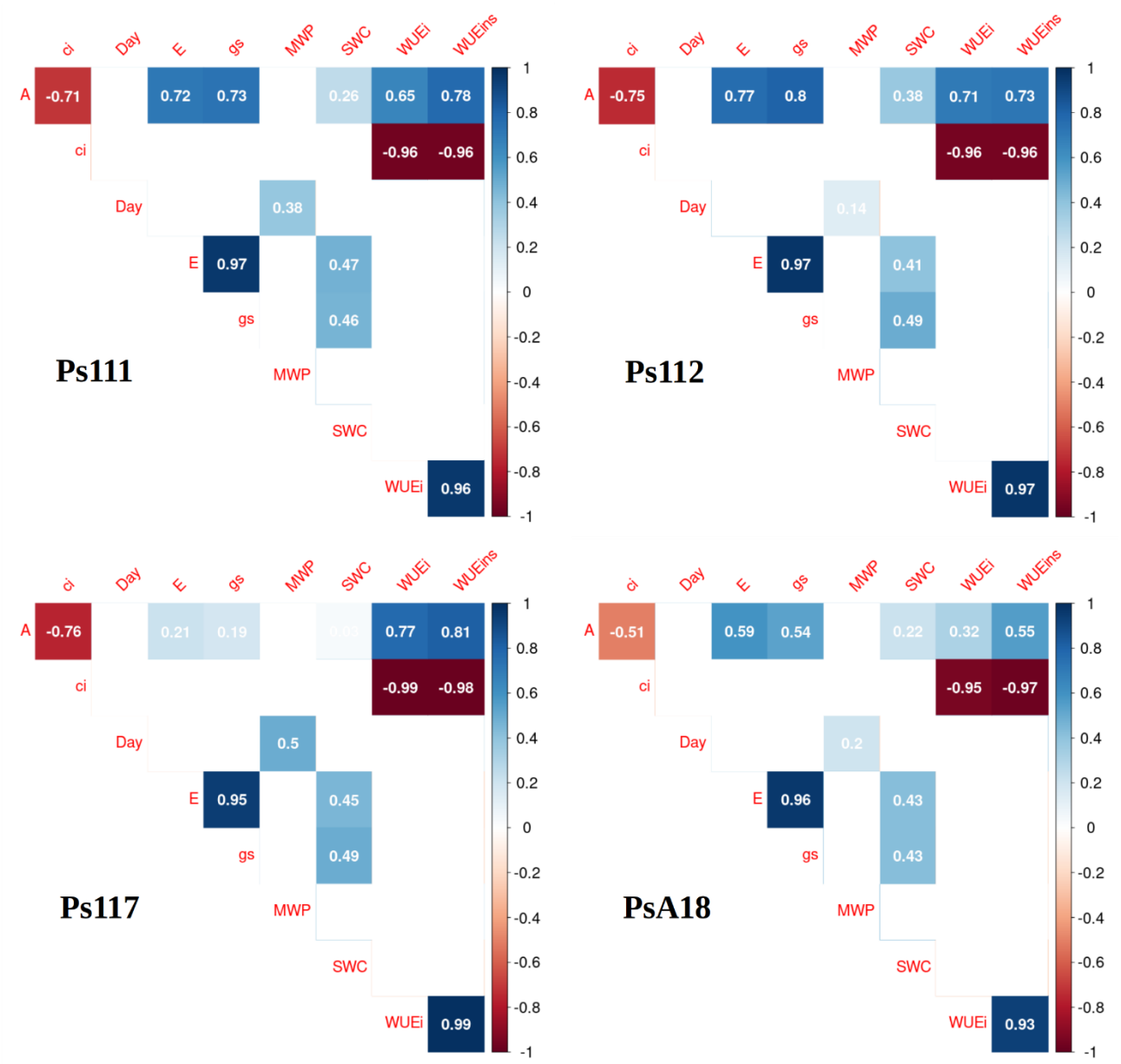

*Figure 5. Correlation matrix based on Spearman's correlation test for relationships between physiological responses following drought treatment in Picea sitchensis. Colours indicate positive (**blue**) to negative (**red**) correlation. Correlation coefficients are shown in **white** inside each square. **Empty (white) squares** indicate absence of significant correlation (**p-value < 0.05**). N = 32-36.*

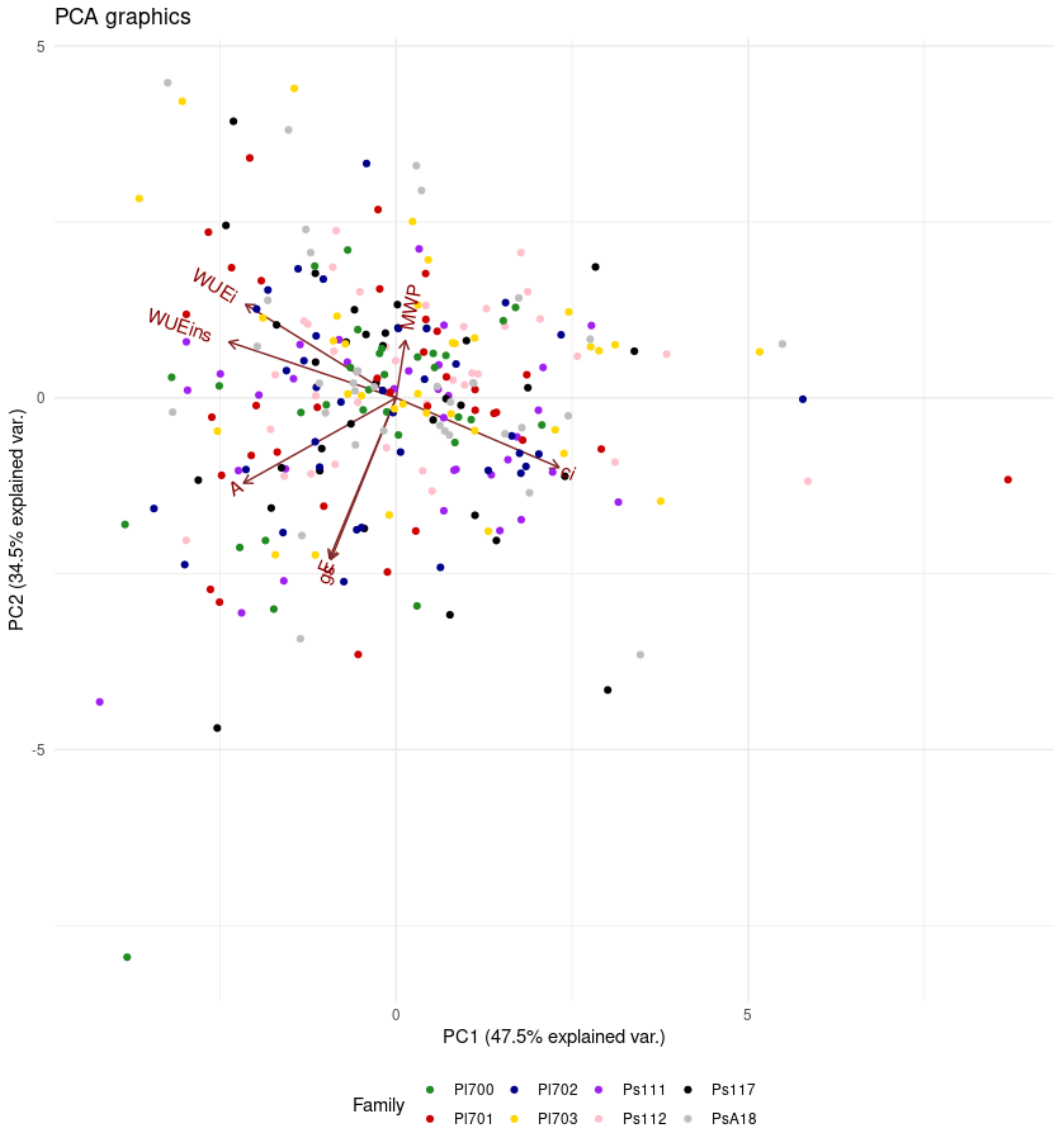

*Figure 6. Principal component analysis (**PCA**) of water status and photosynthesis parameters. All samples and families pooled together. Colours indicate different families. **PC1** = first principal component, **PC2** = second principal component. Ps: P. sitchensis; Pl: P. lutzii. N = 32-36.*

We modelled the relationship between soil volumetric water content (SWC) and key physiological parameters for each family, using quadratic functions (Figure 7). This showed that the relationship with water potential measured at midday (MWP) varied among families and was statistically significant only for *Pl*701 (p-value < 0.01) (Figure 7). Although the second order polynomial function explained only 27% of the total variance (r^2adj = 0.27), *Pl*701 did show a decreasing MWP in response to SWC. This relationship was not as obvious for the remaining families, where MWP did not show significant patterns in response to SWC. We did instead observe a higher level of significance for the relationship of E and g_s with SWC. Only two families – *Pl*700 and *Ps*112 – did not significantly respond to the decrease in SWC (p-value > 0.05). Photosynthetic assimilation trends were poorly explained by SWC, being significantly related only for *Pl*703 (p-value = 0.04).

Similar modelling was carried out with A, g_s and C_i for each of the families (Figure 8). The positive relationship between A and g_s did not show substantial deviations from linearity, although there was some variation among families, with family *Ps*117 showing the highest divergence (r^2adj = 0.22) (Figure 8, left side). A steep decline in photosynthetic A with decreasing g_s was apparent in all families. An increase in C_i was apparent in response to decreasing A. No significant relationship was found between g_s and C_i (Figure 8).

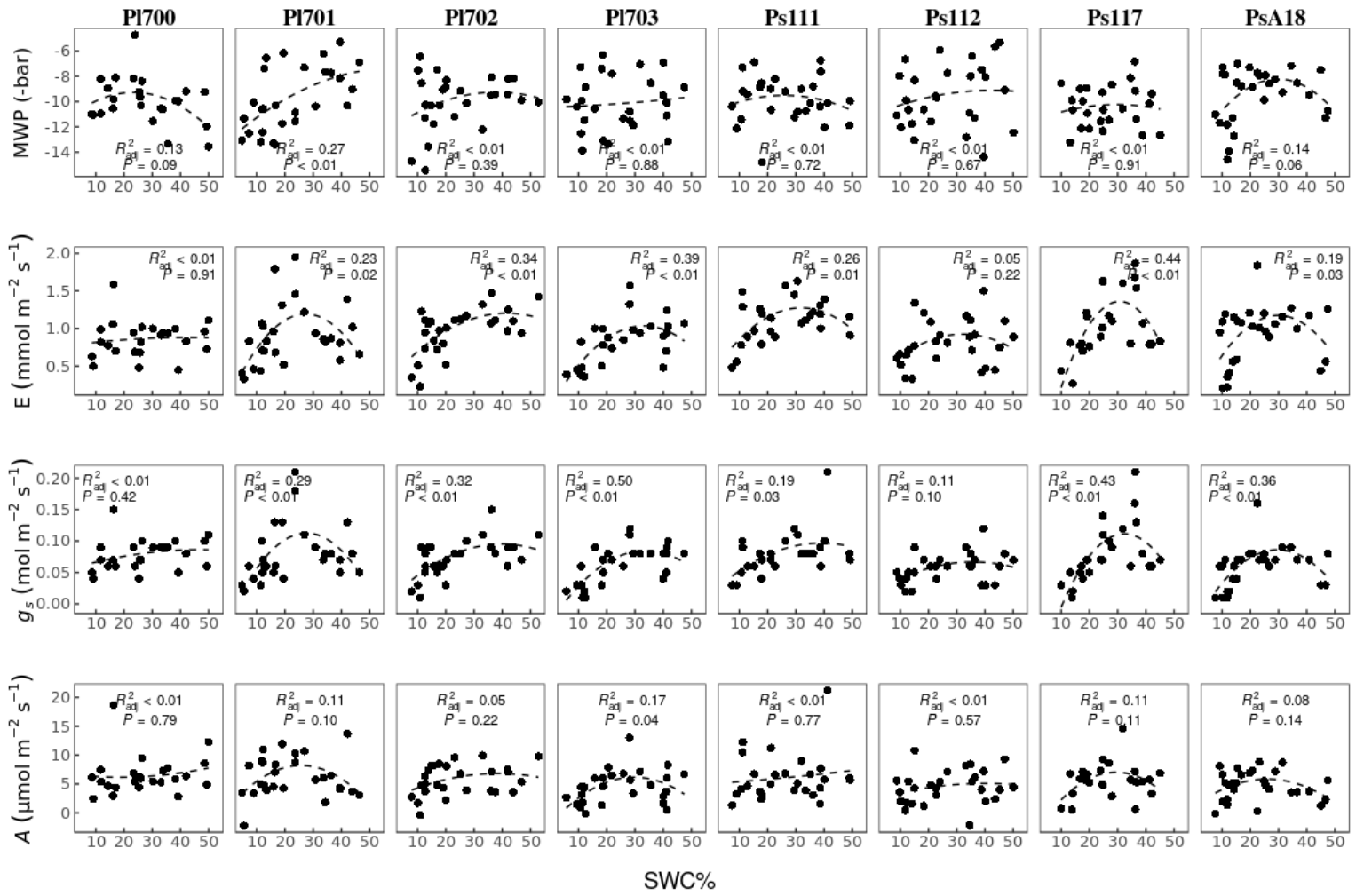

*Figure 7. Relationship between **SWC** and **MWP**, **g_s** and **E** and **A** for P. lutzii (**Pl**) and P. sitchensis (**Ps**) upon drought treatment. N = 32. Quadratic functions are represented by dashed lines. **R^2adj** = adjusted coefficient of determination, **P** = p-value. Only drought-stressed trees are included, while rewatered trees have been excluded, in order to display the shape of the correlation between progression of drought stress and relevant parameters.*

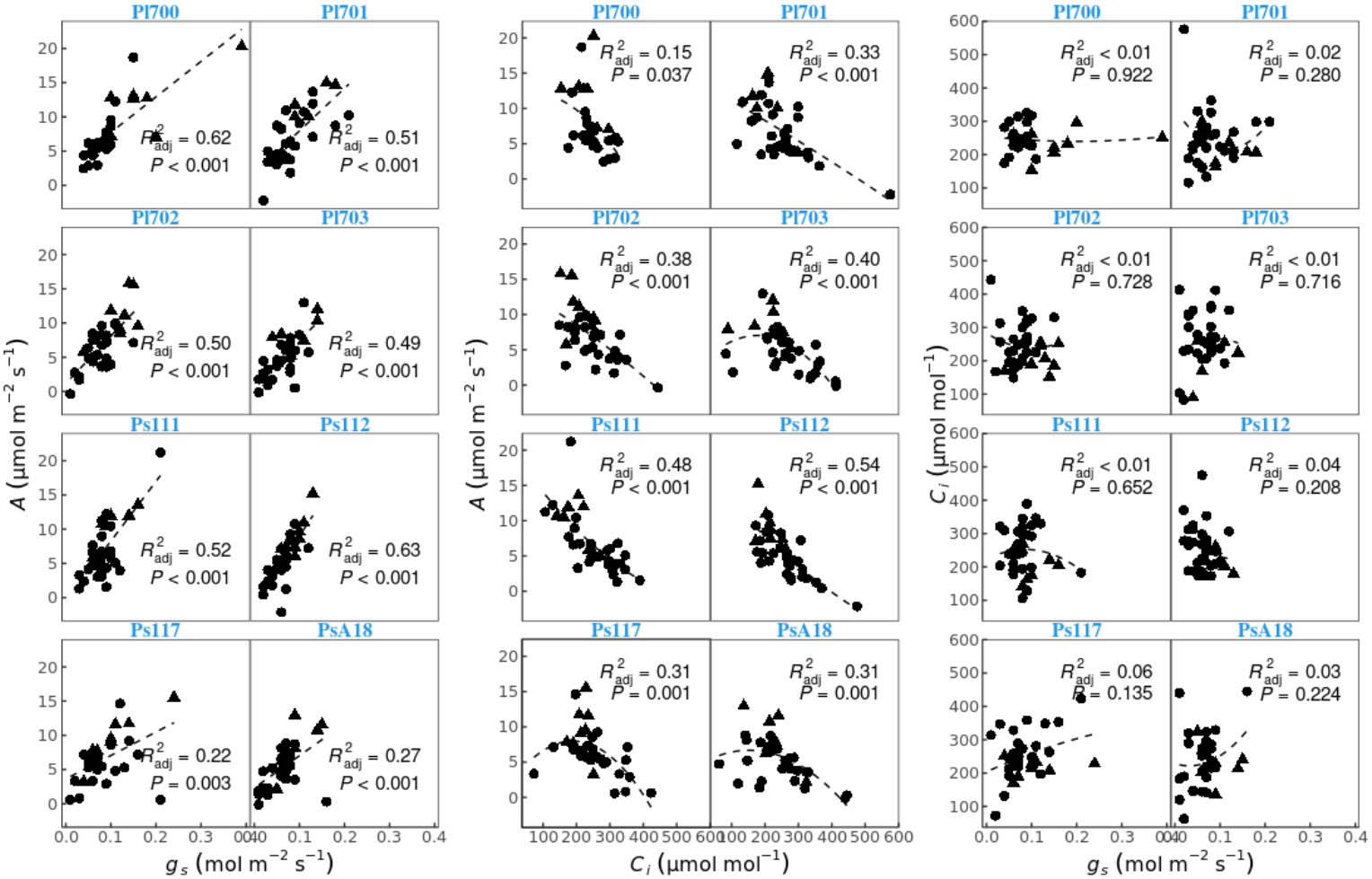

*Figure 8. Relationship between (**A**) net photosynthesis assimilation (A) and g_s, (**B**) net photosynthesis assimilation (A) and Ci and (**C**) g_s and C_i in P. sitchensis (Ps) and P. lutzii (Pl). Quadratic functions and ordinary least squares are represented by dashed lines. **R^2adj** = adjusted coefficient of determination, **P** = p-value. Samples from drought period (**circles**) and rewatering (**triangles**) included. N = 32-36.*

Light response curves

We developed light response curves (LRCs) before, during and after water deficit (Figure 1), to assess how the capacity and performance of the photosynthetic apparatus may change in response to drought stress and recovery. Analysis of the resulting LRCs identified key variables that significantly varied within and between families (Table 5 and 6) and at different time points, but not between species (Table 4).

Table 4. Summary of analysis of variance of P. lutzii and P. sitchensis light response curve parameters. ***LCP*** *(µmol* m^{-2} s^{-1}*),* ***LSP*** *(µmol* m^{-2} s^{-1}*),* $\boldsymbol{A_{sat}}$ *(µmol* m^{-2} s^{-1}*),* ***AQY*** *(mol* mol^{-1}*),* $\boldsymbol{R_d}$ *(µmol* m^{-2} s^{-1}*),* ***theta*** *(dimensionless). Level of significance: p-value < 0.05.* ***Mean*** *= mean values,* ***(SD)*** *= Standard Deviation.*

ANOVA

		Species		
Variable	**N**	*P. lutzii*, *n* = 36[1]	*P. sitchensis*, *n* = 36[1]	**p-value**[2]
LCP	70	26 (17)	29 (18)	0.4
LSP	70	764 (425)	727 (419)	0.7
A_{sat}	70	10.0 (4.8)	9.0 (4.9)	0.4
AQY	70	0.06 (0.06)	0.06 (0.04)	0.8
R_d	70	1.30 (0.84)	1.33 (0.69)	0.9
theta	70	0.60 (0.44)	0.60 (0.43)	>0.9

[1] Mean (SD)

[2] One-way ANOVA

The major changes in photosynthesis were observed in family *Pl*700 (Table 4). When looking for overall differences in mean values of LRC parameters, we observed variability in *A* at light saturation (A_{sat}) (ANOVA p-value = 0.031) and dark respiration (R_d) (ANOVA p-value = 0.002) among families. *Pl*700 showed the highest mean maximum photosynthetic rate with 14.6 µmol CO_2 m^{-2} s^{-1}, whereas *Pl*703 and PsA18 had the lowest (6.9 and 7 µmol CO_2 m^{-2} s^{-1} respectively) and all other families had intermediate values. We found the highest R_d in family *Pl*700 (1.99), followed by *Ps*117 (1.89). *Pl*702 had overall the lowest R_d (0.83). Here light compensation point (LCP, p-value < 0.001), light saturation point (LSP, p-value = 0.004) and light saturated rate of photosynthesis (A_{sat}, p-value = 0.034) showed an increase from well-watered to recovery, across drought stress. The light compensation point significantly increased after re-watering (41 µmol m^{-2} s^{-1}), light saturation point increased upon imposition of drought stress up to 1,045 µmol m^{-2} s^{-1} and 1,289 µmol m^{-2} s^{-1} after re-watering, while light saturated rate of photosynthesis constantly increased from the imposition of drought stress until re-watering from 10.68 to 18.65 µmol CO_2 m^{-2} s^{-1}. In family *Pl*701, light saturated rate of photosynthesis only changed significantly (p-value = 0.03) by increasing upon re-watering compared to the drought-stress period. Family *Pl*703 showed significant changes in apparent quantum yield (AQY) and curvature parameter (theta). Apparent quantum yield was not significantly affected by drought treatment but increased upon re-watering to higher levels compared to drought period (0.063, p-value = 0.044), while curvature parameter progressively moved from 0.86 at the well-watered time point to 0.51 after re-watering (p-value = 0.022). Family *Ps*A18 showed a steep increase in maximum photosynthetic rate upon rewatering, while drought period couldn't be accounted for as it was not possible to estimate LRCs parameters at this time point.

Table 5. Summary of analysis of variance and post hoc multiple comparisons by Tukey test of P. lutzii light response curve parameters. ***0*** *= Pre-drought,* ***1*** *= Drought,* ***2*** *= Rewatering.* ***LCP*** *(µmol* m^{-2} s^{-1}*),* ***LSP*** *(µmol* m^{-2} s^{-1}*),* $\boldsymbol{A_{sat}}$ *(µmol* m^{-2} s^{-1}*),* ***AQY*** *(mol* mol^{-1}*),* $\boldsymbol{R_d}$ *(µmol* m^{-2} s^{-1}*),* ***theta*** *(dimensionless). Significant differences between groups are shown in compact letter display. Level of significance:* ***p-value*** *< 0.05.* ***Mean*** *= mean values, (****SD****) = Standard Deviation.*

	Pl700					Pl701					Pl702					Pl703				
Variable	**N**	*0*, $n = 3$ [1]	*1*, $n = 3$ [1]	*2*, $n = 3$ [1]	**p-value** [2]	**N**	*0*, $n = 3$ [1]	*1*, $n = 3$ [1]	*2*, $n = 3$ [1]	**p-value** [2]	**N**	*0*, $n = 3$ [1]	*1*, $n = 3$ [1]	*2*, $n = 3$ [1]	**p-value** [2]	**N**	*0*, $n = 3$ [1]	*1*, $n = 3$ [1]	*2*, $n = 3$ [1]	**p-value** [2]
LCP	9	16 (1) **a**	21 (3) **a**	41 (4) **b**	**<0.001**	9	54 (9)	21 (20)	23 (15)	0.074	9	24 (10)	18 (8)	12 (8)	0.3	9	28 (21)	36 (27)	14 (11)	0.5
LSP	9	320 (20) **a**	1,045 **b** (330)	1,289 **b** (184)	**0.004**	9	735 (596)	741 (461)	884 (452)	>0.9	9	632 (223)	773 (439)	763 (511)	0.9	9	332 (337)	912 (66)	743 (656)	0.3
A_{sat}	9	10.68 **a** (1.90)	14.47 **ab** (4.13)	18.65 **b** (1.46)	**0.034**	9	7.8 (1.4) **ab**	5.4 (4.4) **a**	13.4 (1.4) **b**	**0.030**	9	9.20 (0.92)	8.67 (6.22)	10.90 (2.61)	0.8	9	6.2 (6.3)	5.8 (1.7)	8.7 (4.1)	0.7
AQY	9	0.11 (0.02)	0.16 (0.18)	0.06 (0.01)	0.5	9	0.047 (0.012)	0.027 (0.012)	0.080 (0.044)	0.12	9	0.053 (0.032)	0.040 (0.010)	0.067 (0.025)	0.5	9	0.040 **ab** (0.017)	0.027 **a** (0.006)	0.063 **b** (0.015)	**0.044**
R_d	9	1.67 (0.35)	2.02 (1.50)	2.28 (0.54)	0.7	9	2.03 (0.40)	0.69 (0.89)	1.44 (0.37)	0.089	9	1.13 (0.36)	0.71 (0.45)	0.65 (0.29)	0.3	9	1.36 (1.42)	0.76 (0.33)	0.79 (0.42)	0.7
theta	9	0.76 (0.02)	-0.01 (1.19)	0.67 (0.05)	0.4	9	0.36 (0.95)	0.68 (0.09)	0.58 (0.11)	0.8	9	0.75 (0.06)	0.70 (0.16)	0.64 (0.19)	0.7	9	0.86 **b** (0.07)	0.68 **ab** (0.07)	0.51 **a** (0.16)	**0.022**

[1] Mean (SD)

[2] One-way ANOVA

Table 6. Summary of analysis of variance and post hoc multiple comparisons by Tukey test of P. sitchensis light response curve parameters. ***0*** *= Pre-drought,* ***1*** *= Drought,* ***2*** *= Rewatering.* ***LCP*** *(µmol* m^{-2} s^{-1}*),* ***LSP*** *(µmol* m^{-2} s^{-1}*),* $\mathbf{A_{sat}}$ *(µmol* m^{-2} s^{-1}*),* ***AQY*** *(mol* mol^{-1}*),* $\mathbf{R_d}$ *(µmol* m^{-2} s^{-1}*),* ***theta*** *(dimensionless) Significant differences between groups are shown in compact letter display. Level of significance:* ***p-value*** *< 0.05.* ***Mean*** *= mean values, (****SD****) = Standard Deviation.*

	Ps111					Ps112					Ps117					PsA18				
Variable	**N**	*0*, *n* = 3 [1]	*1*, *n* = 3 [1]	*2*, *n* = 3 [1]	**p-value** [2]	**N**	*0*, *n* = 3 [1]	*1*, *n* = 3 [1]	*2*, *n* = 3 [1]	**p-value** [2]	**N**	*0*, *n* = 3 [1]	*1*, *n* = 3 [1]	*2*, *n* = 3 [1]	**p-value** [2]	**N**	*0*, *n* = 3 [1]	*1*, *n* = 3 [1]	*2*, *n* = 3 [1]	**p-value** [2]
LCP	9	45 (8) [b]	11 (10) [a]	12 (10) [a]	**0.007**	9	33 (13)	25 (10)	19 (24)	0.6	9	45 (28)	37 (22)	42 (20)	>0.9	7	31 (5)	9 (NA)	30 (16)	0.4
LSP	9	885 (316)	1,126 (214)	682 (454)	0.3	9	419 (359)	612 (398)	421 (341)	0.8	9	565 (388)	622 (394)	1,230 (367)	0.14	7	502 (623)	529 (NA)	996 (289)	0.5
A_{sat}	9	7.5 (1.8)	8.0 (4.7)	13.4 (6.5)	0.3	9	8.53 (2.56)	7.05 (3.81)	11.84 (1.39)	0.2	9	6.2 (3.4)	6.4 (3.9)	17.1 (6.7)	0.055	7	3.92 (1.77) [a]	3.24 (NA)	11.33 [b] (1.00)	**0.006**
AQY	9	0.03 (0.00)	0.05 (0.04)	0.11 (0.07)	0.2	9	0.057 (0.015)	0.043 (0.012)	0.100 (0.053)	0.2	9	0.057 (0.035)	0.043 (0.021)	0.073 (0.040)	0.6	7	0.040 (0.010)	0.080 (NA)	0.057 (0.029)	0.4
R_d	9	1.42 (0.24)	0.64 (0.55)	0.75 (0.22)	0.084	9	1.62 (0.45)	0.99 (0.21)	1.12 (0.76)	0.4	9	1.75 (0.43)	1.56 (1.28)	2.38 (0.49)	0.5	7	1.13 (0.14)	0.55 (NA)	1.50 (0.76)	0.4
theta	9	0.68 (0.23)	-0.17 (1.08)	0.64 (0.09)	0.3	9	0.86 (0.15)	0.70 (0.16)	0.81 (0.05)	0.4	9	0.76 (0.15)	0.72 (0.16)	0.55 (0.07)	0.2	7	0.67 (0.47)	-0.17 (NA)	0.61 (0.15)	0.2

[1] Mean (SD)

[2] One-way ANOVA

Discussion

In this study we assessed the degree of variation in water status and gas exchange dynamics between two species of conifers in the Pinaceae, *P. sitchensis* and its hybrid *P. lutzii* - and their full-sibling breeding families. We did this by imposing an artificial and acute drought stress on potted young seedlings under semi-controlled conditions and by monitoring their responses throughout several weeks, from optimal SWC, through soil water deficit, to rewatering. Both species adopted a conservative water regulation strategy, and the main source of variability was found in g_s and E. Water and gas exchange parameters recovered to higher levels than pre-stress, as a probable mechanism of compensation over drought stress. The photosynthetic apparatus didn't seem to be largely affected by stress. In fact, *P. lutzii* showed signs of resistance under drought conditions, while *P. sitchensis* appeared tolerant. WUE_{ins} was slightly higher in *P. lutzii* compared to *P. sitchensis*.

Changes in soil water content and water potential

SWC drastically decreased from full capacity to less than 10% in all measured pots (Figure 2 and 7). Despite this, we did not observe a consistent reduction in MWP. In fact, MWP was rather stable in all families for the entire duration of the experiment, although variable among measured time points (Figure 2). Some families displayed a more consistent decrease in MWP with increasing soil water deficit, especially *Pl*701, *Pl*703 and *Ps*112. Nevertheless, the change in MWP was small and breeding families didn't differ in mean water status, nor did correlation analysis find any significant links between SWC and MWP (Figure 4 and 5). These results agree with studies on conifer responses to drought showing that members of the Pinaceae such as *Picea spp*. can be very conservative in terms of leaf water status dynamics under drought conditions [28–34]. *Pl*701 was the only family to show an almost linear decrease of MWP with SWC (p-value < 0.01, $R^2_{adj} = 0.27$), which we interpret as a less conservative response to drought stress (Figure 7). *Ps*A18 didn't show a significant response to decreasing SWC (p-value < 0.06, $R^2_{adj} = 0.14$), but together with *Pl*702 appeared to have less of a conservative control over MWP as well. These three families may therefore be the less sensitive to drought conditions among the others, in terms of leaf water status.

Plant stress-physiology and gas exchange

MWP appeared to be decoupled from gas exchange. This was indicated by the lack of relationship between the levels of gas exchange and changes in MWP during soil drying (Figure 7). In fact, our correlation analysis did not show any significant result for both g_s and E in relation to MWP (Figure 4 and 5). This is coherent with the argument that tight stomatal control under limiting water soil conditions is not necessarily associated with conservative regulation of leaf water potential [35], as we have observed previously in Chapter 1 of this work, and that other factors may influence water status and ultimately determine tree death under drought (hydraulic architecture, rooting system). This seems to be the case for family *Pl*700, where maintenance of g_s does not result in a drop of MWP (Figure 7). In contrast, *Ps*117 closed stomata quickly and maintained a rather steady MWP. Overall, g_s and E declined with drought progression in most families (Figure 2 and 7), being significantly correlated with SWC, and were among the main drivers of variation in our experimental dataset, according to PCA (Figure 8). Non-parametric analysis of variance identified significant differences in mean g_s and E between families (Table 3), but not between species (Table 4). *Ps*111, *Pl*702 and *Pl*700 were the families losing more water through their stomata, as indicated by the highest mean rates of gas exchange, while *Ps*A18 had the lowest g_s. The relationship between decreasing SWC and conductance to water vapour was quadratic and significant in all families except for *Pl*700 and *Ps*112 (Figure 7). The parabola suggested a 20-30% SWC response threshold in the seedlings. Other studies have found similar SWC thresholds, where ≈ 20% SWC limits water availability for the plant and triggers physiological responses [36,37]. We found stricter stomatal control, as described by the goodness of fit of the quadratic function and the degree of its curvature, in families *Ps*117, *Pl*703, *Pl*702. In contrast, *Pl*700 didn't appear to be affected by SWC depletion, the almost flat slope of g_s and E indicating loose stomatal control.

MWP was not significantly correlated with *A* (Figure 4 and 5). On the other hand, SWC was correlated with *A* and this relationship was slightly stronger for *P. lutzii* compared to *P. sitchensis*. The time-course of leaf-level assimilation saw a transient increase between the first and second week of water deficit (Figure 2), possibly due to an increase in solar irradiance or the high temperature inside the greenhouse [38]. Afterwards, *A* decreased and recovered only after rewatering. All families seemed to operate around the same level of mean photosynthetic *A* as there were no significant differences (Table 3). The change in photosynthetic *assimilation rate* was highly correlated with water vapor conductance (Figure 8) and the concomitant decrease in g_s and *A* indicated stomatal limitations over photosynthetic carbon assimilation in all families [39–44]. Hence, photosynthesis depended on CO_2

diffusive resistance rather than on leaf water status [45,46]. We in fact observed an inverse relationship between photosynthetic A and C_i, with the latter decreasing as the rate of net photosynthesis increased (Figure 8). It has been shown that non-stomatal limitations intervene in the advanced stages of drought, when g_s decreases past a threshold of around 0.05 mol m^{-2} s^{-1} and eventually leads to photosynthesis failure [47,48]. In our study mean g_s was above that limit, pointing again at a probable stomatal limitation over net photosynthetic rate under our experimental conditions. However, the lack of any clear link between stomatal opening and sub-stomatal CO_2 represents a confounding factor. Therefore, we can't rule out a simple co-regulation of A vs g_s and an effect of non-stomatal limitations of photosynthesis (i.e. a direct effect of stress factors on photosynthesis reactions), as these would contribute to increasing C_i, versus the decrease driven by limited gas exchange and net photosynthesis [40,49–51].

High growth temperatures can affect both stomatal behavior and photosynthesis biochemistry [52]. Stomatal responses vary between species and are still debated [52]. A recent study found that a combination of heat and drought can induce a strong response leading to stomata aperture and loss of water in broadleaf, evergreen isohydric species [53]. We did not observe such dramatic increments in gas exchange in our conifer species. Acclimation of leaf photosynthetic biochemistry to high growth temperatures can intervene, imposing non-stomatal limitations on photosynthesis and reducing its efficiency [54–56]. However, this acclimation response may depend on plant species and functional types, as it has been observed that evergreen woody plants (such as *P. sitchensis*) have greater temperature photosynthetic homeostasis, showing limited changes of photosynthetic rates to increasing growth temperatures [38].

Light response curves

We examined the changes in light use efficiency at key time points as extrapolated from the photosynthetic light response curves (A/PAR) to assess the potential for metabolic damage to the photosynthetic apparatus. This highlighted differences between *P. sitchensis* and *P. lutzii*.

In *P. sitchensis*, the photosynthetic function was largely unaffected by drought stress. Drought can impact the photosynthetic machinery, causing a reduction in maximum photosynthetic rate (A_{sat}), apparent quantum yield (AQY), light saturation point (LSP) and light compensation point (LCP) [57–60]. Analysis of variance showed only a significant increase in maximum photosynthetic rate (A_{sat}) between pre-stress and recovery time points of *Ps*A18 and a nearly significant increase in maximum

photosynthetic rate between the same time points of *Ps*117 (Table 4 and 5). These were large increments in maximum photosynthetic rate in all *P. sitchensis* families upon rewatering compared to starting levels, although non-significant. This, together with the visible but not significant increase in apparent quantum yield and decrease in light compensation point at the rewatering compared to pre-drought time point of all families, could suggest that an acclimation mechanism to limiting conditions other than SWC took place at the beginning of our experiment and rewatering re-established optimal conditions. This could be due to transient acclimation to the elevated temperatures that trees experienced in the greenhouse [38,61–63], which then enhanced photosynthetic functions under non-limiting water conditions [55]. Post-drought overcompensation effects have been found in angiosperm plant systems subject to episodic drought treatments, where rewatering elicited growth and photosynthetic recovery above pre-stress levels [60,64–66].

In contrast, *P. lutzii* had significant changes in photosynthesis biochemistry, that altogether point at a greater resistance to adverse conditions (Table 4 and 6). Families *Pl*700, *Pl*701 and *Pl*702 showed signs of resistance. *Pl*702 was the only Lutz family that was not significantly affected by drought treatment. *Pl*700 increased both light compensation point after rewatering and light saturation point during the drought stress period, indicating a progressive improvement in the use of high photosynthetic light intensity in the time between drought stress and rewatering. Maximum photosynthetic rate (A_{sat}) also increased, both in *Pl*700 and *Pl*701, meaning an improved photosynthetic efficiency under drought stress. Instead, *Pl*703 significantly increased its apparent quantum yield and decreased R_d upon rewatering, which could be interpreted as a sign of improved photochemical capacity and resilience to drought stress.

Water use efficiency under drought and recovery

The ratio between net photosynthetic assimilation and gas conductance represents the water use efficiency (WUE) of the plant at the leaf level. A better mechanistic understanding of plant water use is required to improve crop production [67]; however, the opportunity of including water use efficiency as a trait in tree breeding programs is highly debated and no conclusive evidence has emerged that points at either a decrease [68,69] or increase in tree growth [70–72]. We looked at dynamic changes in water use efficiency by calculating WUE_i (A/g_s) and WUE_{ins} (A/E) for the duration of the experiment. Previous studies have found a positive correlation between water use efficiency - or its proxies - and biomass production [73,74]. Positive correlation of water use efficiency and A, but not g_s nor E (Figure 3 and 4), indicated that increased water use efficiency possibly depended on net photosynthetic gain

increases at relatively constant gas conductance, with possible beneficial effects on biomass production [75,76].

The relationship between water use efficiency and leaf gas exchange parameters had a best fit with a quadratic model, suggesting that no further increments in water use efficiency could be expected once a certain assimilation threshold is passed (Supplementary figure 3 and 4). WUE_{ins} showed significant and opposite changes when compared to the C_i time course. There was a strong and inverse linear relationship between the water use efficiency responses to C_i, with the former decreasing at elevated C_i concentration. A negative correlation between water use efficiency and C_i has previously been modelled and experimentally observed [77,78]. Therefore, C_i could be a good predictor of leaf-level water use efficiency for our study species. When looking at the time course of developing water use efficiency, we did not identify a consistent growth pattern in response to the drought treatment, except for family *Ps*A18, which nevertheless was not significant. A difference emerged between the two species indicating that *P. lutzii* had a slightly higher mean WUE_{ins} compared to *P. sitchensis* (Table 4).

Differences in whole plant water use efficiency and its proxies have been observed in different provenances of *Larix occidentalis* [79]. Here, we found that full-sibling families of Lutz and *P. sitchensis* differed in WUE_{ins} (Table 3). *Pl*700 and *Pl*701 had the highest water use efficiency, while *Ps*111 and *Ps*A18 had the lowest. It appears that a combination of low E and relatively high net photosynthetic rate produced the WUE_{ins} trends we observed in *P. lutzii* families. In contrast, higher transpiration rates did not necessarily translate into higher *A* in *P. sitchensis* families, relegating them to the lower part of the WUE_{ins} spectrum. This could provide additional information for genetic selection of high or low water use efficiency families in the future, whether the target will be more efficient use of water, reduced transpiration, or higher transpiration rates. We didn't find any difference in growth rate as estimated by height and diameter between families (Table 6, Figures 9 and 10), but the evidence we collected suggests *P. lutzii Pl*700 could be the best performing family under our experimental conditions, from the point of view of photochemistry, as indicated by water status, gas exchange measurements, WUE_{ins} and photosynthetic apparatus efficiency.

Conclusions

In this study we assessed variation in physiological responses to a short-term water deficit in full-sibling families of *P. sitchensis* and *P. lutzii* to gain insights into resilience to acute seasonal drought events. We compared water status, gas exchange and photosynthesis performance proxies in potted seedlings. We found significant differences in gas exchange regulation, but these were not necessarily related to water status as observed by midday water potential measurements. Net photosynthetic rate at light saturation was affected by drought stress and led to differences in intrinsic water use efficiency between families and species when combined with transpiration rates, where *P. lutzii* slightly outperformed *P. sitchensis*. No damage to the photosynthetic apparatus was detected and all trees recovered to even higher levels of gas exchange and water potential compared to the beginning of the experiment, indicating possible acclimation mechanisms.

Literature cited

1. Forest Research. Forestry Statistics 2022: A compendium of statistics about woodland, forestry and primary wood processing in the United Kingdom.
2. Cameron AD. Building Resilience into Sitka Spruce (*Picea sitchensis* (Bong.) Carr.) Forests in Scotland in Response to the Threat of Climate Change. *Forests.* 2015;6(2):398-415. doi:10.3390/F6020398
3. Ray D. Impacts of climate change on forestry in Scotland – a synopsis of spatial modelling research. January 2008. ISBN: 978-0-85538-747-1. ISSN: 1756-5758
4. Brown I. Natural environment and natural assets UK Climate Change Risk Assessment 2017 Evidence Report. Chapter 3: Natural environment and natural assets.
5. Locatelli T, Beauchamp K, Perks M, et al. Drought risk in Scottish forests: 1 Executive summary. February 2021. doi:10.7488/era/1292
6. Kennedy-Asser AT, Andrews O, Mitchell DM, Warren RF. Evaluating heat extremes in the UK Climate Projections (UKCP18). *Environmental Research Letters*. 2021;16(1):014039. doi:10.1088/1748-9326/ABC4AD
7. Kendon M, McCarthy M, Jevrejeva S, et al. State of the UK Climate 2021. *International Journal of Climatology*. 2022;42(S1):1-80. doi:10.1002/JOC.7787
8. Spencer JW. Forest resilience in British forests, woods & plantations - the ecological components. *Quarterly Journal of Forestry*. 2018;112(1):53-61.

9. Tew E., Rob Coventry, Emily Fensom and Chris Sorensen. Forest Resilience, Part 2. Practical considerations. *Quarterly Journal of Forestry*. July 2021 Vol 115 No.3
10. Jackson GE, Irvine J, Grace J. Xylem cavitation in Scots pine and Sitka spruce saplings during water stress. *Tree Physiology*. 1995;15(12):783-790. doi:10.1093/TREEPHYS/15.12.783
11. Huang W, Fonti P, Larsen JB, et al. Projecting tree-growth responses into future climate: A study case from a Danish-wide common garden. *Agricultural and Forest Meteorology*. 2017;247:240-251. doi:10.1016/J.AGRFORMET.2017.07.016
12. Grant OM, O'Reilly C. Impact of genetic variation and long-term limited water availability on the ecophysiology of young Sitka spruce (*Picea sitchensis* (Bong.) Carr.). *Tree Physiology*. 2017;37(4):536-549. doi:10.1093/TREEPHYS/TPW093
13. Ovenden TS, Perks MP, Forrester DI, et al. Intimate mixtures of Scots pine and Sitka spruce do not increase resilience to spring drought. *Forest Ecology and Management*. 2022;521:120448. doi:10.1016/J.FORECO.2022.120448
14. Davies S, Bathgate S, Petr M, Gale A, Patenaude G, Perks M. Drought risk to timber production – A risk versus return comparison of commercial conifer species in Scotland. *Forest Policy and Economics*. 2020;117:102189. doi:10.1016/J.FORPOL.2020.102189
15. Committee on Climate Change. Net Zero The UK's contribution to stopping global warming. May 2019.
16. Mason WL, Petr M, Bathgate S. Silvicultural strategies for adapting planted forests to climate change: from theory to practice. *Journal of Forest Science*;58(6):265-277. doi:10.17221/105/2011-JFS
17. Jactel H, Bauhus J, Boberg J, et al. Tree Diversity Drives Forest Stand Resistance to Natural Disturbances. *Current Forestry Reports;*3, 223–243 (2017). doi:10.1007/s40725-017-0064-1
18. Anderegg WRL, Konings AG, Trugman AT, et al. Hydraulic diversity of forests regulates ecosystem resilience during drought. *Nature.* 2018;561(7724):538-541. doi:10.1038/s41586-018-0539-7
19. Schnabel F, Liu X, Kunz M, et al. Species richness stabilizes productivity via asynchrony and drought-tolerance diversity in a large-scale tree biodiversity experiment. *Science Advances*. 2021;7(51):1643. doi:10.1126/SCIADV.ABK1643
20. Fletcher AM, Faulkner R. *A Plan for the Improvement of Sitka Spruce by Selection and Breeding.* Forestry Commission; 1972.
21. Lee S, Matthews R. An Indication of the Likely Volume Gains from Improved Sitka Spruce Planting Stock. Forestry Commission; March 2004. ISSN 1460-3802, ISBN 0-85538-619-3
22. Mochan S, Lee S, Gardiner B. Benefits of improved Sitka spruce: volume and quality of timber. Forest Research; September 2008. ISBN: 973-0-85538-766-2, ISSN: 1756-5758
23. Glombik P, O'Reilly C, Grant OM. Early-height variation between full-sibling families of Sitka spruce growing in Ireland. *Irish Forestry.* 2015;72. Corpus ID: 91057573

24. Stokes V, Lee S, Forster J, Fletcher A. A comparison of Sitka spruce x white spruce hybrid families as an alternative to pure Sitka spruce plantations in upland Britain. *Forestry: An International Journal of Forest Research*. 2018;91(5):650-661. doi:10.1093/FORESTRY/CPY027
25. Stokes VJ, Jinks R, Kerr G. An analysis of conifer experiments in Britain to identify productive alternatives to Sitka spruce. *Forestry.* 2022;96(2):170–187. doi:10.1093/FORESTRY/CPAC035
26. Mitchell RG, Wright KH, Johnson NE. Damage by the Sitka spruce weevil (*Pissodes strobi*) and growth patterns for 10 spruce species and hybrids over 26 years in the Pacific Northwest. *Materials Science, Environmental Science*. 1990;434. doi:10.2737/PNW-RP-434
27. Sang Z, Sebastian-Azcona J, Hamann A, Menzel A, Hacke U. Adaptive limitations of white spruce populations to drought imply vulnerability to climate change in its western range. *Evolutionary Applications*. 2019;12(9):1850-1860. doi:10.1111/EVA.12845
28. Martínez-Vilalta J, Sala A, Piñol J. The hydraulic architecture of Pinaceae - a review. *Plant Ecology.* 2004;171:3-13. doi:10.1023/B:VEGE.0000029378.87169.b1
29. West AG, Hultine KR, Jackson TL, Ehleringer JR. Differential summer water use by Pinus edulis and Juniperus osteosperma reflects contrasting hydraulic characteristics. *Tree Physiology*. 2007;27(12):1711-1720. doi:10.1093/TREEPHYS/27.12.1711
30. Plaut JA, Yepez EA, Hill J, et al. Hydraulic limits preceding mortality in a piñon-juniper woodland under experimental drought. *Plant, Cell & Environment*. 2012;35(9):1601-1617. doi:10.1111/J.1365-3040.2012.02512.X
31. Limousin JM, Bickford CP, Dickman LT, et al. Regulation and acclimation of leaf gas exchange in a piñon–juniper woodland exposed to three different precipitation regimes. *Plant, Cell & Environment*. 2013;36(10):1812-1825. doi:10.1111/PCE.12089
32. Brodribb TJ, McAdam SAM. Abscisic Acid Mediates a Divergence in the Drought Response of Two Conifers. *Plant Physiology* 2013;162(3):1370-1377. doi:10.1104/PP.113.217877
33. Meinzer FC, Woodruff DR, Marias DE, Mcculloh KA, Sevanto S. Dynamics of leaf water relations components in co-occurring iso- and anisohydric conifer species. *Plant, Cell & Environment*. 2014;37(11):2577-2586. doi:10.1111/PCE.12327
34. Voelker SL, DeRose RJ, Bekker MF, Sriladda C, Leksungnoen N, Kjelgren RK. Anisohydric water use behavior links growing season evaporative demand to ring-width increment in conifers from summer-dry environments. *Trees - Structure and Function*. 2018;32(3):735-749. doi:10.1007/S00468-018-1668-1/
35. Martínez-Vilalta J, Garcia-Forner N. Water potential regulation, stomatal behaviour and hydraulic transport under drought: deconstructing the iso/anisohydric concept. *Plant, Cell & Environment*. 2017;40(6):962-976. doi:10.1111/pce.12846
36. Breshears DD, Myers OB, Barnes FJ. Horizontal heterogeneity in the frequency of plant-available water with woodland intercanopy-canopy vegetation patch type rivals that occuring vertically by soil depth. *Ecohydrology*. 2009;2(4):503-519. doi:10.1002/ECO.75

37. Garcia-Forner N, Adams HD, Sevanto S, et al. Responses of two semiarid conifer tree species to reduced precipitation and warming reveal new perspectives for stomatal regulation. *Plant, Cell & Environment*. 2016;39(1):38-49. doi:10.1111/PCE.12588
38. Way DA, Yamori W. Thermal acclimation of photosynthesis: On the importance of adjusting our definitions and accounting for thermal acclimation of respiration. *Photosynthesis Research*. 2014;119(1-2):89-100. doi:10.1007/S11120-013-9873-7
39. Chaves MM. Effects of Water Deficits on Carbon Assimilation. *Journal of Experimental Botany*. 1991;42(1):1-16. doi:10.1093/JXB/42.1.1
40. Escalona JM, Flexas J, Medrano H. Stomatal and non-stomatal limitations of photosynthesis under water stress in field-grown grapevines. *Functional Plant Biology*. 2000;27(1):87-87. doi:10.1071/PP99019_CO
41. Lawlor DW, Cornic G. Photosynthetic carbon assimilation and associated metabolism in relation to water deficits in higher plants. *Plant, Cell & Environment*. 2002;25(2):275-294. doi:10.1046/J.0016-8025.2001.00814.X
42. Peña-Rojas I, Aranda X, Fleck I. Stomatal limitation to CO_2 assimilation and down-regulation of photosynthesis in Quercus ilex resprouts in response to slowly imposed drought. *Tree Physiology*. 2004;24(7):813-822. doi:10.1093/TREEPHYS/24.7.813
43. Aranda I, Rodriguez-Calcerrada J, Robson TM, Cano J, Alte L, Sanchez-Gomez D. Stomatal and non-stomatal limitations on leaf carbon assimilation in beech (*Fagus sylvatica* L.) seedlings under natural conditions. *Forest systems*. 2012;21(3): 405-417. doi:10.5424/fs/2012213-02348
44. Drake JE, Power SA, Duursma RA, et al. Stomatal and non-stomatal limitations of photosynthesis for four tree species under drought: A comparison of model formulations. *Agricultural and Forest Meteorology*. 2017;247:454-466. doi:10.1016/J.AGRFORMET.2017.08.026
45. Medrano H, Escalona JM, Bota J, Gulías J, Flexas J. Regulation of Photosynthesis of C3 Plants in Response to Progressive Drought: Stomatal Conductance as a Reference Parameter. *Annals of Botany*. 2002;89(7):895-905. doi:10.1093/AOB/MCF079
46. Drake JE, Power SA, Duursma RA, et al. Stomatal and non-stomatal limitations of photosynthesis for four tree species under drought: A comparison of model formulations. *Agricultural and Forest Meteorology*. 2017;247:454-466. doi:10.1016/J.AGRFORMET.2017.08.026
47. Flexas J, Bota J, Galmés J, Medrano H, Ribas-Carbó M. Keeping a positive carbon balance under adverse conditions: responses of photosynthesis and respiration to water stress. *Physiologia Plantarum*. 2006;127(3):343-352. doi:10.1111/J.1399-3054.2006.00621.X
48. Galmés J, Medrano H, Flexas J. Photosynthetic limitations in response to water stress and recovery in Mediterranean plants with different growth forms. *New Phytologist*. 2007;175(1):81-93. doi:10.1111/J.1469-8137.2007.02087.X

49. Cornic G, Prioul J -L, Louason G. Stomatal and non-stomatal contribution in the decline in leaf net CO2 uptake during rapid water stress. *Physiologia Plantarum*. 1983;58(3):295-301. doi:10.1111/J.1399-3054.1983.TB04184.X
50. Macfarlane C, White DA, Adams MA. The apparent feed-forward response to vapour pressure deficit of stomata in droughted, field-grown Eucalyptus globulus Labill. *Plant, Cell & Environment*. 2004;27(10):1268-1280. doi:10.1111/J.1365-3040.2004.01234.X
51. Damour G, Vandame M, Urban L. Long-term drought results in a reversible decline in photosynthetic capacity in mango leaves, not just a decrease in stomatal conductance. *Tree Physiology*. 2009;29(5):675-684. doi:10.1093/TREEPHYS/TPP011
52. Moore CE, Meacham-Hensold K, Lemonnier P, et al. The effect of increasing temperature on crop photosynthesis: from enzymes to ecosystems. *Journal of Experimental Botany*. 2021;72(8):2822-2844. doi:10.1093/JXB/ERAB090
53. Marchin RM, Backes D, Ossola A, Leishman MR, Tjoelker MG, Ellsworth DS. Extreme heat increases stomatal conductance and drought-induced mortality risk in vulnerable plant species. *Global Change Biology*. 2022;28(3):1133-1146. doi:10.1111/GCB.15976
54. Bagley J, Rosenthal DM, Ruiz-Vera UM, et al. The influence of photosynthetic acclimation to rising CO_2 and warmer temperatures on leaf and canopy photosynthesis models. *Global Biogeochemical Cycles*. 2015;29(2):194-206. doi:10.1002/2014GB004848
55. Smith NG, Dukes JS. Short-term acclimation to warmer temperatures accelerates leaf carbon exchange processes across plant types. *Global Change Biology*. 2017;23(11):4840-4853. doi:10.1111/GCB.13735
56. Kumarathunge DP, Medlyn BE, Drake JE, et al. Acclimation and adaptation components of the temperature dependence of plant photosynthesis at the global scale. *New Phytologist*. 2019;222(2):768-784. doi:10.1111/NPH.15668
57. Flexas J, Medrano H. Drought-inhibition of Photosynthesis in C3 Plants: Stomatal and Non-stomatal Limitations Revisited. *Annals of Botany*. 2002;89(2):183-189. doi:10.1093/AOB/MCF027
58. Lawlor DW. Limitation to Photosynthesis in Water-stressed Leaves: Stomata vs. Metabolism and the Role of ATP. *Annals of Botany*. 2002;89(7):871-885. doi:10.1093/AOB/MCF110
59. Grassi G, Magnani F. Stomatal, mesophyll conductance and biochemical limitations to photosynthesis as affected by drought and leaf ontogeny in ash and oak trees. *Plant, Cell & Environment*. 2005;28(7):834-849. doi:10.1111/J.1365-3040.2005.01333.X
60. Xu Z, Zhou G, Shimizu H. Are plant growth and photosynthesis limited by pre-drought following rewatering in grass? *Journal of Experimental Botany*. 2009;60(13):3737-3749. doi:10.1093/JXB/ERP216
61. Day ME. Influence of temperature and leaf-to-air vapor pressure deficit on net photosynthesis and stomatal conductance in red spruce (*Picea rubens*). *Tree Physiology*. 2000;20(1):57-63. doi:10.1093/TREEPHYS/20.1.57

62. Song Y, Chen Q, Ci D, Shao X, Zhang D. Effects of high temperature on photosynthesis and related gene expression in poplar. *BMC Plant Biology.* 2014;14(1):1-20. doi:10.1186/1471-2229-14-111
63. Garcia-Forner N, Adams HD, Sevanto S, et al. Responses of two semiarid conifer tree species to reduced precipitation and warming reveal new perspectives for stomatal regulation. *Plant, Cell & Environment*. 2016;39(1):38-49. doi:10.1111/pce.12588
64. Xu ZZ, Zhou GS. Photosynthetic Recovery of a Perennial Grass Leymus chinensis after Different Periods of Soil Drought. 2007;10(3):277-285. doi:10.1626/PPS.10.277
65. Hofer D, Suter M, Buchmann N, Lüscher A. Nitrogen status of functionally different forage species explains resistance to severe drought and post-drought overcompensation. *Agriculture, Ecosystems & Environment*. 2017;236:312-322. doi:10.1016/J.AGEE.2016.11.022
66. Qi M, Liu X, Li Y, et al. Photosynthetic resistance and resilience under drought, flooding and rewatering in maize plants. *Photosynthesis Research*. 2021;148(1-2):1-15. doi:10.1007/S11120-021-00825-3
67. Sinclair TR, Sinclair TR. Is transpiration efficiency a viable plant trait in breeding for crop improvement? *Functional Plant Biology*. 2012;39(5):359-365. doi:10.1071/FP11198
68. Lévesque M, Siegwolf R, Saurer M, Eilmann B, Rigling A. Increased water-use efficiency does not lead to enhanced tree growth under xeric and mesic conditions. *New Phytologist*. 2014;203(1):94-109. doi:10.1111/NPH.12772
69. van der Sleen P, Groenendijk P, Vlam M, et al. No growth stimulation of tropical trees by 150 years of CO_2 fertilization but water-use efficiency increased. *Nature Geoscience*. 2014;8(1):24-28. doi:10.1038/ngeo2313
70. Zhang Jianwei, Marshall JD. Population differences in water-use efficiency of well-watered and water-stressed western larch seedlings. *Canadian Journal of Forest Research*. 1994;24(1):92-99. doi:10.1139/X94-014
71. Marguerit E, Bouffier L, Chancerel E, et al. The genetics of water-use efficiency and its relation to growth in maritime pine. *Journal of Experimental Botany*. 2014;65(17):4757-4768. doi:10.1093/JXB/ERU226
72. Huang R, Zhu H, Liu X, et al. Does increasing intrinsic water use efficiency (iWUE) stimulate tree growth at natural alpine timberline on the southeastern Tibetan Plateau? *Global and Planetary Change*. 2017;148:217-226. doi:10.1016/J.GLOPLACHA.2016.11.017
73. Rasheed F, Dreyer E, Richard B, Brignolas F, Montpied P, le Thiec D. Genotype differences in 13C discrimination between atmosphere and leaf matter match differences in transpiration efficiency at leaf and whole-plant levels in hybrid *Populus deltoides ×nigra*. *Plant, Cell & Environment*. 2013;36(1):87-102. doi:10.1111/J.1365-3040.2012.02556.X
74. Bogeat-Triboulot MB, Buré C, Gerardin T, et al. Additive effects of high growth rate and low transpiration rate drive differences in whole plant transpiration efficiency among black poplar genotypes. *Environmental and Experimental Botany*. 2019;166:103784. doi:10.1016/J.ENVEXPBOT.2019.05.021

75. Voltas J, Serrano L, Herna´ndez M, et al. Carbon Isotope Discrimination, Gas Exchange and Stem Growth of Four Euramerican Hybrid Poplars under Different Watering Regimes. *New Forests*. 2006;31(3):435-451. doi:10.1007/S11056-005-0879-7

76. Flexas J, Galmés J, Gallé A, et al. Improving water use efficiency in grapevines: potential physiological targets for biotechnological improvement. *Australian Journal of Grape and Wine Research*. 2010;16(1):106-121. doi:10.1111/J.1755-0238.2009.00057.X

77. Jones HG. Plants and Microclimate: A Quantitative Approach to Environmental Plant - Hamlyn G. Jones. 2013; doi:10.1017/CBO9780511845727

78. Earl HJ. Stomatal and non-stomatal restrictions to carbon assimilation in soybean (Glycine max) lines differing in water use efficiency. *Environmental and Experimental Botany*. 2002;48(3):237-246. doi:10.1016/S0098-8472(02)00041-2

79. Zhang Jianwei, Marshall JD. Population differences in water-use efficiency of well-watered and water-stressed western larch seedlings. *Canadian Journal of Forest Research*. 1994;24(1):92-99. doi:10.1139/X94-014

Supplementary material

Tables

ANOVA

		Family								
Variable	**N**	**PI700**, N = 5[1]	**PI701**, N = 5[1]	**PI702**, N = 5[1]	**PI703**, N = 5[1]	**Ps111**, N = 5[1]	**Ps112**, N = 5[1]	**Ps117**, N = 5[1]	**PsA18**, N = 5[1]	**p-value**[2]
Height	40	342 (48)	419 (67)	407 (69)	407 (54)	420 (45)	454 (74)	437 (58)	414 (26)	0.2
Diameter	40	4.58 (0.99)	5.30 (0.35)	6.28 (1.55)	4.77 (0.51)	5.46 (0.66)	5.84 (0.79)	5.27 (1.05)	5.26 (1.17)	0.2

[1] Mean (SD)
[2] One-way ANOVA

Supplementary table 1. Summary of analysis of variance of P. lutzii and P. sitchensis growth parameters. ***Height*** *(mm),* ***Diameter*** *(mm). Level of significance:* ***p-value*** *< 0.05.* ***Mean*** *= mean values, (****SD****) = Standard Deviation.*

Figures

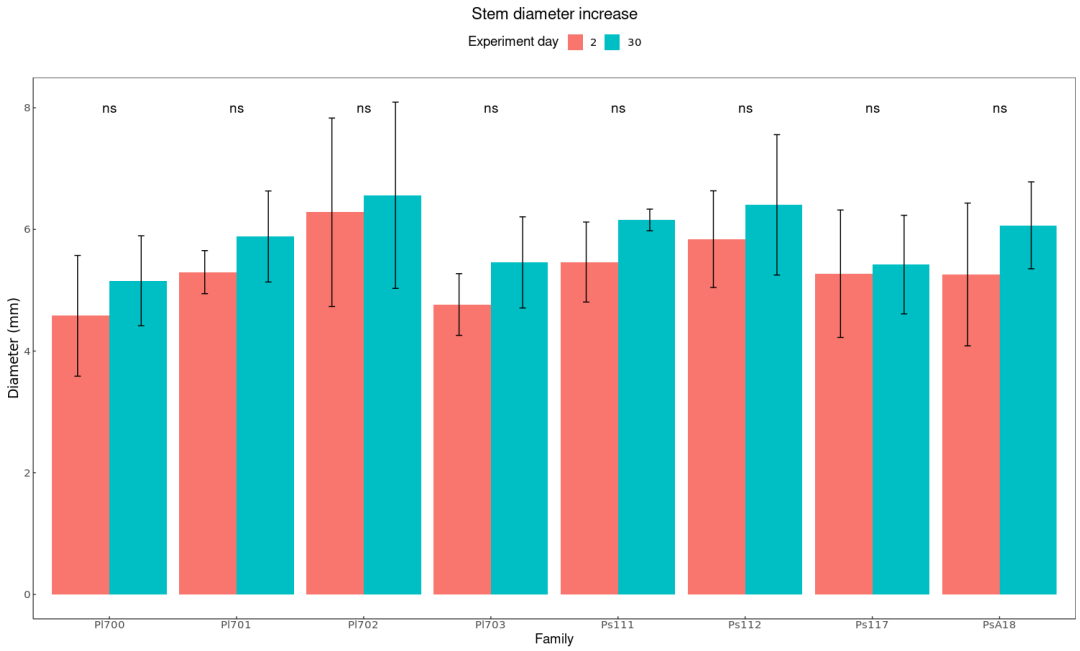

*Supplementary figure 1. Differences in stem diameter of P.sitchensis (Ps111-118) and P. lutzii (Pl700-703) at 2 (**red**) and 30 (**blue**) days since the onset of drought, compared by Student's t-test. Bars are standard deviations. **Ns** = non-significant. N = 5.*

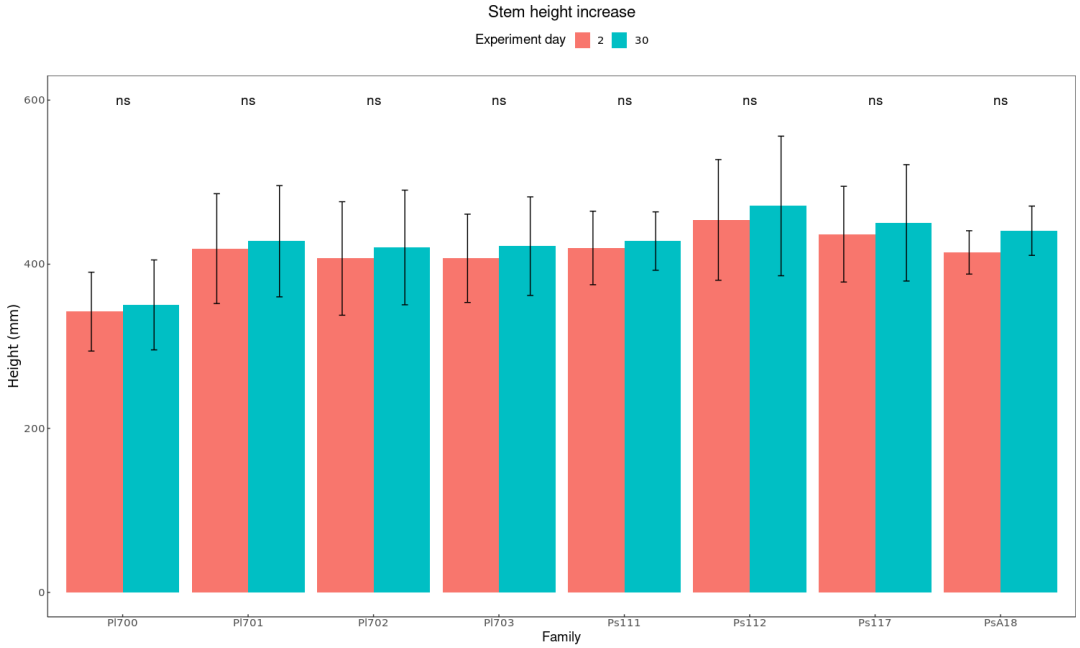

*Supplementary figure 2. Differences in stem height of P.sitchensis (Ps111-118) and P. lutzii (Pl700-703) at 2 (**red**) and 30 (**blue**) days since the onset of drought, compared by Student's t-test. Bars are standard deviations. **Ns** = non-significant. N = 5.*

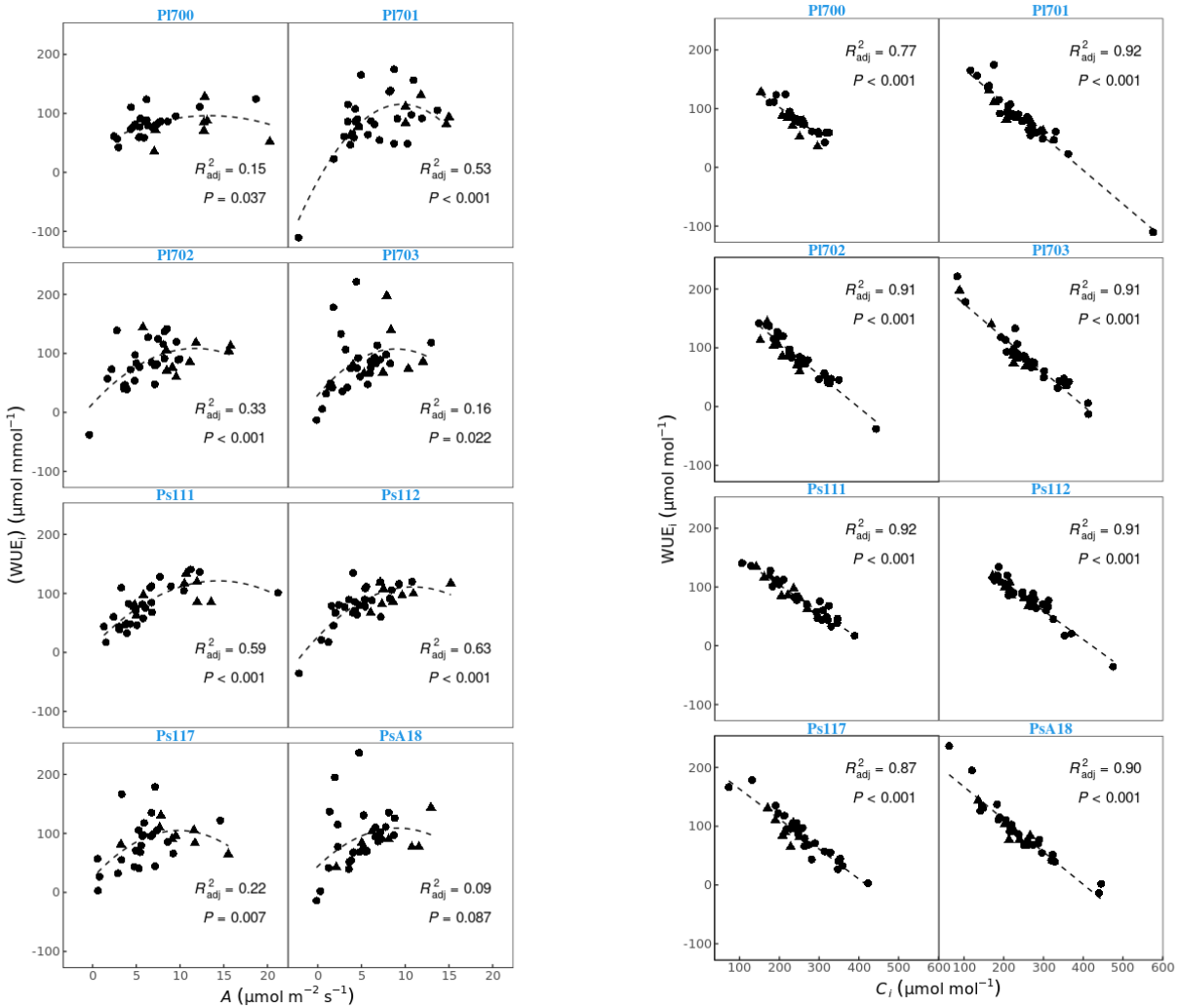

*Supplementary figure 3. (**A**) Relationship between $iWUE_i$ and gs and (**B**) WUE_i and Ci in P. sitchensis (Ps) and P. lutzii (Pl) subjected to drought treatment and recovery. Quadratic functions and ordinary least squares are represented by dashed lines.* ***R2adj*** *= adjusted coefficient of determination,* ***P*** *= p-value. Samples from drought period (**circles**) and rewatering (**triangles**) are included. N = 32-36.*

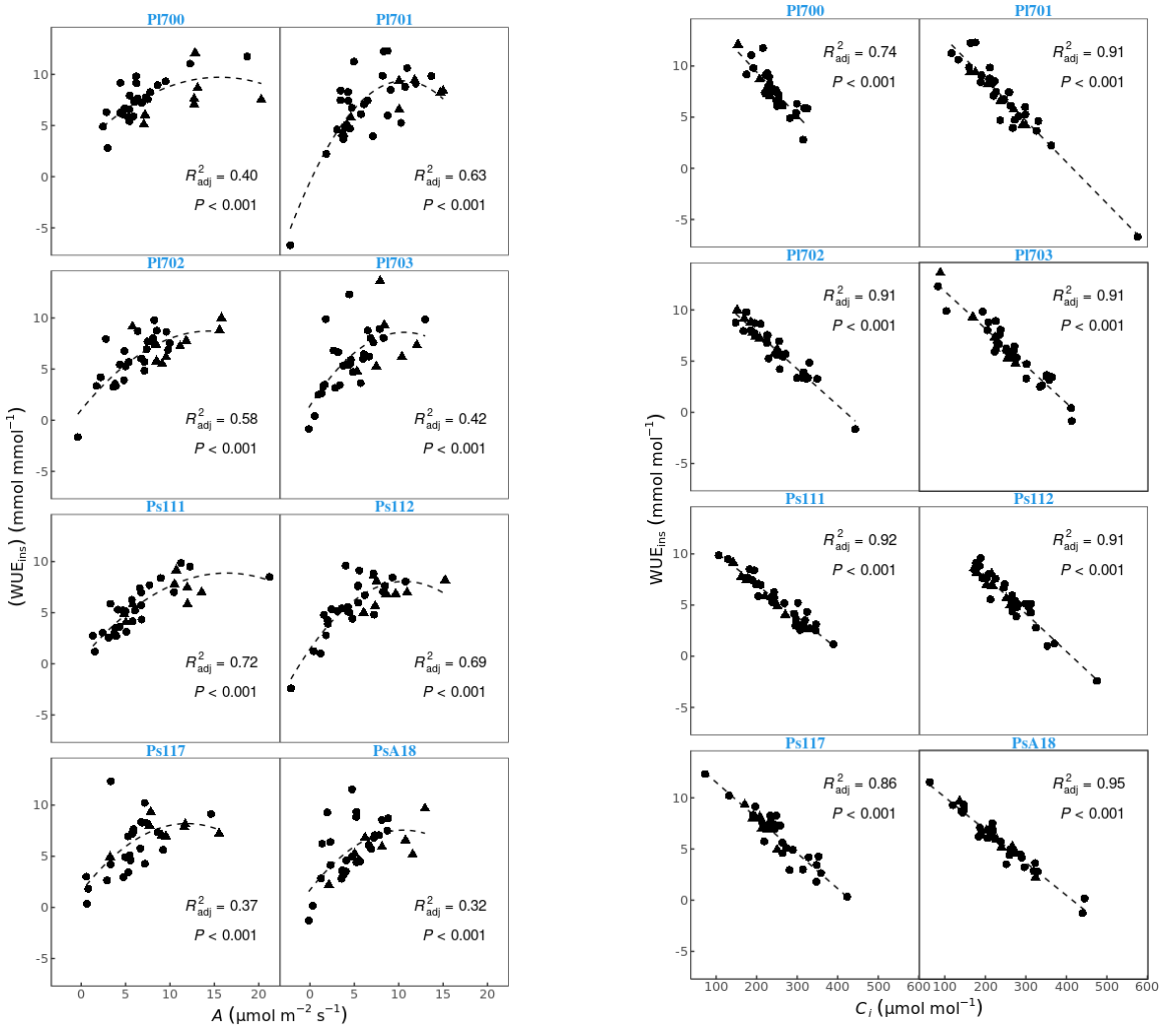

*Supplementary figure 4. (**A**) WUE_{ins} and gs and (**B**) Ci in P. sitchensis (Ps) and P. lutzii (Pl) subjected to drought treatment and recovery. Quadratic functions and ordinary least squares are represented by dashed lines. **R2adj** = adjusted coefficient of determination, **P** = p-value. Samples from drought period (**circles**) and rewatering (**triangles**) are included. N = 32-36.*

General discussion

This work investigated the genetics of conifer drought responses, which are poorly studied. Starting from genomic resources spanning a diverse range of conifer species and families, we pinpointed single-gene mechanisms that may govern the production of species-specific phenotypes under limiting soil water conditions. The genes of interest participate in the abscisic acid (ABA) biosynthesis pathway and appeared conserved across millions of years of evolution. Although not definitive, we bring new evidence that 9-*cis*-epoxycarotenoid dioxygenases (*NCEDs*) fine-tune ABA accumulation in conifer foliage in two diverging modes, depending on phylogenetic history. Characterisation of the coded enzymes is still ongoing, but *in silico* analyses confirmed the high degree of structural conservation for at least two species, implying conserved function. Finally, we inspected variability among cultivars and hybrids of one species particularly important to the UK forestry sector, *Picea sitchensis* (*P. sitchensis*). We discuss our main findings and their implications for future research and industrial applications.

Multispecies drought response characterisation

We successfully identified a continuum of xylem water potential regulation among 9 species of 3 diverging conifer families, in line with the widely accepted view that iso/anisohydric strategies constitute a spectrum of responses [1–3]. We were able to quantify the degree of isohydricity by calculating the slope (σ) of the regression line between MWP and percentage SWC. In agreement with previous reports, we observed that Pinaceae and basal Cupressaceae are positioned at the isohydric end of the spectrum, while derived Cupressaceae and Taxaceae are towards the anisohydric end [4].

ABA profile characterisation

We then correlated water potential, as a proxy of isohydricity, with a metabolic trait such as ABA accumulation. In line with previous studies [4,5], all Pinaceae displayed a Rising (R) type, increasing foliar ABA levels continuously accordingly to their isohydric behaviour. Cupressaceae did tend to show just a transient increase in hormone levels, with *Chamaecyparis lawsoniana* (*C. lawsoniana)* being a clear Peaking (P) type coherently with its strong anisohydric response. In peaking type trees,

high ABA levels only play a role at the early onset of soil drought but are not needed later, as stomatal closure is driven by the low water potentials that these trees are able to withstand [6,7]. By directly considering variation of MWP with SWC and complementing this information with a metabolic trait, our drought experiment confirmed that the iso/anisohydry framework can still be effective in separating tree species based on their drought response. Moreover, our experiment adds to the growing body of evidence suggesting that R/P types of ABA accumulation may be an evolutionary trait that emerged during conifer diversification and adaptation to dry environments [4,6,8].

ABA-related gene identification

We hypothesised that rate limiting *NCEDs*, if functionally conserved, may be the best candidates and the main regulators of contrasting R/P types. We used sequence similarity searches to identify candidate sequences using model *A. thaliana* gene sequences as a reference. To do this, we selected three species that represent their respective families in the drought response spectrum: *P. sitchensis* for the isohydric Pinaceae, *C. lawsoniana* for the extreme anisohydric Cupressacease and *Taxus baccata* (*T. baccata)* for the relatively anisohydric Taxacease. We found several candidate sequences that shared high similarity with *Arabidopsis thaliana (A. thaliana)* genes, indicating that their function and the ABA biosynthesis pathways may be conserved in conifers. This is in line with genomic studies that have identified homologous sequences of *A. thaliana* ABA-related genes in conifers [9–12]. Previous studies mostly focus on Pinaceae and are based on transcriptome production and analysis, with no ABA quantitation. Here, we aimed at testing selected target genes for their timely expression in relation to drought progression and ABA accumulation in a diverse array of conifer species.

ABA biosynthesis contributes to R/P-types

NCED expression levels were responsive to drought stress in *P. sitchensis* and *C. lawsoniana*. *NCEDs* of *P. sitchensis* were upregulated in response to drought stress for the entire duration of the experiment, consistent with our predictions. Instead, *NCEDs* of *C. lawsoniana* were strikingly downregulated, meeting only partially our expectations for the peaking type. In fact, we expected to see a shift in gene expression from up to downregulation. We did not find evidence suggesting that other biosynthetic genes alone could drive ABA accumulation to high levels in any of the species tested. The ABA peak that we observed in *C. lawsoniana* could originate from early upregulation of ClNCEDs which we didn't capture, or by glycosylated stores of ABA. Only one study, to our knowledge, compared gene expression and ABA dynamics in two conifers, Scot pine and Norway

spruce, which are both Pinaceae [13]. The authors found a relationship between *NCED* expression and ABA levels in Norway spruce but not Scot pine, where both increased transiently, and no contribution was observed from other biosynthetic genes. Intriguingly, Pashkovskiy and collaborators observed upregulation of genes coding for β-glycosidases, which free ABA from ABA-GE stores, but no reduction in conjugated ABA of Scot pine and Norway spruce [13].

Catabolism of ABA in R/P-types

We further tested whether catabolic function could contribute to shaping R/P ABA profiles. *P. sitchensis* cytochrome P450 707As (*CYP707As)* were not differentially expressed in response to drought, indicating that catabolism is constitutive under drought, as expected. Instead, *C. lawsoniana CYP707As* were differentially expressed, three of them being downregulated and one being upregulated at about the same time of decreasing levels of ABA. Thus, catabolic function may contribute to modulating ABA levels in Peaking types, although we can only speculate on this as we did not measure phaseic acid (PA), the product of the catabolic reaction. However, a recent study found no contribution of catabolism of ABA, by only quantifying PA levels, in the production of P-types of the conifer *Callitris rhomboidea (C. rhomboidea)* [14]. Instead, the authors detected a significant increase in ABA-GE, indicating that conjugation and not catabolism controls post-peak ABA decrease. *T. baccata* showed some degree of downregulation of *CYP707As*, possibly indicating that catabolic function is switched off to allow ABA accumulation by other sources than de-novo biosynthesis, as we did not detect any significant upregulation of biosynthesis genes for this species.

NCEDs sequence analysis

We inspected our conifer NCED protein sequences to study their degree of homology with known CCD and NCED sequences from model species maize and *A. thaliana* [15–21]. Overall, conifer sequences were more closely related to the reference *Zm*VP14 sequence than those of the CCDs, sharing important protein motifs correlated with carotenoid oxidoreductase activity. Key residues contributing to stereoselectivity for the substrate were also well-conserved between angiosperm and conifer NCEDs, suggesting specific cleavage of the 11-12 bond of 9-cis-violaxanthin and 9-cis-neoxanthin, except for PsNCED2 and *T. baccata* putative NCEDs which harboured some substitutions in the catalytic pocket. This is coherent with their reduced responsiveness to drought in gene expression studies.

NCEDs structural and functional analyses

We used protein sequence information to model the 3D protein structure of each putative conifer NCED. Different algorithms identified all conifer proteins as monomeric epoxycarotenoid dioxygenases able to complex with Fe^{II} and oxygen with a high degree of confidence. All modelled structures were high-quality, falling in the range of native crystal structures. We were able to identify a chloroplast transit peptide at the N-termini of ZmVP14, AtNCED3 and AtCCD4, as expected [18], and PsNCED2, ClNCED1, but not ZmCCD1 and intriguingly not in the remaining six conifer sequences. Transit peptides are made of highly variable sequences, that the prediction software may not capture, as programs are based on limited libraries. Therefore, this result must be carefully considered before excluding the possibility of interaction of the conifer NCEDs with the chloroplast membranes. However, protein membrane interaction simulations showed that putative conifer NCEDs have membrane binding capacity and could localise either on the thylakoid membrane or, if they are not imported inside the organelle, on the chloroplast envelope. Here, they could access their substrates [22,23]. Protein-ligand simulations showed a low energy conformation that suited the optimal position of the substrate inside the catalytic pocket [20] for all putative NCEDs but *Tb*NCED1 and *Tb*NCED2. This is consistent with gene expression studies, where *T. baccata* NCEDs did not respond to drought stress in a substantial way. We can speculate that *Tb*NCEDs may cleave other but similar substrates than neoxanthin and violaxanthin.

Protein cloning, isolation and testing

We successfully cloned and purified PsNCED1, as it was one of the most drought responsive and promising sequences at the structural and functional analysis. It was also the most interesting for industrial applications. This is the first putative conifer NCED to be cloned, to our knowledge. The recombinant protein had to be isolated as a maltose binding protein (MBP)-fusion PsNCED1, due to its low solubility in aqueous solutions and tendency to form inclusion bodies. The MBP-PsNCED1 was then tested to verify its catalytic activity *in vitro*, using neoxanthin as substrate. Unfortunately, no product was detected. The lack of substrate detection suggests that it was degraded during the reaction preparation [24,25].

Stress physiology of *Picea sitchensis* and *Picea lutzii*

We explored variability in drought responses within *P. sitchensis* and its hybrid *Picea lutzii* (*P. lutzii)* - because of their relevance to the forestry market. Both species adopted a conservative water regulation strategy, coherently with our isohydric characterisation and the literature for Pinaceae [5,26], although the stringency of this response varied among families. Stomatal conductance and leaf transpiration were the main drivers of variation among breeding families and could be the main limiting factor affecting photosynthetic gain, more than metabolic photosynthetic damage [27,28]. Interestingly, both species were resilient to drought, as gas exchange parameters recovered to higher levels than pre-stress. This indicates that Sitka and *P. lutzii* have the capacity of adapting to an episodic drought and once water is available can overcompensate by boosting their photosynthetic activity, as observed before in angiosperm plant systems [29–32].

Photosynthesis performance under drought conditions

We calculated photosynthetic Light Response Curves (LRCs) to estimate the impact of drought on photosynthesis biochemistry, by measuring leaf gas exchange. Again, both species appeared resilient to drought stress, as their photosynthetic apparatus fully recovered and overcompensated previous losses upon rewatering, as observed for the gas exchange functions. Moreover, *P. lutzii* showed signs of improved photosynthetic efficiency even under drought conditions, compared to *P. sitchensis*. Previous studies on *P. sitchensis* found homogeneous physiological responses to drought among different breeding families [33,34]. Our findings could help in the choice of genetic lines of interest in Sitka and *P. lutzii*, showing at the same time the possible outcomes of crossing species to produce similar trees with different responsiveness to drought stress [35].

Water use efficiency

We found evidence that sustained net carbon gain under drought stress led to increased water use efficiency (WUE) under our experimental conditions. Instantaneous WUE, measured at leaf level, was somewhat higher in *P. lutzii* compared to *P. sitchensis*. This is in line with the greater resistance to drought stress of the photosynthetic apparatus of *P. lutzii*. These findings, together with the observation of significant variability in leaf transpiration and stomatal conductance, may inform on the selection of suitable genotypes. Overall, *P. lutzii* is promising in terms of photosynthesis gains under our experimental conditions.

Contribution to research on conifers

With our work, we provide evidence that NCEDs conserve their role of rate-limiting enzymes in the biosynthesis of ABA among genetically and phenotypically divergent coniferous species. We also show the role of differential NCED gene expression in controlling R/P-types in at least two conifer species, *P. sitchensis* and *C. lawsoniana*, with contrasting water regulation strategies. Evidence showing that long term expression of NCEDs is essential to produce these ABA profiles was lacking [4,13,14]. We also isolated for the first time a conifer NCED protein, *P. sitchensis* NCED1, and provided evidence of the degree of structural and functional conservation of other conifer NCEDs. The recombinant PsNCED1 protein with its sequence, primer oligos and an experimental protocol for cloning and purification are available, so that downstream applications and testing are possible. These resources integrate genomic and transcriptomics information collected so far in the field of conifer research, and specifically on conifer responses to drought. Finally, we found evidence of variability in drought sensitivity among several breeding families of Sitka and *P. lutzii*, the latter showing increased photosynthetic functions under drought stress conditions. The scientific literature reporting studies on conifer breeding families is rather limited and variability among provenances and genetic lines has been difficult to detect [33,34]. We believe that our findings will help foresters in establishing better breeding practices.

Future research directions

Further work is needed to assess the origin of the ABA peak that we observed in *C. lawsoniana* and the role of catabolism in the removal of active ABA from the cell. Previous studies have provided non-conclusive evidence regarding the role of either mobilisation of ABA-GE stores [13] or *de-novo* biosynthesis [14] in increasing ABA foliage levels. Setting earlier time points for gene expression analysis may help understanding if early *NCED* expression contributes to the ABA peak. ABA-GE mobilisation is catalysed by β-glucosidases [36] and future screenings should account for their expression. We observed timely differential expression of catabolic genes in *C. lawsoniana*, suggesting that they could be involved in the modulation of the ABA response, but Mercado-Reyes and colleagues showed that ABA removal was promoted by conjugation and no change was observed in phaseic acid in *C. rhomboidea* [14]. Abscisic acid conjugation is catalysed by UDP-glucosyltransferases [37], so it will be necessary to quantify both their expression levels and ABA-GE changes during drought.

Our PsNCED1 recombinant protein assay did not yield conclusive evidence about its role in catalysing the cleavage of the 11-12 double bond of neoxanthin, although gene expression study and *in silico* analyses point in that direction. This was likely due to substrate degradation during preparation of the reaction mix. It will be necessary to repeat the experiment under more controlled conditions. Moreover, gene complementation studies *in planta* are ongoing with *A. thaliana* mutants and include *NCED* sequences from *P. sitchensis*, *C. lawsoniana,* and *T. baccata*. This, together with the *in vitro* enzyme assay, will serve to confirm the biological function of the proteins object of our work.

Finally, drought experiments in the field may be needed to test whether our findings apply to natural conditions, longer time scales and older trees. Some studies indicate that physiological responses to drought may depend on tree ontogeny, changing with tree size and age [38–41]. We also found that temperature increased to very high values during our drought experiment on Sitka and *P. lutzii*. It would be interesting to assess the impact of such high temperatures on the drought physiology of these trees, as multiple stresses can influence tree survival on the long term [41].

Impacts and applications

Our work seeks to contribute to the establishment of better-informed breeding programmes in the forestry sector and especially in the UK market, where *P. sitchensis* is still the principal species. We believe that integrating approaches in a multidisciplinary way, can yield quality information to help adapt and potentially mitigate the impacts of climate change as a key for the future of British and global forests. Genomic resources are increasingly available but bridging the gap between genes and phenotype is required to disentangle the relative contribution of evolution and plasticity to tree performance and survival under drought. Knowledge of the genes and pathways involved in different drought responses in diverse species, and how they are regulated under stress, can guide genetic modification or selection of genotypes to produce desired phenotypes, starting from existing germplasm. Much of the research conducted in the forestry field has focused on growth-related and anatomical traits. Knowing the level of intraspecific variation in water and photosynthesis-related traits can inform on the significance of work past and future, as it will allow to pinpoint which breeding lines, that have been selected so far, may adapt to future local conditions and to act by focusing efforts on the promising material.

Literature cited

1. Klein T. The variability of stomatal sensitivity to leaf water potential across tree species indicates a continuum between isohydric and anisohydric behaviours. *Funct Ecol*. 2014;28(6):1313-1320. doi:10.1111/1365-2435.12289
2. Garcia-Forner N, Adams HD, Sevanto S, et al. Responses of two semiarid conifer tree species to reduced precipitation and warming reveal new perspectives for stomatal regulation. *Plant Cell Environ*. 2016;39(1):38-49. doi:10.1111/PCE.12588
3. Ratzmann G, Meinzer FC, Tietjen B. Iso/Anisohydry: Still a Useful Concept. *Trends in Plant Science*. 2019;24(3):191-194. doi:10.1016/J.TPLANTS.2019.01.001
4. Brodribb TJ, McAdam SAM, Jordan GJ, Martins SCV. Conifer species adapt to low-rainfall climates by following one of two divergent pathways. *Proceedings of the National Academy of Sciences*. 2014;111(40):14489-14493. doi:10.1073/pnas.1407930111
5. Brodribb TJ, McAdam SAM. Abscisic Acid Mediates a Divergence in the Drought Response of Two Conifers. *Plant Physiology*. 2013;162(3):1370-1377. doi:10.1104/PP.113.217877
6. Brodribb TJ, McAdam SAM. Abscisic Acid Mediates a Divergence in the Drought Response of Two Conifers. *Plant Physiology*. 2013;162(3):1370-1377. doi:10.1104/pp.113.217877
7. McAdam SAM, Brodribb TJ. The Evolution of Mechanisms Driving the Stomatal Response to Vapor Pressure Deficit. *Plant Physiology*. 2015;167(3):833-843. doi:10.1104/pp.114.252940
8. Nolan RH, Tarin T, Santini NS, McAdam SAM, Ruman R, Eamus D. Differences in osmotic adjustment, foliar abscisic acid dynamics, and stomatal regulation between an isohydric and anisohydric woody angiosperm during drought. *Plant Cell Environ*. 2017;40(12):3122-3134. doi:10.1111/PCE.13077
9. Lorenz WW, Alba R, Yu YS, Bordeaux JM, Simões M, Dean JFD. Microarray analysis and scale-free gene networks identify candidate regulators in drought-stressed roots of loblolly pine (P. taeda L.). *BMC Genomics 2011 12:1*. 2011;12(1):1-17. doi:10.1186/1471-2164-12-264
10. Hu R, Wu B, Zheng H, et al. Global Reprogramming of Transcription in Chinese Fir (Cunninghamia lanceolata) during Progressive Drought Stress and after Rewatering. *International Journal of Molecular Sciences 2015, Vol 16, Pages 15194-15219*. 2015;16(7):15194-15219. doi:10.3390/IJMS160715194
11. Du M, Ding G, Cai Q. The Transcriptomic Responses of Pinus massoniana to Drought Stress. *Forests 2018, Vol 9, Page 326*. 2018;9(6):326. doi:10.3390/F9060326
12. Pervaiz T, Liu SW, Uddin S, Amjid MW, Niu SH, Wu HX. The transcriptional landscape and hub genes associated with physiological responses to drought stress in pinus tabuliformis. *International Journal of Molecular Sciences*. 2021;22(17):9604. doi:10.3390/IJMS22179604/S1

13. Pashkovskiy PP, Vankova R, Zlobin IE, et al. Comparative analysis of abscisic acid levels and expression of abscisic acid-related genes in Scots pine and Norway spruce seedlings under water deficit. *Plant Physiology and Biochemistry*. 2019;140:105-112. doi:10.1016/J.PLAPHY.2019.04.037
14. Mercado-Reyes JA, McAdam S. Extreme drought deactivates ABA biosynthesis. *Authorea Preprints*. March 31, 2022. doi:10.22541/AU.164873604.42418092/V1
15. Sh S, Bc T, Da G, et al. Specific Oxidative Cleavage of Carotenoids by VP14 of Maize. 1997;(August 2015):1872-1874. doi:10.1126/science.276.5320.1872
16. Iuchi S, Kobayashi M, Taji T, et al. Regulation of drought tolerance by gene manipulation of 9-cis-epoxycarotenoid dioxygenase, a key enzyme in abscisic acid biosynthesis in Arabidopsis. *Plant J*. 2001;27(4):325-333. doi:10.1046/J.1365-313X.2001.01096.X
17. Giuliano G, Al-Babili S, von Lintig J. Carotenoid oxygenases: cleave it or leave it. *Trends in Plant Science*. 2003;8(4):145-149. doi:10.1016/S1360-1385(03)00053-0
18. Schwartz SH, Tan BC, McCarty DR, Welch W, Zeevaart JAD. Substrate specificity and kinetics for VP14, a carotenoid cleavage dioxygenase in the ABA biosynthetic pathway. *Biochimica et Biophysica Acta (BBA) - General Subjects*. 2003;1619(1):9-14. doi:10.1016/S0304-4165(02)00422-1
19. Auldridge ME, McCarty DR, Klee HJ. Plant carotenoid cleavage oxygenases and their apocarotenoid products. *Curr Opin Plant Biol*. 2006;9(3):315-321. doi:10.1016/J.PBI.2006.03.005
20. Messing SAJ, Mario Amzel L, Gabelli SB, et al. Structural insights into maize viviparous14, a key enzyme in the biosynthesis of the phytohormone abscisic acid. *Plant Cell*. 2010;22(9):2970-2980. doi:10.1105/tpc.110.074815
21. Daruwalla A, Kiser PD. Structural and mechanistic aspects of carotenoid cleavage dioxygenases (CCDs). *BBA Molecular and Cell Biology of Lipids*. 2020;1865(11). doi:10.1016/J.BBALIP.2019.158590
22. Schwartz SH, Qin X, Zeevaart JAD. Elucidation of the Indirect Pathway of Abscisic Acid Biosynthesis by Mutants, Genes, and Enzymes. *Plant Physiology*. 2003;131(4):1591-1601. doi:10.1104/PP.102.017921
23. Sun T, Yuan H, Cao H, Yazdani M, Tadmor Y, Li L. Carotenoid Metabolism in Plants: The Role of Plastids. *Molecular Plant*. 2018;11(1):58-74. doi:10.1016/J.MOLP.2017.09.010
24. Giossi C, Cartaxana P, Cruz S. Photoprotective Role of Neoxanthin in Plants and Algae. *Molecules*. 2020;25(20). doi:10.3390/MOLECULES25204617
25. Meléndez-Martínez AJ, Mandić AI, Bantis F, et al. A comprehensive review on carotenoids in foods and feeds: status quo, applications, patents, and research needs. 2021;62(8):1999-2049. doi:10.1080/10408398.2020.1867959
26. Mcdowell N, Pockman WT, Allen CD, et al. Mechanisms of Plant Survival and Mortality during Drought : Why Do Some Plants Survive while Others Succumb to Drought. 2008;178(4):719-739.

27. Medrano H, Escalona JM, Bota J, Gulías J, Flexas J. Regulation of Photosynthesis of C3 Plants in Response to Progressive Drought: Stomatal Conductance as a Reference Parameter. *Annals of Botany*. 2002;89(7):895-905. doi:10.1093/AOB/MCF079
28. Drake JE, Power SA, Duursma RA, et al. Stomatal and non-stomatal limitations of photosynthesis for four tree species under drought: A comparison of model formulations. Agricultural and Forest Meteorology. 2017;247:454-466. doi:10.1016/J.AGRFORMET.2017.08.026
29. Xu ZZ, Zhou GS. Photosynthetic Recovery of a Perennial Grass Leymus chinensis after Different Periods of Soil Drought. 2007;10(3):277-285. doi:10.1626/PPS.10.277
30. Xu Z, Zhou G, Shimizu H. Are plant growth and photosynthesis limited by pre-drought following rewatering in grass? *Journal of Experimental Botany*. 2009;60(13):3737-3749. doi:10.1093/JXB/ERP216
31. Hofer D, Suter M, Buchmann N, Lüscher A. Nitrogen status of functionally different forage species explains resistance to severe drought and post-drought overcompensation. *Agric Ecosyst Environ*. 2017;236:312-322. doi:10.1016/J.AGEE.2016.11.022
32. Qi M, Liu X, Li Y, et al. Photosynthetic resistance and resilience under drought, flooding and rewatering in maize plants. *Photosynth Res*. 2021;148(1-2):1-15. doi:10.1007/S11120-021-00825-3
33. Grant OM, O'Reilly C. Impact of genetic variation and long-term limited water availability on the ecophysiology of young Sitka spruce (*Picea sitchensis* (Bong.) Carr.). *Tree Physiology*. 2017;37(4):536-549. doi:10.1093/TREEPHYS/TPW093
34. Grant OM, Montero Ribeiro AF, Glombik P, O'Reilly C. Impact of limited water availability on growth and biomass production of a range of full-sibling Sitka spruce (*Picea sitchensis* (Bong.) Carr.) families. *Forestry: An International Journal of Forest Research*. 2018;91(1):83-97. doi:10.1093/FORESTRY/CPX034
35. Sasani N, Pâques LE, Boulanger G, et al. Physiological and anatomical responses to drought stress differ between two larch species and their hybrid. *Trees - Structure and Function*. 2021;35(5):1467-1484. doi:10.1007/S00468-021-02129-4
36. Xu ZY, Lee KH, Dong T, et al. A Vacuolar β-Glucosidase Homolog That Possesses Glucose-Conjugated Abscisic Acid Hydrolyzing Activity Plays an Important Role in Osmotic Stress Responses in Arabidopsis. *Plant Cell*. 2012;24(5):2184-2199. doi:10.1105/TPC.112.095935
37. Dong T, Hwang I. Contribution of ABA UDP-glucosyltransferases in coordination of ABA biosynthesis and catabolism for ABA homeostasis. *Plant Signal Behav*. 2014;9(APR). doi:10.4161/PSB.28888
38. Cavender-Bares J, Bazzaz FA. Changes in drought response strategies with ontogeny in quercus rubra: Implications for scaling from seedlings to mature trees. *Oecologia*. 2000;124(1):8-18. doi:10.1007/PL00008865/METRICS
39. Grulke NE, Retzlaff WA. Changes in physiological attributes of ponderosa pine from seedling to mature tree. *Tree Physiology*. 2001;21(5):275-286. doi:10.1093/TREEPHYS/21.5.275

40. Mediavilla S, Escudero A. Stomatal responses to drought of mature trees and seedlings of two co-occurring Mediterranean oaks. *Forest Ecology and Management*. 2004;187(2-3):281-294. doi:10.1016/J.FORECO.2003.07.006

41. Niinemets Ü. Responses of forest trees to single and multiple environmental stresses from seedlings to mature plants: Past stress history, stress interactions, tolerance and acclimation. *Forest Ecology and Management*. 2010;260(10):1623-1639. doi:10.1016/J.FORECO.2010.07.054